UNIVERSITY OF SOUTHAMPTON

Novel Amido/Imino, Diamido/Ether and Phenoxyimine Early Transition Metal Complexes

Robin Mark Porter

A Thesis Submitted for the Degree of Doctor of Philosophy

Department Of Chemistry

July 2004

UNIVERSITY OF SOUTHAMPTON

ABSTRACT

FACULTY OF SCIENCE

CHEMISTRY

Doctor of Philosophy

"Novel Amido/Imino, Diamido/Ether and Phenoxyimine Early Transition Metal Complexes"

by Robin Mark Porter

A series of novel, mixed donor amino/imino ligands have been synthesised in high yield and converted to the corresponding lithium amido/imino compounds. Both the amino/imino and the lithium amido/imino compounds were reacted with Group 4 metal complexes to give amido/imino and related complexes of Ti and Zr. Early transition metal complexes of a phenoxyimine ligand were prepared using both aminolysis and salt elimination methodologies. A series of novel diamido-ether ligands were prepared based on a xanthene or dibenzofuran framework, and several Ti complexes were prepared.

The silylamino/imino compounds 2-[CyN=C(CH_3)]C_6H_4N(H)($SiMe_3$) ($L^{TMS}H$) and 2-[CyN=C(CH_3)]C_6H_4N(H)($SiMe_2Bu^t$) ($L^{TBDMS}H$) were synthesised in high yields by reaction of 2-[CyN=C(CH_3)]C_6H_4N(H)Li with Me_3SiCl and Bu^tMe_2SiCl respectively. The arylamino/imino compounds 2-[CyN=C(CH_3)]C_6H_4N(H)(xyl) ($L^{xyl}H$) and 2-[CyN=C(CH_3)]C_6H_4N(H)(mes) ($L^{mes}H$) were prepared in high yields by Buchwald-Hartwig amination of the arylbromides with 2-[CyN=C(CH_3)]$C_6H_4NH_2$. The amino/imino ligands were deprotonated with Bu^nLi to yield the respective lithium amido/imino complexes (LLi).

The zirconium complexes (L^{TMS})$Zr(NMe_2)_2Cl$, (L^{TBDMS})$Zr(NMe_2)_2Cl$, (L^{TMS})$Zr(NEt_2)_2Cl$, and (L^{mes})$Zr(NEt_2)_2Cl$ were synthesised by salt elimination reaction between the appropriate LLi and $Zr(NR_2)_2Cl_2(THF)_2$ compounds. The (L^{TMS})$ZrCl_3$ complex was prepared by reaction of $L^{TMS}Li$ with $ZrCl_4$, as well as by reaction of Me_3SiCl with (L^{TMS})$Zr(NMe_2)_2Cl$ and (L^{TMS})$Zr(NEt_2)_2Cl$; (L^{mes})$ZrCl_3$ was prepared by reaction of Me_3SiCl with $L^{mes}Zr(NEt_2)_2Cl$. The product of reaction between $L^{TBDMS}Li$ and $Zr(NEt_2)_2Cl_2(THF)_2$ was the complex [2-(CyNC=CH_2)-$C_6H_4NSiMe_2Bu^t$]$Zr(NEt_2)Cl(THF)$, in which the amido/imino ligand has been converted to a dianionic amido/vinylamido group. The analogous complex [2-(CyNC=CH_2)-C_6H_4N(mes)]$Zr(NEt_2)Cl(THF)$ was observed as a side product from the reaction of $L^{mes}Li$ with $Zr(NEt_2)_2Cl_2(THF)_2$. The 2:1 complex (L^{TBDMS})$_2ZrCl_2$ was synthesised by reaction of two equivalents of $L^{TBDMS}Li$ with $ZrCl_4(THT)_2$. The complex (L^{TMS})$Zr(NMe_2)_3$ was prepared by an aminolysis reaction between $L^{TMS}H$ and $Zr(NMe_2)_4$, but under forcing conditions the reaction yielded an imido-bridged dimer following Me_3SiNMe_2 elimination.

The results of salt elimination reactions of $L^{xyl}Li$ and $L^{mes}Li$ with $Ti(NMe_2)_2Cl_2$ were complexes of the type 2-[CyNC(CH_3)(NMe_2)]-C_6H_4N(aryl)$Zr(NMe_2)Cl$, in which the amido/imino ligand was converted to a tridentate, dianionic diamido/amino ligand. The minor product of each reaction were the 2-[CyNC(CH_3)(NMe_2)]-C_6H_4N(aryl)$ZrCl_2$ type complexes.

Ethylene polymerisation studies on (L^{TMS})$Zr(NMe_2)_2Cl$, (L^{mes})$Zr(NEt_2)_2Cl$, (L^{mes})$ZrCl_3$ and (L^{TBDMS})$_2ZrCl_2$ with MAO as cocatalyst showed that they possessed low to moderate activity.

A series of phenoxyimine complexes of Ti, Zr and Nb were prepared using the 2-Bu^t-6-[CyN=C(H)]C_6H_4O- (L^{phen}) group. The lithium phenoxyimine complex ($L^{phen}Li$) was prepared and reacted with $Ti(NMe_2)_2Cl_2$ to give (L^{phen})$Ti(NMe_2)Cl_2(HNMe_2)$. Reaction of one equivalent of $L^{phen}H$ with $Ti(NMe_2)_2Cl_2$ gave (L^{phen})$Ti(NMe_2)Cl_2(THF)$; whilst (L^{phen})$_2TiCl_2$, (L^{phen})$_2Ti(NEt_2)_2$, (L^{phen})$_2ZrCl_2$ and (L^{phen})$_2Zr(NEt_2)_2$ were obtained from reaction of two equivalents of $L^{phen}H$ with $Ti(NEt_2)_2Cl_2$, $Ti(NEt_2)_4$, $Zr(NEt_2)_2Cl_2(THF)_2$ and $Zr(NEt_2)_4$ respectively. Reaction of two equivalents of $L^{phen}H$ with $Nb(NEt_2)_4$ yielded the niobium(V) complex (2-*tert*-butyl-6-cyclohexyliminomethyl-phenoxy) [2-*tert*-butyl-6-(1-cyclohexylamido-2-ethylamido-propyl)-phenoxy] niobium diethylamide.

A series of novel diamino-ether ligands were prepared, 4,5-dicyclohexylamino-2,7-di-*tert*-butyl-9,9-dimethyl-xanthene ($N_2O^1H_2$), 4,5-di-(2,4,6-trimethylanilino)-2,7-di-*tert*-butyl-9,9-dimethyl-xanthene ($N_2O^2H_2$) and 4,5-di-(2,4,6-trimethylanilino)-dibenzofuran ($N_2O^3H_2$), by Buchwald-Hartwig amination of the appropriate primary amine with either 4,5-dibromo-2,7-di-*tert*-butyl-9,9-dimethyl-xanthene or 4,5-dibromo-dibenzofuran. The dilithium diamido complex $N_2O^3Li_2$ was prepared by double deprotonation of $N_2O^3H_2$ with Bu^nLi. An alkanolysis reaction between $N_2O^1H_2$ and $Ti(benzyl)_4$ yielded (N_2O^1)$Ti(benzyl)_2$. *In situ* double deprotonation of both $N_2O^1H_2$ and $N_2O^2H_2$ followed by reaction with $Ti(NMe_2)_2Cl_2$ gave the (N_2O)$Ti(NMe_2)_2$ complexes as the product.

Table of Contents

List of Figures

List of Schemes

List of Tables

Acknowledgements

Firstly, I would like to acknowledge the EPSRC for providing the financial support for this project. I would like to thank my supervisor Dr. Andreas A. Danopoulos for his support and assistance throughout the project. I thank the other members of the Danopoulos group (past and present), particularly Dr. Scott Winston, Nikos Tsoureas and Dr. Joseph Wright for their assistance with X-ray crystallography. I wish to acknowledge my friends around the department for their friendship throughout the four years I have spent on this project. Lastly, I thank my family and Mel for all their support during my time at Southampton.

List of Abbreviations

R	alkyl group
Ar	aryl group
X	halogen
M	metal
L	ligand
Me	methyl
Et	ethyl
Pr^i	*iso*-propyl
Bu^t	*tert*-butyl
Cy	cyclohexyl
Ph	phenyl
xylyl	3,5-dimethylphenyl
mesityl	2,4,6-trimethylphenyl
THF	tetrahydrofuran
THT	tetrahydrothiophene
Et_2O	diethylether
Bu^nLi	*n*-butyl lithium
dba	dibenzylideneacetone
BINAP	2,2'-bis(diphenylphosphino)-1,1'-binaphthyl
NMR	nuclear magnetic resonance
CI-GCMS	chemical ionisation gas chromatographic mass spectrometry
δ	chemical shift
ppm	parts per million
s	singlet
d	doublet
t	triplet
m	multiplet
br.	broad
dd	doublet of doublets
dt	doublet of triplets
tt	triplet of triplets
Hz	Hertz

Chapter 1
Introduction

1.1 Amide ligands and metal amides

An amide ligand is a fragment of the form $RR'N^-$ that contains a nitrogen donor atom.[1] It is monoanionic and classed as a hard ligand. A metal amide is classed as a compound that contains one or more $RR'N^-$ ligands bound to a metal M.

(1) (2)

R, R' = H, alkyl, aryl, SiR_3 etc.

Scheme 1.1: Resonance forms of metal-amide bonding.

Metal amides are molecular compounds that have the structural unit (1) (Scheme 1.1). Under the valence bond formalism the metal-amide bond can be represented by the two limiting resonance forms (1) and (2) in Scheme 1.1. Form (2) represents backbonding from the p_z orbital of the nitrogen to a d_π of the transition metal, usually in the form of a M(d)←N(p) interaction. The amide ligand is formally a four-electron donor, when the ionic model of valence electron counting is used.

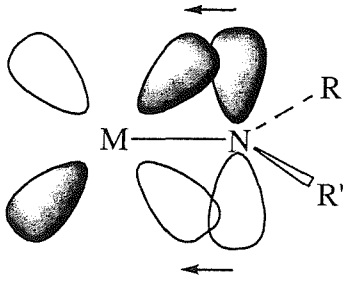

Figure 1.1: Schematic diagram representing the π-bonding in a metal amide.

The geometry of the metal-amide group is described as planar at N, a fact understandable by the sp^2 hybridisation that the nitrogen atom adopts. There are cases where the amide group adopts a bonding geometry in which the nitrogen geometry is close to tetrahedral.

This π-bonding requires suitable vacant d-orbitals on the metal, which are more commonly available on the earlier transition metals rather than the later ones. This explains why the later transition metals less readily form stable compounds with M-NRR' bonds and the higher reactivity of amide groups when coordinated to these metals (eg. Pd-amination, Ir, Rh hydroaminations etc.).[2,3]

The first metal amide, $Zn(NEt_2)_2$ was prepared in 1856 by Frankland.[4] The next example of a transition metal amide was not reported until 1935 with the synthesis of $Ti(NPh_2)_4$.[5] After this, the transition metal amides were discovered in the late 1950's, including $Zr(NMe_2)_4$ and $Zr(NEt_2)_4$.[6] Metal silylamides are analogous ligands ($RR'N^-$ where at least one of R, R' is SiR_3). Electronically, they are similar to dialkylamides but the silicon atom is capable of delocalising electron density by N(p)-Si(d) overlap. Metal silylamides have been studied in detail with bulky SiR_3 groups, especially for the stabilisation of low coordination number compounds.[7-12]

1.2 Single-site olefin polymerisation catalysis

One of the main industrial uses of organometallic catalysts is in the polymerisation and oligomerisation of olefins. More than half of the polyolefins produced annually (*ca.* 1990) utilised (heterogeneous) Ziegler-Natta catalysts.[13] These heterogeneous materials are formed from titanium(III)chloride and aluminium alkyls, or from magnesium chloride/titanium tetrachloride and triethylaluminium.[14] Homogenous Ziegler-Natta systems began to be studied in order to understand the elementary steps of polymerisation. However, they gave rise to a new generation of polymerisation catalysts known as single-site polymerisation catalysts. These provide control over the precise geometry of the catalytically active site, which can lead to precise tailoring of the polymeric microstructures and therefore the mechanical properties of the polymer.

Early work on homogenous catalysts based on Group 4 metals for the polymerisation of ethylene included bis(cyclopentadienyl)titanium(IV) compounds

with an organoaluminium compound as co-catalyst.[15] The activities of these systems were poor and so no industrial applications followed.

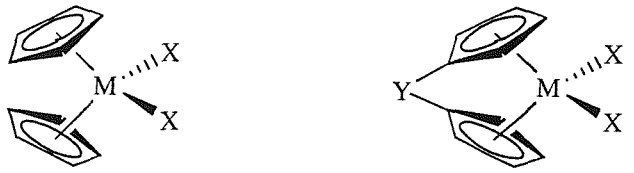

I **II**

Figure 1.2: Group 4 metallocene (**I**) and Group (IV) *ansa*-metallocene (Y=bridging group) (**II**).

New breeds of homogeneous catalysts were developed, based on metallocenes (Figure 1.2, above) and methylalumoxane (MAO). They were 10-100 times more active than the commonly used heterogeneous catalysts and attracted great interest.[16] Using these catalysts it became possible to tailor the properties of the polymers by tuning the geometry of the ligands.[17-21]

1.2.1 Mechanism of polymerisation

MAO is formed by a controlled reaction between trimethylaluminium and water and is a mixture of oligomers.[22-24] The basic oligomer (Figure 1.3, below) forms associates and cage structures which complex additional trimethylaluminium.[13]

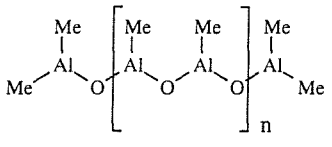

n = ~500

Figure 1.3: Basic oligomer of MAO.

The alumoxane co-catalysts initially alkylate the metallocene component (eq. (1), below) and then form the active species by abstraction of Me^- (eq. (2), below). The active species is generated by dissociation of the metallocene alumoxane complex[25] and the $[alumoxane\text{-}Me]^-$ anion is regarded as weakly or non-

coordinating.[26] A large excess of MAO is usually required, covering an aluminium/metallocene ratio in the range of 50-100 for supported systems and 400-20000 in solution. This means that nearly every zirconocene group is active, forming a single-site catalyst.

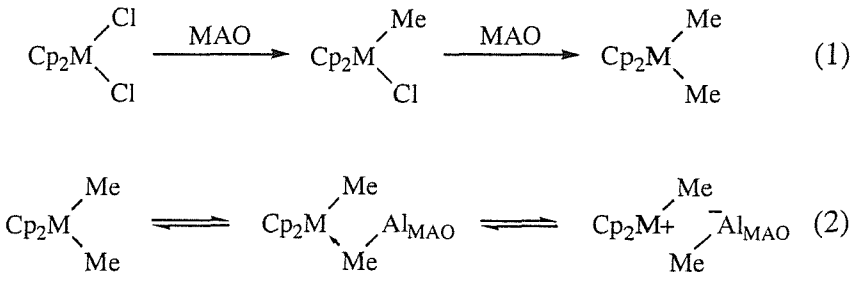

Scheme 1.2: Generation of the active catalytic species by action of MAO on a metallocene.

Using the Group 4 metallocene dichloride catalyst precursors as an example, the polymerisation process occurs according to the Cossee-Arlman mechanism (Scheme 1.3, below).[27] Following the abstraction of a methyl anion the cationic Group 4 metal complex is formally a 14 electron species. Compared to the 16 electron dimethyl precursor the complex is now electron deficient and is therefore more electrophilic, which encourages the coordination of the olefin monomer. Once coordinated, the olefin is inserted into the metal-alkyl bond *via* a four centred transition state.

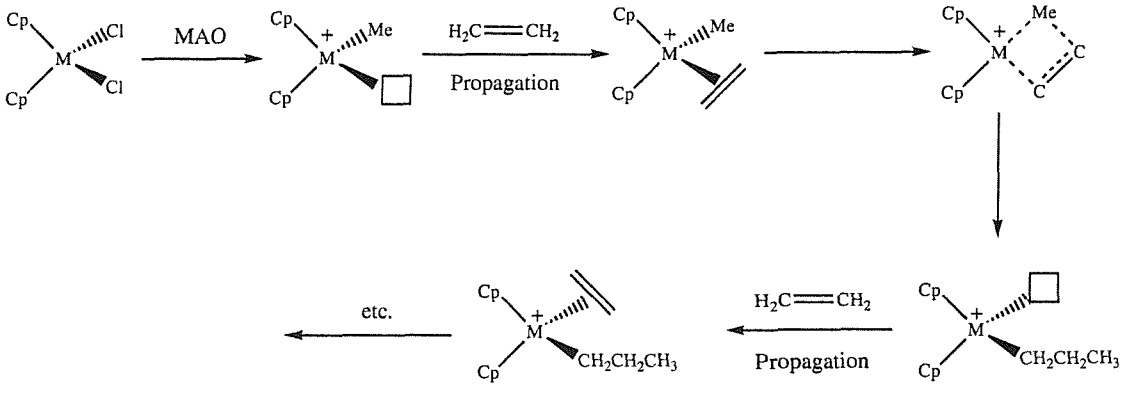

Scheme 1.3: Cossee-Arlman mechanism of single-site olefin polymerisation.

The termination of the polymer chain growth is usually by β-H elimination or by transfer of the polymer chain to the organoaluminium species (if it was used as a cocatalyst). Additionally, a polymerisation that proceeds without chain transfer or elimination reactions can be classed as a living polymerisation. Simply, a living polymerisation occurs with rapid initiation and negligible chain termination or transfer.[18]

1.3 Metal amide complexes as single-site olefin polymerisation catalysts

Since the early 1990's extensive efforts have been devoted to the development of novel ligands for the stabilisation of early transition metals and the potential of these complexes to act as olefin polymerisation catalysts.[28-31] As alternatives to Cp ligands, the alkoxy and amido ligands have received a great deal of attention and proved to be suitable for the stabilisation of early, electron-poor transition metals in medium to high oxidation states. Of these two alternatives the amido ligand offers the greater scope for ligand and complex design due to the potential for double substitution at the donor atom. The amido donor function R_2N^- may be placed into a great variety of structural environments including complex polydentate ligand structures and combined with other donor functionalities.[32] The availability of the two substituent positions at the amido N-donor atom allows for its integration into ligand systems of both podand and macrocyclic topology (Figure 1.4, below). This allows for a well-defined relative orientation of the ligating atoms and many possibilities of steric control. Amido functions may also be combined with other donor functionalities that possess a different formal charge and chemical hardness.

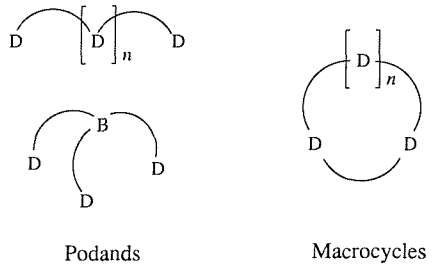

Figure 1.4: Topologies of polydentate ligands (D = donor function, B = bridgehead function)

1.3.1 Linked cyclopentadienyl-amide complexes

A great deal of work has been carried out on the use of ligands featuring a cyclopentadienyl group with a pendant anionic amido group. Indeed, the linked Ti η^5:η^1-Cp-amide complex, or constrained geometry catalyst (complex **III**, Figure 1.5), is a rare example of a commercially exploited "non-metallocene" catalyst. It has been primarily used for the copolymerisation of ethylene with higher α-olefins. Extensive modifications have been carried out on this system and are summarised in a recent review.[33] As well as cyclopentadienyl-amide-based constrained geometry catalysts, complexes based on fluorenyl (complex **IV**, Figure 1.5) and indenyl (complex **V**, Figure 1.5) groups have been found to act as active catalysts for the polymerisation of ethylene and propylene.[34-40]

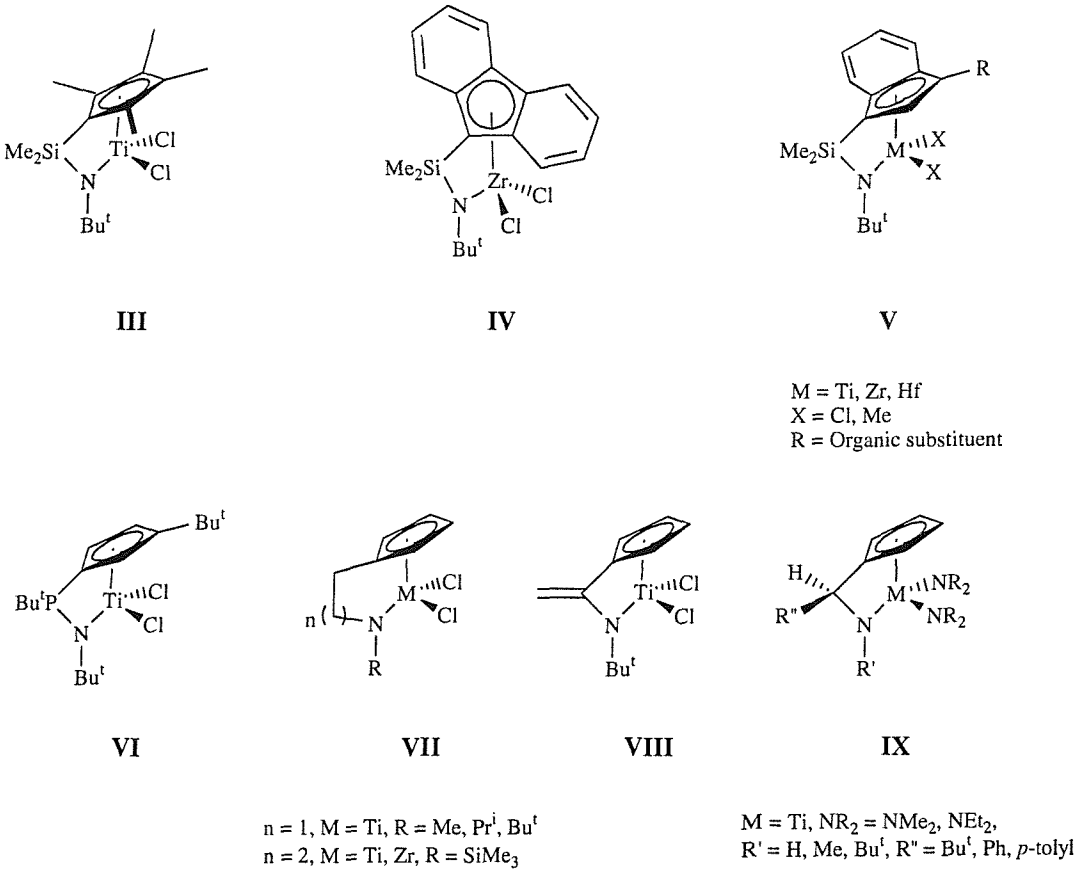

Figure 1.5: Linked Cp-amido complexes **(III)** – **(IX)**.

Various complexes containing an alternative to the dimethylsilyl-bridging group have been reported. A phosphorus-bridged Cp-amide Ti complex (complex **VI**, Figure 1.5) displays high activity and produces linear, high molecular weight

polyethylene.[41] A series of carbon-linked Cp-amide complexes have been synthesised featuring C_1- (complex **VIII** and **IX**, Figure 1.5),[42-44] C_2- (complex **VII**, n=1, Figure 1.5),[45] and C_3-bridging units (complex **VII**, n=2, Figure 1.5).[46] Both types of the C_1-bridged complexes display similar polymerisation activity to the related dimethylsilyl-bridged Zr complexes that are analogous to complex **III** (Figure 1.5).

1.3.2 Chelating diamide ligands

Recently, several academic groups have focused their attention on Group 4 metal complexes containing amide ligands.[28-30] They are promising candidates for olefin polymerisation catalysis due to the lower formal electron count that a cationic diamido Group 4 complex possesses, ($[(R_2N)_2ZrR]^+$ is a ten electron species) compared to that of the dicyclopentadienyl analogue ($[Cp_2ZrR]^+$ is a fourteen electron species). The diamido complex is thus more electron deficient and should more easily attract an electron rich olefin to form the olefin complex, followed by insertion of the double bond into the zirconium-alkyl bond.

A report by Roesky concerns the synthesis of Zr and Hf complexes containing two monoamido ligands bearing bulky substituents on nitrogen (complex **X**, Figure 1.6).[47] When activated with MAO the complex displayed moderate polymerisation activity. McConville and co-workers reported highly active catalysts for the polymerisation of α-olefins based on a chelating diamide ligand bearing bulky aryl groups on nitrogen, with dichloride and dialkyl complexes of Ti and Zr (complex **XI**, Figure 1.6).[48-51] The complexes were not applied to the polymerisation of ethylene but displayed high activity for the polymerisation of α-olefins and, especially, the titanium complexes performed living polymerisation of 1-hexene.[51] Analogous *N*-silyl complexes of Ti and Zr (complex **XII**, Figure 1.6) have been studied and shown to have a low to moderate activity for the polymerisation of ethylene.[52,53] This low activity is possibly due to catalyst deactivation as a result of the instability of the silylamido-zirconium dialkyl systems.[54] A diamide ligand with a C_2-linker (complex **XIII**, Figure 1.6) that gives a five-membered chelate ring gave complexes[55] that possessed lower polymerisation activity than the corresponding six-membered chelate ring systems, above.

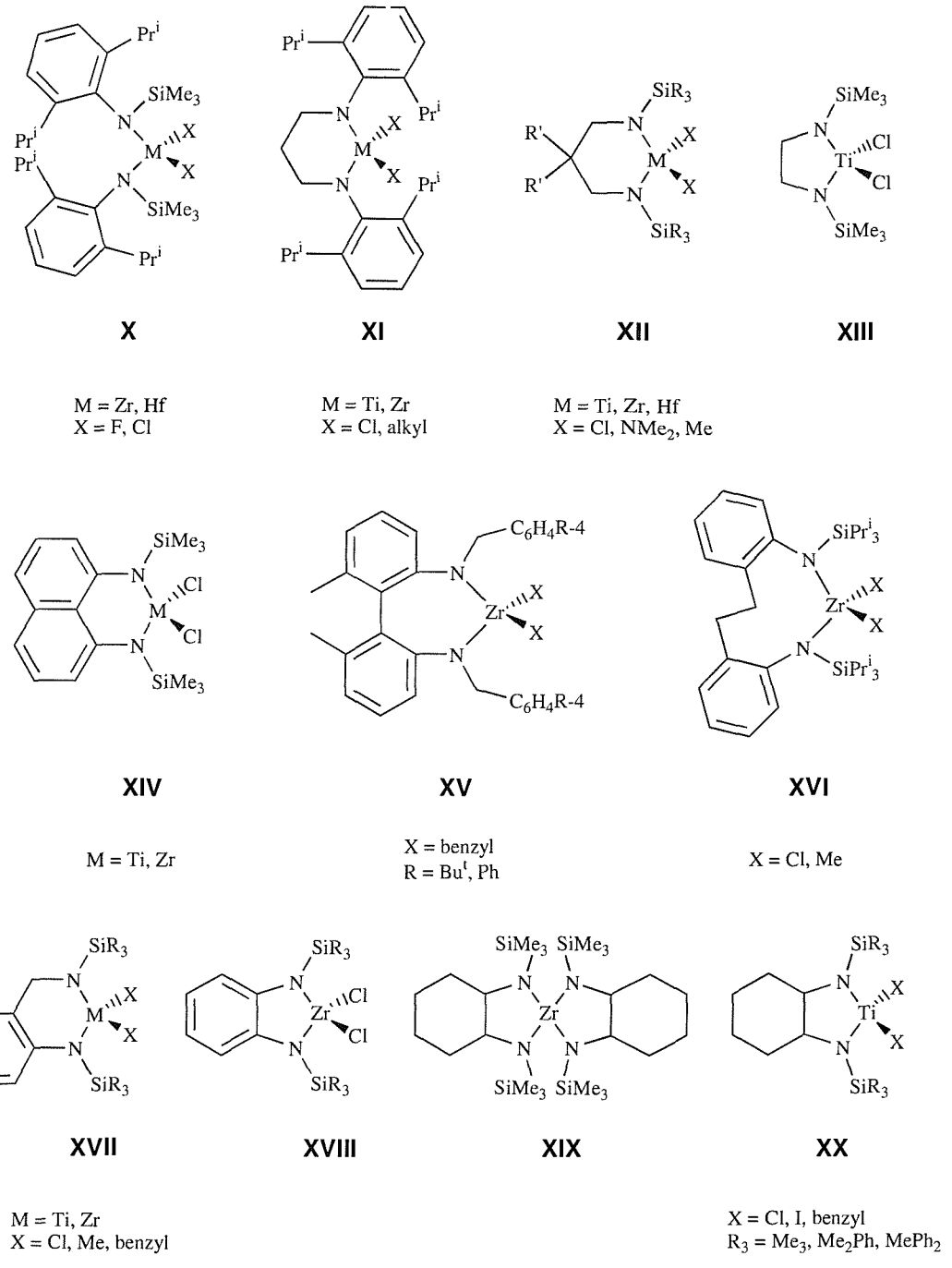

Figure 1.6: Bis-amido complex (**X**) and chelating diamido complexes (**XI**) – (**XX**).

Diamido complexes featuring a fused or linked biphenylene backbone have been studied. The rigid, fused biphenylene complexes featuring silyl-substituted amides (complex **XIV**, Figure 1.6) display very high activity for the polymerisation of ethylene as well as copolymerisation of ethylene with α-olefins.[53,56-59] Two systems based on linked biphenylene backbones both display moderate activities for ethylene polymerisation. The directly linked *o*-phenylene

system[60] (complex **XV**, Figure 1.6) is more conformationally rigid than the system in which the two phenyl rings are seperated by a C_2-spacer[61] (complex **XVI**, Figure 1.6).

Complexes based on diamido phenyl ligands (complexes **XVII** and **XVIII**, Figure 1.6) displayed low activity for ethylene polymerisation.[62-64] Similar complexes based on a 1,2-diamido cyclohexane ligand were prepared for Zr (complex **XIX**, Figure 1.6)[65] and Ti (complex **XX**, Figure 1.6).[66] The Zr complex featured two diamido ligands and displayed moderate activity for ethylene polymerisation when activated with MAO, whilst no data was given for the titanium complexes.

1.3.3 Amide ligands with a neutral donor atom

Many systems have been investigated which feature a diamide ligand with a neutral donor atom. It was anticipated that ligands of this type would lead to the formation of more stable, four-coordinate alkyl cations of titanium and zirconium. Schrock *et al.* have studied several different systems (complex **XXI** - **XXIII**, Figure 1.7) that combine two amido donors with either an ether or a thioether donor.[67-77] Zirconium dialkyl complexes of these ligands were shown to be active for the polymerisation of 1-hexene when activated with a borane activator.

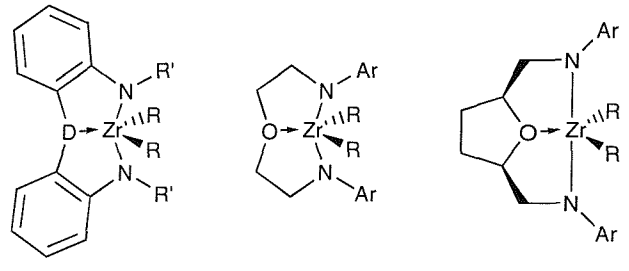

XXI **XXII** **XXIII**

Figure 1.7: Complexes prepared by Schrock featuring a diamide ligand with a neutral ether or thioether donor.

An analogous diamide ligand studied by Bochmann and co-workers features an ether donor with a silyl-backbone (complex **XXIV**, Figure 1.8).[65] Zirconium complexes of the ligand proved to have only moderate activity. A similar activity

was reported for zirconium complexes of a diamide ligand containing a neutral amine donor (complex **XXV**, Figure 1.8).[78]

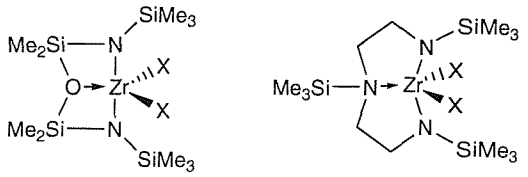

XXIV **XXV**

Figure 1.8: A diamido-ether complex (**XXIV**) and a diamido-amine complex (**XXV**).

McConville and co-workers prepared a series of complexes featuring a diamide ligand with a central pyridyl donor (complex **XXVI**, Figure 1.9).[79, 80] The zirconium complex displayed very high activity for ethylene polymerisation whilst the titanium analogue only gave very low activities. An analogous ligand prepared by both Schrock and Mountford features two amido donors and a pyridyl group arranged in a tripodal fashion (complex **XXVII**, Figure 1.9). Whereas the McConville ligand adopts a *mer* conformation upon coordination, this ligand coordinates in a *fac* fashion. Schrock reported that when activated with $[Ph_3C][B(C_6F_5)_4]$, Zr and Hf complexes of this diamido-pyridine ligand were active for the polymerisation of 1-hexene, with the hafnium derivative performing living polymerisation.[81, 82] Mountford used the ligand to stabilise Group 4 and 5 imido complexes.[83-85]

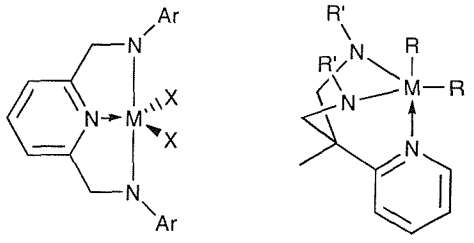

XXVI **XXVII**

Figure 1.9: Diamido-pyridyl complexes reported by McConville (**XXVI**) and Schrock and Mountford (**XXVII**).

1.4 *o*-(Cyclohexylimino-1-ethyl)-anilido ligands

The main focus of this project is concerned with the synthesis of a series of *o*-(cyclohexylimino-1-ethyl)-anilido ligands (**XXVIII**, Figure 1.10) and a study of their behaviour as supporting ligands for early transition metal complexes. The ligands feature a combination of a hard anionic donor (amide) and a softer, neutral donor (imine). The formal electron donation of the two donor groups is four electrons from the amide and two from the imine. This means that the amido/imino ligands have the potential to act as six electron donors. They are therefore isoelectronic to cyclopentadienyl (Cp^-) ligands. It is anticipated that this strong electron donating ability will prove suitable for the electron deficient early transition metals in their high oxidation states.

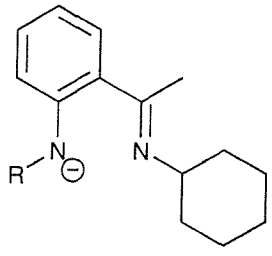

XXVIII

Figure 1.10: *o*-(Cyclohexylimino-1-ethyl)-anilido ligands studied in this project.

The properties of the amido/imino ligands can be varied by altering the nature of the nitrogen substituents. In this project the imino-substituent has remained constant (cyclohexyl), but a variety of silyl and aryl groups have been employed as the amido-substituents. This work is a progression of earlier work within the group that focussed on complexes of the *o*-(*tert*-butyliminomethyl)-*N*-trimethylsilyl-anilido ligand.[86]

These amido/imino ligands share many characteristics with β-diketiminato ligands (**XXIX**, Figure 1.11) (see Introduction, Chapter 4) and salicylaldiminato/phenoxy-imine ligands (**XXX**, Figure 1.11) (see Introduction, Chapter 5). β-Diketiminato ligands are monoanionic N,N donors that form six-membered chelate rings with metals, with the negative charge delocalised around the chelate ring. The area has been recently reviewed.[87] They have been used to

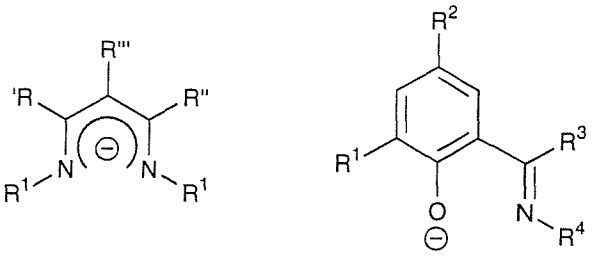

XXIX XXX

Figure 1.11: β-Diketiminato (**XXIX**) and salicylaldiminato/phenoxy-imine (**XXX**) ligands.

prepare metal complexes across the transition series as well as with main group elements. The salicylaldiminato ligand has also been used to prepare metal complexes across the periodic table,[29] but a class of bis-salicylaldiminato Group 4 complexes have proved to be extremely active catalysts for the polymerisation of ethylene and higher olefins.[88, 89]

1.5 Aims

The aims of the research were to investigate and develop novel mixed donor amido/imino ligands based on an *o*-(cyclohexylimino-1-ethyl)-anilido framework, and to study their behaviour as supporting ligands for early transition metals. It was anticipated that these complexes would have potential applications as ethylene polymerisation catalysts. By varying the nature of the nitrogen-substituents, it was hoped that insights into the behaviour of these amido/imino ligands would be gained. These developments could have potential applications to the analogous salicylaldiminato/phenoxy-imine class of ligands.

1.6 References

1. M. F. Lappert, P. P. Power, A. R. Sanger, R. C. Srivastava, *Metal and Metalloid Amides*, Ellis Horwood, Chichester, 1980.

2. J. R. Fulton, A. W. Holland, D. J. Fox, R. G. Bergman, *Acc. Chem. Res.*, 2002, **35**, 44.

3. H. E. Bryndza, W. Tam, *Chem. Rev.*, 1988, **88**, 1163

4. E. Frankland, *Proc. Roy. Soc.*, 1856-57, **8**, 502.

5. O. C. Dermer, W. C. Fernelius, *Z. Anorg. Allg. Chem.*, 1935, **221**, 83.

6. D. C. Bradley, I. M. Thomas, *Proc. Chem. Soc.*, 1959, 225.

7. N. W. Alcock, M. Pierce-Butler, G. R. Willey, *J. Chem. Soc. Chem. Comm.*, 1974, 627.

8. E. C. Alyea, D. C. Bradley, R. G. Copperthwaite, *J. Chem. Soc., Dalton Trans.*, 1972, 1580.

9. D. C. Bradley, *Chem. in Brit.*, 1975, **11**, 393.

10. D. C. Bradley, M. B. Hursthouse, C. W. Newing, A. J. Welch, *J. Chem. Soc. Chem. Comm.*, 1972, 567.

11. D. C. Bradley, M. B. Hursthouse, P. F. Rodesiler, *J. Chem. Soc., Dalton Trans.*, 1972, 2100.

12. K. Issleib, G. Batz, *Z. Anorg. Allg. Chem.*, 1969, **369**, 83.

13. B. Cornils, W. A. Herrmann, *Applied Homogenous Catalysis with Organometallic Compounds*, Wiley-VCH, Weinheim, 1996.

14. H. Sinn, W. Kaminsky, *Adv. Organomet. Chem.*, 1980, **18**, 99.

15. D. S. Breslow, N. R. Newburg, *J. Am. Chem. Soc.*, 1957, **79**, 5072.

16. H. Sinn, W. Kaminsky, H. -J. Vollmer, R. Woldt, *Angew. Chem. Int. Ed. Engl.*, 1980, **19**, 390.

17. G. W. Coates, *J. Chem. Soc., Dalton Trans.*, 2002, 467.

18. G. W. Coates, P. D. Hustad, S. Reinartz, *Angew. Chem. Int. Ed.*, 2002, **41**, 2236.

19. M. Bochmann, *J. Chem. Soc., Dalton Trans.*, 1996, 255.

20. H. H. Brintzinger, D. Fischer, R. Mülhaupt, B. Rieger, R. M. Waymouth, *Angew. Chem. Int. Ed. Engl.*, 1995, **34**, 1143.

21. H. G. Alt, A. Köppl, *Chem. Rev.*, 2000, **100**, 1205.

22. A. Andresen, H. –G. Cordes, J. Herwig, W. Kaminsky, A. Merck, R. Mottweiler, J. Pein, H. Sinn, H. –J. Vollmer, *Angew. Chem. Int. Ed. Engl.*, 1976, **15**, 630.

23. H. Sinn, W. Kaminsky, H. –J. Vollmer, R. Woldt, *Angew. Chem. Int. Ed. Engl.*, 1980, **19**, 390.

24. S. Pasynkiewicz, *Polyhedron*, 1990, **9**, 429.

25. R. F. Jordan, *Adv. Organomet. Chem.*, 1991, **32**, 325.

26. M. Bochmann, *Angew. Chem. Int. Ed. Engl.*, 1992, **31**, 1181.

27. F. A. Cotton, G. Wilkinson, *Advanced Inorganic Chemistry*, 5th Edition, Wiley-Interscience, NY, 1988.

28. G. J. P. Britovsek, V. C. Gibson, D. F. Wass, *Angew. Chem. Int. Ed.*, 1999, **38**, 428.

29. V. C. Gibson, S. K. Spitzmesser, *Chem. Rev.*, 2003, **103**, 283.

30. R. Kempe, *Angew. Chem. Int. Ed.*, 2000, **39**, 468.

31. W. E. Piers, D. J. H. Emslie, *Coord. Chem. Rev.*, 2002, **233-234**, 131.

32. L. H. Gade, *Chem. Commun.*, 2000, 173.

33. A. L. McKnight, R. M. Waymouth, *Chem. Rev.*, 1998, **98**, 2587.

34. A. Reb, H. G. Alt, *J. Mol. Catal. A: Chem.*, 2001, **174**, 35.

35. H. G. Alt, K. Fottinger, W. Milius, *J. Organomet. Chem.*, 1999, **572**, 21.

36. H. G. Alt, A. Reb, *J. Mol. Catal. A: Chem.*, 2001, **175**, 43.

37. H. G. Alt, A. Reb, W. Milius, A. Weis, *J. Organomet. Chem.*, 2001, **628**, 169.

38. H. G. Alt, A. Reb, K. Kundu, *J. Organomet. Chem.*, 2001, **628**, 211.

39. T. Hasan, A. Ioku, K. Nishii, T. Shiono, T. Ikeda, *Macromolecules*, 2001, **34**, 3142.

40. J. Klosin, W. J. Kruper, P. N. Nickias, G. R. Roof, P. De Waele, K. A. Abboud, *Organometallics*, 2001, **20**, 2663.

41. V. V. Kotov, E. V. Avtomonov, J. Sundermeyer, K. Harms, D. A. Lemenovskii, *Eur. J. Inorg. Chem.*, 2002, 678.

42. L. Duda, G. Erker, R. Fröhlich, F. Zippel, *Eur. J. Inorg. Chem.*, 1998, 1153.

43. K. Kunz, G. Erker, S. Döring, R. Fröhlich, G. Kehr, *J. Am. Chem. Soc.*, 2001, **123**, 6181.

44. K. Kunz, G. Erker, S. Döring, S. Bredeau, G. Kehr, R. Fröhlich, *Organometallics*, 2002, **21**, 1031.

45. D. van Leusen, D. J. Beetstra, B. Hessen, J. H. Teuben, *Organometallics*, 2000, **19**, 4084.

46. P. T. Gomes, M. L. H. Green, A. M. Martins, *J. Organomet. Chem.*, 1998, **551**, 133.

47. S. A. A. Shah, H. Dorn, A. Voigt, H. W. Roesky, E. Parisini, H. –G. Schmidt, M. Noltemeyer, *Organometallics*, 1996, **15**, 3176.

48. J. D. Scollard, D. H. McConville, J. J. Vittal, *Organometallics*, 1995, **14**, 5478.

49. J. D. Scollard, D. H. McConville, *J. Am. Chem. Soc.*, 1996, **118**, 10008.

50. J. D. Scollard, D. H. McConville, N. C. Payne, J. J. Vittal, *Macromolecules*, 1996, **29**, 5241.

51. J. D. Scollard, D. H. McConville, S. J. Rettig, *Organometallics*, 1997, **16**, 1810.

52. C. Lorber, B. Donnadieu, R. Choukroun, *Organometallics*, 2000, **19**, 1963.

53. C. H. Lee, Y. H. La, J. W. Park, *Organometallics*, 2000, **19**, 344.

54. R. R. Schrock, S. W. Seidel, Y. Schrodi, W. M. Davis, *Organometallics*, 1999, **18**, 428.

55. S. Tinkler, R. J. Deeth, D. J. Duncalf, A. McCamley, *Chem. Commun.*, 1996, 2623.

56. K. Nomura, N. Naga, K. Takaoki, *Macromolecules*, 1998, **31**, 8009.

57. C. H. Lee, Y. H. La, S. J. Park, J. W. Park, *Organometallics*, 1998, **17**, 3648.

58. K. Nomura, N. Naofumi, K. Takaoki, A. Imai, *J. Mol. Catal. A: Chem.*, 1998, **130**, 209.

59. K. Nomura, K. Oya, Y. Imanishi, *Polymer*, 2000, **41**, 2755.

60. F. G. N. Cloke, T. J. Geldbach, P. B. Hitchcock, J. B. Love, *J. Organomet. Chem.*, 1996, **506**, 343.

61. Y. M. Jeon, S. J. Park, J. Heo, K. Kim, *Organometallics*, 1998, **17**, 3161.

62. Y. M. Jeon, J. Heo, W. M. Lee, T. H. Chang, K. Kim, *Organometallics*, 1999, **18**, 4107.

63. R. M. Gauvin, C. Lorber, R. Choukroun, B. Donnadieu, J. Kress, *Eur. J. Inorg. Chem.*, 2001, 2337.

64. S. Daniele, P. B. Hitchcock, M. F. Lappert, P. G. Merle, *J. Chem. Soc., Dalton Trans.*, 2001, 13.

65. N. A. H. Male, M. Thornton-Pett, M. Bochmann, *J. Chem. Soc., Dalton Trans.*, 1997, 2487.

66. B. Tsuie, D. C. Swenson, R. F. Jordan, *Organometallics*, 1997, **16**, 1392.

67. R. Baumann, W. M. Davis, R. R. Schrock, *J. Am. Chem. Soc.*, 1997, **119**, 3830.

68. D. D. Graf, W. M. Davis, R. R. Schrock, *Organometallics*, 1998, **17**, 5820.

69. R. Baumann, R. R. Schrock, *J. Organomet. Chem.*, 1998, **557**, 69.

70. R. Baumann, R. Stumpf, W. M. Davis, L. C. Liang, R. R. Schrock, *J. Am. Chem. Soc.*, 1999, **121**, 7822.

71. R. R. Schrock, R. Baumann, S. M. Reid, J. T. Goodman, R. Stumpf, W. M. Davis, *Organometallics*, 1999, **18**, 3649.

72. L. C. Liang, R. R. Schrock, W. M. Davis, *Organometallics*, 2000, **19**, 2526.

73. J. T. Goodman, R. R. Schrock, *Organometallics*, 2001, **20**, 5205.

74. R. R. Schrock, L. C. Liang, R. Baumann, W. M. Davis, *J. Organomet. Chem.*, 1999, **591**, 163.

75. M. Aizenberg, L. Turculet, W. M. Davis, F. Schattenmann, R. R. Schrock, *Organometallics*, 1998, **17**, 4795.

76. M. A. Flores, M. R. Manzoni, R. Baumann, W. M. Davis, R. R. Schrock, *Organometallics*, 1999, **18**, 3220.

77. D. D. Graf, R. R. Schrock, W. M. Davis, R. Stumpf, *Organometallics*, 1999, **18**, 843.

78. A. D. Horton, J. de With, A. J. van der Linden, H. van de Weg, *Organometallics*, 1996, **15**, 2672.

79. F. Guérin, D. H. McConville, J. J. Vittal, *Organometallics*, 1996, **15**, 5586.

80. F. Guérin, D. H. McConville, N. C. Payne, *Organometallics*, 1996, **15**, 5085.

81. P. Mehrkhodavandi, P. J. Bonitatebus, R. R. Schrock, *J. Am. Chem. Soc.*, 2000, **122**, 7841.

82. P. Mehrkhodavandi, R. R. Schrock, *J. Am. Chem. Soc.*, 2001, **123**, 10746.

83. S. M. Pugh, A. J. Blake, L. H. Gade, P. Mountford, *Inorg. Chem.*, 2001, **40**, 3992.

84. S. M. Pugh, D. J. M. Trösch, M. E. G. Skinner, L. H. Gade, P. Mountford, *Organometallics*, 2001, **20**, 3531.

85. A. J. Blake, P. E. Collier, L. H. Gade, P. Mountford, J. Lloyd, S. M. Pugh, M. Schubart, M. E. G. Skinner, D. J. M. Trösch, *Inorg. Chem.*, 2001, **40**, 870.

86. R. M. Porter, S. Winston, A. A. Danopoulos, M. B. Hursthouse, *J. Chem. Soc., Dalton Trans.*, 2002, 3290.

87. L. Bourget-Merle, M. F. Lappert, J. R. Severn, *Chem. Rev.*, 2002, **102**, 3031.

88. Y. Suzuki, H. Terao, T. Fujita, *Bull. Chem. Soc. Jpn.*, 2003, **76**, 1493.

89. S. Matsui, T. Fujita, *Catal. Today*, 2001, **66**, 63.

Chapter 2

Mixed Donor Amido/Imino Ligands

2.1 Introduction

There is currently great interest in the study of ligand architectures incorporating amido functional groups as non-metallocene spectators, especially in organometallic complexes of the early transition metals.[1,2,3,4] The well-known electronic characteristics of the amido group and its facile incorporation into tunable ligand backbones provide unique opportunities for the design of complexes with catalytic activity.[1] Seminal contributions in this area have shown the viability of single site polymerisation catalysts based on chelating or functionalised amido ligands. The area has been recently reviewed.[4,5] Furthermore, organometallic complexes with Schiff bases, mainly salicylaldimines (2-$RN{=}C(H)C_6H_4O^-$, R=alkyl or aryl) and their derivatives have been extensively explored.[6] Some exhibit high activity or living behaviour in polymerisation reactions.[6,7] The attractive features of these ligands are easy synthetic accessibility and steric and electronic tuning by substitution of the aromatic ring or the imine carbon.[6] In contrast, the coordination chemistry of the anionic ligands that formally originate from the salicylaldiminato group by replacement of the PhO^- group with the isoelectronic $PhNR^-$ have received less attention,[8] even though the tuning opportunities in this case are even broader (Scheme 2.1). This is possibly due to the synthetic difficulties associated with the synthesis of this ligand system. The series of amino/imino and amido/imino ligands synthesised in this project are shown below (Scheme 2.1) and demonstrate some of the tuning opportunities afforded by the ligand system.

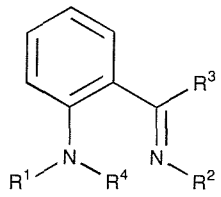

(**2.2**), R^1=$SiMe_3$, R^2=Cy, R^3=Me, R^4=H; (**2.3**), R^1=$SiMe_3$, R^2=Cy, R^3=Me, R^4=Li.

(**2.4**), R^1=$SiMe_2Bu^t$, R^2=Cy, R^3=Me, R^4=H; (**2.5**), R^1=$SiMe_2Bu^t$, R^2=Cy, R^3=Me, R^4=Li.

(**2.6**), R^1=3,5-dimethylphenyl, R^2=Cy, R^3=Me, R^4=H; (**2.7**), R^1=3,5-dimethylphenyl, R^2=Cy, R^3=Me, R^4=Li.

(**2.8**), R^1=2,4,6-trimethylphenyl, R^2=Cy, R^3=Me, R^4=H; (**2.9**), R^1=2,4,6-trimethylphenyl, R^2=Cy, R^3=Me, R^4=Li.

(**2.10**), R^1=2,4,6-trimethylphenyl, R^2=Cy, R^3=H, R^4=H; (**2.11**), R^1=2,4,6-trimethylphenyl, R^2=Cy, R^3=H, R^4=Li.

Scheme 2.1: Amino/imino and amido/imino ligands synthesised in this project.

2.1.1 Palladium-catalysed amination of aryl halides

The synthesis of the ligands (**2.6**), (**2.8**), and (**2.10**) required the formation of a C-N bond between nitrogen and an aromatic carbon to give a diaryl amine species. Traditional synthetic methods for these compounds are hindered by several problems. Reagents containing functional groups are often incompatible with procedures involving nitration, reduction or substitution and so the use of protection and deprotection steps is necessary. Reductive amination, involving the synthesis of an imine from an arylamine and the subsequent reduction of the imine, is not applicable to the synthesis of a diarylamine species. Copper mediated (Ullmann-type) substitutions of aryliodides by nitrogen nucleophiles occur at high temperatures, are typically substrate specific, and often give products from diarylation.

In order to avoid these problems it was decided to employ the recently developed palladium-catalysed coupling chemistry to form the new C-N bond from an aryl bromide by substitution of the bromide with an aniline. Palladium catalysed coupling chemistry between aryl halides and amines has recently been reviewed.[9] The origins of this methodology can be found in the 1980s when palladium complexes bearing monodentate phosphines were used as a catalyst in the coupling

of aryl bromides with trialkyltin amides.[10] An example of this type of reaction is shown below (Scheme 2.2)

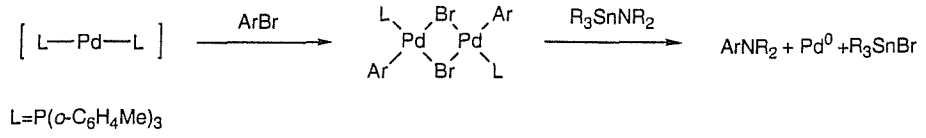

Scheme 2.2: Palladium-phosphine complex catalysed coupling of an aryl bromide with a trialkyltin amide.

The toxicity, thermal instability, and air-sensitivity of the tin-amides, as well as the narrow selection of arylhalides that undergo the coupling reaction and the poor atom economy of the transformations severely limit their scope.

In 1995 both Hartwig and Buchwald reported results on the tin-free amination of aryl halides.[11,12] The catalytic system comprised an aryl halide, an amine, a base and a Pd catalyst. The reactions were initially carried out at 80-100 °C in toluene and the first catalysts that were employed were $[PdCl_2\{P(o\text{-}C_6H_4Me)_3\}_2]$ and $[Pd\{P(o\text{-}C_6H_4Me)_3\}_2]$. The activity under these conditions was low for primary amines compared to secondary amines. In addition, coupling of a primary amine with an aryl bromide, was always accompanied by the formation of large amounts of arenes as side products. Mechanistic studies would later show that the arenes were formed as a result of β-hydrogen elimination instead of reductive elimination (Scheme 2.3).[13,14]

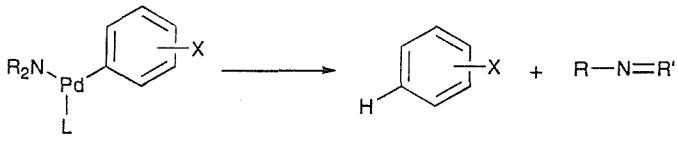

Scheme 2.3: β-Hydrogen elimination at a palladium centre leading to an arene and an imine.

A second generation of catalysts based on palladium complexes bearing chelating phosphines proved capable of performing aminations of aryl halides with primary alkyl amines as well as anilines. The palladium complexes that were used as catalysts employed BINAP and DPPF as ligands.[15,16,17]

More recently, non-phosphine ligands have been utilised for the palladium catalysts. An extensive amount of research has been focused on the use of Arduengo type N-heterocyclic carbene ligands. Catalysts of this type have been found to be extremely active. As with the palladium phosphine complexes the catalyst can either be preformed or generated *in situ*, in this case from $Pd(dba)_2$, the imidazolium/imidazolinium salt and a base.[18,19]

The exact mechanism of palladium-catalysed amination of aryl halides is not definitively known. The generally accepted mechanism for the Pd/BINAP-catalysed amination of aryl bromides, as proposed by Wolfe and Buchwald, is shown below (Scheme 2.4).[17]

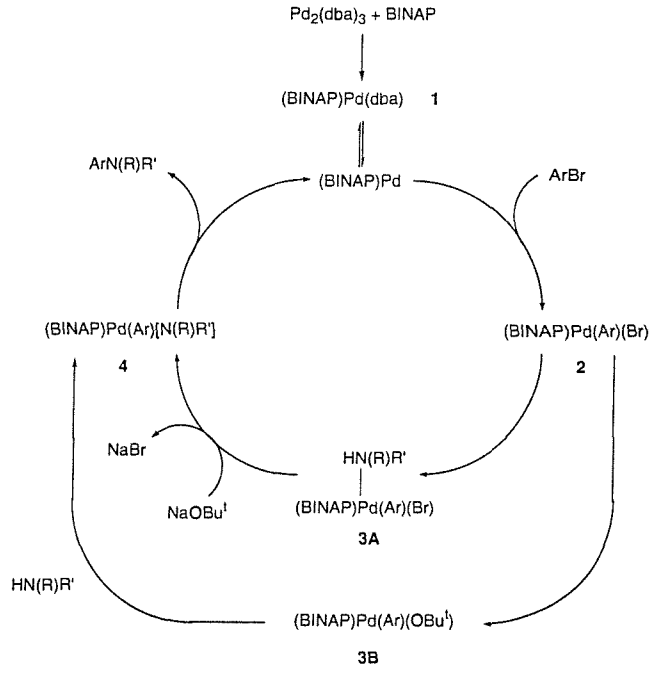

Scheme 2.4: Mechanism for the Pd/BINAP-catalysed amination of aryl bromides.

Initially, mixing BINAP with $Pd_2(dba)_3$ gives the complex (BINAP)Pd(dba) **1**. The next step is thought to be dissociation of the remaining dba ligand followed by oxidative addition of the aryl bromide to give the (BINAP)Pd(Ar)(Br) **2** complex. The mechanism then follows one of two paths, the first of which involves coordination of the amine **3A** followed by deprotonation to give an amido complex **4**. The second possible route involves reaction between the base $NaOBu^t$ and complex **2** to give (BINAP)Pd(Ar)(OBu^t) **3B**. This complex then reacts with

the amine to give complex **4** by protonolysis of the butoxide ligand. The final step is a reductive elimination of complex **4** to give the desired aryl amine product as well as regenerating the Pd(0) catalyst.

This mechanism differs from that proposed for systems involving a palladium catalyst bearing mondentate phosphine ligands. In this case the Pd(0) complex is a 14-electron two-coordinate species that loses one phosphine ligand before the oxidative addition of the aryl halide. The mechanism then proceeds in a similar fashion to that described above for the Pd(BINAP) case.

2.1.2 2-Pyridyl-azaallyl ligand

Lappert and co-workers synthesised a 2-pyridyl-azaallyl ligand class that is analogous to (**2.3**) and (**2.5**).[20] It was synthesised by reaction of RCN (R=Ph, Bu^t) with $[Li\{C(SiMe_3)(H)(C_5H_4N\text{-}2)(Et_2O)\}]_2$ to give the lithium salt of the ligand. A crystallographic study of one representative showed that the pyridyl group inhibited the delocalisation of the anionic charge and prevented the ligand from acting as a typical β-diketiminato group.

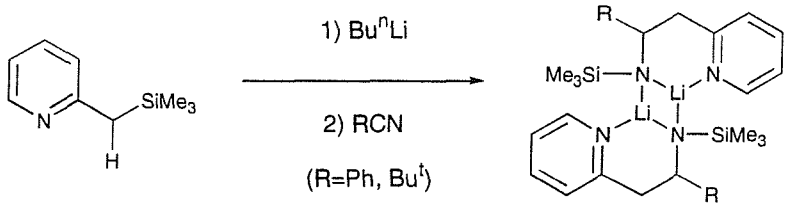

Scheme 2.5: Lappert's synthesis of a lithium pyridyl-azaallyl ligand.

2.1.3 2-(1-Aryliminomethyl)-*N*-(aryl)-anilide ligand

Piers has recently reported the synthesis of a ligand that is similar to (**2.6**), (**2.8**), and (**2.10**) (Scheme 2.6).[21] The 2-(2,6-diisopropylphenyliminomethyl)-*N*-(2,6-diisopropylphenyl)-aniline ligand was synthesised in two stages from *o*-fluorobenzaldehyde. The first step forms the imine and is followed by a nucleophilic aromatic displacement of fluoride using a lithium-anilide reagent. This synthesis illustrates the difficulties associated with utilising aromatic nucleophilic substitution reactions to form the bond between N^- and an aromatic carbon; the second step of the sequence proceeding in only 41% yield. The

amino/imino ligand was then deprotonated by reaction with Bu^nLi to yield the lithium-amido/imino species.

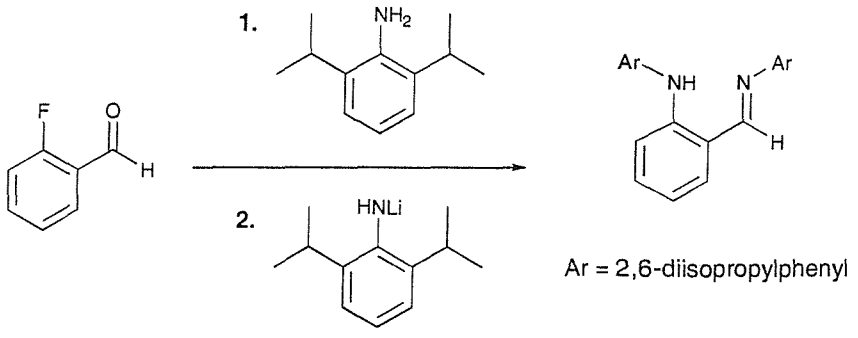

Scheme 2.6: Piers' synthesis of the 2-(2,6-diisopropylphenyliminomethyl)-*N*-(2,6-diisopropylphenyl)-aniline ligand.

Results and Discussion

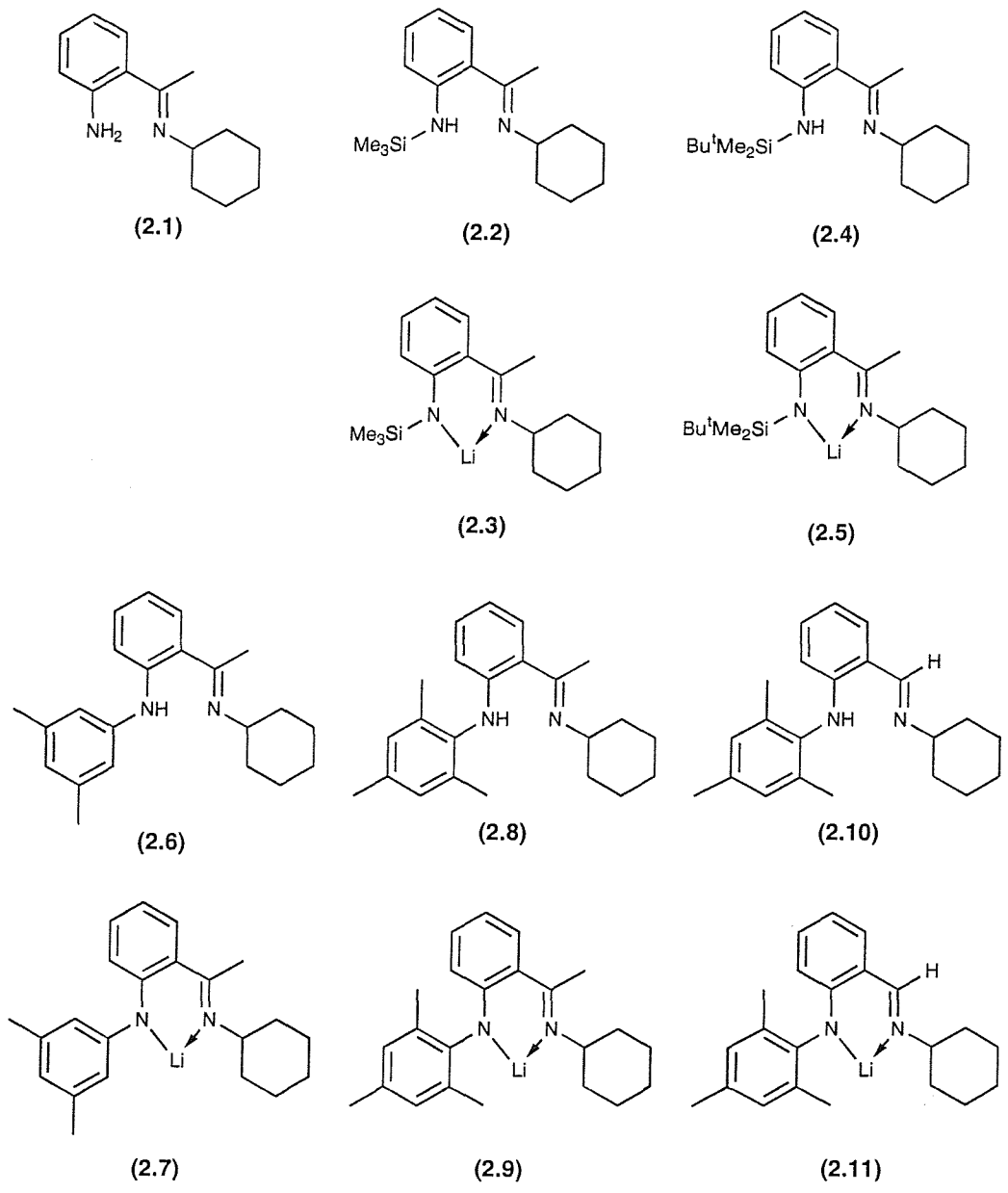

Figure 2.1: Amino/imino and lithium amido/imino ligands synthesised.

2.2 Synthesis of 2-(1-cyclohexylimino-ethyl)-aniline (2.1)

The starting material that was utilised in the synthesis of the amino/ketimine and amido/ketimine ligands (**2.2**)-(**2.9**) reported here was 2-(1-cyclohexylimino-ethyl)-aniline (**2.1**). It was prepared by the condensation reaction of *o*-aminoacetophenone with a large excess of cyclohexylamine (*ca.* seven-fold excess) to afford the Schiff base in multigram quantities. It was necessary to

employ forcing conditions in the synthesis of (**2.1**), the reaction being performed in toluene at 100 °C in the presence of 4 Å molecular sieves. The completion of the reaction was followed by CI-GCMS. The molecular ion in the mass spectrum of the product had a m/z of 217 corresponding to MH^+.

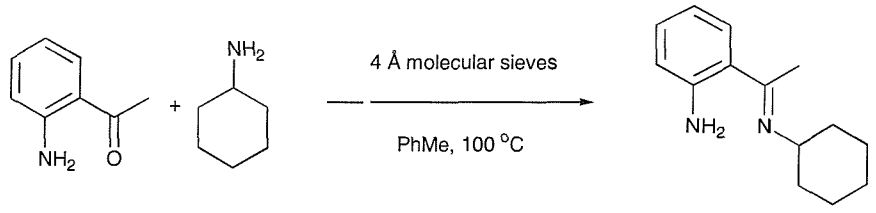

Scheme 2.7: Synthesis of 2-(1-cyclohexylimino-ethyl)-aniline (**2.1**).

2.2.1 NMR spectroscopy for (2.1)

The ^1H and $^{13}C\{^1H\}$ NMR spectra of (**2.1**) are straightforward. The CH_2 groups of the cyclohexyl ring give rise to a series of multiplets between 1.2 and 1.9 ppm in the ^1H NMR spectrum and three signals in the $^{13}C\{^1H\}$ NMR spectrum. The cyclohexyl ring CH group that is bonded to the imine nitrogen appears at 59.80 ppm in the $^{13}C\{^1H\}$ NMR spectrum and as a triplet of triplets at 3.58 ppm in the ^1H NMR spectrum. The ketimino methyl group appears as a singlet at 2.30 ppm in the ^1H NMR spectrum and at 16.26 ppm in the $^{13}C\{^1H\}$ NMR spectrum. The four aromatic protons give rise to one doublet of doublets, one doublet of triplets and two overlapping signals between 6.6 and 7.5 ppm in the ^1H NMR spectrum and six signals in the $^{13}C\{^1H\}$ NMR spectrum. The imine carbon appears as the most downfield signal in the $^{13}C\{^1H\}$ NMR spectrum at 165.65 ppm and the amine protons give rise to a broad singlet in the ^1H NMR spectrum at 6.55 ppm.

2.3 Synthesis of 2-(1-cyclohexylimino-ethyl)-*N*-(trialkylsilyl)-aniline compounds (2.2) and (2.4)

The two *N*-silyl-substituted amino/imino compounds (**2.2**) and (**2.4**) were synthesised by deprotonation of the free aniline (**2.1**) with Bu^nLi followed by quenching of the resulting lithium amide with trimethylchlorosilane and *tert*-butyldimethylchlorosilane, respectively (Scheme 2.8). An analogous method has

been used previously to synthesise 2-(*tert*-butyliminomethyl)-*N*-(trimethylsilyl)-aniline within the Danopoulos group.[22]

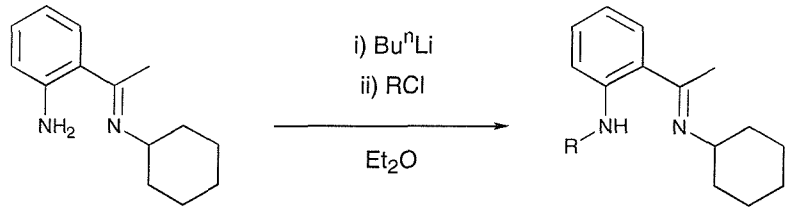

R=SiMe$_3$ (**2.2**); R=SiMe$_2$Bu^t (**2.4**).

Scheme 2.8: Synthesis of 2-(1-cyclohexylimino-ethyl)-*N*-(trimethylsilyl)-aniline (**2.2**) and 2-(1-cyclohexylimino-ethyl)-*N*-(*tert*-butyldimethylsilyl)-aniline (**2.4**).

The trimethylsilyl-substituted ligand (**2.2**) was isolated as a yellow, moisture sensitive oil in excellent yield. The analogous trimethylsilyl-amino/aldimino compound that was prepared previously within the Danopoulos group was isolated as a colourless oil.[22]

Problems growing crystals suitable for diffraction studies of zirconium complexes incorporating the trimethylsilyl-amino/imino ligand (see Chapter 3) lead us to synthesise the bulkier amino/imino ligand (**2.4**). Following deprotonation of (**2.1**) with Bu^{n}Li the lithium amido species was quenched with *tert*-butyldimethyl chlorosilane to yield (**2.4**) as a light brown solid in high yield.

2.3.1 NMR spectroscopy for (2.2) and (2.4)

The position of the signals due to the ligand backbone of (**2.2**) and (**2.4**) in the ^{1}H and ^{13}C{^{1}H} NMR spectra vary little compared to (**2.1**) (Table 2.1). The silylmethyl groups appear between 0.3 and 0.4 ppm in the ^{1}H NMR spectrum and at *ca.* 0.3 ppm in the ^{13}C{^{1}H} NMR spectrum. The protons of the *tert*-butyl group of (**2.4**) appear at 1.0 ppm with the methyl carbons at 27.21 ppm and the tertiary carbon at 18.96 ppm. The introduction of a silyl-substituent on the amine nitrogen results in a downfield shift of the NH to 10.00 (**2.2**) and 9.77 ppm (**2.4**). The imine carbons of (**2.2**) and (**2.4**) (165.95 and 166.59 ppm respectively) are shifted little relative to (**2.1**).

Table 2.1: A comparison of selected ^{1}H and $^{13}C\{^{1}H\}$ NMR data for the compounds (**2.1**), (**2.2**) and (**2.4**).[a]

Compound	(2.1)	(2.2)	(2.4)
Imine CH_3	2.30	2.32	2.31
$SiCH_3$	-	0.35	0.29
$SiC(CH_3)_3$	-	-	1.01
Cyclohexyl C*H*	3.58	3.60	3.55
NH/NH_2	6.55	10.00	9.77
Imine CH_3	16.26	15.27	16.49
$SiCH_3$	-	0.31	-3.31
$SiC(CH_3)_3$	-	-	18.96
$SiC(CH_3)_3$	-	-	27.21
Cyclohexyl *C*H	59.80	59.23	60.52
Imine *C*=N	165.65	165.95	166.59

[a] Spectral data expressed in ppm; solvent = $CDCl_3$.

2.4 Synthesis of lithium [2-(1-cyclohexylimino-ethyl)-*N*-(trialkylsilyl)-anilide] compounds (2.3) and (2.5)

Compounds (**2.2**) and (**2.4**) were converted into the corresponding lithium amido/imino species by deprotonation of the parent amine with $Bu^{n}Li$. The *N*-silyl anilines were dissolved in petroleum and cooled to –78 °C. Vigorous stirring was required to prevent (**2.4**) from being precipitated out of solution at –78 °C. After addition of $Bu^{n}Li$ at –78 °C and stirring overnight at RT, the reactions produce the desired lithium amido/imino compounds, the bulk of which are precipitated out of solution. Since the compounds have partial solubility in petroleum, cooling the reaction mixture back to –78 °C before isolating them by filtration increases the isolated yield. Both the lithium trimethylsilylamido/imino (**2.3**) and lithium *tert*-butyldimethylsilylamido/imino (**2.5**) compounds were isolated as extremely air and moisture sensitive white, crystalline solids.

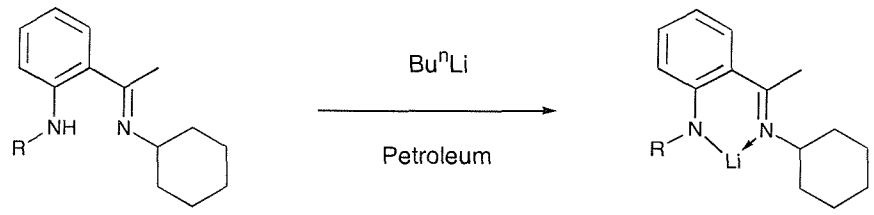

R=$SiMe_3$ (**2.3**); R=$SiMe_2Bu^t$ (**2.5**).

Scheme 2.9: Synthesis of lithium [2-(1-cyclohexylimino-ethyl)-*N*-(trimethylsilyl)-anilide] (**2.3**) and lithium [2-(1-cyclohexylimino-ethyl)-*N*-(*tert*-butyldimethylsilyl)-anilide] (**2.5**).

2.4.1 NMR spectroscopy for (2.3) and (2.5)

The ^1H and $^{13}C\{^1H\}$ NMR spectra of compounds (**2.3**) and (**2.5**) are very similar to those of their amine precursors (**2.2**) and (**2.4**). The one major difference is the absence of a peak assignable to the amine proton, which is therefore strong evidence that deprotonation has taken place. ^7Li NMR experiments on both compounds each gave rise to one lithium resonance at *ca.* 4 ppm (relative to LiCl).

Table 2.2: A comparison of selected ^1H, $^{13}C\{^1H\}$ and ^7Li NMR data for the compounds (**2.3**) and (**2.5**).[a]

Compound	**(2.3)**	**(2.5)**
Imine CH_3	2.23	2.30
$SiCH_3$	0.36	0.36
$SiC(CH_3)_3$	-	1.18
Cyclohexyl C*H*	3.56	3.62
Imine CH_3	20.29	20.26
$SiCH_3$	3.90	0.23
$SiC(CH_3)_3$	-	21.44
$SiC(CH_3)_3$	-	28.91
Cyclohexyl *C*H	61.15	60.90
Imine *C*=N	168.92	169.24
Li[b]	4.06	3.92

[a] Spectral data expressed in ppm; solvent = d^5-pyridine.

[b] Relative to LiCl in D_2O.

2.4.2 X-ray diffraction study on lithium [2-(1-cyclohexylimino-ethyl)-*N*-(trimethylsilyl)-anilide] (2.3)

X-ray diffraction quality crystals of (**2.3**) were grown by cooling a saturated petroleum solution to –30 °C to give the product as yellow prisms.

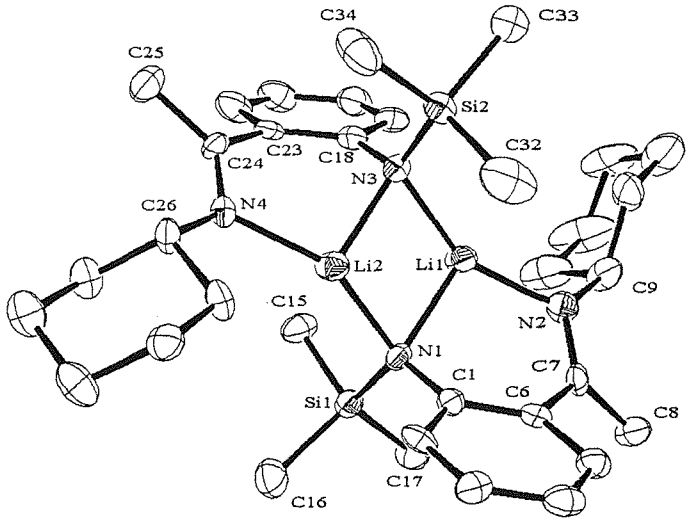

Figure 2.2: ORTEP representation of the crystal structure of lithium [2-(1-cyclohexylimino-ethyl)-*N*-(trimethylsilyl)-anilide] (**2.3**) (50% probability thermal ellipsoids). Hydrogens are omitted for clarity.

The molecule is a centrosymmetric dimer containing two amido/imino ligands that link the two lithium atoms *via* bridging amide nitrogens. Each lithium atom is also bound by an imine nitrogen, giving a coordination number of three. The central Li_2N_2 ring is almost planar with an inter-lithium distance of 2.415(9)Å. The Li-N(imine) [1.970(8) and 1.982(8)Å] and the Li-N(amide) [range 1.978(8)-1.997(8)Å, mean 1.987(16)Å] bond lengths are very similar, although normally the imine-lithium bond length would be expected to be longer than the amide-lithium bond. This may be due to the bridging nature of the amide groups in this compound.

The C=N bond length [1.280(5) and 1.287(5)Å] and the planar geometry about the imine bond suggests that the anionic charge of the amide group is not delocalised around the chelate ring of the ligand. It is therefore plausible that the benzene ring incorporated in the ligand backbone inhibits the delocalisation of the

negative charge of the amide group. This constitutes a difference between this ligand framework and the typical β-diketiminato ligands, where π-electron delocalisation results in equal bonds.[23]

The structure of **(2.3)** shares many characteristics with the structure of the lithium pyridyl-azaallyl compound $[Li\{N(SiMe_3)C(Bu^t)C(H)(C_5H_4N\text{-}2)\}]_2$ reported by Lappert.[20] This is also a centrosymmetric dimer with bridging trimethylsilylamides in which the lithium nitrogen bond to the neutral pyridyl nitrogen is shorter than the bonds to the amide nitrogen. The Li-N(amide) bond lengths [range 2.012(9)-2.032(6)Å] are close to those of **(2.3)**.

2.5 Synthesis of 2-(1-cyclohexyliminoalkyl)-*N*-(phenyl)-aniline compounds (2.6), (2.8) and (2.10)

Having observed the breaking of the nitrogen-silicon bond to give a zirconium imido complex whilst performing a transamination reaction between two equivalents of **(2.2)** and $Zr(NMe_2)_4$ (Chapter 3), it was decided to replace the silyl substituents with aryl groups. The phenyl group was chosen because:

(i) The nitrogen-carbon bond is stronger than the nitrogen-silicon bond.

(ii) It cannot be involved in elimination reactions giving rise to metal-ligand multiple bonds.

(iii) The second phenyl ring would adopt a conformation such that its plane would be perpendicular to that of the backbone phenyl ring, giving rise to different steric features. Once the ligand was complexed to a metal, depending on the substituents of the phenyl group, this could allow for steric blocking of the metal centre, in the space above and below the chelate ring of the ligand. This would be beneficial if the complexes proved to have potential as polymerisation catalysts, because the amide bound metal centre of the catalyst would be better protected from attack by other molecules.

The three ligands, 2-(1-cyclohexylimino-ethyl)-*N*-(3,5-dimethylphenyl)-aniline **(2.6)**, 2-(1-cyclohexylimino-ethyl)-*N*-(2,4,6-trimethylphenyl)-aniline **(2.8)** and 2-(cyclohexyliminomethyl)-*N*-(2,4,6-trimethylphenyl)-aniline **(2.10),** were synthesised using Buchwald-Hartwig palladium catalysed coupling of an aniline and an aryl-bromide (Schemes 2.10, 2.11, and 2.12). The less sterically hindered

3,5-dimethylphenyl-substituted aniline was synthesised using a palladium(0)-BINAP/NaOBu^t catalyst system.[16,17] The catalyst loading was 5 mol. % of both $Pd(dba)_2$ and *rac*-BINAP, with two equivalents of NaOBu^t as the base. The reaction was performed in xylenes at 140 °C, and was adjudged to be complete after five days by following with CI-GCMS. The product **(2.6)** was isolated as a bright yellow solid in high yield following two kugelrohr distillations. One distillation was necessary to remove the residual xylenes and the second to separate the product from involatile material.

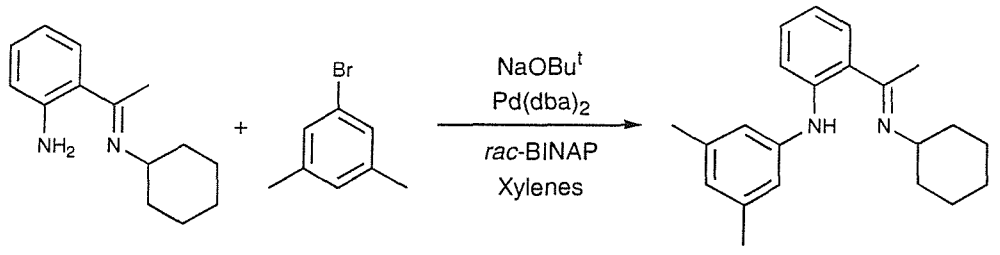

Scheme 2.10: Synthesis of 2-(1-cyclohexylimino-ethyl)-*N*-(3,5-dimethylphenyl)-aniline **(2.6)**.

Following the successful synthesis of **(2.6)** an attempt was made to synthesise the analogous 2,4,6-trimethylphenyl-substituted aniline. Using the same conditions as for the synthesis of **(2.6),** but employing 2,4,6-trimethylbromobenzene as the arylbromide, resulted in slow conversion of **(2.1)** to **(2.8)**. By following the reaction using CI-GCMS it was observed that complete conversion of 1 mmol of **(2.1)** took one week, too slow to be of synthetic use. The reason for this lower reactivity is possibly due to the increased steric demands of the mesityl group. The reaction was then tried with a palladium-carbene complex acting as the catalytically active species. Palladium-carbene complexes are conveniently generated *in situ* from a palladium(0) complex, an imidazolinium chloride and a base.[18,19] We employed a catalytic system that had already been studied ($Pd(dba)_2$, 1,3-bis-(2,6-diisopropyl-phenyl)-imidazolinium chloride and NaOBu^t) and we found it to be much quicker than the *rac*-BINAP system for the coupling of 2-(1-cyclohexylimino-ethyl)-aniline with 2,4,6-trimethylbromobenzene. Following some optimisation of the reaction conditions the catalyst loading employed was 0.75 mol. % of $Pd(dba)_2$ and 1.50 mol. % of the

imidazolinium chloride with 1.43 equivalents of $NaOBu^t$ as the base. Performing the reaction in 1,4-dioxane at 105 °C gave complete conversion in three days. Following an aqueous work up the compound was purified using the same method as (**2.6**) to yield 2-(1-cyclohexylimino-ethyl)-*N*-(2,4,6-trimethylphenyl)-aniline (**2.8**) as a viscous, bright yellow oil in high yield.

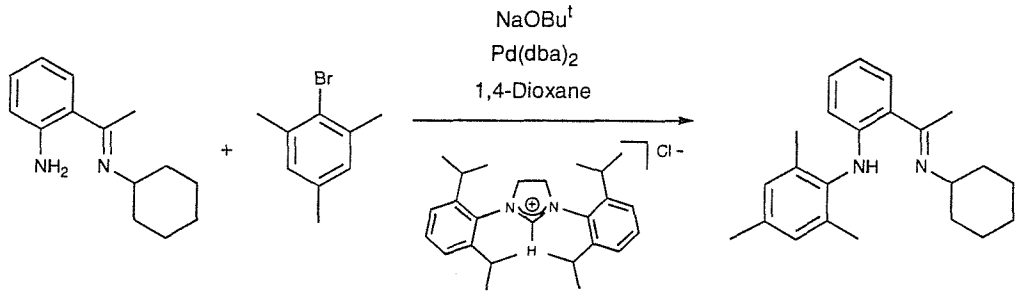

Scheme 2.11: Synthesis of 2-(1-cyclohexylimino-ethyl)-*N*-(2,4,6-trimethylphenyl)-aniline (**2.8**).

Following the synthesis of (**2.8**), further attempts were made to synthesise analogous amino/imino compounds with bulkier aryl substituents on the amino-nitrogen by utilising the $Pd(dba)_2$/imidazolinium chloride system. Coupling reactions of 2,4,6-triisopropylbromobenzene and 2,4,6-tri-*tert*-butylbromobenzene with (**2.1**) were unsuccessful. By following these reactions using CI-GCMS it was observed that a small trace of product was produced in the case of the reaction with 2,4,6-triisoproplybromobenzene. The reaction would not proceed any further despite performing the reaction with a higher catalyst loading. In the case of the reaction with 2,4,6-tri-*tert*-butylbromobenzene there was no trace of any product by GCMS. It is most likely that this lack of reactivity is attributable to the increased steric demands of the arylbromides.

Following the results obtained from the reactions of the amido/ketimino ligands with titanium and zirconium complexes, an effort was undertaken to synthesise the analogous amino/aldimino compound 2-cyclohexyliminomethyl-*N*-(2,4,6-trimethylphenyl)-aniline (**2.10**). This would have enabled us to investigate how the ligand behaviour differs depending on whether it contains an aldimino or a ketimino group. The $Pd(dba)_2$/imidazolinium chloride/$NaOBu^t$ catalyst system was also employed in attempts to couple 2,4,6-trimethylbromobenzene with

2-(cyclohexyliminomethyl)-aniline. All attempts to couple these two compounds failed. The reason for the failure to couple these two compounds is unclear given the relative ease with which (**2.6**) and (**2.8**) were prepared.

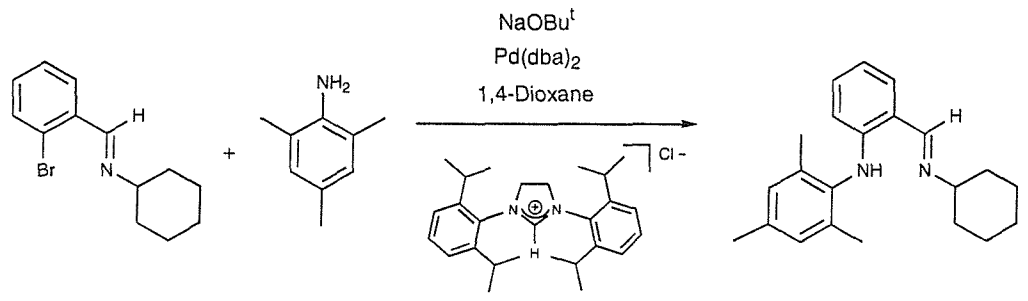

Scheme 2.12: Synthesis of 2-(cyclohexyliminomethyl)-*N*-(2,4,6-trimethylphenyl)-aniline (**2.10**).

The synthesis of (**2.10**) was then attempted by coupling 2-cyclohexyliminomethyl-bromobenzene with 2,4,6-trimethylaniline using the palladium-carbene catalyst. The small scale (2 mmol) reaction was adjudged to be complete after five days by CI-GCMS. The same work-up procedure that was employed in the synthesis of (**2.6**) and (**2.8**) afforded (**2.10**) as a yellow oil in good yield. The long reaction time and higher catalyst loading (5% $Pd(dba)_2$ and 10% imidazolinium chloride) meant that this method of was not practical for the large scale synthesis of (**2.10**). For metal complexation studies to be performed using (**2.10**) as a ligand, a faster and more efficient ligand synthesis needs to be developed.

2.5.1 NMR spectroscopy for (2.6), (2.8), and (2.10)

As with the *N*-silyl substituted amino/imino ligands (**2.2**) and (**2.4**) discussed above, a peak of high diagnostic value in the ^{1}H NMR spectra of these compounds is the low field resonance assignable to the amine proton. In the spectra of the silylamino/ketimino compounds the amine proton resonates at *ca.* 10 ppm in $CDCl_3$. In the spectra of the arylamino/ketimino compounds (**2.6**) and (**2.8**) it appears further downfield at 11.90 and 11.71 ppm, respectively. The amine proton of the arylamino/aldimino compound (**2.10**) resonates at 10.70 ppm, which is also

further downfield than its corresponding trimethylsilyl-substituted amino/imino derivative (9.9 ppm).[22]

Table 2.3: A comparison of selected ^{1}H and $^{13}C\{^{1}H\}$ NMR data for the compounds **(2.6)**, **(2.8)** and **(2.10)**.[a]

Compound	**(2.6)**	**(2.8)**	**(2.10)**
Imine CH_3	2.34	2.42	-
Imine *H*	-	-	8.47
Aryl CH_3[b]	2.32	2.23, 2.38	2.19, 2.35
Cyclohexyl *CH*	3.62	3.70	3.18
N*H*	11.90	11.71	10.70
Imine CH_3	16.59	15.22	-
Aryl CH_3[b]	22.12	18.43, 20.87	18.33, 20.91
Cyclohexyl *C*H	59.59	58.93	69.54
Imine *C*	165.80	165.23	161.50

[a] Spectral data expressed in ppm; solvent = $CDCl_3$.

[b] For **(2.8)** and **(2.10)** the first value given is that of the methyl group in the 4-position and the second value is that of the two methyl groups in the 2- and 6-positions.

Other characteristic peaks in the NMR spectra of **(2.6)** and **(2.8)** include the ketimino methyl group at *ca.* 2.3-2.4 ppm (^{1}H NMR spectra) and 15-17 ppm ($^{13}C\{^{1}H\}$ NMR spectra). There is no corresponding peak for **(2.10)** which has an aldimine proton, which gives rise to a peak at 8.47 ppm in the ^{1}H NMR spectrum. The methyl groups of the *N*-aryl group appear in the same region as the imino methyls. The two methyl substituents of the 3,5-dimethylphenyl group **(2.6)** appear as single resonances in both the proton and carbon NMR spectra whilst the three methyl groups of the mesityl ring in **(2.8)** and **(2.10)** appear as two signals in a 2:1 ratio. For **(2.6)** and **(2.8)** the methine CH of the cyclohexyl group appears in the same region as for the silyl-substituted compounds (between *ca.* 3.5 and 3.7 ppm). For **(2.10)** it appears further upfield at 3.18 ppm. The furthest downfield peak in the $^{13}C\{^{1}H\}$ NMR spectrum is due to the imine carbon. In the ketimine compounds **(2.6)** and **(2.8)** it appears at 165.80 and 165.23 ppm, respectively. In the aldimine group of **(2.10)** it is more upfield at 161.50 ppm.

2.6 Synthesis of lithium [2-(1-cyclohexylimino-alkyl)-*N*-(aryl)-anilide] compounds (2.7), (2.9) and (2.11)

The lithium amido/imino compounds (**2.7**), (**2.9**) and (**2.11**) were readily obtained in high yield by reaction of Bu^nLi with the amino/imino compounds (**2.6**), (**2.8**) and (**2.10**) (Scheme 2.13) following the same procedure as for (**2.3**) and (**2.5**). As with (**2.3**) and (**2.5**), the resulting lithium complexes have low solubility in petroleum and precipitate out of solution as the reaction progresses. Unlike (**2.3**) and (**2.5**), which are white solids, the lithium arylamido/imino compounds are brightly coloured. Compounds (**2.7**) and (**2.11**) are yellow whilst (**2.9**) is orange.

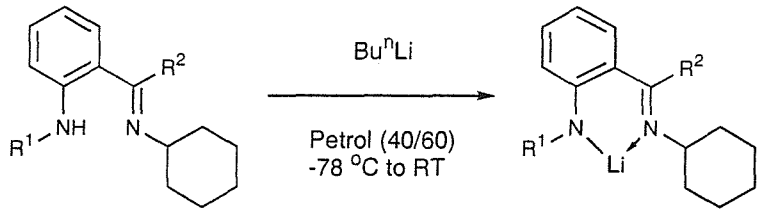

(**2.7**) R^1=xylyl, R^2=Me; (**2.9**) R^1=mesityl, R^2=Me; (**2.11**) R^1=mesityl, R^2=H.

Scheme 2.13: Synthesis of lithium [2-(1-cyclohexylimino-ethyl)-*N*-(3,5-dimethylphenyl)-anilide] (**2.7**), lithium [2-(1-cyclohexylimino-ethyl)-*N*-(2,4,6-trimethylphenyl)-anilide] (**2.9**) and lithium [2-(cyclohexyliminomethyl)-*N*-(2,4,6-trimethylphenyl)-anilide] (**2.11**).

2.6.1 NMR spectroscopy for compounds (2.7), (2.9) and (2.11)

The most diagnostic feature of the ^1H NMR spectra of (**2.7**), (**2.9**) and (**2.11**) is the absence of a peak assignable to an amine proton. This is strong evidence that deprotonation has occurred to give the amido/imino compounds. The spectra of the three lithium amido/imino compounds contain peaks assignable to the rest of the ligand backbone but shifted slightly relative to the parent amino/imino compounds. This evidence coupled with the observation that the reaction products are extremely air and moisture sensitive solids, strongly supports the conclusion that the isolated compounds are the proposed lithium amido/imino compounds.

The NMR spectra of (**2.7**) (solvent = C_6D_6) are surprisingly complicated when compared to those of (**2.9**) and (**2.11**) as well as to the lithium

silylamido/imino compounds. There is one major set of peaks in the ^{1}H and $^{13}C\{^{1}H\}$ NMR spectra corresponding to the anticipated lithium amide species. In addition, there are much less intense peaks in the same regions as the major peaks. This is also evident in a ^{7}Li NMR spectrum where a major peak at 1.77 ppm is accompanied by a smaller peak at 1.22 ppm. Similar pairing of peaks is observed in the ^{1}H NMR spectrum for the resonances assignable to a methine cyclohexyl proton α to the imino-nitrogen. The ratio of integrals of the major peaks to the minor peaks is *ca.* 4:1, which is in agreement with the ratio of the intensities of the two peaks in the ^{7}Li NMR spectrum. The minor peaks are not attributable to unreacted or reprotonated amine, but rather to different aggregation of the molecules in solution. A single crystal X-ray diffraction study on **(2.7)** (see below) yielded a trimeric structure, whereas **(2.3)** and **(2.9)** proved to have a dimeric structure in the solid state. It is possible that in the case of **(2.7)** in solution there is a mixture or equilibrium of dimers and trimers.

The position of peaks assignable to the ketimine methyl group, the methine cyclohexyl group and the imine carbon appear in similar positions for both **(2.7)** and **(2.9)** (Table 2.4). The spectra differ in the number of peaks present due to the aryl substituent of the amide group and the cyclohexyl ring. The methyls of the xylyl ring of **(2.7)** appear as two resonances in both the ^{1}H (2.00 and 2.57 ppm) and $^{13}C\{^{1}H\}$ (22.34 and 22.48 ppm) NMR spectra. The three aromatic protons appear as three singlets in the ^{1}H NMR spectrum (6.22, 6.26, 6.86 ppm), and there is a total of twelve peaks for the two phenyl rings in the $^{13}C\{^{1}H\}$NMR spectrum. This contrasts with **(2.9)**, where the three methyl groups of the mesityl ring give rise to only two peaks in a 2:1 ratio in both the ^{1}H (2.05 and 2.24 ppm) and $^{13}C\{^{1}H\}$ (19.83 and 21.61 ppm) NMR spectra. The two aromatic protons in the 3 and 5 positions of the mesityl ring appear as one peak at 6.77 ppm and there are only ten peaks in the $^{13}C\{^{1}H\}$ NMR spectrum assignable to the two phenyl rings. This suggests that the mesityl ring of **(2.9)** is freely rotating but the xylyl ring of **(2.7)** is not. The $^{13}C\{^{1}H\}$ NMR spectrum of **(2.7)** contains six peaks assignable to the cyclohexyl group whilst that of **(2.9)** contains only four, suggesting that two pairs of the carbons in the cyclohexyl group of **(2.9)** are rapidly interconverting, but not in **(2.7)**.

The ^{1}H NMR spectrum of **(2.11)** shows that the mesityl ring behaves in the same way as in **(2.9)** and appears to possess free rotation about the C-N bond. As

with the amino/imino compounds, the methine cyclohexyl proton is shifted *ca.* 0.4 ppm upfield relative to (**2.7**) and (**2.9**).

Table 2.4: A comparison of selected ^{1}H, $^{13}C\{^{1}H\}$ and ^{7}Li NMR data for the compounds (**2.7**), (**2.9**) and (**2.11**).[a]

Compound	**(2.7)**[b]	**(2.9)**	**(2.11)**
Imine CH_3	1.86	2.00	-
Imine *H*	-	-	8.06
Aryl CH_3[c]	2.00, 2.57	2.05, 2.24	2.11, 2.25
Cyclohexyl *CH*	2.95	3.06	2.67
Aryl aromatic *CH*	6.22, 6.26, 6.86	6.77	6.81
Imine CH_3	17.83	19.31	-
Aryl CH_3[c]	22.34, 22.48	19.83, 21.61	-
Cyclohexyl *C*H	61.09	61.10	-
Imine *C*	169.41	170.88	-
Li[d]	1.77	1.91	-

[a] Spectral data expressed in ppm; solvent = C_6D_6.

[b] The data reported here is that of the major species.

[c] For (**2.9**) and (**2.11**) the first value given is that of the two methyl groups in the 2- and 6-positions and the second value is that of the methyl group in the 4-position.

[d] Relative to LiCl in D_2O.

2.6.2 X-ray diffraction study on lithium [2-(1-cyclohexylimino-ethyl)-*N*-(3,5-dimethylphenyl)-anilide] (2.7)

X-ray diffraction quality crystals of (**2.7**) were obtained by cooling a saturated petroleum solution to –30 °C to give the compound as yellow blocks.

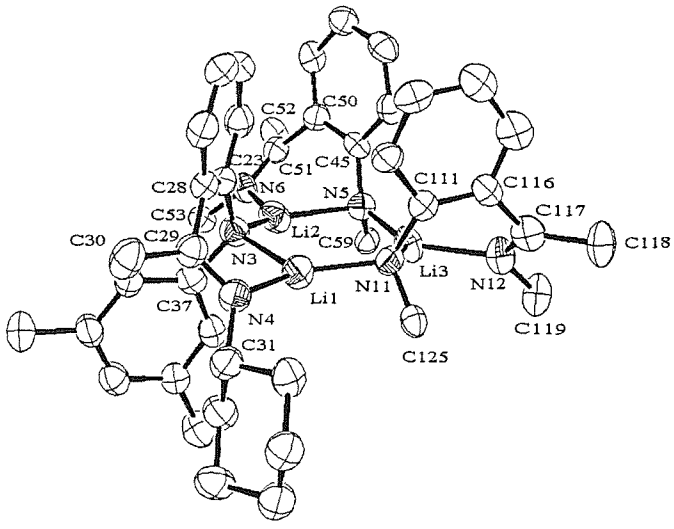

Figure 2.3: ORTEP representation of the crystal structure of lithium [2-(1-cyclohexylimino-ethyl)-*N*-(3,5-dimethylphenyl)-anilide] (**2.7**) (50% probability thermal ellipsoids). Two cyclohexyl rings [C(55)-(58) and C(120)-(124)] and two 3,5-dimethylphenyl groups [C(60)-(66) and C(126)-(132)] are omitted for clarity. Hydrogens are omitted for clarity.

The molecule exhibits a trimeric structure in which the three amido nitrogens and the three lithium atoms are located on the corners of a distorted cyclohexane chair conformer. The three amido/imino groups are arranged such that the three *ortho*-substituted phenyl rings that link the amide and imine moieties are located on one side of the near planar Li_3N_3 ring whilst the alternating cyclohexyl and xylyl rings are on the other, giving a "cisoid" arrangement. The lithium coordination sphere comprises two amide groups and one imine nitrogen giving three coordinate lithium environments. The Li-N(amide) bond lengths lie in the range 1.942(10)-2.048(10)Å and the Li-N(imine) bonds are between 2.026(10)-2.047(10)Å. Each amido nitrogen has one lithium bond shorter than the other [eg. Li(1)-N(3) 2.042(9)Å; Li(2)-N(3) 1.942(10)Å]. The longer bonds are those that are part of the amido/imino chelate rings. The Li-N bond lengths are similar to those observed in the dimeric structures of (**2.3**) and (**2.9**). The internal Li-N-Li angles [range 104.5(4)-109.3(4)°, mean 107.3(10)°] of the Li_3N_3 ring are smaller than the internal N-Li-N angles [range 126.9(5)-132.3(5)°, mean 129.6(12)°].

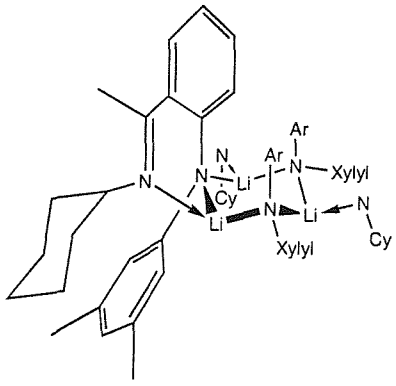

Figure 2.4: Schematic diagram representing the solid state structure of lithium [2-(1-cyclohexylimino-ethyl)-*N*-(3,5-dimethylphenyl)-anilide] (**2.7**).

The angles about the imine groups suggest a planar geometry and the C=N double bonds [range 1.269(6)-1.291(6)Å, mean 1.277(15)Å] lie in the normal range. The differences between the lengths of the C=N double bond and the C(aryl)-N(amide) single bond lengths [range 1.392(6)-1.405(6)Å, mean 1.397(15)Å] within the chelate rings suggests that the presence of the aryl group in the chelate ring of the ligand inhibits the delocalisation of the negative charge. This correlates with the behaviour of the lithium-silylamido/imino ligand (**2.3**) that was observed in the solid state.

Similar crystal structures containing a central Li_3N_3 ring display both planar and puckered geometries. The reported structure of the $Li(Me_2[9]aneN_3)$ trimer by Mountford[24] possesses a near planar Li_3N_3 ring in which the four coordinate Li atoms are each further bound by two amino nitrogens of the macrocyclic groups. As with (**2.7**), the Li-N-Li angles [range 101.75(14)-103.68(14)°] are smaller than the N-Li-N angles [range 135.27(17)-137.34(17)°]. Each Li atom possesses two inequivalent amide bonds, with the Li-N bond contained within the chelate of the macrocyclic ligand being longer than the Li-N bond to the second macrocycle [e.g. Li(1)-N(9) 2.030(3)Å; Li(1)-N(39) 1.977(3)Å], in an analogous fashion to (**2.7**).

A similarly planar Li_3N_3 ring is contained within the structure of the benzyl(trimethylsilyl)amidolithium trimer reported by Mulvey.[25] The amide substituents are arranged in a "cisoid" manner and there is an increased difference between the Li-N-Li bond angles [range 92.6(2)-94.8(2)°] and the N-Li-N angles [range 145.1(2)-147.0(2)°]. Due to the simple nature of the amido ligand it is not

capable of chelating and so the Li-N bond lengths are equivalent [range 1.940(4)-1.977(4)Å].

A pair of structures of C_3-chiral tripodal amido ligands reported by Gade[26] demonstrates puckered examples of Li_3N_3 rings. The structures of $HC\{SiMe_2N(Li)[(S)\text{-}1\text{-}phenylethyl]\}_3$ and $HC\{SiMe_2N(Li)[(R)\text{-}1\text{-}indanyl]\}_3$ possess a heteroadamantane core containing the Li_3N_3 ring. There is weak internal solvation of the Li atoms by the pendant aryl groups. The Li-N bond lengths lie in a similar range to those of (**2.7**). It is possible that the puckering of the Li_3N_3 ring is enhanced by the tripodal ligand architecture and the solvation by the aryl groups.

2.6.3 X-ray diffraction study on lithium [2-(1-cyclohexylimino-ethyl)-*N*-(2,4,6-trimethylphenyl)-anilide] (2.9)

X-ray diffraction quality crystals of (**2.9**) were obtained by cooling a saturated petroleum solution to –30 °C to give the compound as orange blocks.

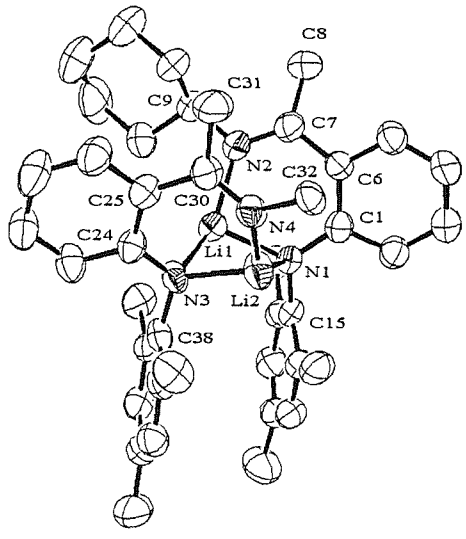

Figure 2.5: ORTEP representation of the crystal structure of lithium [2-(1-cyclohexylimino-ethyl)-*N*-(2,4,6-trimethylphenyl)-anilide] (**2.9**) (50% probability thermal ellipsoids). One cyclohexyl ring [C(33)-(37)] has been omitted for clarity. Hydrogens are omitted for clarity.

The molecule is dimeric with the amide nitrogens bridging the two lithium atoms to give an asymmetric puckered Li_2N_2 ring. Each lithium atom is further

coordinated to an imine nitrogen to give a lithium coordination number of three. The Li-N(amide) [1.924(8)-2.178(9)Å] and Li-N(imine) [1.952(8) and 1.974(9)Å] bond lengths are comparable to those observed for the dimer (**2.3**) and the trimer (**2.7**). As in the previous structures, (**2.9**) shows a planar geometry about the imino C=N bonds at 1.293(5) and 1.306(5)Å. As in the structure of (**2.7**), both amido nitrogens possess one Li-N bond shorter than the other [eg. Li(1)-N(1) 1.950(8)Å; Li(2)-N(1) 2.178(9)Å]. The difference between the two bond lengths is more pronounced in the structure of (**2.9**) than in (**2.7**). A significant difference is that in (**2.9**) it is the shorter Li-N(amide) bond that is part of the amido/imino chelate ring, whereas in (**2.7**) it is the longer bond that is contained in the chelate ring. The geometry of the dimer is different to that observed for (**2.3**). In (**2.9**) the Li_2N_2 ring is puckered, whereas in (**2.3**) it is observed to be almost planar. The dimeric structure of (**2.3**) is centrosymmetric while (**2.9**) features a "cisoid" arrangement, placing the two mesityl rings on the same side of the Li_2N_2 ring. The two aromatic rings are arranged "face to face" (see Fig. 2.5). It is possible that there is a π-stacking interaction that promotes this more sterically hindered conformation over that of the conformation displayed by the dimer in (**2.3**). This arrangement would seem to prohibit the free rotation of the mesityl rings as observed in the NMR data suggesting that this geometry is not adopted in solution.

Table 2.5: A comparison of selected structural data between the complexes (**2.7**) and (**2.9**).[a]

Compound	**(2.7)**	**(2.9)**
Li-N(amide) (shorter bond)[b]	1.952(24)	1.937(11)
Li-N(amide) (longer bond)[b]	2.038(23)	2.125(13)
Li-N(imine)	2.035(24)	1.963(12)
C=N	1.277(15)	1.300(7)
Li-Li (inter lithium distance)	3.213(30)	2.362(11)
N-Li-N (bite angle)	95.6(10)	96.7(6)
N-Li-N (amide nitrogens)	129.6(12)	101.0(6)
Li-N-Li	107.3(10)	71.0(4)

[a] Mean bond lengths in Å, mean angles in °.

[b] Each bridging amide possesses one N-Li bond shorter than the other.

2.7 Conclusions

The condensation reaction of *o*-aminoacetophenone with cyclohexylamine to afford 2-(1-cyclohexylimino-ethyl)-aniline (**2.1**) has been carried out in good yield. Two silyl-amino/imino compounds (**2.2**) and (**2.4**) were synthesised in high yield by the action of Bu^nLi on (**2.1**) and the subsequent quenching of the resultant lithium amide species with a chlorotrialkylsilane. The two corresponding lithium silylamido/imino compounds (**2.3**) and (**2.5**) were synthesised by deprotonating the secondary-amino moieties with Bu^nLi.

The primary amine of (**2.1**) was substituted with bulky aryl rings to give two arylamino/imino compounds (**2.6**) and (**2.8**). The new C-N bonds were formed using a palladium catalyst to couple (**2.1**) with the appropriate arylbromide. The coupling reaction proceeded in high yield although it was sensitive to the sterics of the arylbromide. The resultant arylamino/imino compounds were deprotonated with Bu^nLi to give the lithium amido/imino compounds (**2.7**) and (**2.9**).

All attempts to extend the palladium catalysed coupling to the reaction of the analogous aldimine-containing compound 2-cyclohexyliminomethyl-aniline with 2,4,6-trimethylbromobenzene were unsuccessful. It was however possible to couple 2-cyclohexyliminomethyl-bromobenzene with 2,4,6-trimethylaniline, but in a lower yield than that achieved with the ketimine containing compounds and with increased reaction times. The resultant arylamino/imino compound was deprotonated with Bu^nLi to give the corresponding lithium-arylamido/imino compound.

In conclusion, the methodology to synthesise a series of amino/ketimino ligands in high yield in which the amine nitrogen is substituted with either a trialkylsilyl group or an aryl ring has been developed. This seems to be complimentary to the method developed by Piers.[21] The corresponding lithium amido/imino compounds, which were obtained in high yield by reaction with Bu^nLi, show a remarkable structural diversity dependant on the size and nature of the *N*-substituent.

2.8 Experimental

The following compounds were prepared following literature methods: 1,3-bis-(2,6-diisopropyl-phenyl)-imidazolinium.[27]

2.8.1 2-(1-Cyclohexylimino-ethyl)-aniline (2.1).

2-Aminoacetophenone (10.0 g, 74.1 mmol) was dissolved in toluene (100 cm^3) and to the solution were added activated 4Å molecular sieves and cyclohexylamine (63 cm^3, 552 mmol). The resulting orange mixture was stirred at 100 °C in a closed vessel under reduced pressure for 4 days. After completion, filtration of the sieves and removal of the volatiles under reduced pressure gave a light brown solid, which was crystallised from petroleum as a white solid that was isolated, washed with cold petroleum and dried to yield **(2.1)**.

Yield: 10.12 g, 63%.

$\delta_H(CDCl_3)$ 1.25-1.90 (10H, m, cyclohexyl CH_2s), 2.30 (3H, s, imine CH_3), 3.58 (1H, tt, cyclohexyl CH α to imine N), 6.55 (2H, br s, NH_2), 6.65 (2H, m, aromatic), 7.10 (1H, dt, aromatic), 7.50 (1H, dd, aromatic).

$^{13}C\{^1H\}$ $\delta_C(CDCl_3)$ 16.26 (imine CH_3), 25.42, 26.52, 34.79 (cyclohexyl CH_2s), 59.80 (cyclohexyl CH α to imine N), 116.52, 117.52 (aromatic CHs), 122.20 (quaternary aromatic), 129.93, 130.37 (aromatic CHs), 148.82 (quaternary aromatic), 165.65 (ArC(Me)=N(Cy)).

2.8.2 2-(1-Cyclohexylimino-ethyl)-*N*-(trimethylsilyl)-aniline (2.2).

To a cooled (-78 °C), stirred solution of **(2.1)** (5.90 g, 27.3 mmol) in diethyl ether (150 cm^3), was added slowly *via* cannula Bu^nLi (12.3 cm^3 of 2.45 M solution in hexanes, 30 mmol). After complete addition, the bright yellow solution was stirred at –78 °C for 1h, allowed to reach room temperature and stirred for 2 h. Trimethylchlorosilane (3.8 cm^3, 30 mmol) was then added *via* syringe and the mixture was stirred for 15 h giving a light yellow suspension. Concentration to *ca.* 50 cm^3, followed by addition of petroleum (150 cm^3), filtration of the precipitated LiCl and removal of the volatiles under reduced pressure gave a dark orange oil which was purified by a vacuum distillation. The product was isolated as a bright yellow oil (b.p. 140 °C, 0.05 mm Hg).

Yield: 6.74 g, 86%.

$\delta_H(CDCl_3)$ 0.35 (9H, s, silyl C*H*$_3$Si), 1.10-1.90 (10H, m, cyclohexyl C*H*$_2$s), 2.32 (3H, s, imine C*H*$_3$), 3.60 (1H, tt, cyclohexyl C*H* α to imine N), 6.70 (1H, dt, aromatic), 6.83 (1H, dd, aromatic), 7.17 (1H, dt, aromatic), 7.54 (1H, dd, aromatic), 10.00 (1H, s, N*H*).

$^{13}C\{^1H\}$ $\delta_C(CDCl_3)$ 0.31 (silyl *C*H$_3$Si), 15.27 (imine *C*H$_3$), 24.91, 26.24, 35.08 (cyclohexyl *C*H$_2$s), 59.23 (cyclohexyl *C*H α to imine N), 115.72, 117.78 (aromatic *C*Hs), 122.86 (quaternary aromatic), 130.00, 130.23 (aromatic *C*Hs), 150.66 (quaternary aromatic), 165.95 (Ar*C*(Me)=N(Cy)).

2.8.3 Lithium [2-(1-cyclohexylimino-ethyl)-*N*-(trimethylsilyl)-anilide] (2.3).

To a cooled (-78 °C), stirred solution of **(2.2)** (4.58 g, 15.9 mmol) in petroleum (150 cm^3) was added slowly *via* cannula Bu^{n}Li (7.1 cm^3, of 2.45 M solution in hexanes, 17.5 mmol). The mixture was stirred at -78 °C for 1 h, allowed to reach room temperature and stirred for 15 h. This produced a light yellow suspension. From this the product was isolated by filtration as a white, extremely air sensitive solid (3.2 g), which was dried *in vacuo*. The mother liquor was reduced to *ca.* 30 cm^3 and cooled to -30 °C for 12 h giving a second crop (0.8 g). X-ray diffraction quality crystals were grown from a saturated petroleum solution of **(2.3)** that was cooled to -30 °C.

Yield: 4.0 g, 86%.

Mp: 223 °C (dec).

$\delta_H(C_6D_6)$ 0.06 (9H, s, silyl C*H*$_3$Si), 1.10-1.90 (10H, m, cyclohexyl C*H*$_2$s), 1.98 (3H, s, imine C*H*$_3$), 3.27-3.38 (1H, br t, cyclohexyl C*H* α to imine N), 6.82-6.88 (2H, m, aromatic), 7.21 (1H, dd, aromatic), 7.31 (1H, dd, aromatic).

$^{13}C\{^1H\}$ $\delta_C(C_6D_6)$ 1.78 (silyl *C*H$_3$Si), 19.56 (imine *C*H$_3$), 25.19, 25.25, 26.10, 34.38 (cyclohexyl *C*H$_2$s), 60.19 (cyclohexyl *C*H α to imine N), 117.22, 129.77, 129.91, 130.68 (aromatic *C*Hs), 130.75, 156.71 (quaternary aromatics), 170.12 (Ar*C*(Me)=N(Cy)).

δ_H(d^5-pyridine) 0.36 (9H, s, silyl C*H*$_3$Si), 1.10-2.00 (10H, m, cyclohexyl C*H*$_2$s), 2.23 (3H, s, imine C*H*$_3$), 3.56 (1H, br t, cyclohexyl C*H* α to imine N), 6.45 (1H, dt, aromatic), 7.17-7.23 (2H, m, aromatics), 7.29 (1H, dd, aromatics).

$^{13}C\{^1H\}$ δ_C(d^5-pyridine) 3.90 (silyl *C*H$_3$Si), 20.29 (imine *C*H$_3$), 26.00, 26.62, 34.79 (cyclohexyl *C*H$_2$s), 61.15 (cyclohexyl *C*H α to imine N), 109.42, 125.92,

129.48, 131.39 (aromatic *C*Hs), 131.94, 161.99 (quaternary aromatics), 168.92 (Ar*C*(Me)=N(Cy)).

δ_{Li}(d^5-pyridine) 4.06

Found: C, 68.5; H, 8.9; N, 12.5. $C_{17}H_{27}Li_1N_2Si_1$ requires C, 69.4; H, 9.2; N, 9.5%.

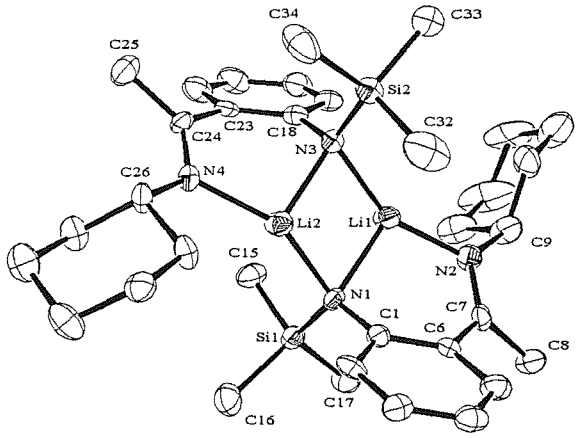

Figure 2.6: ORTEP representation of the crystal structure of lithium [2-(1-cyclohexylimino-ethyl)-*N*-(trimethylsilyl)-anilide] (**2.3**) (50% probability thermal ellipsoids). Hydrogens are omitted for clarity.

Table 2.6: Selected bond lengths (Å) and angles (°) for (**2.3**).

N(1)-Li(1)	1.989(8)	N(1)-Li(2)	1.982(8)
N(3)-Li(1)	1.978(8)	N(3)-Li(2)	1.997(8)
N(2)-Li(1)	1.970(8)	N(4)-Li(2)	1.982(8)
Li(1)-Li(2)	2.415(9)	N(1)-Si(1)	1.703(4)
N(1)-C(1)	1.407(5)	C(1)-C(6)	1.419(5)
C(6)-C(7)	1.491(5)	C(7)-N(2)	1.287(5)
C(7)-C(8)	1.517(6)	N(2)-C(9)	1.462(5)
N(3)-Si(2)	1.698(4)	N(3)-C(18)	1.404(6)
C(18)-C(23)	1.426(6)	C(23)-C(24)	1.484(6)
C(24)-N(4)	1.280(5)	C(24)-C(25)	1.510(6)
N(4)-C(26)	1.479(5)		
N(1)-Li(1)-N(2)	99.6(4)	N(1)-Li(1)-N(3)	105.4(3)
N(2)-Li(1)-N(3)	153.5(4)	N(3)-Li(2)-N(4)	97.4(3)
N(3)-Li(2)-N(1)	104.9(3)	N(4)-Li(2)-N(1)	152.1(4)
Li(1)-N(1)-Li(2)	74.9(3)	Li(1)-N(3)-Li(2)	74.8(3)
C(1)-N(1)-Si(1)	119.6(3)	Li(1)-N(1)-C(1)	102.5(3)

N(1)-C(1)-C(6)	123.7(6)	C(1)-C(6)-C(7)	124.3(4)
C(6)-C(7)-N(2)	119.2(4)	C(7)-N(2)-Li(1)	117.1(3)
C(6)-C(7)-C(8)	116.5(4)	C(8)-C(7)-N(2)	124.2(4)
C(7)-N(2)-C(9)	121.0(4)	C(9)-N(2)-Li(1)	119.6(4)
C(18)-N(3)-Si(2)	123.9(3)	Li(2)-N(3)-C(18)	102.5(3)
N(3)-C(18)-C(23)	123.9(3)	C(18)-C(23)-C(24)	123.2(4)
C(23)-C(24)-N(4)	119.1(4)	C(24)-N(4)-Li(2)	117.2(3)
C(23)-C(24)-C(25)	116.5(4)	C(25)-C(24)-N(4)	124.4(4)
C(24)-N(4)-C(26)	122.7(4)	C(26)-N(4)-Li(2)	117.3(3)

2.8.4 2-(1-Cyclohexylimino-ethyl)-*N*-(*tert*-butyldimethylsilyl)-aniline (2.4).

To a cooled (–78 °C), solution of **(2.1)** (4.00 g, 18.5 mmol) in diethyl ether (150cm^3), was added slowly *via* cannula Bu^{n}Li (8.3cm^3 of 2.45M solution in hexanes, 20.4 mmol). The mixture was then stirred at –78 °C for 1 h, allowed to reach room temperature and stirred for a further 2 h. To this, was added *via* cannula a solution of *tert*-butyldimethylchlorosilane (3.07 g, 20.4 mmol) in diethyl ether (20 cm^3) and stirring was continued for a further 15 h resulting in the formation of a brown solution and LiCl precipitate. The mixture was concentrated to *ca.* 50 cm^3 and petroleum (150 cm^3) was added to induce complete precipitation of LiCl. Filtration and removal of the volatiles *in vacuo* gave the product as a light brown solid.

Yield: 4.71 g, 77%.

$\delta_H(CDCl_3)$ 0.29 (6H, s, silyl C*H*$_3$S), 1.01 (9H, s, SiC(C*H*$_3$)$_3$), 1.2-1.9 (10H, m, cyclohexyl C*H*$_2$S), 2.31 (3H, s, imine C*H*$_3$), 3.55 (1H, tt, cyclohexyl C*H* α to imine N), 6.64 (1H, dt, aromatic), 6.83 (1H, dd, aromatic), 7.10 (1H, dt, aromatic), 7.50 (1H, dd, aromatic), 9.77 (1H, br. s, N*H*).

$^{13}C\{^1H\}$ $\delta_C(CDCl_3)$ -3.31 (silyl *C*H$_3$S), 16.49 (imine *C*H$_3$), 18.96 (Si*C*(CH$_3$)$_3$), 25.86, 26.52 (cyclohexyl *C*H$_2$S), 27.21 (SiC(*C*H$_3$)$_3$), 35.03 (cyclohexyl *C*H$_2$), 60.52 (cyclohexyl *C*H α to imine N), 115.93, 118.50 (aromatic *C*Hs), 123.23 quaternary aromatic), 130.15, 130.41 (aromatic *C*Hs), 150.65 (quaternary aromatic), 166.59 (Ar*C*(Me)=N(Cy)).

2.8.5 Lithium [2-(1-cyclohexylimino-ethyl)-*N*-(*tert*-butyldimethylsilyl)-anilide] (2.5).

To a cooled (–78 °C), stirred solution of **(2.4)** (2.74 g, 8.30 mmol) in petroleum (100cm^3) was slowly added *via* cannula Bu^{n}Li (3.6 cm^3 of 2.45M solution, 8.7 mmol). The mixture was stirred at –78 °C for 1 h, allowed to reach room temperature and stirred for 15 h. This produced a light yellow suspension. From this the product was isolated by filtration as a white, extremely air sensitive solid (1.7 g), which was dried *in vacuo*. The mother liquor was reduced to *ca.* 30 cm^3 and cooled to –30 °C for 12 h giving a second crop of **(2.5)** (0.5 g).

Yield 2.2 g, 79%.

Mp: 240 °C (dec).

$\delta_H(C_6D_6)$ -0.15 (3H, s, silyl C*H*$_3$) -0.08 (3H, s, silyl C*H*$_3$), 0.90 (9H, s, SiC(C*H*$_3$)$_3$) 1.1-2.2 (10H, m, cyclohexyl C*H*$_2$s), 1.95 (3H, s, imine C*H*$_3$), 3.29 (1H, br t, cyclohexyl C*H* α to imine N), 6.77 (1H, dt, aromatic), 7.10 (1H, dd, aromatic), 7.18 (1H, dd, aromatic), 7.24 (1h, dt, aromatic).

δ_H(d^5-pyridine) 0.36 (6H, s, silyl C*H*$_3$s), 1.18 (9H, s, SiC(C*H*$_3$)$_3$), 1.2-2.1 (10H, m, cyclohexyl C*H*$_2$s), 2.30 (3H, s, imine C*H*$_3$), 3.62 (1H, br t, cyclohexyl C*H* α to imine N), 6.46 (1H, t, aromatic), 7.16 (1H, dt, aromatic), 7.22-7.30 (2H, m, aromatics).

^{13}C{^{1}H} δ_C(d^5-pyridine) 0.23 (silyl *C*H$_3$s), 20.26 (imine *C*H$_3$), 21.44 (Si*C*(CH$_3$)$_3$), 25.99, 26.63 (cyclohexyl *C*H$_2$s), 28.91 (SiC(*C*H$_3$)$_3$), 34.5.06 (cyclohexyl *C*H$_2$), 60.90 (cyclohexyl *C*H α to imine N), 110.20, 127.73, 129.21, 130.81 (aromatic *C*Hs), 132.92, 161.92 (quaternary aromatics), 169.24 (Ar*C*(Me)=N(Cy)).

δ_{Li}(d^5-pyridine) 3.92

Found: C, 69.7; H, 9.5; N, 9.4. $C_{20}H_{33}Li_1N_2Si_1$ requires C, 71.4; H, 9.9; N, 8.3%.

2.8.6 2-(1-Cyclohexylimino-ethyl)-*N*-(3,5-dimethylphenyl)-aniline (2.6).

An ampoule was loaded with **(2.1)** (5.400 g, 25 mmol), NaOBu^t (4.805 g, 50.0 mmol), Pd(dba)$_2$ (0.718 g, 1.25 mmol) and *rac*-BINAP (0.778 g, 1.25 mmol). Xylenes (150 ml) were added before 3,5-dimethylbromobenzene (3.5 cm^3, 25.5 mmol) was added to the resulting suspension. The ampoule was closed under

reduced pressure and the mixture was stirred at 140 °C for 5 days. After cooling, the xylene solution was filtered and the volatiles removed *in vacuo* to yield a dark brown residue, which was dissolved in diethyl ether (50 ml) and extracted with water (3 x 50 ml). The organic extract was dried with $MgSO_4$ and the volatiles were removed *in vacuo*. The resulting dark brown residue was transferred to a kugelrohr and the product was distilled at 200 °C at 0.05 mm Hg to yield a bright yellow oil. Upon cooling to room temperature the oil solidified to yield (**2.6**) as a pale yellow solid.

Yield: 6.581 g, 82%.

Mp: 59-63 °C.

$\delta_H(CDCl_3)$ 1.00-1.95 (10H, m, cyclohexyl C*H*$_2$s), 2.32 (6H, s, xylyl C*H*$_3$s), 2.34 (3H, s, imine C*H*$_3$), 3.62 (1H, tt, cyclohexyl C*H* α to imine N), 6.65 (1H, s, xylyl aromatic), 6.78 (1H, t, aromatic), 6.87 (2H, s, xylyl aromatic), 7.20 (1H, t, aromatic), 7.44 (1H, d, aromatic), 7.59 (1H, d, aromatic), 11.90 (1H, br. s, N*H*).

$^{13}C\{^1H\}$ $\delta_C(CDCl_3)$ 16.59 (imine *C*H$_3$), 22.12 (xylyl *C*H$_3$s), 25.27, 26.48, 34.66 (cyclohexyl *C*H$_2$s), 59.59 (cyclohexyl *C*H α to imine N), 115.82, 117.57, 118.67 (aromatic *C*Hs), 123.80 (quaternary aromatic), 124.09, 130.17, 130.35 (aromatic *C*Hs), 139.50, 142.92, 145.61 (quaternary aromatics), 165.80 (Ar*C*(Me)=N(Cy)).

$\delta_H(C_6D_6)$ 1.10-1.80 (10H, m, cyclohexyl C*H*$_2$s), 1.85 (3H, s, imine C*H*$_3$), 2.13 (6H, s, xylyl C*H*$_3$s), 3.35 (1H, m, cyclohexyl C*H* α to imine N), 6.56 (1H, s, xylyl aromatic), 6.72 (1H, dt, aromatic), 7.07 (2H, s, xylyl aromatics), 7.09 (1H, dt, aromatic), 7.40 (1H, dd, aromatic), 7.64 (1H, dd, aromatic), 12.46 (1H, s, N*H*).

$^{13}C\{^1H\}$ $\delta_C(C_6D_6)$ 16.14 (imine *C*H$_3$), 22.15 (xylyl *C*H$_3$s), 25.40, 26.75, 34.96 (cyclohexyl *C*H$_2$s), 59.51 (cyclohexyl *C*H α to imine N), 116.12, 117.62, 119.87 (aromatic *C*Hs), 123.54 (quaternary aromatic), 124.91, 130.68, 130.89 (aromatic *C*Hs), 139.67, 143.54, 147.01 (quaternary aromatics), 166.16 (Ar*C*(Me)=N(Cy)).

Found: C, 81.8; H, 8.6; N, 8.2. $C_{22}H_{28}N_2$ requires C, 82.5; H, 8.8; N, 8.7%.

2.8.7 Lithium [2-(1-cyclohexyliminolethyl)-*N*-(3,5-dimethylphenyl)-anilide] (2.7).

To a cooled (-78 °C), stirred solution of (**2.6**) (6.581 g, 20.57 mmol) in petroleum (100 cm^3), was added slowly *via* cannula Bu^nLi (9.3 cm^3 of 2.45 M solution in hexanes, 22.6 mmol). The mixture was stirred at –78 °C for 1 h, allowed to reach room temperature and stirred for 15 h. This produced an orange/yellow suspension. The solid was isolated by filtration and dried *in vacuo* to yield (**2.7**) as an orange, air sensitive solid. The mother liquor was cooled to -30 °C to yield a second crop of (**2.7**) as yellow, X-ray diffraction quality crystals.

Yield: 5.50 g, 82%.

Mp: 285 °C (dec).

Major product:

$\delta_H(C_6D_6)$ 0.65-1.75 (10H, m, cyclohexyl C*H*$_2$s), 1.86 (3H, s, imine C*H*$_3$), 2.00 (3H, s, xylyl C*H*$_3$), 2.57 (3H, s, xylyl C*H*$_3$), 2.85-3.05 (1H, m, cyclohexyl C*H* α to imine N), 6.10 (1H, d, aromatic), 6.22 (1H, s, xylyl aromatic), 6.26 (1h, s, xylyl aromatic), 6.82 (1H, t, aromatic), 6.86 (1H, s, xylyl aromatic), 6.95 (1H, dt, aromatic), 7.04 (1H, dd, aromatic).

$^{13}C\{^1H\}$ $\delta_C(C_6D_6)$ 17.83 (imine *C*H$_3$), 22.34, 22.48 (xylyl *C*H$_3$s), 25.71, 26.08, 26.39, 32.92, 33.51 (cyclohexyl *C*H$_2$s), 61.09 (cyclohexyl *C*H α to imine N), 112.38, 116.49, 117.40, 120.02, 128.07, 129.04, 132.03 (aromatic *C*Hs), 136.42, 139.93, 139.95, 152.89, 159.87 (quaternary aromatics), 169.41 (Ar*C*(Me)=N(Cy)).

$\delta_{Li}(C_6D_6)$ 1.77.

Minor peaks:

$\delta_H(C_6D_6)$ 1.76 (s), 1.83 (s), 1.92 (s), 1.94 (s), 1.96 (s), 1.98 (s), 2.02 (s), 2.59 (s, C*H*$_3$s), 2.75-2.88 (m, cyclohexyl C*H* α to imine N), 6.12 (d), 6.19 (t), 6.37 (s), 6.41 (s), 7.14 (t), 7.44 (m), 7.59 (t), 7.76 (d, aromatics).

$^{13}C\{^1H\}$ $\delta_C(C_6D_6)$ 18.12, 21.79, 21.91, 22.42 (*C*H$_3$s), 26.48, 26.63, 26.70, 31.66, 32.14, 32.83, 33.42 (cyclohexyl *C*H$_2$s), 61.17, 61.27 (cyclohexyl *C*Hs α to imine N), 111.68, 111.81, 113.60, 114.69, 115.86, 117.20, 118.03, 118.23, 119.66, 119.90, 128.21, 129.44, 129.53, 129.82, 130.22, 131.55, 131.60 (aromatic *C*Hs), 136.06, 136.24, 136.63, 139.53, 141.60, 141.73, 142.32, 142.86, 157.70, 158.57, 159.27, 169.49, 169.95, 170.08 (quaternary aromatics and Ar*C*(Me)=N(Cy)).

$\delta_{Li}(C_6D_6)$ 1.22.

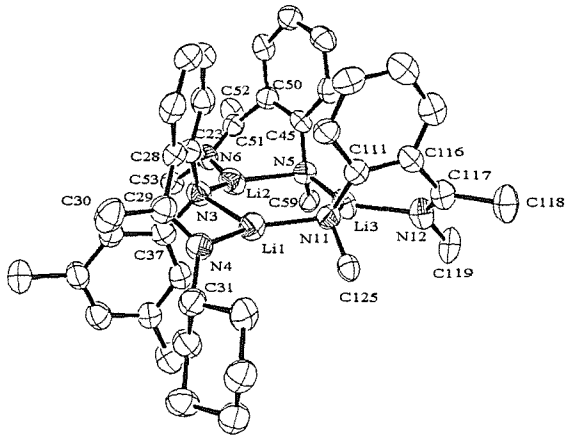

Figure 2.7: ORTEP representation of the crystal structure of lithium [2-(1-cyclohexylimino-ethyl)-*N*-(3,5-dimethylphenyl)-anilide] **(2.7)** (50% probability thermal ellipsoids). Two cyclohexyl rings [C(55)-(58) and C(120)-(124)] and two 3,5-dimethylphenyl groups [C(60)-(66) and C(126)-(132)] are omitted for clarity. Hydrogens are omitted for clarity.

Table 2.7: Selected bond lengths (Å) and angles (°) for **(2.7)**.

Li(1)-N(11)	1.943(9)	Li(1)-N(3)	2.042(9)
Li(1)-N(4)	2.029(10)	Li(2)-N(3)	1.942(10)
Li(2)-N(6)	2.037(10)	Li(2)-N(5)	2.037(10)
Li(3)-N(5)	1.946(10)	Li(3)-N(11)	2.038(9)
Li(3)-N(12)	2.036(10)	Li(1)-Li(2)	3.233(12)
Li(1)-Li(3)	3.181(12)	Li(2)-Li(3)	3.195(13)
N(3)-C(37)	1.390(6)	N(3)-C(23)	1.394(6)
N(4)-C(29)	1.275(6)	N(4)-C(31)	1.465(6)
N(5)-C(59)	1.398(6)	N(5)-C(45)	1.392(6)
N(6)-C(51)	1.269(6)	N(6)-C(53)	1.469(6)
N(11)-C(125)	1.379(6)	N(11)-C(111)	1.405(6)
N(12)-C(117)	1.291(6)	N(12)-C(119)	1.467(7)
C(23)-C(28)	1.425(7)	C(28)-C(29)	1.490(8)
C(29)-C(30)	1.520(7)	C(45)-C(50)	1.416(7)
C(50)-C(51)	1.481(7)	C(51)-C(52)	1.515(7)
C(111)-C(116)	1.419(7)	C(116)-C(117)	1.492(7)
C(117)-C(118)	1.518(7)		
N(3)-Li(1)-N(11)	128.0(5)	N(3)-Li(2)-N(5)	129.1(5)
N(5)-Li(3)-N(11)	130.6(5)	Li(1)-N(3)-Li(2)	108.5(4)

Li(2)-N(5)-Li(3)	106.7(4)	Li(3)-N(11)-Li(1)	106.0(4)
N(3)-Li(1)-N(4)	96.8(4)	N(5)-Li(2)-N(6)	96.2(4)
N(11)-Li(3)-N(12)	94.3(4)	C(37)-N(3)-C(23)	121.4(5)
N(3)-C(23)-C(28)	125.5(5)	C(23)-C(28)-C(29)	122.8(5)
C(28)-C(29)-N(4)	119.1(5)	C(28)-C(29)-C(30)	116.8(5)
C(30)-C(29)-N(4)	124.1(5)	C(29)-N(4)-Li(1)	111.2(5)
C(29)-N(4)-C(31)	121.2(5)	C(31)-N(4)-Li(1)	126.7(5)
C(59)-N(5)-C(45)	121.1(4)	N(5)-C(45)-C(50)	124.3(5)
C(45)-C(50)-C(51)	123.3(5)	C(50)-C(51)-N(6)	117.3(5)
C(50)-C(51)-C(52)	117.6(5)	C(52)-C(51)-N(6)	125.1(5)
C(51)-N(6)-Li(2)	113.1(4)	C(51)-N(6)-C(53)	121.7(4)
C(53)-N(6)-Li(2)	123.2(4)	C(125)-N(11)-C(111)	120.5(4)
N(11)-C(111)-C(116)	124.7(5)	C(111)-C(116)-C(117)	122.5(5)
C(116)-C(117)-N(12)	118.3(5)	C(116)-C(117)-C(118)	116.0(5)
C(118)-C(117)-N(12)	125.6(5)	C(117)-N(12)-Li(3)	114.2(5)
C(117)-N(12)-C(119)	122.1(5)	C(119)-N(12)-Li(3)	122.9(4)

2.8.8 2-(1-Cyclohexylimino-ethyl)-*N*-(2,4,6-trimethylphenyl)-aniline (2.8).

An ampoule was loaded with **(2.1)** (8.600 g, 39.8 mmol), $NaOBu^t$ (5.500 g, 57.0 mmol), $Pd(dba)_2$ (0.172 g, 0.30 mmol), and 1,3-bis-(2,6-diisopropyl-phenyl)-imidazolinium chloride (0.256 g, 0.60 mmol). 1,4-Dioxane (75 cm^3) was added before 2,4,6-trimethylbromobenzene (6.70 cm^3, 43.8 mmol) was added to the resulting suspension. The ampoule was closed under reduced pressure and stirred at 105 °C for 3 days. After cooling, the solution was diluted with water (100 cm^3) and extracted with diethyl ether (3 x 100 ml). The organic extracts were combined and washed with a saturated brine solution before being dried with $MgSO_4$. The volatiles were then removed *in vacuo* to yield a brown residue, which was transferred to a kugelrohr. The product was distilled at 250 °C at 0.05 mm Hg and **(2.8)** was isolated as a bright yellow oil.

Yield: 10.99 g, 83%.

$\delta_H(CDCl_3)$ 1.20-1.95 (10H, m, cyclohexyl CH_2s), 2.24 (6H, s, mesityl CH_3s), 2.38 (3H, s, mesityl CH_3), 2.42 (3H, s, imine CH_3), 3.69 (1H, tt, cyclohexyl CH α to imine N), 6.27 (1H, d, aromatic), 6.67 (1H, t, aromatic), 7.02 (2H, s, mesityl aromatics), 7.10 (1H, t, aromatic), 7.66 (1H, d, aromatic), 11.71 (1H, br. s, N*H*).

$^{13}C\{^1H\}$ $\delta_C(CDCl_3)$ 15.22 (imine CH_3), 18.43, 20.87 (mesityl CH_3s), 24.68, 25.78, 34.23 (cyclohexyl CH_2s), 58.93 (cyclohexyl CH α to imine N), 112.28, 114.42 (aromatic CHs), 119.82 (quaternary aromatic), 128.88, 129.36, 130.01 (aromatic CHs), 134.82, 136.03, 136.18, 148.11 (quaternary aromatics), 165.23 (ArC(Me)=N(Cy)).

$\delta_H(C_6D_6)$ 1.05-1.80 (10H, m, cyclohexyl CH_2s), 1.91 (3H, s, CH_3), 2.19 (3H, s, CH_3), 2.29 (6H, s, mesityl CH_3s), 3.40 (1H, tt, cyclohexyl C*H* α to imine N), 6.53 (1H, dd, aromatic), 6.67 (1H, dt, aromatic), 6.88 (2H, s, mesityl aromatics), 7.05 (1H, dt, aromatic), 7.46 (1H, dd, aromatic), 12.05 (1H, s, N*H*).

$^{13}C\{^1H\}$ $\delta_C(C_6D_6)$ 15.67 (imine *C*H_3), 19.41, 21.68 (mesityl *C*H_3s), 25.53, 26.66, 35.15 (cyclohexyl *C*H_2s), 59.58 (cyclohexyl *C*H α to imine N), 113.45, 115.72 (aromatic *C*Hs), 120.96 (quaternary aromatic), 130.22, 130.68, 131.39 (aromatic *C*Hs), 135.70, 136.83, 137.39, 149.66 (quaternary aromatics), 166.60 (Ar*C*(Me)=N(Cy)).

2.8.9 Lithium [2-(1-cyclohexylimino-ethyl)-*N*-(2,4,6-trimethylphenyl)-anilide] (2.9).

To a cooled (-78 °C), stirred solution of **(2.8)** (5.630 g, 16.83 mmol) in petroleum (150 cm^3) was added slowly *via* cannula Bu^nLi (7.40 cm^3 of 2.45 M solution in hexanes, 18.13 mmol). The mixture was stirred at –78 °C for 1 h, allowed to reach room temperature and stirred for 17 h. This produced a bright orange suspension in a bright red solution. The product was isolated by filtration, washed with petrol (30 cm^3) and dried *in vacuo* to yield **(2.9)** as an orange, air sensitive solid. The mother liquor was cooled to –30 °C to yield a second crop of **(2.9)** as orange, X-ray diffraction quality crystals.

Yield: 4.25 g, 74%.

Mp: 167-170 °C.

$\delta_H(C_6D_6)$ 0.80-1.65 (10H, m, cyclohexyl CH_2s), 2.00 (3H, s, imine CH_3), 2.05 (6H, s, mesityl CH_3s), 2.24 (3H, s, mesityl CH_3), 3.06 (1H, br t, cyclohexyl C*H* α to imine N), 6.48 (1H, dt, aromatic), 6.61 (1H, br d, aromatic), 6.77 (2H, s, mesityl aromatics), 6.96 (1H, dt, aromatic), 7.41 (1H, br d, aromatic).

$^{13}C\{^1H\}$ $\delta_C(C_6D_6)$ 19.31 (imine *C*H_3), 19.83 (mesityl *C*H_3s), 21.61 (mesityl *C*H_3), 26.25, 26.33, 35.06 (cyclohexyl *C*H_2s), 61.10 (cyclohexyl *C*H α to imine N), 112.54, 120.74 (aromatic *C*Hs), 124.74, 130.17 (quaternary aromatics), 130.72 (aromatic *C*H), 131.60 (mesityl aromatic *C*Hs), 132.50 (quaternary aromatic), 132.90 (aromatic *C*H), 152.37, 159.05 (quaternary aromatics), 170.88 (Ar*C*(Me)=N(Cy)).

$\delta_{Li}(C_6D_6)$ 1.91

Found: C, 80.3; H, 8.6, 7.8. $C_{23}H_{29}LiN_2$ requires C, 81.2; H, 8.6; N, 8.2%.

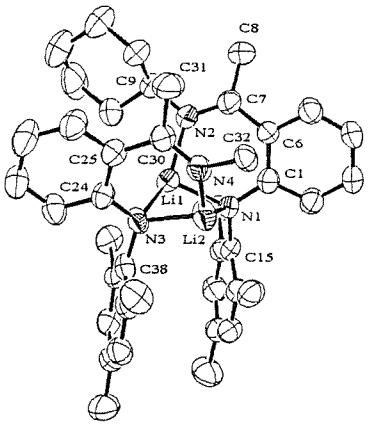

Figure 2.8: ORTEP representation of the crystal structure of lithium [2-(1-cyclohexylimino-ethyl)-*N*-(2,4,6-trimethylphenyl)-anilide] **(2.9)** (50% probability thermal ellipsoids). One cyclohexyl ring [C(33)-(37)] has been omitted for clarity. Hydrogens are omitted for clarity.

Table 2.8: Selected bond lengths (Å) and angles (°) for **(2.9)**.

Li(1)-N(1)	1.950(8)	Li(1)-N(3)	2.071(9)
Li(2)-N(1)	2.178(9)	Li(2)-N(3)	1.924(8)
Li(1)-N(2)	1.952(8)	Li(2)-N(4)	1.974(9)
Li(1)-Li(2)	2.362(11)	N(1)-C(15)	1.429(5)
N(1)-C(1)	1.389(5)	N(2)-C(7)	1.306(5)
N(2)-C(9)	1.472(5)	N(3)-C(38)	1.432(5)
N(3)-C(24)	1.371(5)	N(4)-C(30)	1.293(5)
N(4)-C(32)	1.474(5)	C(1)-C(6)	1.435(6)
C(6)-C(7)	1.487(6)	C(7)-C(8)	1.516(6)
C(24)-C(25)	1.428(6)	C(25)-C(30)	1.493(6)
C(30)-C(31)	1.524(6)		
N(1)-Li(1)-N(3)	102.4(4)	N(1)-Li(2)-N(3)	99.5(4)
Li(1)-N(1)-Li(2)	69.6(3)	Li(1)-N(3)-Li(2)	72.4(3)
N(1)-Li(1)-N(2)	96.9(4)	N(3)-Li(2)-N(4)	96.4(4)
C(15)-N(1)-C(1)	118.7(3)	Li(1)-N(1)-C(1)	122.6(3)
N(1)-C(1)-C(6)	122.4(4)	C(1)-C(6)-C(7)	125.4(4)
C(6)-C(7)-N(2)	122.1(4)	C(6)-C(7)-C(8)	115.4(4)
C(8)-C(7)-N(2)	122.5(4)	C(7)-N(2)-Li(1)	125.1(4)
C(7)-N(2)-C(9)	118.7(4)	C(9)-N(2)-Li(1)	115.7(3)
C(38)-N(3)-C(24)	116.0(3)	Li(2)-N(3)-C(24)	122.5(4)
N(3)-C(24)-C(25)	122.8(4)	C(24)-C(25)-C(30)	125.3(4)

C(25)-C(30)-N(4)	121.0(4)	C(25)-C(30)-C(31)	116.6(4)
C(31)-C(30)-N(4)	122.2(4)	C(30)-N(4)-Li(2)	121.3(4)
C(30)-N(4)-C(32)	120.2(4)	C(32)-N(4)-Li(2)	115.5(4)

Table 2.9: Crystallographic parameters for **(2.3)**, **(2.7)** and **(2.9)**.

Compound	**(2.3)**	**(2.7)**	**(2.9)**
Chemical Formula	$C_{34}H_{54}Li_2N_4Si_2$	$C_{66}H_{81}Li_3N_6$	$C_{46}H_{58}Li_2N_4$
Formula Weight	588.87	979.19	680.84
Crystal System	Orthorhombic	Triclinic	Orthorhombic
Space Group	*Pna2₁*	*P-1*	*Pbca*
a/Å	30.959(6)	13.9493(8)	14.6329(7)
b/Å	9.919(2)	19.9645(8)	17.3919(7)
c/Å	11.8838(4)	23.3181(15)	31.7930(18)
α/°	90.0	109.670(2)	90.0
β/°	90.0	104.223(2)	90.0
γ/°	90.0	90.457(4)	90.0
V/Å^3	3649.4(10)	5898.2(6)	8091.1(7)
Z	4	4	8
T/K	150	120	120
μ/mm^{-1}	0.124	0.063	0.064
F(000)	1280	2112	2944
No. Data collected	17720	35444	11147
No. Unique data	4403	11225	5978
R_{int}	0.1083	0.1188	0.0902
Final $R(\|F\|)$ for $I>2\sigma(I)$	0.0482	0.0751	0.0848
Final $R(F^2)$ for all data	0.1002	0.1793	0.1968

2.8.10 2-(Cyclohexyliminomethyl)-*N*-(2,4,6-trimethylphenyl)-aniline (2.10).

An ampoule was loaded with [*o*-(cyclohexyl)iminomethyl]-bromobenzene (0.532 g, 2.0 mmol), NaOBu^t (0.28 g, 3.0 mmol), Pd(dba)$_2$ (0.057 g, 0.10 mmol), and 1,3-bis-(2,6-diisoproply-phenyl)-imidazolinium chloride (0.085 g, 0.20 mmol). 1,4-Dioxane (20 cm^3) was added before 2,4,6-trimethylaniline (0.31 cm^3, 2.2 mmol) was added to the resulting suspension. The ampoule was closed under reduced pressure and stirred at 105 °C for 5 days. After cooling, the solution was diluted with water (20 cm^3) and extracted with diethyl ether (3 x 30 ml). The organic extracts were combined and washed with a saturated brine solution before being dried with $MgSO_4$. The volatiles were then removed *in vacuo* to yield a brown residue, which was transferred to a kugelrohr. The product was distilled from the residue at 250 °C at 0.05 mm Hg to yield **(2.10)** as a dark yellow oil.

Yield: 0.435 g, 68%.

$\delta_H(CDCl_3)$ 1.1-1.9 (10H, m, cyclohexyl C*H*$_2$s), 2.19 (6H, s, mesityl C*H*$_3$s), 2.35 (3H, s, mesityl C*H*$_3$), 3.18 (1H, br t, cyclohexyl C*H* α to imine N), 6.23 (1H, dd, aromatic), 6.67 (1H, dt, aromatic), 6.99 (2H, s, mesityl aromatics), 7.11 (1H, dt, aromatic), 7.27 (1H, dd, aromatic), 8.47 (1H, s, (ArC(*H*)=N(Cy)), 10.70 (1H, s, N*H*).

$^{13}C\{^1H\}$ $\delta_C(CDCl_3)$ 18.33, 20.91 (mesityl *C*H$_3$s), 24.56, 25.74, 34.83 (cyclohexyl *C*H$_2$s), 69.54 (cyclohexyl *C*H α to imine N), 111.38, 114.95 (aromatic *C*Hs), 117.32 (quaternary aromatic), 128.93 (mesityl aromatic *C*Hs), 130.66, 133.32 (aromatic *C*Hs), 135.36, 135.71, 136.28, 147.97 (quaternary aromatics), 161.50 (Ar*C*(H)=N(Cy).

2.8.11 Lithium-[(2-cyclohexyliminomethyl)-*N*-(2,4,6-trimethylphenyl)-anilide] (2.11).

To a stirred, cooled (-78 °C) solution of **(2.10)** (0.40 g, 1.25 mmol) in petroleum (30 cm^3) was added slowly *via* cannula Bu^{n}Li (0.60 cm^3 of 2.45 M solution in hexanes, 1.5 mmol). The mixture was stirred at –78 °C for 1 h, allowed to reach room temperature and stirred for 17 h. This produced a yellow suspension that was isolated by filtration to yield **(2.11)** as a yellow solid.

Yield: 0.258 g, 64%.

$\delta_H(C_6D_6)$ 0.7-1.7 (10H, m, cyclohexyl C*H*$_2$s), 2.11 (6H, s, mesityl C*H*$_3$s), 2.25 (3H, s, mesityl C*H*$_3$), 2.67 (1H, br t, cyclohexyl C*H* α to imine N), 6.35-6.55 (2H, m, aromatics), 6.81 (2H, s, mesityl aromatics), 7.02 (1H, t, aromatic), 7.22 (1H, d, aromatic), 8.06 (1H, s, (ArC(*H*)=N(Cy)).

2.9 References

1. L. H. Gade, *Chem. Commun.*, 2000, 173.
2. L. H. Gade, *Angew. Chem. Int. Ed.*, 2000, **39**, 2658.
3. R. Kempe, *Angew. Chem. Int. Ed.*, 2000, **39**, 468.
4. V. C. Gibson, S. K. Spitzmesser, *Chem. Rev.*, 2003, **103**, 283.
5. G. J. P. Britovsek, V. C. Gibson, D. F. Wass, *Angew. Chem. Int. Ed.*, 1999, **38**, 428.
6. Y. Suzuki, H. Terao, T. Fujita, *Bull. Chem. Soc. Jpn.*, 2003, **76**, 1493.
7. G. W. Coates, P. D. Hustad, S. Reinartz, *Angew. Chem. Int. Ed.*, 2002, **41**, 2236.

8. C. Weymann, A. A. Danopoulos, G. Wilkinson, T. K. N. Sweet, M. B. Hursthouse, *Polyhedron,* 1996, **15**, 3605.
9. J. F. Hartwig, *Angew. Chem. Int. Ed.,* 1998, **37**, 2046.
10. M. Kosugi, M. Kameyama, T. Migita, *Chem. Lett.*, 1983, 927.
11. J. Louie, J. F. Hartwig, *Tetrahedron Lett.,* 1995, **36**, 3609.
12. A. S. Guram, R. A. Rennels, S. L. Buchwald, *Angew. Chem. Int. Ed. Engl.,* 1995, **34**, 1348.
13. J. F. Hartwig, S. Richards, D. Barañano, F. Paul, *J. Am. Chem. Soc.*, 1996, **118**, 3626.
14. U. K. Singh, E. R. Strieter, D. G. Blackmond, S. L. Buchwald, *J. Am. Chem. Soc.*, 2002, **124**, 14104.
15. M. S. Driver, J. F. Hartwig, *J. Am. Chem. Soc.*, 1996, **118**, 7217.
16. J. P. Wolfe, S. Wagaw, S. L. Buchwald, *J. Am. Chem. Soc.*, 1996, **118**, 7215.
17. J. P. Wolfe, S. L. Buchwald, *J. Org. Chem.,* 2000, **65**, 1144.
18. J. Huang, G. Grasa, S. P. Nolan, *Org. Lett.,* 1999, **1**, 1307.
19. S. R. Stauffer, S. Lee, J. P. Stambuli, S. L. Hauck, J. F. Hartwig, *Org. Lett.,* 2000, **2**, 1423.
20. B.–J. Deelman, M. F Lappert, H.-K Lee, T. C. W. Mak, W.-P Leung, P.-R. Wei, *Organometallics*, 1997, **16**, 1247.
21. P. G. Hayes, G. C. Welch, D. J. H. Emslie, C. L. Noack, W. E. Piers, M. Parvez, *Organometallics*, 2003, **22**, 1577.
22. R. M. Porter, S. Winston, A. A. Danopoulos, M. B. Hursthouse, *J. Chem. Soc., Dalton Trans.,* 2002, 3290.
23. M. Stender, R. J. Wright, B. E. Eichler, J. Prust, M. M. Olmstead, H. W. Roesky, P. P. Power, *J. Chem. Soc., Dalton Trans.*, 2001, 3465.
24. S. R. Dubberley, P. Mountford, N. Adams, *Acta Cryst.*, 2002, **E58**, m342.
25. D. R. Armstrong, D. R. Baker, F. J. Craig, R. E. Mulvey, W. Clegg, L. Horsburgh, *Polyhedron*, 1996, **15**, 3533.
26. L. H. Gade, P. Renner, H. Memmler, F. Fecher, C. H. Galka, M. Laubender, S. Radojevic, M. McPartlin, J. W. Lauher, *Chem. Eur. J.*, 2001, **7**, 2563.
27. A. J. Arduengo, III, R. Krafczyk, R. Schmutzler, H. A. Craig, J. R. Goerlich, W. J. Marshall, M. Unverzagt, *Tetrahedron*, 1999, **55**, 14523.

Chapter 3

2-(1-Cyclohexylimino-ethyl)-*N*-(trialkylsilyl)-anilide and Related Complexes of Zirconium(IV)

3.1 Introduction

3.1.1 Amido/imino transition metal complexes

A novel 2-(*tert*-butyliminomethyl)-6-methylanilide complex of Mn(II) was synthesised and structurally characterised by Wilkinson and co-workers in 1995 (Scheme 3.1).[1] The structure of the complex consisted of a four-coordinate tetrahedral manganese atom chelated by two $(Bu^t)N{=}C(H)C_6H_3(Me)NH$- ligands. The complex was the unexpected product of the reaction between five equivalents of $Li(NHC_6H_3Me_2\text{-}2,6)$ and $Mn(NBu^t)_3Cl$.

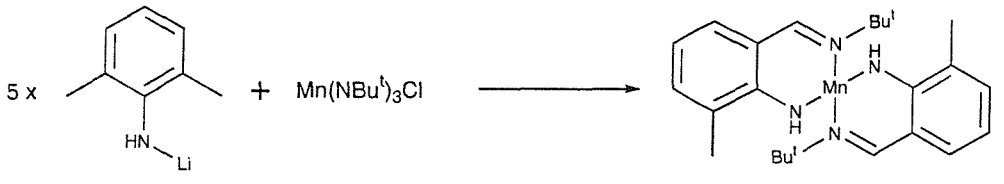

Scheme 3.1: Synthesis of $Mn[(Bu^t)N{=}C(H)C_6H_3(Me)NH]_2$ reported by Wilkinson.

Wilkinson subsequently initiated a study to seek a rational synthetic method for analogous metal complexes to the manganese example.[2] The similar $2\text{-}(Bu^t)N{=}C(H)C_6H_4NH_2$ ligand was synthesised and used to prepare complexes of the type $M[2\text{-}(Bu^t)N{=}C(H)C_6H_4NH]_2$ (M = Mn, Fe, Co, Ni). These compounds were synthesised by interaction of two equivalents of the monolithium salt of the secondary amine ligand and $MnBr_2$, $FeBr_2$, $CoCl_2$, and $NiCl_2(dme)$, respectively. The Mn, Fe, and Co complexes were also obtained by interaction of $\{M[N(SiMe_3)_2]_2\}_2$ (M = Mn, Co) or $Fe[N(SiMe_3)_2]_2$ with four and two equivalents of $2\text{-}(Bu^t)N{=}C(H)C_6H_4NH_2$, respectively.

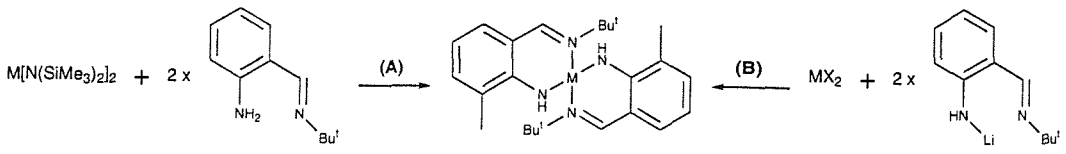

Scheme 3.2: Synthesis of $M[(Bu^t)N=C(H)C_6H_4NH]_2$ complexes from the interaction of either: (**A**) the free amine with $M[N(SiMe_3)_2]_2$ or (**B**) the lithium amide with MX_2, reported by Wilkinson.

When the reaction of the dimer $\{Mn[N(SiMe_3)_2]_2\}_2$ with only two equivalents of the $2\text{-}(Bu^t)N=C(H)C_6H_4NH_2$ ligand was carried out,[2] the product was the dimer $\{(Me_3Si)_2NMn[(Bu^t)N=C(H)C_6H_4NH]\}_2$, which contained bridging amido nitrogens. Each Mn atom was bonded by four N atoms in a distorted octahedral environment so that each ligand chelated one Mn and bridged to the other (Scheme 3.3, below). The bridges were unsymmetrical with Mn-N distances differing by *ca.* 0.075 Å, with the shorter bond being contained within the chelate ring.

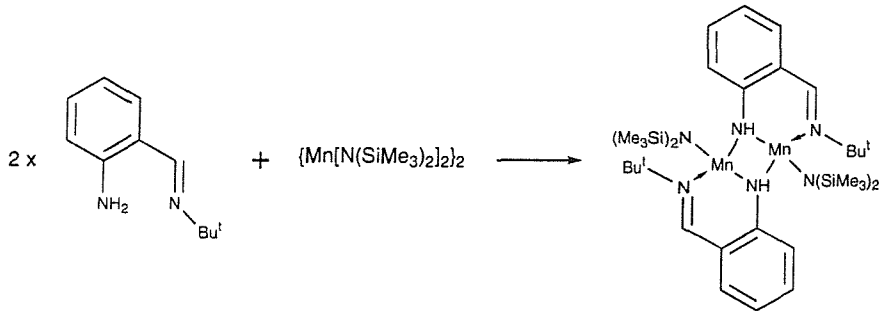

Scheme 3.3: Synthesis of the dimer $\{(Me_3Si)_2NMn[(Bu^t)N=C(H)C_6H_4NH]\}_2$ reported by Wilkinson.

The ligands studied by Wilkinson did not feature a second substituent on the amide nitrogen, making it a primary amide. Danopoulos and co-workers synthesised an analogous ligand by taking the ligand studied by Wilkinson and substituting one of the amino protons for a trimethylsilyl group.[3] This ligand was introduced onto a Zr(IV) centre by interaction of one equivalent of the lithium amido/imino species with $ZrCl_4$, and of two equivalents with $ZrCl_4(THT)_2$, to give both the 1:1 and the 2:1 Zr(IV) complexes. Both complexes were isolated as

extremely air sensitive, yellow, crystalline solids and were structurally characterised.[3]

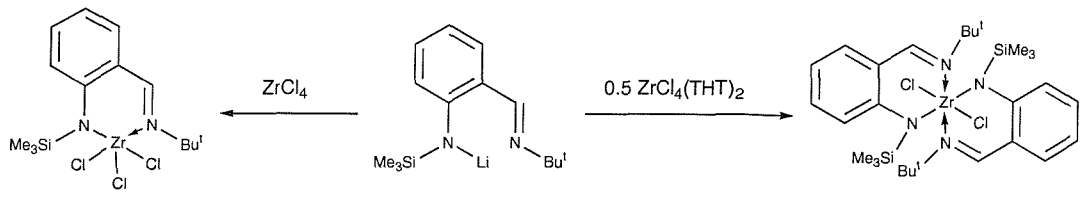

Scheme 3.4: Synthesis of 1:1 and 2:1 2-(Bu^t)N=C(H)C_6H_4N($SiMe_3$) complexes of Zr(IV) reported by Danopoulos.

Danopoulos also observed an unexpected ligand rearrangement in the reaction of one equivalent of the free amine, 2-(Bu^t)N=C(H)C_6H_4NH($SiMe_3$), with $Zr(NMe_2)_2Cl_2(THF)_2$ in PhMe at 95 °C.[3] Instead of the expected $LZr(NMe_2)Cl_2$ type complex, the resultant dimeric complex contained a diamido/monoamino, tridentate ligand which was formally the result of the *tert*-butylimine group inserting into the zirconium-dimethylamide bond. This observation demonstrates the "non-innocence" of the *tert*-butylaldimine moiety, although the reaction conditions were relatively harsh.

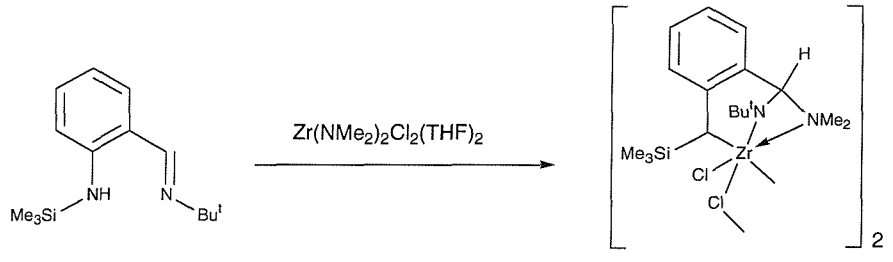

Scheme 3.5: Synthesis of the dimeric Zr(IV) complex involving the conversion of the amido/imino ligand into a diamido/monoamino ligand reported by Danopoulos.

3.1.2 2-Pyridyl-azaallyl complexes of zirconium

Lappert and co-workers synthesised zirconium complexes[4] of the 2-pyridyl-azaallyl ligands they had prepared.[5] The complexes were synthesised by reaction of two equivalents of the lithium 2-pyridyl-azaallyl ligand with $ZrCl_4$ (Scheme 3.6). The complexes comprise two 2-pyridyl-azaallyl groups and two chloride

ligands. The complexes possess distorted octahedral geometry with *cis* chlorides and *trans* amides. Lappert also reported a series of analogous 2-quinolyl-azaallyl zirconium complexes.[4]

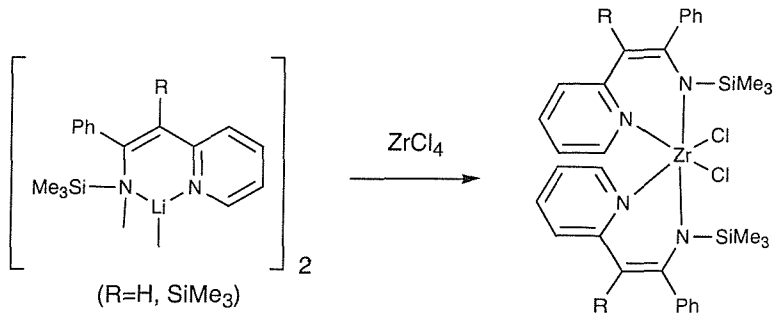

Scheme 3.6: Lappert's synthesis of bis-2-pyridyl-azaallyl zirconium dichloride complexes.

In a subsequent step, one of the 2:1 complexes was converted into the mono-2-pyridyl-azaallyl zirconium trichloride complex by reaction with one equivalent of $ZrCl_4$ (Scheme 3.7). Ethylene polymerisation catalysis studies (using MAO as co-catalyst) showed that the 2:1 complexes possessed no activity but the 1:1 complex possessed moderate activity.

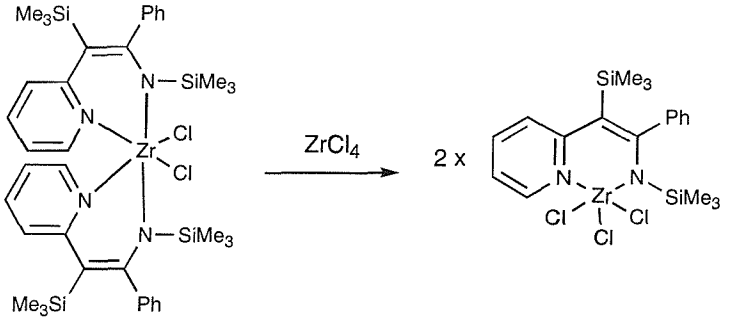

Scheme 3.7: Conversion of the bis-2-pyridyl-azaallyl zirconium dichloride complex to the mono-2-pyridyl-azaallyl zirconium trichloride.

Results and Discussion

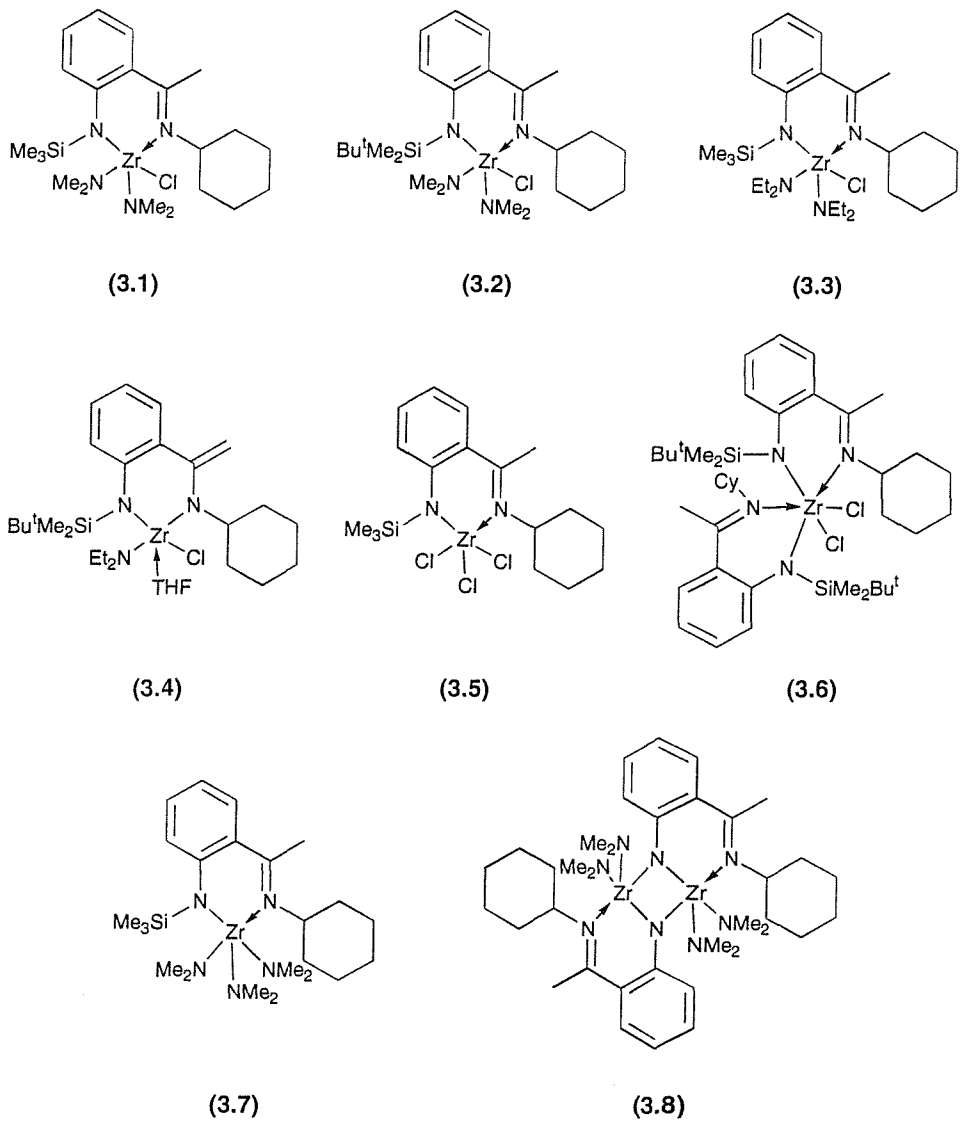

Figure 3.1: Zirconium complexes **(3.1)**–**(3.8)** synthesised.

3.2 Salt metathesis reactions between lithium silylamido/imino compounds and $Zr(NR_2)_2Cl_2(THF)_2$ complexes

The three amido/imino zirconium complexes **(3.1)**, **(3.2)** and **(3.3)** of the type $LZr(NR_2)_2Cl$ were prepared *via* salt metathesis reactions between either $Zr(NMe_2)_2Cl_2(THF)_2$ or $Zr(NEt_2)_2Cl_2(THF)_2$ with the lithium silylamido/imino compounds **(2.3)** and **(2.5)**. The complexes were synthesised in moderate to good yield by reaction of the lithium amido/imino compound with the zirconium starting material and isolated as extremely air and moisture sensitive orange or yellow

crystalline solids. It was necessary to purify the resultant complexes by recrystallisation from petroleum to remove reprotonated silylamino/imino ligand from the reaction products.

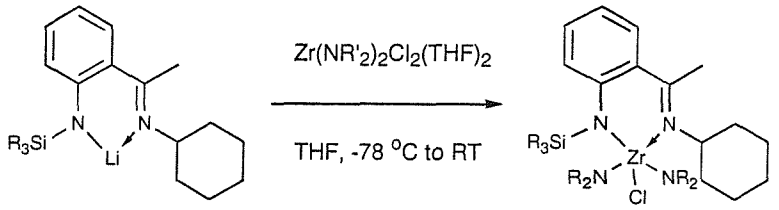

SiR_3=$SiMe_3$, NR'_2=NMe_2 (**3.1**); SiR_3=$SiMe_2Bu^t$, NR'_2=NMe_2 (**3.2**); SiR_3=$SiMe_3$, NR'_2=NEt_2 (**3.3**).

Scheme 3.8: Synthesis of (**3.1**), (**3.2**) and (**3.3**).

Single crystal X-ray diffraction studies on (**3.2**) and (**3.3**) showed that the complexes possessed distorted trigonal bipyramidal geometries about the zirconium centres. NMR spectroscopic studies showed that the two dialkylamido ligands were inequivalent in solution.

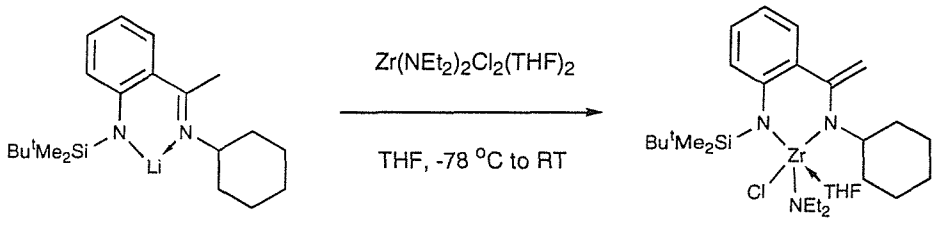

Scheme 3.9: Synthesis of (**3.4**).

An unexpected result was obtained from an attempt to prepare the analogous $LZr(NR_2)_2Cl$ type complex from the reaction of (**2.5**) with $Zr(NEt_2)_2Cl_2(THF)_2$. The isolated product was complex (**3.4**), in which the 2-(1-cyclohexylimino-ethyl)-*N*-(*tert*-butyldimethylsilyl)-anilide ligand has been converted into a 2-(1-cyclohexylamido-vinyl)-*N*-(*tert*-butyldimethylsilyl)-anilide species (Scheme 3.9). The zirconium centre also bears one diethylamido, one chloride and one THF ligand. The structure of the complex was determined by a single crystal X-ray diffraction study and confirmed by the NMR data that was obtained (see below).

Here the ligand is acting as a chelating dianionic diamide species containing the unusual vinylamide donor in conjunction with the silylamide moiety. Unlike most conventional diamide or β-diketiminate ligands this novel diamide ligand contains two inequivalent amide groups giving an asymmetric diamide ligand.

It was unclear how complex (**3.4**) was formed given that complexes (**3.1**), (**3.2**) and (**3.3**), the anticipated products from salt elimination reactions, were isolated previously. An initial hypothesis to explain the formation of (**3.4**) was that following the salt elimination reaction to give the anticipated $LZr(NR_2)_2Cl$ species, there occurred an intermolecular deprotonation of the imine methyl group by a second molecule of bulky, basic lithium silylamido/imino. This step would resemble enolate formation in analogous enolisable ketones. Isomerisation of the coordinated en-iminato to the vinyl-amido species would give the observed product.

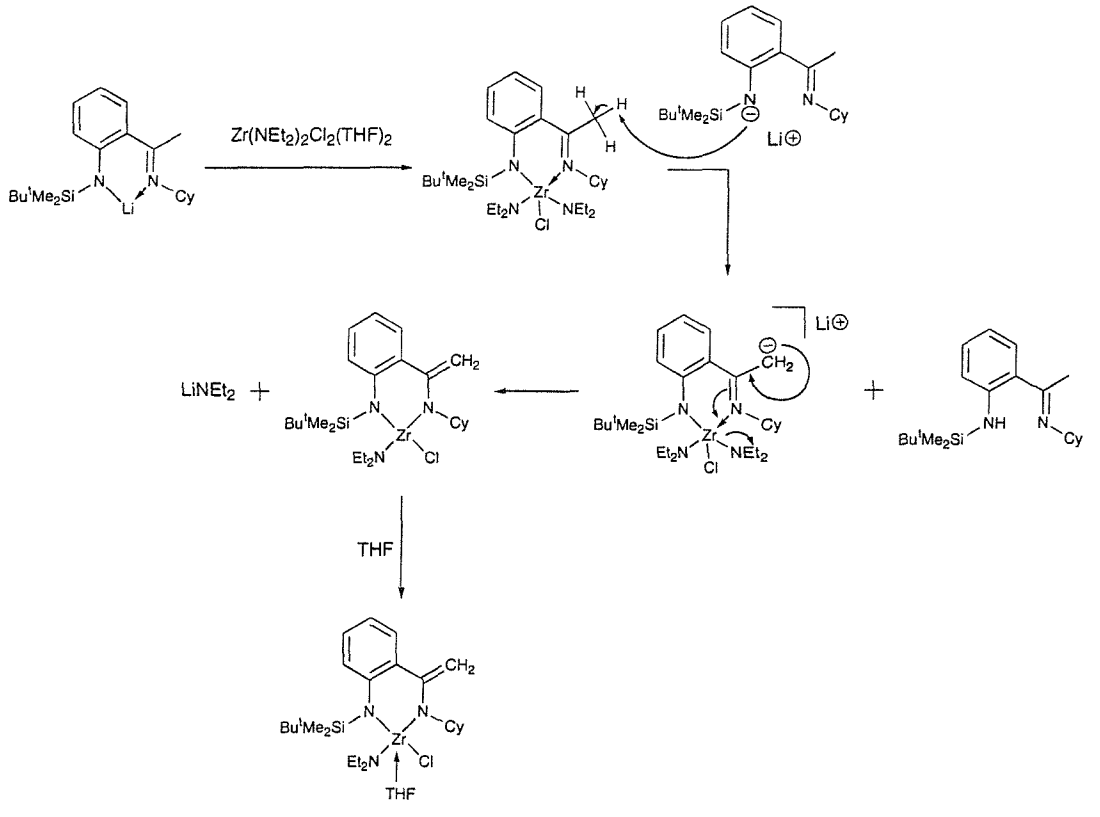

Scheme 3.10: Postulated mechanism for the formation of (**3.4**)**:** (i) intermolecular deprotonation of the imine methyl group by a molecule of the lithium silylamido/imino compound; (ii) isomerisation and formation of (**3.4**).

This mechanistic scheme (above) appears unlikely for several reasons:

(i) It seems unlikely that diethylamide would act as a leaving group to facilitate the migration of the negative charge and formation of the second amido moiety in the bidentate ligand.

(ii) The maximum yield of **(3.4)** expected, based on the above model, is only 50% (based on zirconium) since one equivalent of the silylamido/imino lithium acts as a base. In fact, **(3.4)** was isolated in 45% yield after recrystallisation from petroleum. Attempts were made to optimise the yield by altering the ratio of silylamido/imino lithium to zirconium to 2:1 but there was no change in the isolated yield of **(3.4)**.

(iii) Attempts were made to add a second equivalent of silylamido/imino lithium compound **(2.5)** to the preformed $LZr(NEt_2)_2Cl$ complex **(3.3)** but the rearrangement to the silylamido/vinylamido ligand was not observed. There is no reaction apparent by ^1H NMR spectroscopy and the two starting materials are the only species detectable by NMR spectroscopy following the reaction.

(iv) If lithium diethylamide was formed as a byproduct of this mechanism it would not be unreasonable to anticipate that it would then react with **(3.4)** to substitute the chloride ligand for diethylamide and give lithium chloride as the by product.

Given that this reaction has occurred when using the bulkier ligand and the zirconium complex with the bulkier diethylamide ligands, a release of the steric congestion around the zirconium centre may be the driving force for the transformation. It is therefore possible that steric crowding about the metal centre promotes the insertion of the cyclohexylimine group into a zirconium-diethylamide bond to give a monoamino/diamido species (Scheme 3.11, below). This species could then undergo an E1 type reaction involving the dissociation of the diethylamine group followed by loss of a neighbouring proton to give the olefin. In this case the diamide ligand is formed initially, before elimination gives the olefin group. The first mechanism involved a simultaneous formation of the olefin and the second amide group.

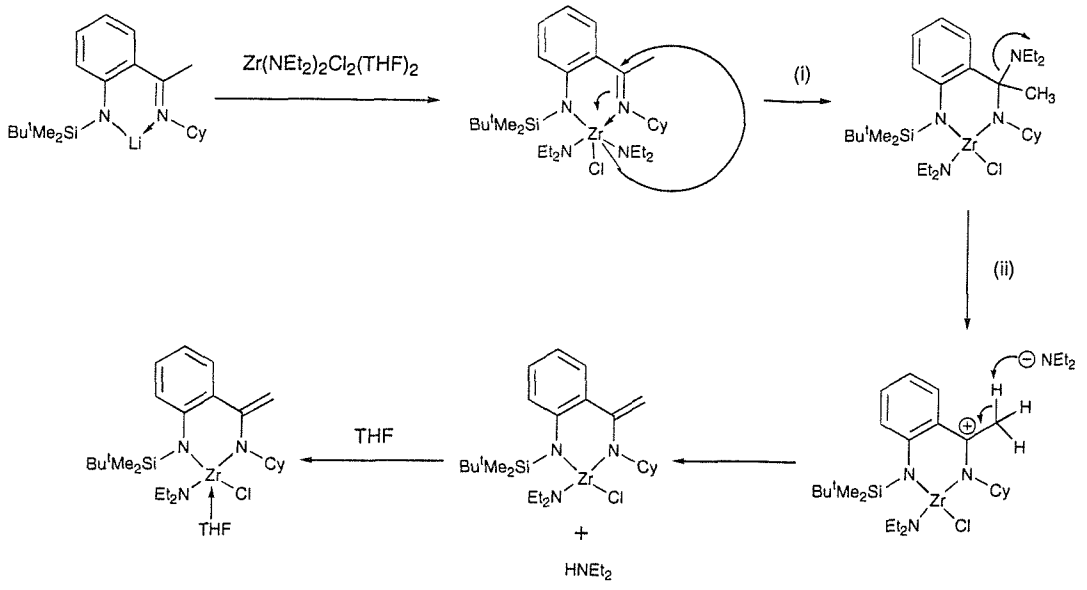

Scheme 3.11: Proposed insertion and elimination mechanism for the formation of **(3.4)**: (i) insertion of the cyclohexylimine group into a zirconium-diethylamide bond; (ii) elimination of $HNEt_2$ to give the vinylamido group.

Evidence to support the insertion postulated in this mechanism of the formation of **(3.4)** is provided by the synthesis and characterisation of several similar titanium complexes (see Chapter 4) and a zirconium complex previously reported by the Danopoulos group. In these cases, the amido/imino ligand has been converted to a monoamino/diamido species similar to the one postulated in the formation of **(3.4)** (see Figure 3.2).

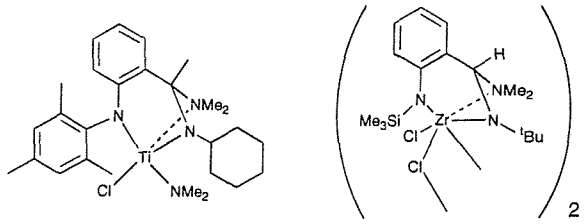

A. **B.**

Figure 3.2: Structures of **A**: complex **(4.9)** from Chapter 4; and **B**: a previously reported structure by Danopoulos.

Further evidence to support the proposed mechanism is provided by the detection of a similar complex **(4.2)** as a minor product from the reaction of the arylamido/imino lithium **(2.9)** with $Zr(NEt_2)_2Cl_2(THF)_2$ (see Chapter 4). The major

product (**4.1**) was the anticipated amido/imino zirconium complex of the type $LZr(NEt_2)_2Cl$.

When attempts were made to react $Zr(NR_2)_2Cl_2(THF)_2$ (R=Me, Et) with two equivalents of (**2.3**) or (**2.5**), it was observed that it was not possible to form a $L_2Zr(NR_2)_2$ type complex. ^1H NMR spectroscopy showed that the product of the reaction was the $LZr(NR_2)_2Cl$ complex and unreacted lithium amido/imino. This suggests that the steric demands of two silylamido/imino ligands and two dialkylamido groups on a zirconium(IV) centre are too great. In contrast, L_2ZrCl_2 complexes with the less bulky chloride ligands have been synthesised. It is also notable that it is possible to synthesise $L_2Zr(NR_2)_2$ type complexes using a phenoxy/imine ligand instead of a silylamido/imino ligand (see Chapter 5). The reduced steric demand of the phenoxy group, which lacks a second substituent on the oxygen donor atom, may be invoked to explain this difference.

3.2.1.1 NMR spectroscopy for (3.1), (3.2) and (3.3)

The ^1H and $^{13}C\{^1H\}$ NMR spectra of the three amido/imino zirconium complexes [(**3.1**)-(**3.3**)] of the type $LZr(NR_2)_2Cl$ contain peaks assignable to the silylamido/imino ligand backbone as well as the dialkylamide ligands. The peaks due to the amido/imino ligand occur in similar positions to those of the amino/imino and the lithium amido/imino compounds (see Chapter 2), and are compared in Table 3.1.

Table 3.1: A comparison of selected ^{1}H and $^{13}C\{^{1}H\}$ NMR data for (**3.1**), (**3.2**) and (**3.3**).[a]

Compound	**(3.1)**	**(3.2)**	**(3.3)**
SiCH_3	0.33	0.54, 0.67	0.35
Si[C(CH_3)]	-	0.76	-
Imine CH_3	1.72	1.82	1.77
Cycohexyl CH	3.41	3.45	multiplet[c]
N(CH_3)$_2$	2.86, 2.97	2.67, 3.03	-
N(CH_2CH_3)$_2$	-	-	0.91, 1.07
N(CH_2CH_3)$_2$	-	-	multiplet[c]
SiCH_3	3.22	-1.11, 2.06	3.20
Si[C(CH_3)][b]	-	21.37, 28.21	-
Imine CH_3	21.29	21.72	21.78
Cycohexyl CH	64.38	64.77	64.40
N(CH_3)$_2$	43.67, 44.41	43.99, 44.33	-
N(CH_2CH_3)$_2$	-	-	14.28, 14.41
N(CH_2CH_3)$_2$	-	-	42.70, 43.06
C=N	169.12	170.48	169.52

[a] Spectral data expressed in ppm; solvent = C_6D_6.

[b] The first value given is that of the tertiary carbon.

[c] It is not possible to report accurate values here because the diethylamide CH_2s and the methine cyclohexyl CH appear as an overlapping multiplet.

The data show the dialkylamide ligands to be inequivalent in solution. The dimethylamide ligands of (**3.1**) and (**3.2**) appear as two singlets in both the ^{1}H and $^{13}C\{^{1}H\}$ NMR spectra, each proton signal integrating as six protons. The diethylamide ligands of (**3.3**) give a more complicated pattern. They appear in the $^{13}C\{^{1}H\}$ NMR spectrum as two signals at *ca.* 14 ppm assignable to the methyl groups and two signals at *ca.* 43 ppm assignable to the CH_2 groups. In the ^{1}H NMR spectrum, the CH_3s appear as two triplets, each integrating as six protons, at 0.91 and 1.07 ppm, whilst the CH_2s appear as four multiplets between 3.1 and 3.7 ppm, with a total integration of eight protons. If the complexes adopt the same distorted trigonal bipyramidal geometry in solution as they do in the solid state then the inequivalence of the dialkylamide ligands could be due to the asymmetry of the amido/imino ligand. This could possibly be because one dialkylamide is located near the trialkylsilyl group and the other is near to the cyclohexyl group.

3.2.1.2 NMR spectroscopy for (3.4)

The NMR spectra of **(3.4)** do not contain resonances due to an imine methyl group as those of **(3.1)**-**(3.3)** do. The protons of the newly formed vinyl group appear as two singlets in the ^{1}H NMR spectrum at 4.24 and 4.39 ppm. These couple to the CH_2 peak at 88.36 ppm in a C-H correlation experiment. The vinyl carbon which links the phenyl ring and the cyclohexylamide nitrogen is now shifted slightly upfield [relative to the position of the imine carbon in complexes **(3.1)**-**(3.3)**] to 156.80 ppm. The diethylamide ligand appears in the ^{1}H NMR spectrum as a triplet at 0.76 ppm (for the two methyl groups) and two broad signals at 2.81 and 3.01 ppm (for the CH_2s), and as two signals at 14.56 and 42.79 ppm in the $^{13}C\{^{1}H\}$ NMR spectrum. The signals due to THF appear at 1.32 and 3.69 ppm as broad triplets in the proton spectrum and at 25.78 and 70.25 ppm in the $^{13}C\{^{1}H\}$ NMR spectrum. The resonances assignable to the methine CH of the cyclohexyl group bound to the vinylamido-nitrogen appear in very similar positions (3.40 ppm in the ^{1}H NMR spectrum and 63.58 ppm in the $^{13}C\{^{1}H\}$ NMR spectrum) to those due to the analogous methine CHs that are bound to an imino-nitrogen in complexes **(3.1)**-**(3.3)**.

3.2.2 X-ray diffraction studies of (3.2), (3.3) and (3.4)

The structures of all three complexes show that they adopt distorted trigonal bipyramidal geometries. In both **(3.2)** and **(3.3)** the axial positions are occupied by the imine nitrogen and the chloride ligand with the three stronger π-donating amide groups in the equatorial plane. In the structure of **(3.4)** the axial positions are occupied by the vinylamide nitrogen and the molecule of THF with the silylamido and dialkylamide groups and the chloride ligand in the equatorial plane.

Table 3.2: A comparison of selected structural data for **(3.2)**, **(3.3)** and **(3.4)**.[a]

Compound	**(3.2)**	**(3.3)**	**(3.4)**
Zr-N (silyl)	2.082(7)	2.112(4)	2.052(2)
Zr-N (cyclohexyl)	2.431(7)	2.460(4)	2.1290(19)
N-C (imine)	1.309(11)	1.285(7)	1.392(3)
C-C	1.519(13)	1.518(7)	1.348(3)
N-C (cyclohexyl)	1.486(10)	1.478(7)	1.472(3)
N-Zr-N	80.2(2)	76.61(15)	89.5(8)

[a] Bond lengths in Å, angles in °.

The short imine bond lengths in complexes **(3.2)** and **(3.3)** [1.309(11) and 1.285(7)Å] demonstrate that the double bond nature is maintained upon coordination of the ligand to the zirconium centre. They contrast with the increased bond length between the vinyl carbon and the cyclohexylamide nitrogen in **(3.4)** [1.392(3)Å], which therefore indicates the single nature of the bond in **(3.4)**. There is also a pronounced difference in the C-C bond lengths between the imine carbon and the methyl group. The distances are typical of a C-C single bond in **(3.2)** and **(3.3)** [1.519(13) and 1.518(7)Å], but in **(3.4)** the bond length of 1.348(3)Å is typical of an olefin. The Zr-N bond lengths also support the transformation from a cyclohexylimine group to a vinylamide species. In **(3.2)** and **(3.3)** the zirconium-nitrogen bond distances to the imine group [2.431(7) and 2.460(4)Å] are significantly longer than the Zr-N bond length to the vinylamide nitrogen [2.1290(19)Å], which is comparable to the Zr-N(amide) bond lengths reported here.

3.2.2.1 X-ray diffraction study on (3.2)

X-ray diffraction quality crystals of [2-(1-cyclohexylimino-ethyl)-*N*-(*tert*-butyldimethylsilyl)-anilide] zirconium chloride bis-dimethylamide **(3.2)** were obtained by cooling a saturated petroleum solution to –30 °C to give the compound as yellow blocks.

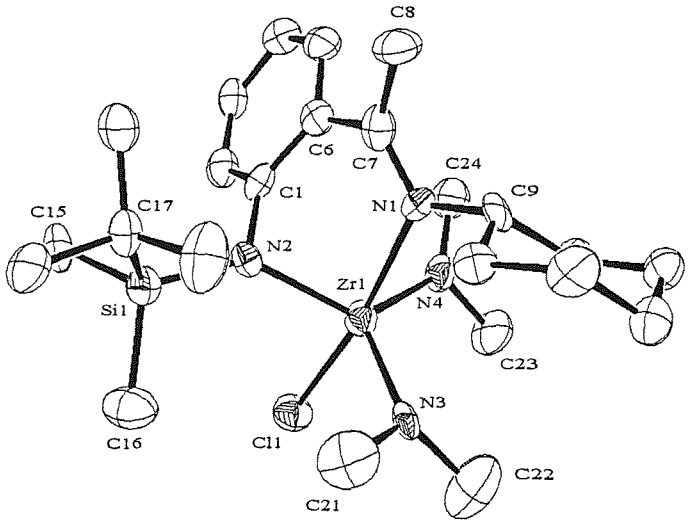

Figure 3.3: ORTEP representation of the crystal structure of [2-(1-cyclohexylimino-ethyl)-*N*-(*tert*-butyldimethylsilyl)-anilide] zirconium chloride bis-dimethylamide (**3.2**) (50% probability thermal ellipsoids). Hydrogens are omitted for clarity.

The zirconium-amide bond length of 2.082(7)Å is markedly shorter than the zirconium-imine bond length of 2.431(7)Å. This fact coupled with the difference in the C-N bond lengths of N(2)-C(1) [1.422(10)Å] and N(1)-C(7) [1.309(11)Å] confirms that the anionic charge is localised on the amide. The amido/imino ligand possesses a bite angle of 80.2(2)° about the zirconium centre and the six-membered chelate ring is non-planar. This planar nature of the amide group demonstrates that the lone pair of the nitrogen is involved in π-bonding to the metal. The bond lengths between the zirconium centre and the dimethylamide [N(3)-Zr(1) 2.039(8) and N(4)-Zr(1) 2.070(7)Å] and chloride [Cl(1)-Zr(1) 2.500(3)Å] ligands are typical of a zirconium(IV) complex and are comparable to the other similar complexes reported here.

3.2.2.2 X-ray diffraction study on (3.3)

X-ray diffraction quality crystals of [2-(1-cyclohexylimino-ethyl)-*N*-(trimethylsilyl)-anilide] zirconium chloride bis-diethylamide (**3.3**) were obtained by cooling a saturated petroleum solution to –30 °C to give the compound as yellow cubes.

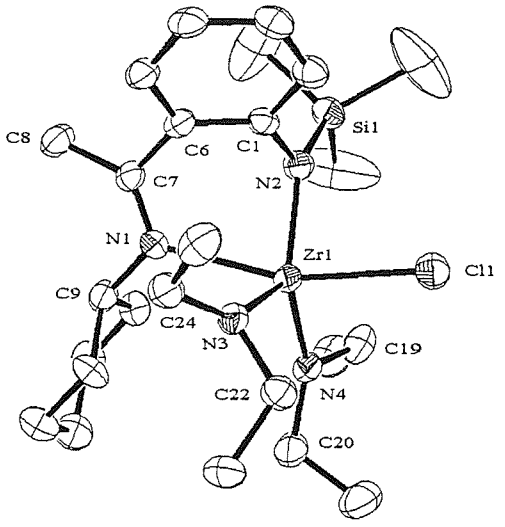

Figure 3.4: ORTEP representation of the crystal structure of [2-(1-cyclohexylimino-ethyl)-*N*-(trimethylsilyl)-anilide] zirconium chloride bis-diethylamide (**3.3**) (50% probability thermal ellipsoids). Hydrogens are omitted for clarity.

As with the structure of (**3.2**), the zirconium-amide bond length [2.112(4)Å] is much shorter than the zirconium-imine bond [2.460(4)Å]. The zirconium-nitrogen bond lengths of the amido/imino ligand are very similar to those of the bulkier ligand in complex (**3.2**), but the bite angle of the ligand is smaller, being 76.61(15)° [compared to 80.2(2)° in (**3.2**)]. The geometry of the silylamide group is planar, suggesting that like (**3.2**), there is a strong π-bonding interaction with the metal. The bond lengths to the diethylamide [N(3)-Zr(1) 2.047(4) and N(4)-Zr(1) 2.054(5)Å] and chloride [Cl(1)-Zr(1) 2.5021(13)Å] ligands are again typical and very similar to those of (**3.2**).

3.2.2.3 X-ray diffraction study on (3.4)

X-ray diffraction quality crystals of [2-(1-cyclohexylamido-vinyl)-*N*-(*tert*-butyldimethylsilyl)-anilide] zirconium chloride diethylamide tetrahydrofuran (**3.4**) were obtained by cooling a saturated petroleum solution to –30 °C to give the compound as yellow cubes.

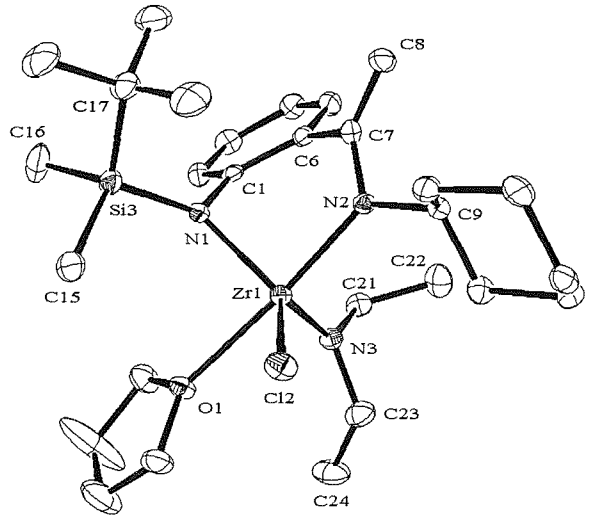

Figure 3.5: ORTEP representation of the crystal structure of [2-(1-cyclohexylamido-vinyl)-*N*-(*tert*-butyldimethylsilyl)-anilide] zirconium chloride diethylamide tetrahydrofuran **(3.4)** (50% probability thermal ellipsoids). Hydrogens are omitted for clarity.

Although the 1-cyclohexylimino-ethyl group has been converted into a 1-cyclohexylamido-vinyl species and the zirconium-nitrogen bond is shorter [2.1290(19)Å], it remains longer than that to the silylamido group [N(1)-Zr(1) 2.052(2)Å]. The six-membered chelate ring of the dianionic ligand is still puckered, but the bite angle is 89.5(8)° and is larger than in the amido/imino ligands of complexes **(3.2)** and **(3.3)**. The Zr-Cl [2.4503(7)Å] and zirconium-diethylamide [2.019(2)Å] bond lengths remain typical, and the zirconium-THF bond length is 2.3625(16)Å.

3.3 Synthesis of [2-(1-cyclohexylimino-ethyl)-*N*-(trimethylsilyl)-anilide] zirconium trichloride (3.5)

In previous work within the Danopoulos group an amido/imino complex of the type $LZrCl_3$ had been prepared by reacting the lithium amido/imino compound with $ZrCl_4$.[3] In this previous case it was an amido/aldimino ligand rather than the amido/ketimino ligands being studied here.

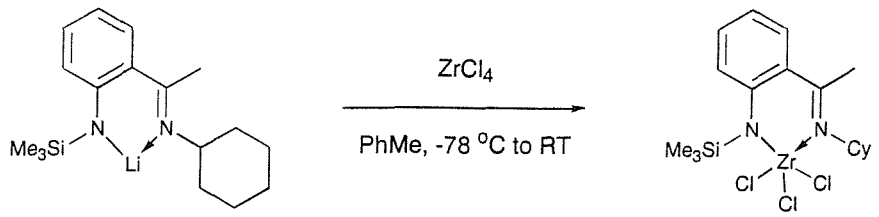

Scheme 3.12: Synthesis of (**3.5**) *via* a salt metathesis reaction.

This method was repeated using (**2.3**) (Scheme 3.12) and the product of the reaction was a bright orange solid. The solid was not soluble in C_6D_6 but a ^1H NMR spectrum was obtained in CD_2Cl_2 which, although it contained peaks assignable to the amido/imino ligand backbone, appeared to be due to a complicated mixture of products. It is possible that the complex is not inert to the CD_2Cl_2 solvent and reacted in some way. The identification of the product as [2-(1-cyclohexylimino-ethyl)-*N*-(trimethylsilyl)-anilide] zirconium trichloride is therefore based on the satisfactory elemental analysis that was obtained (found: C, 42.4; H, 6.0; N, 6.4. $C_{17}H_{27}N_2SiCl_3Zr$ requires C, 42.1; H, 5.6; N, 5.8%).

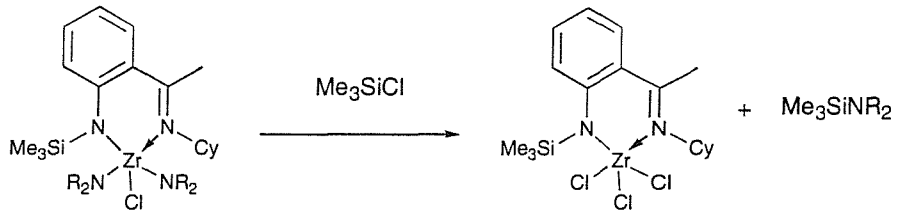

NR_2=NMe_2 (**3.1**); NR_2=NEt_2 (**3.3**).

Scheme 3.13: Synthesis of (**3.5**) by reaction of Me_3SiCl with (**3.1**) and (**3.3**).

It was also possible to replace the dimethylamido/diethylamido groups in complexes (**3.1**) and (**3.3**) with chlorides by reaction of each complex with trimethylchlorosilane (Scheme 3.13). When these reactions were performed on a small scale in Young's tap NMR tubes it was possible to follow the progress of the reaction and to witness the disappearance of the peaks due to the dialkylamide ligands and see the appearance of peaks due to the the product and the Me_3SiNR_2 byproduct. These peaks disappeared upon removing the volatiles from the NMR tubes *in vacuo* to leave a set of peaks assignable to the product.

When (**3.5**) was formed by substitution of dialkylamide ligands for chlorides the product was soluble in C_6D_6. This suggests that it is possible that the product from these reactions is a monomeric species, whereas that formed by reaction of the lithium amido/imino compound with polymeric $ZrCl_4$ gives a dimeric complex.

3.3.1 NMR spectroscopy for (3.5)

The method of synthesising (**3.5**) by substitution of the dialkylamide ligands of complexes (**3.1**) and (**3.3**) gave a product with the same NMR data from both starting materials. The ^1H NMR spectrum contains only resonances assignable to the amido/imino ligand backbone. The trimethylsilyl group resonates at 0.25 ppm and the imino-methyl resonance appears at 1.61 ppm. The methine cyclohexyl CH appears at a position of 3.46 ppm, which is typical when compared to complexes (**3.1**)-(**3.4**), and the aromatic resonances lie between 6.8 and 7.3 ppm.

3.4 Synthesis of bis-[2-(1-cyclohexylimino-ethyl)-*N*-(*tert*-butyldimethylsilyl)-anilide] zirconium dichloride (3.6)

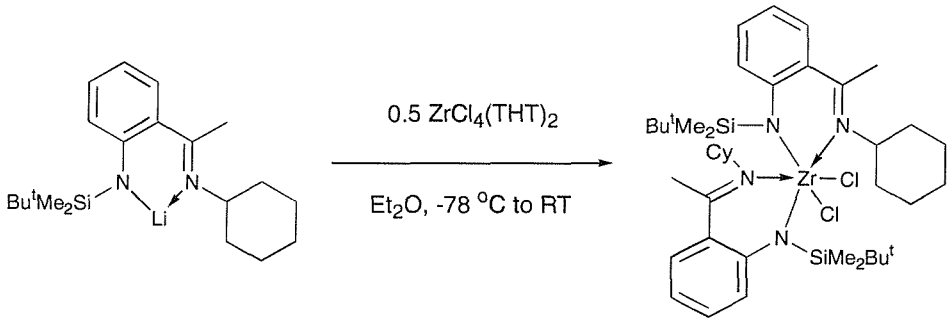

Scheme 3.14: Synthesis of (**3.6**).

A zirconium(IV) complex bearing two 2-(1-cyclohexylimino-ethyl)-*N*-(*tert*-butyldimethylsilyl)-anilide ligands and two chlorides was synthesised by reaction of two equivalents of the lithium amido/imino (**2.5**) with $ZrCl_4(THT)_2$ in diethyl ether (Scheme 3.14, above). The crude product was recrystallised from petroleum to give (**3.6**) in moderate yield as yellow, extremely air sensitive crystals. Complex (**3.6**) was identified by analytical and spectroscopic methods and the structure confirmed by X-ray crystallography. This synthesis followed a procedure

employed in the formation of an analogous 2:1 complex by Danopoulos using the trimethylsilylamido/aldimino ligand (Scheme 3.15, below).[3]

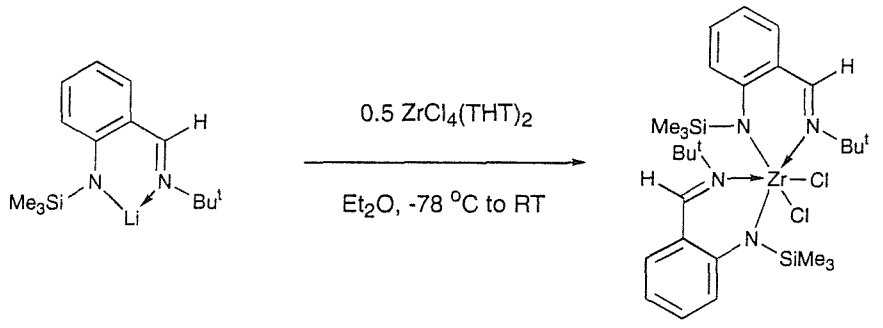

Scheme 3.15: Previous synthesis of bis-[2-(*tert*-butyliminomethyl)-*N*-(trimethylsilyl)-anilide] zirconium dichloride within the Danopoulos group.

3.4.1 NMR spectroscopy for (3.6)

Complex (**3.6**) possessed poor solubility in C_6D_6 and as a result a satisfactory carbon NMR spectrum was not recorded. The proton NMR spectrum of (**3.6**) contained broadened peaks for the imine methyl groups and the silylalkyl groups. This suggests that the complex contains two inequivalent amido/imino ligands, which is in agreement with the results of a single crystal X-ray diffraction study (see below). The *tert*-butyl groups appear as a broad singlet at 0.64 ppm with the silylmethyl groups as a very broad signal between –0.45 and 0.25 ppm. The imine methyl groups appear as a broad singlet between 2.0 and 2.2 ppm.

3.4.2 X-ray diffraction study on (3.6)

X-ray diffraction quality crystals of bis-[2-(1-cyclohexylimino-ethyl)-*N*-(*tert*-butyldimethylsilyl)-anilide] zirconium dichloride (**3.6**) were obtained by cooling a saturated petroleum solution to –30 °C to give the compound as yellow prisms.

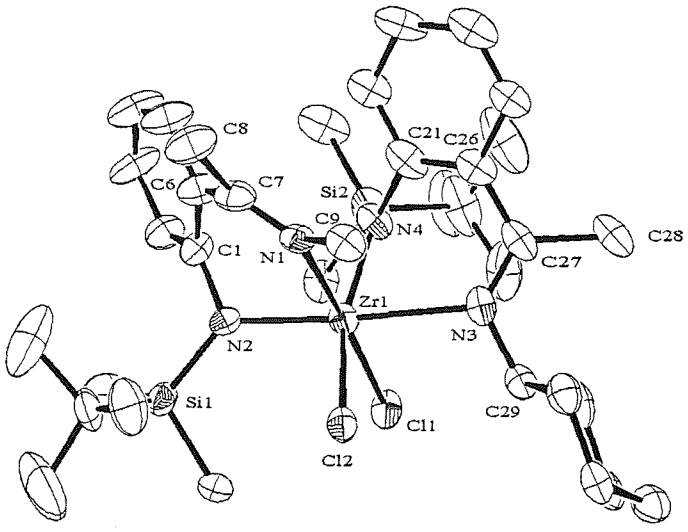

Figure 3.6: ORTEP representation of the crystal structure of bis-[2-(1-cyclohexylamido-vinyl)-*N*-(*tert*-butyldimethylsilyl)-anilide] zirconium dichloride (**3.6**) (50% probability thermal ellipsoids). One cyclohexyl group is removed for clarity [C(10)-C(14)]. Hydrogens are omitted for clarity.

The complex adopts a distorted octahedral geometry with *cis* chlorides. The two amido/imino ligands are inequivalent with the amide nitrogen of one *trans* to the imine nitrogen of the other. This leaves one chloride *trans* to an amide group, and the other *trans* to an imine group. This is the same geometry adopted by the analogous complex prepared previously.[3] It differs from the bis-phenoxy/imine zirconium/titanium dichloride complexes, in which the complexes are C_2-symmetric with the phenoxy groups of each ligand *trans* to one another with *cis* chlorides and imine groups (see Chapter 5). It is possible that a C_2-symmetric geometry for a bis-amido/imino zirconium dichloride complex is sterically unfavourable due to the bulk of the silyl-substituents on the amide groups.

The two zirconium-amide bond lengths are very similar, that of the amide group *trans* to the imine nitrogen [N(2)-Zr(1) 2.111(4)Å] is slightly longer than that which is *trans* to a chloride [N(4)-Zr(1) 2.090(4)Å]. There is a more pronounced difference between the two zirconium-imine bonds, with that of the imine group *trans* to the amide nitrogen [N(3)-Zr(1) 2.459(4)Å] being *ca.* 0.1Å longer than that of the imine group *trans* to the chloride [N(1)-Zr(1) 2.366(4)Å]. The zirconium-chloride bond lengths are typical, with that of the chloride *trans* to

the amide group [Cl(2)-Zr(1) 2.4938(13)Å] slightly longer than that which is *trans* to the imine group [Cl(1)-Zr(1) 2.4417(13)Å]. These observed bond lengths reflect the relative *trans* influence of the functional groups involved.

The bite angles of the puckered chelate rings are 81.06(14) and 78.06(15)° and so remain comparable to the bite angle of 80.2(2)° observed for the same ligand in the mono-amido/imino zirconium complex (**3.2**). The imine bond lengths [C(7)-N(1) 1.272(6) and C(27)-N(3) 1.293(6)Å] clearly show that the imine double bond is still present in both ligands upon complexation, and is shorter than the carbon-nitrogen bond between the amide nitrogen and the benzene ring [N(2)-C(1) 1.419(6) and N(4)-C(21) 1.438(6)Å].

The geometry adopted by the two amido/imino ligands in (**3.6**) differs from the bis-2-pyridyl-azaallyl zirconium dichloride complex reported by Lappert which possesses C_2 symmetry with *trans* amides, *cis* pyridines and *cis* chlorides.[4] The Zr-N(amide) [2.141(3)Å] and Zr-Cl [2.434(1)Å] bond lengths are both comparable to those observed in (**3.6**). It is interesting to note that the Zr-N(pyridine) bond lengths [2.354(3)Å] are similar to the Zr-N(imine) bond lengths in (**3.6**).

3.5 Transamination reactions between 2-(1-cyclohexylimino-ethyl)-*N*-(trimethylsilyl)-aniline (2.2) and $Zr(NMe_2)_4$

A small scale transamination reaction between 2-(1-cyclohexylimino-ethyl)-*N*-(trimethylsilyl)-aniline (**2.2**) and $Zr(NMe_2)_4$ was performed in a 1:1 ratio in a Young's tap NMR tube in C_6D_6 at 50 °C over three days to produce [2-(1-cyclohexylimino-ethyl)-*N*-(trimethylsilyl)-anilide] zirconium tris-dimethylamide (**3.7**).

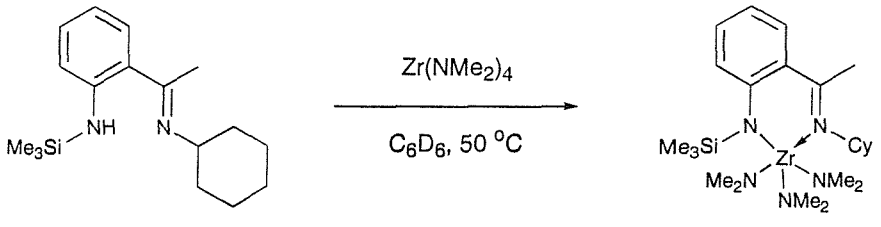

Scheme 3.16: Synthesis of (**3.7**).

The reaction was followed by proton NMR spectroscopy and adjudged to be complete based on the disappearance of the amine proton resonance at 10.4 ppm and the shifting of the methyl and aryl resonances. The dimethylamide resonance also shifted slightly and the ratio of its integral to those of the amido/imino peaks also decreased, which is consistent with the loss of a dimethylamide ligand from the starting material. The reaction was also marked by the appearance of a doublet at *ca.* 2.1 ppm assignable to dimethylamine, which disappeared when the volatiles were removed *in vacuo*. When the reaction was scaled up in toluene the reaction did not appear to proceed in a clean fashion and it was impossible to isolate (**3.7**) from the reaction mixture.

An unexpected result was obtained from an attempt to perform the transamination reaction between $Zr(NMe_2)_4$ and two equivalents of (**2.2**) in toluene at 100 °C. The only product that was isolated was the imido/imino zirconium dimer (**3.8**).

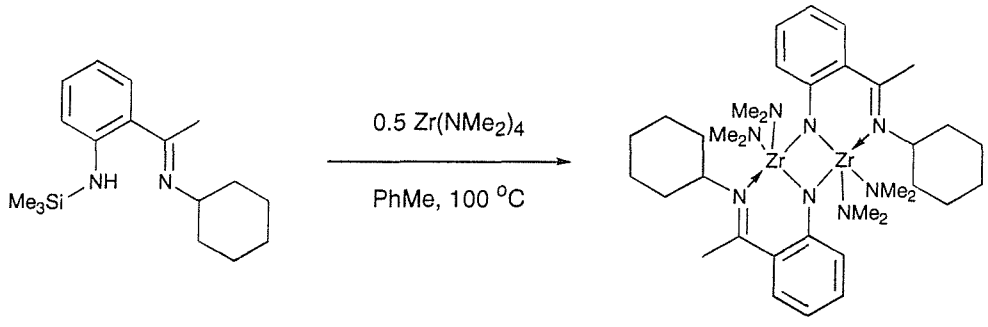

Scheme 3.17: Synthesis of the imido/imino zirconium dimeric complex (**3.8**).

The imido moiety has been formed by the loss of the trimethylsilyl-substituent from the amide group. The most probable mechanism for the formation of (**3.8**) involves an initial transamination step to form complex (**3.7**), which then undergoes either an intermolecular or intramolecular elimination of Me_3SiNMe_2 to generate the imido moiety. If the elimination is intramolecular then dimerisation gives the observed complex (**3.8**).

Following the crystallisation of the product from petroleum it was not possible to redissolve the crystals in inert solvents in order to obtain a proton NMR spectrum.

3.5.1 NMR spectroscopy for (3.7)

The three dimethylamide ligands appear as one singlet with an integral ratio of approximately 2:1 to the trimethylsilyl resonance, which is consistent with a complex containing three NMe_2 groups and one $SiMe_3$. The NMe_2 resonance is shifted slightly from its position in the starting material (2.96 ppm) to 2.99 ppm. The fact that the three NMe_2 ligands appear as a single resonance suggests that there is fast exchange between equatorial and axial sites if the complex adopts the same distorted trigonal bipyramidal geometry as the $LZr(NR_2)_2Cl$ type complexes (**3.2**) and (**3.3**). The trimethylsilyl resonance shifts slightly from 0.30 to 0.26 ppm but the imine methyl resonance remains in the same position. The methine cyclohexyl resonance is shifted from 3.35 to 3.40 ppm. There is considerable shifting of the aromatic peaks, which is further evidence of the reaction.

3.5.2 X-ray diffraction study on complex (3.8)

X-ray diffraction quality crystals of the imido/imino zirconium complex (**3.8**) were obtained by cooling a saturated petroleum solution to –30 °C to give the compound as orange cubes.

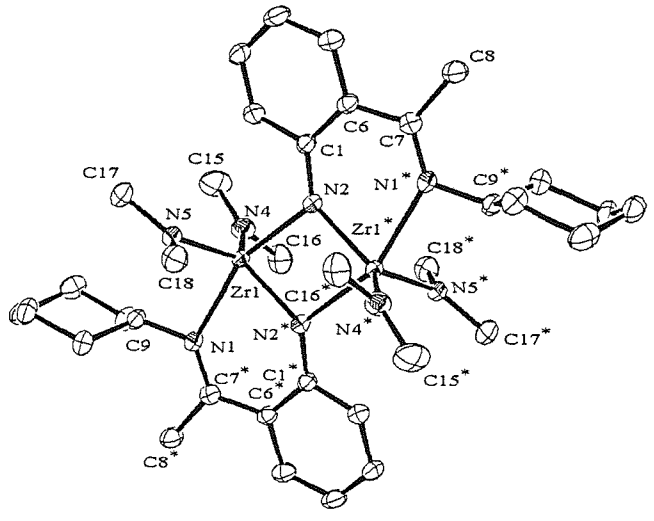

Figure 3.7: ORTEP representation of the crystal structure of the imido/imino zirconium dimer (**3.8**) (50% probability thermal ellipsoids). Hydrogens are omitted for clarity.

The complex is dimeric with bridging imido groups. Each zirconium centre is further bound by one imine nitrogen and two dimethylamide ligands giving a coordination number of five. The geometry about each zirconium centre is best described as distorted trigonal bipyramidal, with the equatorial plane consisting of two dimethylamide ligands and one imido nitrogen, and the axial positons occupied by the second imido-nitrogen and the imine nitrogen. The angle between the two axial groups is 158.24(5)° and shows how distorted the trigonal bipyramid is. The imido nitrogens do not bond symmetrically to both zirconium centres and one bond is *ca.* 0.15Å longer than the other [N(2)-Zr(1*) 2.0652(14) and N(2)-Zr(1) 2.2187(15)Å]. The shorter zirconium-imido bond is contained within the chelate ring of the imido/imino ligand. The zirconium-imine [2.3069(14)Å] and the zirconium-dimethylamide [N(4)-Zr(1) 2.0623(16) and N(5)-Zr(1) 2.0653(14)Å] bond lengths are typical and are comparable to the other complexes reported here.

It is interesting to note that the chelate ring of the imido/imino ligand is planar in (**3.8**). This contrasts with the amido/imino ligand in complexes (**3.2**), (**3.3**) and (**3.6**) and the diamido ligand in (**3.4**) in which the chelate rings are all puckered. The bite angle of the imido/imino ligand [N(2*)-Zr(1)-N(1) 80.11(5)°] remains very similar to those observed in the amido/imino ligands in complexes (**3.2**), (**3.3**) and (**3.6**). The carbon-nitrogen bond of 1.359(2)Å between the imido-nitrogen and the benzene ring is shorter than that between the silylamido-nitrogen and the benzene ring in the other complexes reported here, which is typically *ca.* 1.42-1.43Å. The imino bond length of 1.300(2)Å shows that it retains the double bond character in this complex.

3.6 Preliminary ethylene polymerisation studies

The activity of (**3.1**) and (**3.6**) for ethylene polymerisation catalysis in the presence of MAO was studied following a standardised procedure.[6] They display moderate polymerisation activity, 8.8 and 3.0 g $mmol^{-1}$ bar^{-1} h^{-1} respectively, at room temperature.

3.7 Conclusions

Three silylamido/imino zirconium complexes (**3.1**)-(**3.3**) of the type $LZr(NR_2)_2Cl$ (R=Me, Et) have been prepared *via* salt metathesis reactions of the lithium amido/imino ligand (**2.3**) or (**2.5**) with $Zr(NR_2)_2Cl_2(THF)_2$. The complexes were prepared in moderate to good yields as air/moisture sensitive crystalline solids.

The attempted salt metathesis reaction between (**2.5**) and $Zr(NEt_2)_2Cl_2(THF)_2$ gave as the only product (**3.4**), in which the amido/imino ligand had undergone a rearrangement to a diamido ligand. This was the result of the 1-cyclohexylimino-ethyl group being converted into a 1-cyclohexylamido-vinyl group. This possibly involved the insertion of the cyclohexylimino group into the zirconium-diethylamide bond to give a monoamino/diamido species, followed by elimination of diethylamine from the ligand backbone to generate the olefin. This demonstrates that the 1-cyclohexylimino-ethyl group is not inert and can undergo rearrangements that alter the nature of the amido/imino ligand.

The $LZrCl_3$ complex (**3.5**) of the trimethylsilylamido/imino ligand was synthesised by both salt metathesis reaction between (**2.3**) and $ZrCl_4$; and by action of trimethylchlorosilane on the $LZr(NR_2)_2Cl$ (R=Me, Et) type complexes (**3.1**) and (**3.3**) to substitute the dialkylamide ligands for chlorides.

A bis-amido/imino zirconium complex (**3.6**), incorporating the *tert*-butyldimethylsilylamido/imino ligand, of the type L_2ZrCl_2 was synthesised by salt metathesis reaction between two equivalents of (**2.5**) and $ZrCl_4(THT)_2$. A crystallographic study of the compound showed how sterically crowded the coordination sphere of the zirconium centre is, and indicated why these ligands display a preference for mono-amido/imino complexes rather than bis-amido/imino complexes.

It was possible to prepare the $LZr(NMe_2)_3$ complex (**3.7**) by a transamination reaction between the amino/imino ligand (**2.2**) and $Zr(NMe_2)_4$. However, an attempt to react two equivalents of (**2.2**) with $Zr(NMe_2)_4$ resulted in the isolation of the imido/imino dimer (**3.8**). A pair of imido nitrogens, generated by the loss of the trimethylsilyl substituents (by elimination with a dimethylamide ligand as Me_3SiNMe_2), bridge the two Zr(IV) centres. This demonstrates that the amido-silicon bond is not stable at high temperatures in the presence of dialkylamide ligands bound to zirconium.

Preliminary ethylene polymerisation studies on (**3.1**) and (**3.6**) with an excess of MAO showed them to act as moderate polymerisation catalysts.

3.8 Experimental

The following compounds were prepared following literature methods: $Zr(NMe_2)_2Cl_2(THF)_2$,[7] $Zr(NEt_2)_2Cl_2(THF)_2$,[7] $ZrCl_4(THT)_2$,[8] $Zr(NMe_2)_4$.[9]

3.8.1 [2-(1-Cyclohexylimino-ethyl)-*N*-(trimethylsilyl)-anilide] zirconium chloride bis-dimethylamide (3.1).

To a stirred, cooled (-78 °C) solution of $Zr(NMe_2)_2Cl_2(THF)_2$ (0.790 g, 2 mmol) in THF (80 cm^3), was added slowly *via* cannula a cooled (-78 °C) solution of (**2.3**) (0.588 g, 2 mmol) in THF (40 cm^3). The light yellow mixture was stirred at –78 °C for 1 h, allowed to reach room temperature and stirred for 15 h to give an orange solution. The volatiles were removed *in vacuo* and the residue extracted into petroleum (3 x 50 cm^3). Filtration through Celite, concentration of the filtrate to *ca.* 25 cm^3 and cooling at –30 °C for 15 h gave (**3.1**) as an orange solid (0.40 g). Further concentration of the supernatant and cooling gave further product (0.12 g).

Yield: 0.52 g, 52%.

$\delta_H(C_6D_6)$ 0.33 (9H, s, silyl CH_3s), 1.05-1.95 (10H, m, cyclohexyl CH_2s), 1.72 (3H, s, imine CH_3), 2.86 (6H, s, $N(CH_3)_2$), 2.97 (6H, s, $N(CH_3)_2$), 3.41 (1H, tt, cyclohexyl C*H* α to imine N), 6.70 (1H, dt, aromatic), 7.06 (2H, m, aromatic), 7.28 (1H, dd, aromatic).

$^{13}C\{^1H\}$ $\delta_C(C_6D_6)$ 3.22 (silyl CH_3s), 21.29 (imine CH_3), 26.21, 26.41, 27.35, 31.99, 32.85 (cyclohexyl CH_2s), 43.67 ($N(CH_3)_2$), 44.41 ($N(CH_3)_2$), 64.38 (cyclohexyl C*H* α to imine N), 121.86, 129.79, 131.82, 132.12 (aromatic *C*Hs), 133.33, 146.19 (quaternary aromatics), 169.12 (Ar*C*(Me)=N(Cy)).

Found: C, 49.7; H, 7.8; N, 10.0. $C_{21}H_{39}N_4SiClZr$ requires C, 50.2; H, 7.8; N, 11.2%.

3.8.2 [2-(1-Cyclohexylimino-ethyl)-*N*-(*tert*-butyldimethylsilyl)-anilide] zirconium chloride bis-dimethylamide (3.2).

To a stirred, cooled (-78 °C) solution of $Zr(NMe_2)_2Cl_2(THF)_2$ (0.198 g, 0.5 mmol) in THF (20 cm^3) was added slowly *via* cannula a cooled (-78 °C) solution of (**2.5**) (0.168 g, 0.5 mmol) in THF (20 cm^3). The reaction mixture was stirred at -78 °C for 1 h before reaching room temperature and stirring for a further 15 h. The volatiles were removed *in vacuo* and the residue extracted into petroleum (100

cm^3). Filtration through Celite, concentration of the filtrate to 10 cm^3 and cooling at –30 °C for 15 h gave (**3.2**) as yellow, X-ray diffraction quality crystals (0.05 g).

Yield: 0.05 g, 18%.

$\delta_H(C_6D_6)$ 0.54 (3H, s, silyl CH_3), 0.67 (3H, s, silyl CH_3), 0.76 (9H, s, $SiC(CH_3)_3$), 1.2-1.9 (10H, m, cyclohexyl CH_2s), 1.82 (3H, s, imine CH_3), 2.67 (6H, s, $N(CH_3)_2$), 3.03 (6H, s, $N(CH_3)_2$), 3.45 (1H, br t, cyclohexyl CH α to imine N), 6.67 (1H, dt, aromatic), 6.96-7.05 (2H, m, aromatics), 7.50 (1H, dd, aromatic).

$^{13}C\{^1H\}$ $\delta_C(C_6D_6)$ –1.11 (silyl CH_3), 2.06 (silyl CH_3), 21.37 ($SiC(CH_3)_3$), 21.72 (imine CH_3), 26.25, 26.52, 27.50 (cyclohexyl CH_2s), 28.21 ($SiC(CH_3)_3$), 32.21, 32.33 (cyclohexyl CH_2s), 43.99 ($N(CH_3)_2$), 44.33 ($N(CH_3)_2$), 64.77 (cyclohexyl CH α to imine N), 121.85, 129.76, 131.39, 131.87 (aromatic CHs), 134.11, 146.64 (quaternary aromatics), 170.48 (ArC(Me)=N(Cy)).

Found: C, 53.25; H, 8.57; N, 10.87. $C_{24}H_{45}N_4SiClZr$ requires C, 52.95; H, 8.33; N, 10.29%.

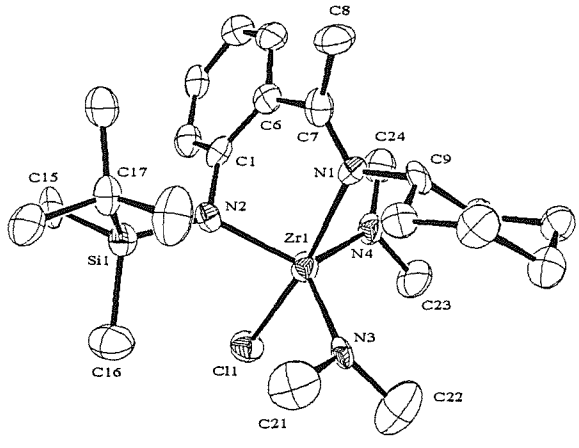

Figure 3.8: ORTEP representation of the crystal structure of [2-(1-cyclohexylimino-ethyl)-*N*-(*tert*-butyldimethylsilyl)-anilide] zirconium chloride bis-dimethylamide (**3.2**) (50% probability thermal ellipsoids). Hydrogens are omitted for clarity.

Table 3.3: Selected bond lengths (Å) and angles (°) for (**3.2**).

N(1)-Zr(1)	2.431(7)	N(2)-Zr(1)	2.082(7)
N(3)-Zr(1)	2.039(8)	N(4)-Zr(1)	2.070(7)

Cl(1)-Zr(1)	2.500(3)	N(2)-Si(1)	1.752(7)
C(1)-N(2)	1.422(10)	C(1)-C(6)	1.424(12)
C(6)-C(7)	1.463(12)	C(7)-N(1)	1.309(11)
C(7)-C(8)	1.519(13)	C(9)-N(1)	1.486(10)
C(21)-N(3)	1.370(13)	C(22)-N(3)	1.490(12)
C(23)-N(4)	1.437(11)	C(24)-N(4)	1.418(11)
N(2)-Zr(1)-N(1)	80.2(2)	N(3)-Zr(1)-N(4)	116.2(3)
N(3)-Zr(1)-N(2)	119.9(3)	N(4)-Zr(1)-N(2)	123.2(3)
N(1)-Zr(1)-Cl(1)	172.27(17)	C(1)-N(2)-Zr(1)	101.0(4)
C(1)-N(2)-Si(1)	120.0(5)	Si(1)-N(2)-Zr(1)	138.4(4)
C(6)-C(1)-N(2)	120.9(8)	C(1)-C(6)-C(7)	123.8(8)
N(1)-C(7)-C(6)	118.6(8)	N(1)-C(7)-C(8)	123.3(8)
C(6)-C(7)-C(8)	118.0(8)	C(7)-N(1)-Zr(1)	117.2(6)
C(7)-N(1)-C(9)	118.2(8)	C(9)-N(1)-Zr(1)	124.6(5)
C(21)-N(3)-Zr(1)	116.9(7)	C(22)-N(3)-Zr(1)	131.1(6)
C(21)-N(3)-C(22)	107.7(9)	C(23)-N(4)-Zr(1)	113.5(6)
C(24)-N(4)-Zr(1)	133.9(5)	C(23)-N(4)-C(24)	112.6(7)

3.8.3 [2-(1-Cyclohexylimino-ethyl)-*N*-(trimethylsilyl)-anilide] zirconium chloride bis-diethylamide (3.3).

To a stirred, cooled (-78 °C) solution of $Zr(NEt_2)_2Cl_2(THF)_2$ (0.225 g, 0.5 mmol) in THF (20 cm^3) was added slowly *via* cannula a cooled (-78 °C) solution of **(2.3)** (0.147 g, 0.5 mmol) in THF (20 cm^3). The reaction mixture was stirred at -78 °C for 1 h before being allowed to reach room temperature and stirred for a further 15 h. The volatiles were removed *in vacuo* and the residue extracted into petroleum (100 cm^3). Filtration through Celite, concentration of the filtrate to *ca.* 10 cm^3 and cooling at –30 °C for 15 h gave **(3.3)** as yellow, X-ray diffraction quality crystals (0.150 g).

Yield 0.150 g, 54%.

$\delta_H(C_6D_6)$ 0.35 (9H, s, silyl CH_3s), 0.8-2.2 (10H, m, cyclohexyl CH_2s), 0.91 (6H, t, $N(CH_2CH_3)_2$), 1.07 (6H, t, $N(CH_2CH_3)_2$), 1.77 (3H, s, imine CH_3), 3.17 (2H, br s, $N(CH_2CH_3)_2$), 3.3-3.7 (7H, m, cyclohexyl C*H* α to imine N and three signals for $N(CH_2CH_3)_2$), 6.75 (1H, dt, aromatic), 6.96-7.09 (2H, m, aromatics), 7.31 (1H, dd, aromatic).

$^{13}C\{^1H\}$ $\delta_C(C_6D_6)$ 3.20 (silyl CH_3s), 14.28, 14.41 ($N(CH_2CH_3)_2$), 21.78 (imine CH_3), 26.22, 26.57, 26.61, 32.29, 32.83 (cyclohexyl CH_2s), 42.70, 43.06 ($N(CH_2CH_3)_2$), 64.40 (cyclohexyl CH α to imine N), 121.92, 129.53, 131.85,

132.53 (aromatic*C*Hs), 134.70, 146.52 (quaternary aromatics), 169.52 (Ar*C*(Me)=N(Cy)).

Found: C, 54.05; H, 8.60; N, 10.15. $C_{25}H_{47}N_4SiClZr$ requires C, 53.77; H, 8.48; N, 10.03%.

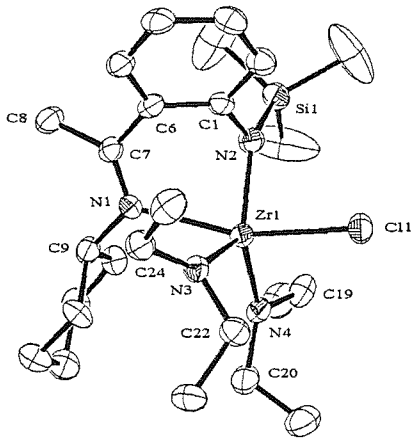

Figure 3.9: ORTEP representation of the crystal structure of [2-(1-cyclohexylimino-ethyl)-*N*-(trimethylsilyl)-anilide] zirconium chloride bis-diethylamide **(3.3)** (50% probability thermal ellipsoids). Hydrogens are omitted for clarity.

Table 3.4: Selected bond lengths (Å) and angles (°) for **(3.3)**.

N(1)-Zr(1)	2.460(4)	N(2)-Zr(1)	2.112(4)
N(3)-Zr(1)	2.047(4)	N(4)-Zr(1)	2.054(5)
Cl(1)-Zr(1)	2.5021(13)	N(2)-Si(1)	1.724(4)
C(1)-N(2)	1.426(7)	C(1)-C(6)	1.414(7)
C(6)-C(7)	1.494(8)	C(7)-N(1)	1.285(7)
C(7)-C(8)	1.518(7)	C(9)-N(1)	1.478(7)
C(22)-N(3)	1.473(7)	C(24)-N(3)	1.464(7)
C(19)-N(4)	1.451(7)	C(20)-N(4)	1.466(7)
N(2)-Zr(1)-N(1)	76.61(15)	N(3)-Zr(1)-N(2)	128.42(18)
N(4)-Zr(1)-N(2)	119.53(17)	N(3)-Zr(1)-N(4)	110.78(17)
N(1)-Zr(1)-Cl(1)	162.13(11)	Zr(1)-N(2)-C(1)	98.5(3)
C(1)-N(2)-Si(1)	115.2(4)	Si(1)-N(2)-Zr(1)	146.3(3)
C(6)-C(1)-N(2)	121.0(5)	C(1)-C(6)-C(7)	121.0(5)
N(1)-C(7)-C(6)	118.5(4)	N(1)-C(7)-C(8)	126.2(5)
C(6)-C(7)-C(8)	115.3(5)	C(7)-N(1)-Zr(1)	116.8(4)
C(7)-N(1)-C(9)	118.8(4)	C(9)-N(1)-Zr(1)	124.4(3)
C(22)-N(3)-Zr(1)	108.7(3)	C(24)-N(3)-Zr(1)	137.3(3)
C(24)-N(3)-C(22)	113.5(4)	C(19)-N(4)-Zr(1)	110.9(4)

C(20)-N(4)-Zr(1)	131.2(4)	C(19)-N(4)-C(20)	116.1(5)

3.8.4 [2-(1-Cyclohexylamido-vinyl)-*N*-(*tert*-butyldimethylsilyl)-anilide] zirconium chloride diethylamide tetrahydrofuran (3.4).

To a cooled (-78 °C), stirred solution of $Zr(NEt_2)_2Cl_2(THF)_2$ (0.225 g, 0.5 mmol) in THF (20 cm^3) was added slowly *via* cannula a solution of **(2.5)** (0.168 g, 0.5 mmol) in THF (20 cm^3). The light yellow mixture was stirred at –78 °C for 1h, allowed to reach room temperature and stirred for 15 h giving a yellow solution. Removal of the THF *in vacuo* was followed by extraction of the residue into petroleum (50 cm^3), The supernatant solution was then filtered and concentrated to *ca* 20 cm^3 and before cooling to –30 °C for 15 h gave orange, X-ray diffraction quality crystals.

Yield 0.135 g, 45%.

$\delta_H(C_6D_6)$ 0.27 (3H, s, silyl C*H*$_3$), 0.44 (3H, s, silyl C*H*$_3$), 0.76 (6H, t, N(CH_2CH_3)$_2$), 1.02 (9H, s, SiC(C*H*$_3$)$_3$), 0.8-2.4 (10H, m, cyclohexyl C*H*$_2$s), 1.32 (4H, m, THF), 2.81 (2H, br s, N(C*H*$_2$CH$_3$)$_2$), 3.01 (2H, br s, N(C*H*$_2$CH$_3$)$_2$), 3.40 (1H, tt, cyclohexyl C*H* α to vinylamide N), 3.69 (4H, t, THF), 4.24 (1H, s, C=C*H*$_2$), 4.39 (1H, s, C=C*H*$_2$), 6.90-7.02 (2H, m, aromatics), 7.10 (1H, dt, aromatic), 7.67 (1H, dd, aromatic).

$^{13}C\{^1H\}$ $\delta_C(C_6D_6)$ –1.57 (silyl C*H*$_3$s), 14.56 (N(CH_2*C*H$_3$)$_2$), 20.70 (Si*C*(CH$_3$)$_3$), 25.78 (THF), 26.42, 26.61 (cyclohexyl *C*H$_2$s), 27.33 (SiC(*C*H$_3$)$_3$), 32.93, 34.54 (cyclohexyl *C*H$_2$s), 42.79 (N(*C*H$_2$CH$_3$)$_2$), 63.58 (cyclohexyl *C*H α to vinylamide N), 70.25 (THF), 88.36 (ArC(N)=*C*H$_2$), 124.34, 128.45, 129.14 (aromatic *C*Hs), 130.26 (quaternary aromatic), 131.99 (aromatic *C*H), 140.71 (quaternary aromatic), 156.80 (Ar*C*(N)=CH$_2$).

Found: C, 56.36; H, 8.54; N, 7.15. $C_{28}H_{50}N_3SiOClZr$ requires C, 56.10; H, 8.41; N, 7.01%.

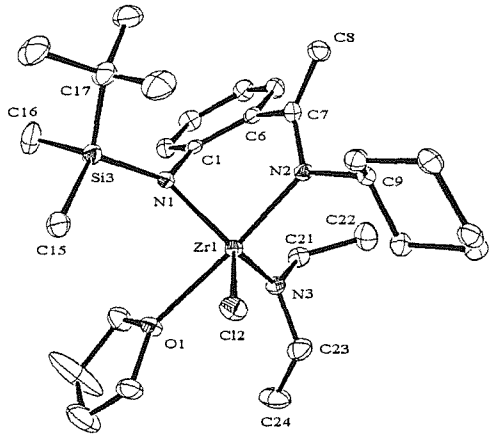

Figure 3.10: ORTEP representation of the crystal structure of [2-(1-cyclohexylamido-vinyl)-*N*-(*tert*-butyldimethylsilyl)-anilide] zirconium chloride diethylamide tetrahydrofuran (**3.4**) (50% probability thermal ellipsoids). Hydrogens are omitted for clarity.

Table 3.5: Selected bond lengths (Å) and angles (°) for (**3.4**).

N(1)-Zr(1)	2.052(2)	N(2)-Zr(1)	2.1290(19)
N(3)-Zr(1)	2.019(2)	Cl(2)-Zr(1)	2.4503(7)
Zr(1)-O(1)	2.3625(16)	C(1)-N(1)	1.426(3)
N(1)-Si(3)	1.755(2)	C(1)-C(6)	1.416(8)
C(6)-C(7)	1.499(4)	C(7)-N(2)	1.392(3)
C(7)-C(8)	1.348(3)	C(9)-N(2)	1.472(3)
C(17)-Si(3)	1.901(3)	C(15)-Si(3)	1.866(3)
C(16)-Si(3)	1.864(3)	C(21)-N(3)	1.465(3)
C(23)-N(3)	1.469(3)		

N(1)-Zr(1)-N(2)	89.5(8)	N(3)-Zr(1)-N(1)	115.42(9)
N(1)-Zr(1)-Cl(2)	119.55(6)	N(3)-Zr(1)-Cl(2)	122.11(7)
N(2)-Zr(1)-O(1)	174.85(7)	C(1)-N(1)-Zr(1)	104.00(15)
C(1)-N(1)-Si(3)	122.57(17)	Si(3)-N(1)-Zr(1)	132.89(13)
C(6)-C(1)-N(1)	120.5(2)	C(1)-C(6)-C(7)	123.1(2)
N(2)-C(7)-C(6)	115.1(2)	C(8)-C(7)-C(6)	117.7(3)
C(8)-C(7)-N(2)	127.1(3)	C(7)-N(2)-Zr(1)	118.02(16)
C(7)-N(2)-C(9)	115.00(19)	C(9)-N(2)-Zr(1)	126.96(16)
C(21)-N(3)-Zr(1)	133.21(17)	C(23)-N(3)-Zr(1)	110.21(18)
C(21)-N(3)-C(23)	114.4(2)		

Table 3.6: Crystallographic parameters for **(3.2)**, **(3.3)** and **(3.4)**.

Compound	**(3.2)**	**(3.3)**	**(3.4)**
Chemical Formula	$C_{24}H_{45}Cl_1N_4Si_1Zr_1$	$C_{25}H_{47}Cl_1N_4Si_1Zr_1$	$C_{28}H_{50}Cl_1N_3O_1Si_1Zr_1$
Formula Weight	544.40	558.43	599.47
Crystal System	Triclinic	Monoclinic	Monoclinic
Space Group	*P-1*	$P2_1/n$	$P2_1/n$
a/Å	9.293(5)	17.2365(7)	14.4679(4)
b/Å	11.022(6)	9.3683(5)	12.2609(3)
c/Å	15.424(9)	18.9138(13)	18.0837(6)
α/°	77.235(17)	90	90.0
β/°	87.70(2)	106.866(2)	104.3480(10)
γ/°	66.486(13)	90	90.0
V/Å^3	1410.8(14)	2922.8(3)	3107.80(15)
Z	2	4	4
T/K	150(2)	150(2)	150(2)
μ/mm^{-1}	0.544	0.527	0.502
F(000)	576	1184	1272
No. Data collected	8991	9956	12852
No. Unique data	5852	6424	7048
R_{int}	0.1214	0.0745	0.0506
Final $R(\|F\|)$ for $I>2\sigma(I)$	0.0985	0.0722	0.0419
Final $R(F^2)$ for all data	0.2069	0.2078	0.0912

3.8.5 [2-(1-Cyclohexylimino-ethyl)-*N*-(trimethylsilyl)-anilide] zirconium trichloride (3.5).

To a stirred, cooled (-78 °C) suspension of $ZrCl_4$ (0.233 g, 1 mmol) in toluene (50 cm^3) was added slowly *via* cannula a solution of **(2.3)** in toluene (50 cm^3). After completion of addition the reaction mixture was stirred at –78 °C for 1 h, allowed to reach room temperature and the resulting yellow solution was stirred for 24 h after which period it turned to an orange suspension. The supernatant was filtered and the toluene removed *in vacuo*. The residue was washed with petroleum (5 x 10 cm^3) yielding the product as an orange solid.

Yield: 0.11 g, 23%.

Found: C, 42.4; H, 6.0; N, 6.4. $C_{17}H_{27}N_2SiCl_3Zr$ requires C, 42.1; H, 5.6; N, 5.8%.

3.8.6 [2-(1-Cyclohexylimino-ethyl)-*N*-(trimethylsilyl)-anilide] zirconium trichloride (3.5).

Complex (**3.1**) (0.032 g, 0.07 mmol) was dissolved in C_6D_6 and placed in an NMR tube fitted with a Young's PTFE tap. Trimethylchlorosilane (8 drops) was added to the solution and the closed NMR tube was heated at 50 °C for 48 h. The volatiles were removed *in vacuo* to yield the product as a yellow oil.

$\delta_H(C_6D_6)$ 0.25 (9H, s, silyl CH_3s), 0.9-2.6 (10H, m, cyclohexyl CH_2s), 1.61 (3H, s, imine CH_3), 3.46 (1H, tt, cyclohexyl C*H* α to imine N), 6.88 (1H, dt, aromatic), 6.95-7.05 (2H, m, aromatics), 7.15-7.22 (1H, m, aromatic).

3.8.7 [2-(1-Cyclohexylimino-ethyl)-*N*-(trimethylsilyl)-anilide]-zirconium trichloride (3.5).

To a solution of (**3.3**) (0.200 g, 0.36 mmol) in benzene at room temperature was added *via* syringe trimethylchlorosilane (0.110 g, 1.00 mmol). The bright yellow solution was stirred for 15 h resulting in a very pale orange solution. The volatiles were removed *in vacuo* to yield the product as pale orange powder.

Yield: 0.165 g, 94%.

$\delta_H(C_6D_6)$ 0.25 (9H, s, silyl CH_3s), 0.9-2.6 (10H, m, cyclohexyl CH_2s), 1.59 (3H, s, imine CH_3), 3.44 (1H, tt, cyclohexyl C*H* α to imine N), 6.85 (1H, dt, aromatic), 6.95-7.05 (2H, m, aromatics), 7.15-7.22 (1H, m, aromatic).

3.8.8 Bis-[2-(1-cyclohexylamido-vinyl)-*N*-(*tert*-butyldimethylsilyl)-anilide] zirconium dichloride (3.6).

To a stirred and cooled (-78 °C) solution of $ZrCl_4(THT)_2$ (0.205 g, 0.5 mmol) in diethyl ether (50 cm^3)was added *via* cannula a solution of (**2.5**) (0.336 g, 1 mmol) in diethyl ether (50 cm^3). The reaction was stirred at –78 °C for 1 h, allowed to reach room temperature and then stirred for 24 h. From the pale yellow suspension the diethyl ether was removed *in vacuo* and the residue was extracted into petroleum (*ca.* 150 cm^3). The extracts were filtered, concentrated to *ca.* 25 cm^3 and the solution cooled to –30 °C to produce pale yellow crystals.

Yield 0.11 g, 27%.

$\delta_H(C_6D_6)$ -0.45-0.25 (12H, br. s, silyl CH_3s), 0.64 (18H, s, $SiC(CH_3)_3$), 1.10-1.90 (20H, m, cyclohexyl CH_2s), 2.00-2.20 (6H, br. s, imine CH_3s), 2.6-2.8 (2H, m, cyclohexyl C*H* α to imine N), 6.6-7.5 (8H, m, aromatics).

Found: C, 57.3; H, 8.0; N, 6.7. $C_{40}H_{66}N_4Si_2Cl_2Zr$ requires C, 58.5; H, 8.1; N, 6.8%.

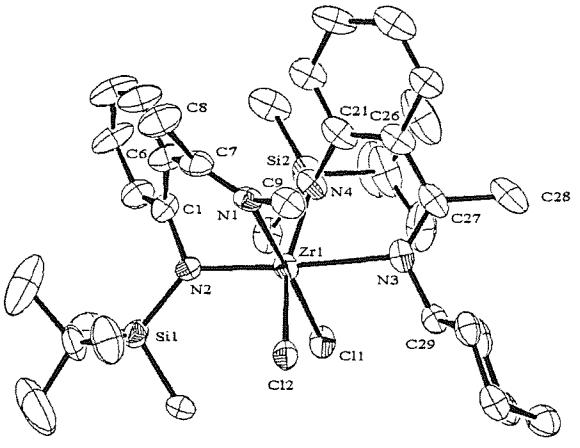

Figure 3.11: ORTEP representation of the crystal structure of bis-[2-(1-cyclohexylamido-vinyl)-*N*-(*tert*-butyldimethylsilyl)-anilide] zirconium dichloride (**3.6**) (50% probability thermal ellipsoids). One cyclohexyl group is removed for clarity [C(10)-C(14)]. Hydrogens are omitted for clarity.

Table 3.7: Selected bond lengths (Å) and angles (°) for (**3.6**).

N(1)-Zr(1)	2.366(4)	N(2)-Zr(1)	2.111(4)
N(3)-Zr(1)	2.459(4)	N(4)-Zr(1)	2.090(4)
Cl(1)-Zr(1)	2.4417(13)	Cl(2)-Zr(1)	2.4938(13)
N(2)-Si(1)	1.763(4)	N(2)-C(1)	1.419(6)
C(1)-C(6)	1.405(7)	C(6)-C(7)	1.495(7)
C(7)-N(1)	1.272(6)	C(7)-C(8)	1.522(7)
N(1)-C(9)	1.496(6)	N(4)-Si(2)	1.766(4)
N(4)-C(21)	1.438(6)	C(21)-C(26)	1.394(8)
C(26)-C(27)	1.474(7)	C(27)-N(3)	1.293(6)
C(27)-C(28)	1.516(7)	N(3)-C(29)	1.485(6)
N(1)-Zr(1)-N(2)	81.06(14)	N(3)-Zr(1)-N(4)	78.06(15)
N(2)-Zr(1)-N(3)	174.70(13)	N(1)-Zr(1)-Cl(1)	171.78(10)
N(4)-Zr(1)-Cl(2)	158.10(11)	Cl(1)-Zr(1)-Cl(2)	90.23(5)
Zr(1)-N(2)-C(1)	112.0(3)	Si(1)-N(2)-C(1)	118.3(3)
Si(1)-N(2)-Zr(1)	129.6(2)	N(2)-C(1)-C(6)	123.0(5)

C(1)-C(6)-C(7)	123.9(5)	C(6)-C(7)-N(1)	119.9(4)
C(8)-C(7)-N(1)	125.8(5)	C(6)-C(7)-C(8)	114.3(5)
C(7)-N(1)-Zr(1)	123.0(3)	C(7)-N(1)-C(9)	122.0(4)
C(9)-N(1)-Zr(1)	114.9(3)	Zr(1)-N(4)-C(21)	115.6(3)
Zr(1)-N(4)-Si(2)	127.6(2)	Si(2)-N(4)-C(21)	116.7(3)
N(4)-C(21)-C(26)	122.3(5)	C(21)-C(26)-C(27)	123.2(5)
C(26)-C(27)-N(3)	120.0(5)	C(28)-C(27)-N(3)	124.1(5)
C(26)-C(27)-C(28)	115.9(4)	C(27)-N(3)-Zr(1)	123.8(3)
C(29)-N(3)-Zr(1)	113.1(3)	C(27)-N(3)-C(29)	122.4(4)

3.8.9 [2-(1-Cyclohexylimino-ethyl)-*N*-(trimethylsilyl)-anilide] zirconium tris-dimethylamide (3.7).

$Zr(NMe_2)_4$ (0.067 g, 0.25 mmol) and **(2.2)** (0.072 g, 0.25 mmol) were dissolved in C_6D_6 and were placed in an NMR tube fitted with a Young's PTFE tap The tube was heated at 50 °C for 72 h during which period the progress of the reaction was monitored by NMR. After completion of the reaction the volatiles were removed *in vacuo* and the product was obtained as an orange oil which was characterised by NMR after redissolving in C_6D_6.

$\delta_H(C_6D_6)$ 0.26 (9H, s, silyl CH_3s), 1.00-1.80 (10H, m, cyclohexyl CH_2s), 1.84 (3H, s, imine CH_3), 2.99 (18H, s, $N(CH_3)_2$), 3.40 (1H, tt, cyclohexyl *CH* α to imine N), 6.72 (1H, dt, aromatic), 7.05-7.12 (2H, m, aromatic), 7.25 (1H, dd, aromatic).

3.8.10 Imido/imino zirconium dimeric complex (3.8).

$Zr(NMe_2)_4$ (0.134 g, 0.5 mmol) was dissolved in toluene (15 cm^3) and added *via* cannula to an ampoule containing **(2.2)** (0.288 g, 1.0 mmol). The reaction was heated at 100 °C for 24 hours and the toluene removed *in vacuo*. X-ray diffraction quality crystals were grown from a saturated petroleum solution. Once the crystals were formed it was not possible to dissolve them in inert deuterated solvents in order to obtain spectroscopic data.

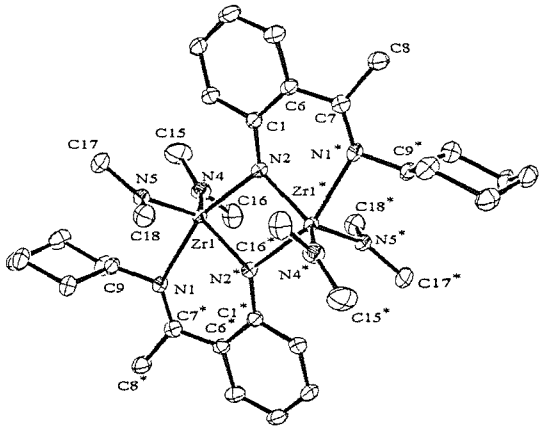

Figure 3.12: ORTEP representation of the crystal structure of the imido/imino zirconium dimer **(3.8)** (50% probability thermal ellipsoids). Hydrogens are omitted for clarity.

Table 3.8: Selected bond lengths (Å) and angles (°) for **(3.8)**.

N(2)-Zr(1*)	2.0652(14)	N(2)-Zr(1)	2.2187(15)
N(1)-Zr(1)	2.3069(14)	N(4)-Zr(1)	2.0623(16)
N(5)-Zr(1)	2.0653(14)	C(1)-N(2)	1.359(2)
C(1)-C(6)	1.439(2)	C(6)-C(7)	1.469(2)
N(1)-C(7*)	1.300(2)	N(1)-C(9)	1.489(2)
C(15)-N(4)	1.448(3)	C(16)-N(4)	1.455(3)
C(17)-N(5)	1.446(2)	C(18)-N(5)	1.449(2)
Zr(1)-Zr(1*)	3.3262(3)		

N(2*)-Zr(1)-N(1)	80.11(5)	N(2)-Zr(1)-N(1)	158.24(5)
N(4)-Zr(1)-N(2*)	119.77(6)	N(2*)-Zr(1)-N(5)	117.18(6)
N(4)-Zr(1)-N(5)	122.57(6)	Zr(1*)-N(2)-Zr(1)	101.81(6)
C(1)-N(2)-Zr(1*)	134.29(12)	C(1)-N(2)-Zr(1)	122.50(11)
N(2)-C(1)-C(6)	125.94(15)	C(1)-C(6)-C(7)	123.59(15)
N(1*)-C(7)-C(6)	120.98(16)	N(1*)-C(7)-C(8)	122.66(16)
C(6)-C(7)-C(8)	116.34(15)	C(7*)-N(1)-Zr(1)	133.18(12)
C(7*)-N(1)-C(9)	123.32(15)	C(9)-N(1)-Zr(1)	103.47(10)
C(15)-N(4)-Zr(1)	132.96(15)	C(16)-N(4)-Zr(1)	115.43(13)
C(15)-N(4)-C(16)	111.59(18)	C(17)-N(5)-Zr(1)	130.40(13)
C(18)-N(5)-Zr(1)	117.79(11)	C(17)-N(5)-C(18)	111.20(15)

Table 3.9: Crystallographic parameters for **(3.6)** and **(3.8)**.

Compound	**(3.6)**	**(3.8)**
Chemical Formula	$C_{40}H_{66}Cl_2N_4Si_2Zr_1$	$C_{18}H_{30}N_4Zr_1$
Formula Weight	821.27	393.68
Crystal System	Monoclinic	Monoclinic
Space Group	$P2_1/n$	$P2_1/n$
a/Å	10.494(2)	8.7107(2)
b/Å	31.860(6)	18.7443(4)
c/Å	14.365(3)	11.8704(2)
α/°	90.0	90.0
β/°	106.39(3)	103.130(1)
γ/°	90.0	90.0
V/Å^3	4607.6(16)	1187.48(7)
Z	4	4
T/K	150(2)	150(2)
μ/mm^{-1}	0.436	0.588
F(000)	1744	824
No. Data collected	45007	27335
No. Unique data	9212	4320
R_{int}	0.1328	0.0396
Final $R(\|F\|)$ for $I>2\sigma(I)$	0.0667	0.0269
Final $R(F^2)$ for all data	0.1685	0.0834

3.8.11 Ethylene polymerisation catalysis.

Complex **(3.1)** (0.050 g, 0.09 mmol) was dissolved in toluene (100 ml) in a glass pressure bottle. MAO (10% weight in toluene) (66.3 ml, 100 mmol) was added to the solution of **(3.1)**. This was stirred for 30 minutes at room temperature. The toluene solution was then saturated with ethylene at a pressure of 7 bar for 2 hours. A white solid was formed in the toluene solution during the catalytic run. After 2 hours the ethylene was blown off the system and the polymerization quenched by the addition of ethanol (5 ml). The polymeric solid that was produced was filtered away from the toluene solution and stirred over night in a 20 vol.-% ethanolic hydrochloric acid solution, then washed with water and ethanol and dried *in vacuo*.

Average yield of polyethylene produced: 9.068 g. This corresponds to a catalyst activity of *ca.* 8.8 g/mmol/bar/h. The melting point of the polyethylene was 210-220 °C.

This procedure was followed for **(3.6)** but on half the scale. The yield of polyethylene was 2.114 g. This corresponds to a catalyst activity of 3.02 g/mmol/bar/h. The melting point of the polyethylene was 217-230 °C.

3.9 References

1. A. A. Danopoulos, G. Wilkinson, T. K. N. Sweet, M. B. Hursthouse, *J. Chem. Soc. Dalton Trans.*, 1995, 205.
2. C. Weymann, A. A. Danopoulos, G. Wilkinson, T. K. N. Sweet, M. B. Hursthouse, *Polyhedron*, 1996, **15**, 3605.
3. R. M. Porter, S. Winston, A. A. Danopoulos and M. B. Hursthouse, *J. Chem. Soc. Dalton Trans.*, 2002, 3290.
4. B.-J. Deelman, P. B. Hitchcock, M. F. Lappert, H.-K. Lee, W.-P. Leung, *J. Organomet. Chem.*, 1996, **513**, 281.
5. B.-J Deelman, M. F Lappert, H.-K Lee, T. C. W. Mak, W.-P Leung, P.-R. Wei, *Organometallics*, 1997, **16**, 1247.
6. W. Kaminsky, R. Engehausen, K. Zoumis, *Makromol. Chem.*, 1992, **193**, 1643.
7. S. Brenner, R. Kempe, P. Arndt, *Z. Anorg. Allg. Chem.*, 1995, **621**, 2021.
8. F. M. Chung, A. D. Westland, *Can. J. Chem.*, 1969, **47**, 195.
9. D. C. Bradley, I. M. Thomas, *J. Chem. Soc.*, 1960, 3857.

Chapter 4

2-(1-Cyclohexylimino-ethyl)-*N*-(aryl)-anilide and Related Complexes of Titanium(IV) and Zirconium(IV)

4.1 Introduction

4.1.1 *N,N*-diaryl-β-diketiminate metal complexes

There has been a great interest in the study of β-diketiminate ligands in which the nitrogens are substituted with aryl groups. A series of different types of β-diketiminate complexes are depicted below (Scheme 4.1). The ligand syntheses often involve the condensation of a carbonyl with the appropriate aniline, and so the phenyl substituent can easily be introduced into the ligand framework.[1] This ease of synthesis allows for the phenyl group to be readily altered and thus steric effects can be studied.

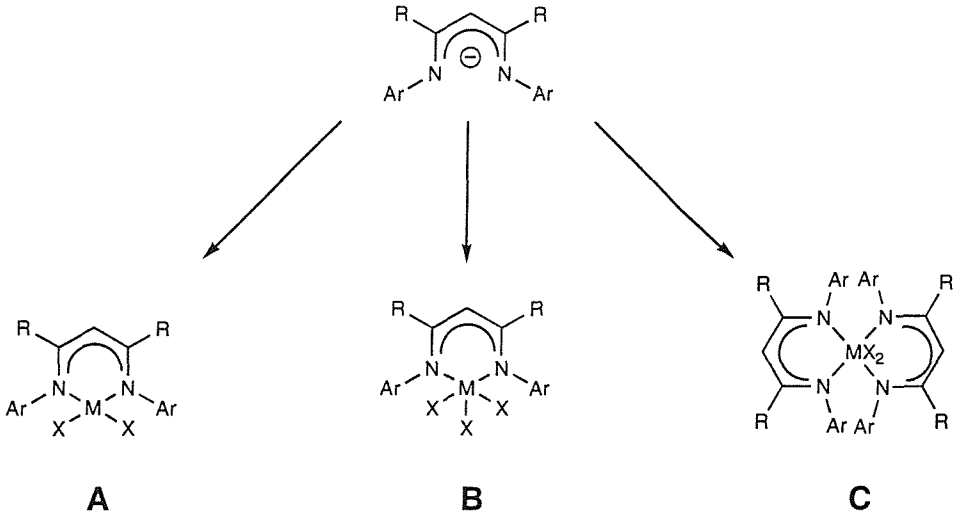

Scheme 4.1: The diaryl-substituted β-diketiminate ligand and three classes of Group 4 Metal complexes.

Three mono β-diketiminate complexes of the type $LMCl_2(THF)_2$ (M=Ti, V, Cr) utilising the $(Ph)_2$nacnac ligand [$(Ph)_2$nacnac = *N,N*-diphenyl-2,4-pentanediimine anion] were reported by Theopold and co-workers.[2] All three complexes were shown to be active ethylene polymerisation catalysts when activated with MAO. Similar work was reported by Budzelaar and co-workers

where a series of six *N*,*N*-diphenyl-β-diketiminate ligands were used to make LMX_2 (M=Ti, V; X=Cl, Me) type complexes.[3] In all of the cases studied it was possible to convert the $LVCl_2$ complexes to the $LVMe_2$ complexes by use of a suitable alkylating agent. The $LTiMe_2$ complexes were only stable if the *N*-phenyl group was 2,6-disubstituted. When cationic complexes were generated from the $LMMe_2$ species it was only the titanium complexes that were active for the polymerisation of α-olefins.

A series of mono *N*,*N*-diphenyl-β-diketiminate complexes of the type LMX_3 (M=Ti, Zr) have been prepared by Smith[4,5] utilising the $(o\text{-}MeC_6H_4)_2$nacnac and the $(2,6\text{-}Me_2C_6H_3)_2$nacnac ligands. The other ligands in these complexes include chlorides, dimethylamides and a mixture of the two. A zirconium complex bearing three benzyl groups was observed to undergo loss of toluene upon thermolysis to give a complex in which one of the *N*-phenyl groups has undergone orthometalation.[5]

Smith[4] and Collins[6] both reported a series of bis *N*,*N*-diphenyl-β-diketiminate complexes of the type L_2MX_2 (M=Ti, Zr; X=Cl, NMe_2). Structurally characterised examples showed that the β-diketiminate ligands did not possess equal bonds between the nitrogens and the metal. The geometry of the complexes placed two nitrogens *trans* to one another and the other two *trans* to the X ligands. The M-N bonds to the nitrogens *trans* to the X ligands were longer than those to the other nitrogens by *ca* 0.05-0.1Å.

4.1.2 2-(1-Aryliminomethyl)-*N*-(aryl)-anilide cationic yttrium complexes

Recent work reported by Piers concerns the synthesis of organoyttrium complexes of the 2-(1-aryliminomethyl)-*N*-(aryl)-anilide ligand (see Introduction, Chapter 2).[7] The ligand is shown to be capable of stabilising bis-alkyl yttrium complexes which act as precursors to cationic organoyttrium complexes. As yet, no catalytic data is reported. As mentioned previously, Piers' ligand is extremely similar to the arylamido/imino ligands reported in this thesis.

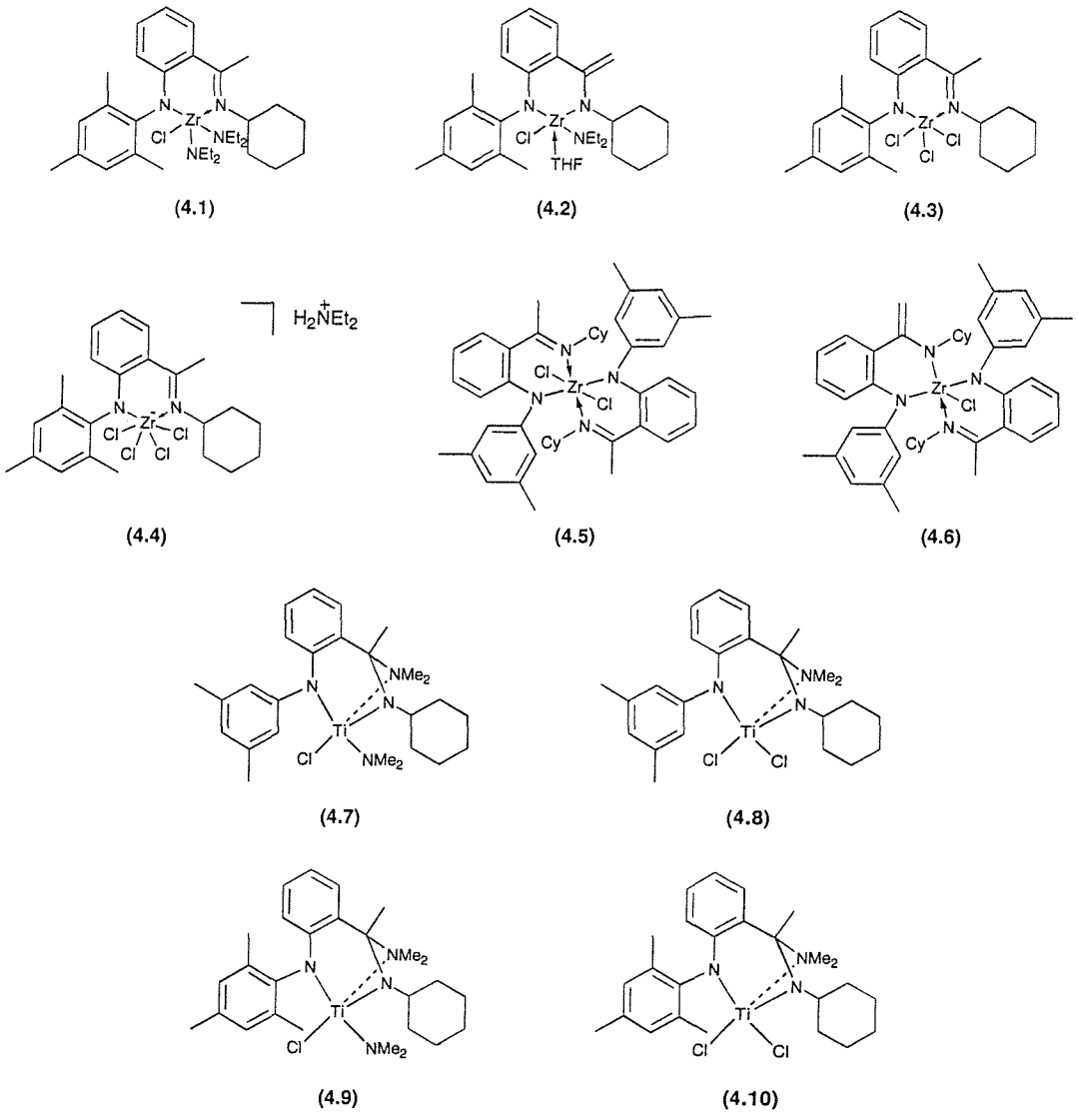

Figure 4.1: Zirconium (**4.1**)-(**4.6**) and titanium complexes (**4.7**)-(**4.10**) synthesised.

4.2 Synthesis of mono-arylamido/imino and related zirconium(IV) complexes

The salt elimination reaction between lithium [2-(1-cyclohexylimino-ethyl)-*N*-(2,4,6-trimethylphenyl)-anilide] (**2.9**) and $Zr(NEt_2)_2Cl_2(THF)_2$ afforded the [2-(1-cyclohexylimino-ethyl)-*N*-(2,4,6-trimethylphenyl)-anilide] zirconium chloride bis-diethylamide complex (**4.1**) in good yield. The addition was performed at -78 °C and the reaction allowed to reach RT. After stirring overnight the volatiles were removed and the bright orange residue extracted into petroleum.

Following a filtration through Celite to remove lithium chloride, the orange filtrate was concentrated and cooled to –30 °C to yield (**4.1**) as orange/yellow crystals.

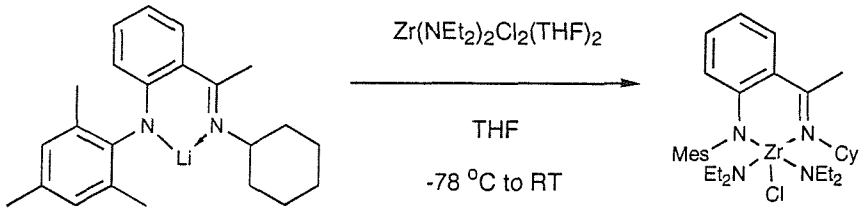

Scheme 4.2: Synthesis of (**4.1**).

It was essential to purify the compound by crystallisation due to the seemingly unavoidable presence of protonated amino/imino ligand (**2.8**) in the reaction mixture. In addition, the product was sometimes contaminated by the presence of a species that was identified as the arylamido/(cyclohexylamido)vinyl containing complex (**4.2**). This complex (**4.2**) was analogous to (**3.4**),[8] and because this was the second time we had observed this type of complex a concerted effort was made in order to understand the mechanism of its formation. Three main possibilities seemed apparent to us:

1. There was a small amount of a di-lithiated species present in the lithium amido/imino compound, which would then coordinate to the zirconium centre *via* a salt elimination reaction.
2. Upon coordination to the zirconium centre, the methyl group was undergoing deprotonation by a molecule of lithium amido/imino followed by a rearrangement to give the observed product.
3. The coordination of the ligand to the metal would occur, followed by an insertion of the cyclohexylimine group into a zirconium-diethylamide bond and elimination of one molecule of diethylamine across the carbon-carbon bond to give the vinylamide species.

The first possibility was discounted based on the ^{1}H, $^{13}C\{^{1}H\}$ and ^{7}Li NMR spectra of the lithium arylamido/imino compound (**2.9**), which showed no evidence of the presence of a second lithium species.

To test the second postulate the salt elimination reaction was performed using two equivalents of the lithium amido/imino ligand. This resulted in no more of the vinylamide containing complex being formed than in the 1:1 reactions. The ^{1}H NMR spectrum of the reaction mixture showed that the major species was still the 1:1 complex (**4.1**) and some unreacted lithium amido/imino (**2.9**).

Impure samples of the complex (**4.2**) were obtained in varying quantities from the reaction of (**2.9**) with $Zr(NEt_2)_2Cl_2(THF)_2$, following the removal from the system of the majority of (**4.1**) by crystallisation from petroleum. This enabled ^{1}H and $^{13}C\{^{1}H\}$ NMR spectra to be recorded for samples which were *ca.* 80% (**4.2**), but analytical data could not be obtained.

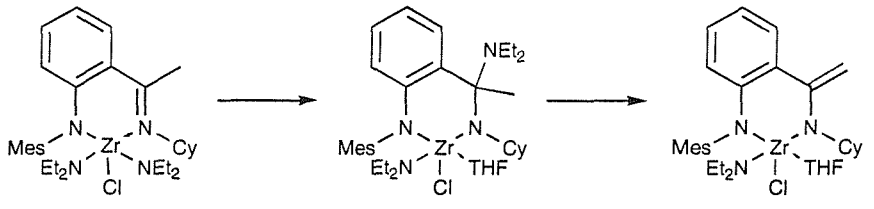

(4.1) **(4.2)**

Scheme 4.3: Proposed insertion-elimination mechanism for the conversion of (**4.1**) into (**4.2**).

The proposed mechanism for the formation of (**4.2**) is analogous to that discussed earlier for (**3.4**) (Chapter 3). It is highly plausible that following the formation of (**4.1**) there is a relatively low energy barrier to the formation of (**4.2**) *via* the insertion of the cyclohexylimine group into the zirconium-diethylamide bond. Since the insertion observed in (**3.4**) occurs when the bulkier *tert*-butyldimethylsilyl (rather than trimethylsilyl) and diethylamide (rather than dimethylamide) groups are employed it is reasonable to assume that the insertion is favoured because it reduces steric crowding about the zirconium centre.

Further indirect evidence for the existence of the diamido/amine containing intermediate is provided by the isolation of the 2-(1-cyclohexylamido-1-dimethylamino-ethyl)-*N*-(aryl)-anilide tripodal complexes (most likely formed by the insertion of the cyclohexylimino group into a titanium-dimethylamide bond) in (**4.7**), (**4.8**), (**4.9**) and (**4.10**) as discussed below. The facility of this transformation in the titanium system is possibly due to the smaller size of the metal center. Scott

reports an analogous migration of a benzyl group from a titanium and zirconium centre to the imine carbon of a linked bis-phenoxyimine ligand.[9,10] Piers observes similar behaviour in phenoxyimine complexes of scandium and yttrium where alkyls[11,12] and a hydride[13] are observed to migrate.

All attempts to introduce the arylamido/imino ligand onto a titanium(IV) or zirconium(IV) centre by transamination reactions between the amino/imino species [(**2.6**) or (**2.8**)] with $M(NR_2)_4$ or $M(NR_2)_2Cl_2$ starting materials (M=Ti, Zr, R= Me, Et) repeatedly failed. Despite performing the reactions in many different solvents at different temperatures the ^1H NMR spectra of the reactions always showed the presence of unreacted starting materials. The reason for this lack of reactivity of the amino/imino ligand is not clear and ensured that salt elimination reactions were the only route available to us to access arylamido/imino metal complexes.

It was possible to convert complex (**4.1**) into the [2-(1-cyclohexylimino-ethyl)-*N*-(2,4,6-trimethylphenyl)-anilide] zirconium trichloride complex (**4.3**) by reaction with an excess of trimethylchlorosilane in benzene. The product was obtained as an air and moisture sensitive bright yellow solid in high yield. It had very low solubility in benzene and other non-polar solvents and precipitated out of the reaction mixture as it was formed. The product was soluble in donor solvents allowing the NMR spectra to be recorded in d^8-THF. In addition to peaks assignable to (**4.3**), there were a series of minor peaks due to the free amino/imino ligand as well as benzene. Placing *ca.* 200 mg of (**4.3**) on a filter frit and washing it with *ca.* 200 cm^3 of petroleum failed to remove these impurities. This suggests that the impurities are trapped within the solid product and are only released upon dissolution of (**4.3**).

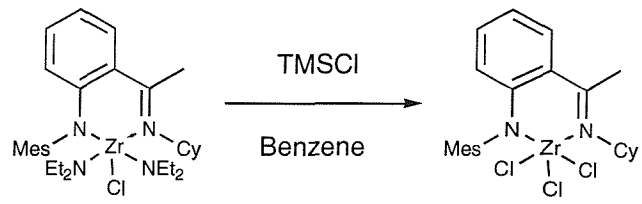

Scheme 4.4: Conversion of (**4.1**) into (**4.3**).

Repeated attempts to grow single crystals for an X-ray diffraction study of (**4.3**) finally yielded the anionic zirconium(IV) complex (**4.4**). A small crop of crystals was grown by slow diffusion of petroleum into a THF solution of (**4.3**). The six-coordinate zirconium complex is bound to one amido/imino ligand and four chloride ligands and the counter ion is a diethylammonium cation. We are not certain on how (**4.4**) was formed (especially the source of the cation). One explanation may involve partial decomposition (hydrolysis) of Me_3SiNEt_2 possibly trapped within the solid product during the long crystallisation.

Repeated attempts to react (**4.3**) with alkyl lithium reagents such as methyl lithium, neopentyl lithium, phenyl lithium and benzyl lithium as well as $LiNHBu^t$ yielded only complex reaction mixtures. Given the fact that several instances have been observed where the cyclohexylimino group has inserted into metal-amide bonds it is not inconceivable that a similar insertion is occurring if any metal-alkyl complexes are formed. The NMR spectra of these reactions were too complicated to identify any of the products and no crystals were grown suitable for a single crystal X-ray diffraction study.

4.2.1 NMR spectroscopy for compounds (4.1) and (4.2)

The NMR spectra of (**4.1**) are consistent with the trigonal bipyramidal geometry that is maintained in the solid state as shown by a single crystal X-ray diffraction study. As in the NMR spectra of the lithium amide (**2.9**), the methyls in the 2- and 6-positions and the aromatic CHs in the 3- and 5-positions each appear as singlets in both the proton and carbon NMR spectra. The cyclohexyl group again appears as four peaks in the $^{13}C\{^1H\}$ NMR spectrum. The four CH_2 groups of the diethylamide ligands appear as one peak in the $^{13}C\{^1H\}$ NMR spectrum but as two overlapping multiplets in the ^1H NMR spectrum. The four CH_3 groups of the diethylamide ligands appear as one peak in the $^{13}C\{^1H\}$ NMR spectrum and

one triplet in the ^{1}H NMR spectrum. This is different from the analogous N-silyl substituted $LZr(NEt_2)_2Cl$ complex **(3.3)** which had two signals for the four CH_3 groups of the diethylamide ligands in both the ^{1}H and $^{13}C\{^{1}H\}$ NMR spectra. The positions of the other peaks due to the ligand backbone are all comparable to the silylamido/imino zirconium complexes bearing two dialkylamides and a chloride ligand described in the previous chapter.

The ^{1}H NMR spectrum of **(4.2)** contains three methyl resonances in the ratio of 1:1:1, all assignable to the mesityl group. In contrast to **(4.1)**, in this complex the two sides of the mesityl group are inequivalent, giving rise to six aromatic signals in the $^{13}C\{^{1}H\}$ NMR spectrum assignable to the mesityl ring. There is no resonance for an imino methyl group but instead two singlets at 4.52 and 4.96 ppm, which integrate as one proton each. These are assignable to the two vinyl protons and appear in similar positions to those of **(3.4)**. In a C-H NMR correlation experiment both signals are coupled to a CH_2 carbon signal at 102.77 ppm. The latter is shifted downfield relative to the corresponding signal of **(3.4)** which appears at 88.7 ppm. The methine cyclohexyl carbon appears at 61.06 ppm and is shifted slightly upfield relative to **(4.1)**.

The diasterotopic protons of the CH_2 segments of the diethylamide ligand appear as two broadened multiplets at *ca.* 2.9 and 3.4 ppm and one carbon signal at 41.26 ppm. The methyl groups appear as a triplet at 0.90 ppm in the ^{1}H NMR spectrum and a signal at 13.14 ppm in the $^{13}C\{^{1}H\}$ NMR spectrum. The coordinated THF appears in the ^{1}H NMR spectrum at 3.78 and 1.26 ppm, and in the $^{13}C\{^{1}H\}$ NMR spectrum at 25.98 and 71.75 ppm.

4.2.2 X-ray diffraction study on (4.1)

X-ray diffraction quality crystals of **(4.1)** were grown by cooling a saturated petroleum solution to –30 °C to give the product as yellow blocks.

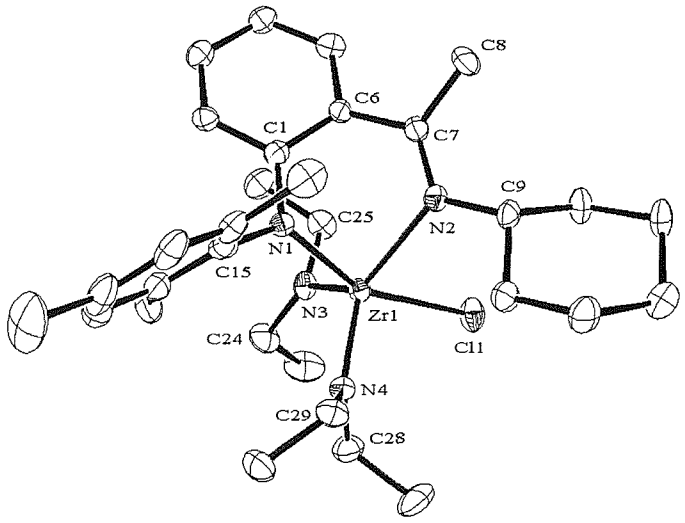

Figure 4.2: ORTEP representation of the crystal structure of [2-(1-cyclohexylimino-ethyl)-*N*-(2,4,6-trimethylphenyl)-anilide] zirconium chloride bis-diethylamide (**4.1**) (50% probability thermal ellipsoids). Hydrogens are omitted for clarity.

The molecule adopts a distorted trigonal bipyramidal geometry similar to the analogous $LZr(NR_2)_2Cl$ type complexes (**3.2**) and (**3.3**) synthesised using the silylamido/imino ligands. The structure of complex (**4.1**) differs from those of (**3.2**) and (**3.3**) in the way the donor atoms are arranged in the distorted trigonal bipyramid. In the structures of (**3.2**) and (**3.3**) the equatorial plane consists of the silylamide nitrogen and the two dialkylamides, with the imine nitrogen and the chloride occupying the axial sites. In the structure of (**4.1**) the equatorial sites are occupied by the two dialkylamides and the imine nitrogen leaving the chloride and arylamide nitrogen in the axial sites. The zirconium-arylamide [2.180(2)Å] and the zirconium-imine [2.315(2)Å] bond distances are comparable to those of (**3.2**) and (**3.3**). The bite angle of the amido/imino ligand [75.51(8)°] is comparable to that of the ligand in (**3.3**) [76.61(15)°], but *ca.* 5° more acute than that of the bulkier ligand in complex (**3.2**). The planarity of the arylamide group indicates a strong π-bonding interaction with zirconium. The C(7)-N(2) bond length of 1.300(3)Å and the C(7)-C(8) distance of 1.500(4)Å shows that the imine bond is maintained in this complex. The zirconium-diethylamide bond distances [Zr(1)-N(3) 2.027(2);

Zr(1)-N(4) 1.999(2)Å] and the zirconium-chloride bond length [2.5228(9)Å] are typical.[4,6,8]

The trigonal bipyramidal structure of **(4.1)** differs from the square pyramidal structure of an analogous β-diketiminate zirconium(IV) complex of the type $LZr(NMe_2)_2Cl$ reported by Smith.[4] The apical position is occupied by a dimethylamide and the β-diketiminate ligand bonds to the metal centre in a more symmetric manner [Zr-N 2.249(2), 2.319(2)Å] than the amido/imino ligand in **(4.1)**. It is interesting to note that the bond lengths to the β-diketiminate ligand are closer in magnitude to the imine in **(4.1)** than the amide.

4.2.3 NMR spectroscopy for complex (4.3)

The conversion of **(4.1)** to **(4.3)** by reaction with trimethylchlorosilane[4,14] was first carried out as an NMR scale reaction in C_6D_6. This resulted in the precipitation of **(4.3)** as a bright yellow solid within the NMR tube. When the reaction was scaled up, the ^1H and $^{13}C\{^1H\}$ NMR spectra of **(4.3)** were recorded in d^8-THF. The four methyl groups of the ligand appear as three signals in the ratio 2:1:1 with the methyl groups in the 2- and 6-positions of the mesityl ring being equivalent. The cyclohexyl CH which is α to the imine nitrogen is greatly shifted downfield in the ^1H NMR spectrum relative to the other compounds reported here and appears at 5.08 ppm. The carbon resonance appears at a fairly typical position of 66.17 ppm and their correlation was confirmed by a C-H correlation experiment.

4.2.4 X-ray diffraction study on (4.4)

X-ray diffraction quality crystals of [2-(1-cyclohexylimino-ethyl)-*N*-(2,4,6-trimethylphenyl)-anilide] zirconium tetrachloride diethylammonium salt **(4.4)** were obtained by layering a THF solution of **(4.1)** with petroleum. Slow diffusion of the petroleum layer into the THF solution afforded **(4.4)** as yellow blocks.

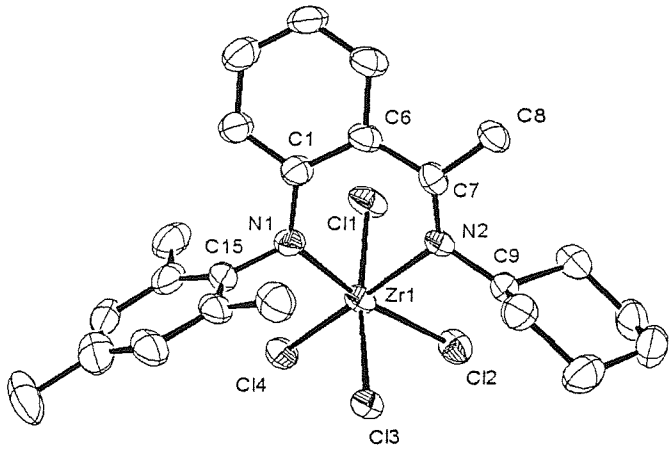

Figure 4.3: ORTEP representation of the crystal structure of the anion from the [2-(1-cyclohexylimino-ethyl)-*N*-(2,4,6-trimethylphenyl)-anilide] zirconium tetrachloride diethylammonium salt (**4.4**) (50% probability thermal ellipsoids). Hydrogens are removed for clarity.

The structure consists of one [2-(1-cyclohexylimino-ethyl)-*N*-(2,4,6-trimethylphenyl)-anilide] ligand and four chlorides bound to a zirconium(IV) centre. This means that the complex is monoanionic and this charge is balanced by a diethylammonium cation. The unit cell also contains two molecules of THF. The coordination geometry of the anion is distorted octahedral with a bite angle for the amido/imino ligand of 79.85(13)°. The zirconium-amide [2.118(4)Å] and zirconium-imine [2.289(3)Å] bond lengths are similar to those in (**4.1**). The zirconium-chloride bond lengths are within the typical range. The imine bond length of 1.293(5)Å is comparable to those found in the other complexes reported here.

4.3 X-ray diffraction studies on bis-(arylamido/imino) and related zirconium(IV) complexes

The X-ray crystal structures of two zirconium complexes each containing two amido/imino or related ligands were recorded. The crystals of complex (**4.5**), a bis-amido/imino zirconium dichloride species, were obtained from a reaction between one equivalent of lithium amido/imino (**2.7**) and $CpZrCl_3$ in very low

yield as part of a complicated mixture. The ^{1}H NMR spectrum of a reaction aliquot was also complicated, and the crystals isolated were only used for structure determination. The crystal structure that is included here provides useful comparison to the analogous *tert*-butyldimethylsilyl-substituted complex (**3.6**). Surprisingly, repeated attempts to synthesise (**4.5**) by using a rational methodology, i.e. reaction of two equivalents of (**2.7**) with $ZrCl_4(THT)_2$, were unsuccessful.

Complex (**4.6**) contains one amido/imino ligand, one arylamido/vinylamido ligand, and one chloride. The arylamido/vinylamido ligand is the 3,5-xylyl substituted analogue of the silylamido/vinylamido ligand observed in complex (**3.4**) and the mesitylamido/vinylamido ligand postulated in complex (**4.2**). As with complex (**4.5**), only the crystal structure of (**4.6**) was obtained. This was because only a small crop of crystals could be isolated from a petroleum solution of the reaction products and therefore there was not enough material to record the NMR spectra. The crystals were obtained from a reaction that was thought to be between one equivalent of (**2.7**) and $Zr(NMe_2)_2Cl_2(THF)_2$, but subsequently it was found that the zirconium starting material had undergone decomposition in the glove box. Therefore the structure is only included here due to its novelty since it represents the only example in which the 2-(1-cyclohexylimino-ethyl)-*N*-(3,5-dimethylphenyl)-anilide and 2-(1-cyclohexylamido-vinyl)-*N*-(aryl)-anilide ligands coexist on the same metal centre.

4.3.1 X-ray diffraction study on (4.5)

X-ray diffraction quality crystals of (**4.5**) were grown by cooling a saturated petroleum solution to –30 °C to give the product as orange plates.

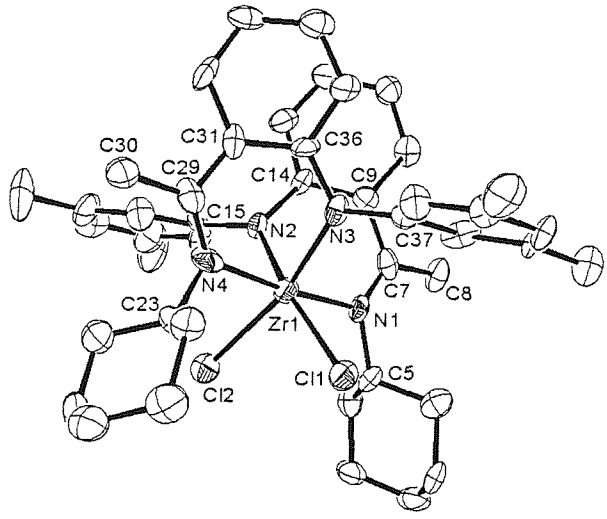

Figure 4.4: ORTEP representation of the crystal structure of isomer A of bis-[2-(1-cyclohexylimino-ethyl)-*N*-(2,4,6-trimethylphenyl)-anilide] zirconium dichloride (**4.5A**) (50% probability thermal ellipsoids). Hydrogens are omitted for clarity.

The unit cell of (**4.5**) contained two different coordination isomers of the complex. In isomer A (**4.5A**) (Figure 4.4, above) the two amido/imino ligands are arranged such that the two imine groups are *trans* to each other and the two *cis* amides are each *trans* to a chloride ligand. This means that the geometry of the complex is distorted octahedral with *cis* chlorides. In isomer B (**4.5B**) (Figure 4.5, below) the amido/imino ligands are arranged such that the imine group of one ligand is *trans* to the amide group of the other ligand. The two *cis* chlorides are *trans* to the remaining amide and the imine groups. Despite the different coordination geometry the complex remains distorted octahedral with *cis* chlorides.

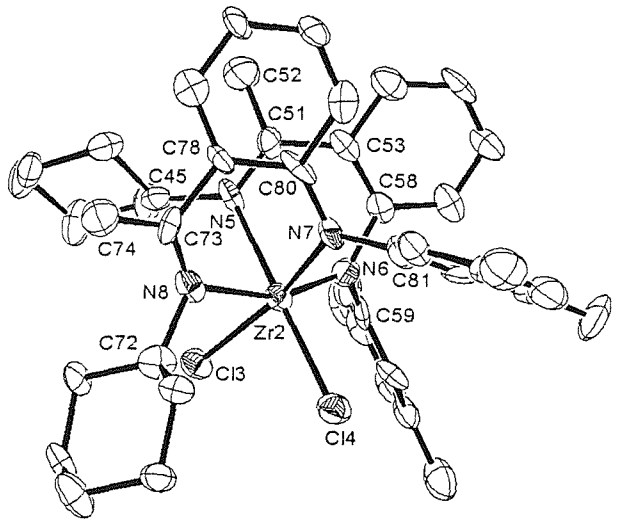

Figure 4.5: ORTEP representation of the crystal structure of isomer B of bis-[2-(1-cyclohexylimino-ethyl)-*N*-(2,4,6-trimethylphenyl)-anilide] zirconium dichloride (**4.5B**) (50% probability thermal ellipsoids). Hydrogens are omitted for clarity.

The average bite angle of the amido/imino ligand in each isomer is very similar [(**4.5A**) 77.7(6)°; (**4.5B**) 76.7(6)°]. The Cl-Zr-Cl angle is larger in (**4.5A**) than in (**4.5B**) [(**4.5A**) 94.91(12)°; (**4.5B**) 91.65(12)°]. This is possibly because with the lower symmetry geometry of (**4.5B**), the xylyl and cyclohexyl rings are placed in closer proximity to one another. They would therefore repel each other more and result in the amido/imino ligands forcing the chlorides closer together. The more symmetrical geometry of (**4.5A**) results in those rings being further away from one another and so the chloride ligands are not forced closer together. In comparison, the analogous L_2ZrCl_2 complex (**3.6**), featuring the bulkier *tert*-butyldimethylsilyl substituted amido/imino ligand, adopts the coordination geometry displayed by (**4.5B**). The larger bite angle of the ligand in (**3.6**) [79.56(21)°] and corresponding smaller Cl-Zr-Cl angle [90.23(5)°] suggest that as the steric bulk of the amido-substituent is increased the *cis* chlorides are forced closer together. The same arrangement is adopted in the bis-[2-cyclohexyliminomethyl-*N*-(trimethylsilyl)-anilide] zirconium dichloride complex prepared previously within the Danopoulos group,[8] suggesting that this geometry is favoured over the C_2 symmetric geometry of (**4.5A**) in amido/imino L_2ZrCl_2

complexes despite the steric constraints. The same geometry as (**4.5A**) is almost universally adopted by the many isoelectronic phenoxy/imine L_2ZrCl_2 complexes reported in both this thesis (Chapter 5) and the literature.[15,16,17]

The zirconium-amide and zirconium-imine bond lengths are similar in both isomers [(**4.5A**) Zr-N(amide) 2.117(14)Å, Zr-N(imine) 2.253(15)Å; (**4.5B**) Zr-N(amide) 2.100(16)Å, Zr-N(imine) 2.308(15)Å] and the zirconium-chloride bond lengths lie within the typical range. The planar nature of the amide groups again implies that they are acting as strong π-donors. The carbon-nitrogen bond lengths of the imine group [(**4.5A**) 1.304(23); (**4.5B**) 1.305(22)Å] are typical of C=N double bond and show that the imine moiety is still present in all four ligands in both isomers, and has not undergone any of the rearrangement reactions observed in here.

4.3.2 X-ray diffraction study on (4.6)

X-ray diffraction quality crystals of (**4.6**) were grown by cooling a saturated petroleum solution to –30 °C to give the product as orange needles.

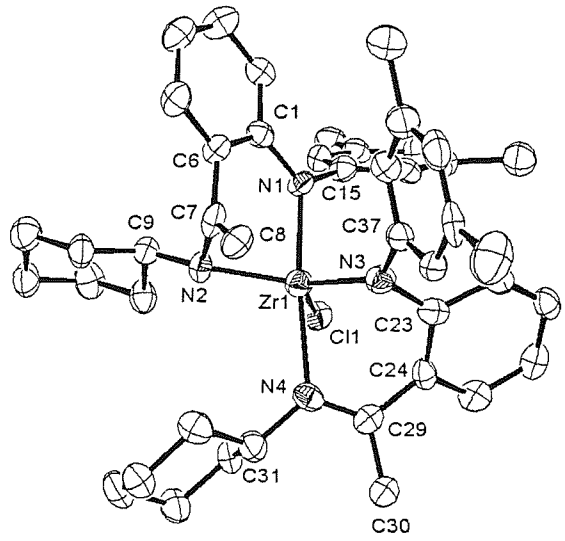

Figure 4.6: ORTEP representation of the crystal structure of [2-(1-cyclohexylimino-ethyl)-*N*-(3,5-dimethylphenyl)-anilide] [2-(1-cyclohexylamido-vinyl)-*N*-(3,5-dimethylphenyl)-anilide] zirconium chloride (**4.6**) (50% probability thermal ellipsoids). Hydrogens are omitted for clarity.

The structure of (**4.6**) consists of a regular amido/imino ligand, an arylamido/vinylamido ligand, and one chloride about a zirconium(IV) centre. The increased C(7)-N(2) bond length [1.416(8)Å] shows that there is no imine group present in the diamide ligand. This contrasts with the imine bond length [C(29)-N(4) 1.296(7)Å] in the amido/imino ligand. The difference in the carbon-carbon bond lengths of the diamide ligand [C(7)-C(8) 1.329(8)Å] and the amido/imino ligand [C(29)-C(30) 1.510(7)Å] is also strong evidence of the fact that there is an olefin present in the diamide ligand. The olefin bond length and the C(vinyl)-N(amide) bond lengths of (**4.6**) are very similar to those observed in complex (**3.4**). The bite angle of the arylamido/vinylamido ligand [N(1)-Zr(1)-N(2) 84.01(18)°] is larger than that of the amido/imino ligand [N(3)-Zr(1)-N(4) 80.04(18)°]. The three zirconium-amide bond lengths [Zr(1)-N(1) 2.172(4)Å; Zr(1)-N(2) 2.054(5)Å; Zr(1)-N(3) 2.122(5)Å] are similar and are significantly shorter than the zirconium-imine bond length [Zr(1)-N(4) 2.356(5)Å]. As in the other complexes reported here in which the cyclohexylimine group is converted into an amide group, the Zr-N bond length is shorter than that of the aryl or silyl substituted amide.

4.4 Formation of a 2-(1-cyclohexylamido-1-dimethylamino-ethyl)-*N*-(aryl)-anilide tripodal ligand *via* reaction of (2.7) and (2.9) with $Ti(NMe_2)_2Cl_2$

An unexpected result was obtained when reacting the amido/imino lithium compounds (**2.7**) and (**2.9**) with $Ti(NMe_2)_2Cl_2$. The amido/imino ligand was converted to a diamido/amino species and acted as a tridentate donor to the titanium(IV) centre. This ligand is dianionic and formally a ten electron donor.

The reaction of (**2.7**) or (**2.9**) with $Ti(NMe_2)_2Cl_2$ produced a mixture of two products. One product was identified as containing the diamido/amino ligand, a dimethylamide and a chloride, whilst the second product contained the diamido/amino ligand and two chlorides. The dimethylamide containing complex is the major product in both reactions (>5:1).

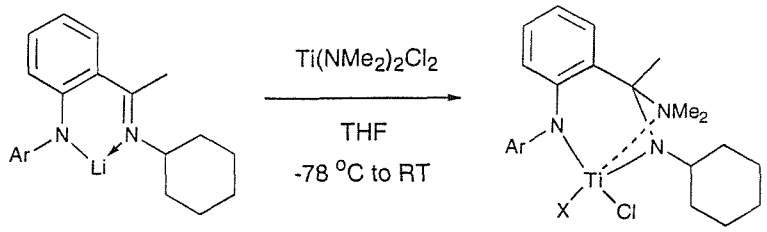

(**4.7**) Ar = xylyl, X = NMe_2; (**4.8**) Ar = xylyl, X = Cl.

(**4.9**) Ar = mesityl, X= NMe_2; (**4.10**) Ar = mesityl, X = Cl.

Scheme 4.5: Reactions between the lithium-amido/imino compounds (**2.7**) and (**2.9**) with $Ti(NMe_2)_2Cl_2$ to give (**4.7**), (**4.8**), (**4.9**) and (**4.10**).

The most likely mechanism for the formation of the tripodal ligand involves the insertion of the cyclohexylimine group into the titanium-dimethylamide bond. In the case of (**4.7**) and (**4.9**), the first step of the mechanism would be the salt metathesis reaction between the lithium amido/imino species and $Ti(NMe_2)_2Cl_2$. This would eliminate lithium chloride and give the anticipated $LTi(NMe_2)_2Cl$ type complex. The insertion of the cyclohexylimine group into the titanium-dimethylamide bond would then occur to give (**4.7**) and (**4.9**).

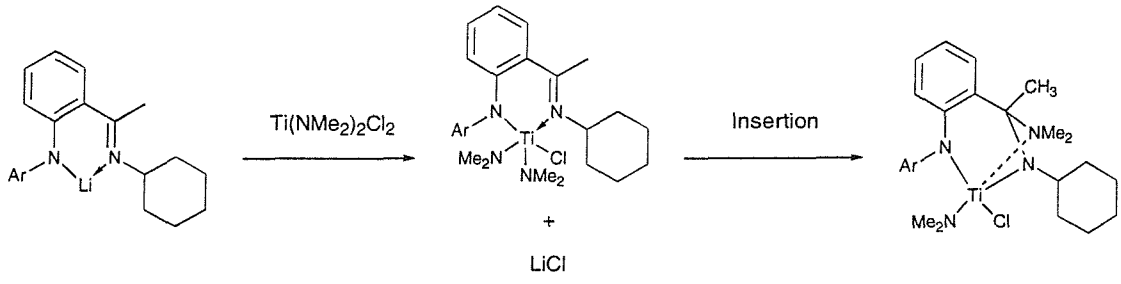

Scheme 4.6: Proposed mechanism for the formation of (**4.7**) and (**4.9**).

The salt metathesis mechanism does not appear to account for the presence of the minor, dichloride complexes (**4.8**) and (**4.10**). These complexes are very similar to a zirconium complex prepared previously in the Danopoulos group.[8] In this case the generation of a tripodal ligand was the result of a transamination reaction between 2-(*tert*-butyliminomethyl)-*N*-(trimethylsilyl)-aniline and $Zr(NMe_2)_2Cl_2(THF)_2$ performed at 100 °C in toluene. The dimeric dichloride species was isolated in low yield and identified as one part of a complicated

reaction mixture. It is likely in this case that the ligand is coordinated to the zirconium centre after the transamination reaction and the *tert*-butylimino group then rapidly inserts into the zirconium-nitrogen bond of the remaining dimethylamide ligand.

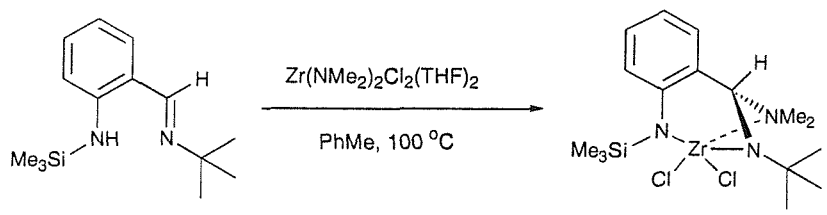

Scheme 4.7: Preparation of a complex containing a similar tripodal ligand within the Danopoulos group.

It seemed possible that (**4.8**) and (**4.10**) are formed by the same insertion mechanism as (**4.7**) and (**4.9**) after a small amount of the lithium amido/imino ligand is reprotonated in the reaction vessel, before performing a transamination reaction with $Ti(NMe_2)_2Cl_2$. To test this hypothesis, transamination reactions were attempted between (**2.6**) and (**2.8**) with $Ti(NMe_2)_2Cl_2$ in THF, toluene, d^8-toluene and d^6-benzene. When performed at the same temperature as the salt metathesis reactions there were no transamination reactions observed for either ligand in any of the solvents. When the temperature of the reactions was increased incrementally no reaction could be observed until the temperature was raised above 100 °C when the reaction would darken considerably and the resultant NMR spectra were extremely broad and did not match the NMR spectra of any of the identified products. This suggests that it is unlikely that a transamination reaction occurs at RT in the reaction vessel between $Ti(NMe_2)_2Cl_2$ and some regenerated amino/imino ligand. Another possibility is that in the salt metathesis reaction a small proportion of lithium dimethylamide is eliminated instead of lithium chloride. This appears unlikely and it remains unclear how (**4.8**) and (**4.10**) are formed.

4.4.1 X-ray diffraction study on (4.8)

X-ray diffraction quality crystals of (**4.8**) were grown by cooling a saturated petroleum solution to –30 °C to give the product as red blocks.

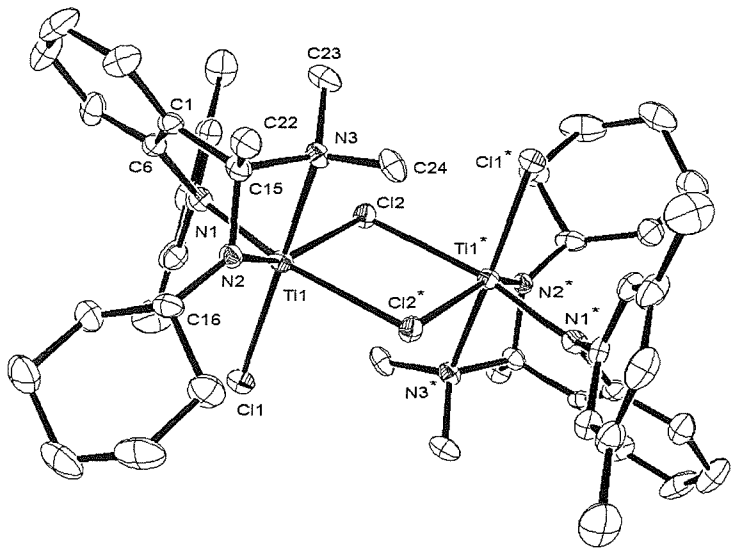

Figure 4.7: ORTEP representation of the crystal structure of [2-(1-cyclohexylamido-1-dimethylamino-ethyl)-*N*-(3,5-dimethylphenyl)-anilide] titanium dichloride (**4.8**) (50% probability thermal ellipsoids). Hydrogens are omitted for clarity.

Compound (**4.8**) is a centrosymmetric dimer with bridging chlorides. The titanium centres are formally six-coordinate with distorted octahedral geometry. The tripodal ligand occupies one face of the distorted octahedron. The titanium-nitrogen bond lengths support the presence of two anionic amide groups and one neutral amine group [Ti(1)-N(1) 1.954(3); Ti(1)-N(2) 1.890(3); Ti(1)-N(3) 2.224(3)Å]. This is also supported by the absence of the imine double bond [C(15)-N(2) 1.470(4)Å] and the bond angles about the dative amine. With the cyclohexylamide group separated from the dative amine group by one carbon, a highly strained four membered metallocycle is formed with a chelate angle of 65.64(11)°. Despite the strain present at the cyclohexylamide group it remains essentially planar, as does the xylylamide group. The three bite angles of the tripodal ligand [N(1)-Ti(1)-N(2) 90.11(12)°; N(2)-Ti(1)-N(3) 65.64(11)°; N(1)-

Ti(1)-N(3) 87.35(11)°] are comparable to the analogous zirconium complex synthesised previously.

4.4.2 X-ray diffraction study on (4.9)

X-ray diffraction quality crystals of (**4.9**) were grown by cooling a saturated petroleum solution to –30 °C to give (**4.9**) as orange plates.

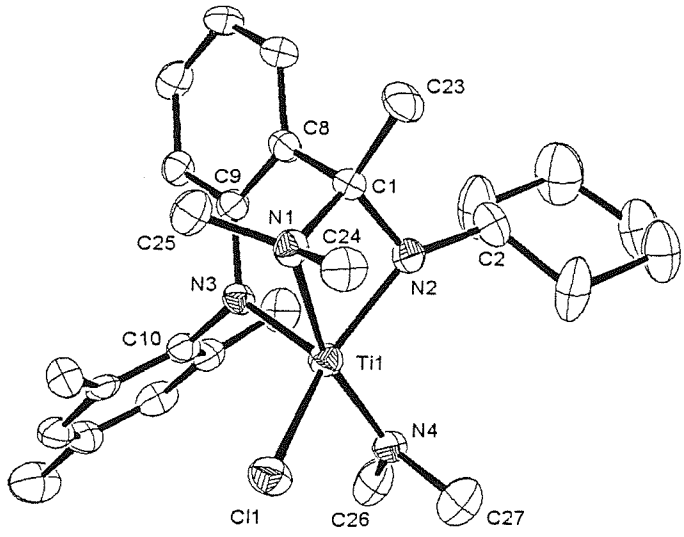

Figure 4.8: ORTEP representation of the crystal structure of [2-(1-cyclohexylamido-1-dimethylamino-ethyl)-*N*-(2,4,6-trimethylphenyl)-anilide] titanium chloride dimethylamide (**4.9**) (50% probability thermal ellipsoids). Hydrogens are omitted for clarity.

The structure of complex (**4.9**) is monomeric with a five coordinate titanium centre. The geometry about titanium is best described as distorted trigonal bipyramidal with the two amide nitrogens and the chloride ligand in the equatorial plane [N(2)-Ti(1)-N(3) 95.19(16)°; N(2)-Ti(1)-Cl(1) 132.94(13)°; N(3)-Ti(1)-Cl(1) 118.74(12)°] and with the dimethylamide and the amine nitrogens occupying the axial positions [N(1)-Ti(1)-N(4) 159.36(17)°]. As with the structure of (**4.8**), the different nature of the nitrogen atoms is clearly demonstrated by the titanium-nitrogen bond lengths with the three amide bonds [N(3)-Ti(1) 1.934(4); N(2)-Ti(1) 1.914(4); N(4)-Ti(1) 1.918(4)Å] being shorter than the Ti-N(amine) bond [N(1)-Ti(1) 2.291(4)Å]. The two amide groups are planar. The C(1)-N(2) bond length of

1.480(6)Å again demonstrates the absence of the imine moiety. The bite angles of the tripodal ligand [N(3)-Ti(1)-N(2) 95.19(16)°; N(2)-Ti(1)-N(1) 64.95(15)°; N(1)-Ti(1)-N(3) 87.04(16)°] are comparable to those of the analogous ligand in complex (**4.8**).

4.4.3 NMR spectroscopy for compounds (4.7), (4.8), (4.9) and (4.10)

The newly generated chiral carbon in the tripodal ligands appears in the $^{13}C\{^{1}H\}$ NMR spectra at *ca.* 86 ppm. It is sp^3 hybridized but it is α to both the cyclohexylamide group and the dimethylamine group. The methyl group located on this carbon atom is shifted upfield relative to the amido/imino ligand and now appears between 1.25 and 1.50 ppm. The two methyl groups of the amine moiety are diastereotopic and are separated by 0.3-0.6 ppm in the ^{1}H NMR spectra, appearing between 1.78 and 2.51 ppm. The two amine methyl groups appear as two signals between 39.5 and 43.5 ppm in the $^{13}C\{^{1}H\}$ NMR spectra. The dimethylamide group of (**4.7**) and (**4.9**) appears as a singlet at *ca.* 3.15 ppm and is typical of a dimethylamide ligand bound to titanium(IV). The methyls of the xylyl group in (**4.7**) and (**4.8**) are equivalent and appear as one signal in both the ^{1}H and $^{13}C\{^{1}H\}$ NMR spectra, whilst the xylyl ring appears as four aromatic signals in the $^{13}C\{^{1}H\}$ NMR spectrum. This contrasts with the mesityl group of (**4.9**) and (**4.10**), of which the three methyl groups are all inequivalent and appear as three signals. The six aromatic carbons of the mesityl ring are all inequivalent and appear as six signals in the $^{13}C\{^{1}H\}$ NMR spectrum. Although the methyl groups situated in the 2 and 6 position of the mesityl ring are inequivalent, the two aromatic protons in the 3 and 5 positions appear as a broad singlet that is coupled to two separate aromatic carbons in a CH correlation experiment.

4.5 Preliminary ethylene polymerisation catalysis studies

The catalytic activity of (**4.1**) and (**4.3**) for the polymerisation of ethylene in the presence of MAO was studied under standardised conditions.[18] They display moderate polymerisation activity, 2.7 and 4.1 g $mmol^{-1}$ bar^{-1} h^{-1} respectively, at room temperature. These values are both inferior compared to the activity of the silylamido/imino zirconium complex (**3.1**).

4.6 Conclusions

The zirconium(IV) complex of the type $LZr(NEt_2)_2Cl$ (**4.1**) was synthesised in good yield by salt metathesis reaction between the lithium amido/imino ligand (**2.9**) and $Zr(NEt_2)_2Cl_2(THF)_2$. The arylamido/vinylamido complex (**4.2**) was also detected in this reaction in variable quantities, suggesting that the olefin might be formed by migration of a diethylamide to the imine carbon followed by elimination of diethylamine across the carbon-carbon bond. It is possible that this rearrangement reduces steric clash about the zirconium centre. The amido/imino zirconium trichloride complex (**4.3**) was synthesised by action of trimethylchlorosilane on (**4.1**), which upon standing in a THF/petroleum mix gave the anionic amido/imino zirconium tetrachloride complex (**4.4**).

The X-ray crystal structures of two zirconium complexes each bearing two amido/imino or related ligands were recorded. Complex (**4.5**) was the L_2ZrCl_2 type complex of the 3,5-xylylamido/imino ligand and the unit cell contained two different coordination isomers. Complex (**4.6**) was of the type LL'ZrCl where L=amido/imino and L'=amido/vinylamido and illustrated another case where the amido/imino ligand was converted into the dianionic, olefin containing species.

Two titanium(IV) complexes (**4.7**) and (**4.9**) were synthesised from salt metathesis reactions between $Ti(NMe_2)Cl_2$ and the lithium amido/imino ligands (**2.7**) and (**2.9**). In these complexes the amido/imino ligand had been converted into a diamido/amino tripodal ligand, apparently by a migration of dimethylamide to the imine carbon. This type of ligand is possibly an intermediate in the formation of the amido/vinylamido type ligand observed in complexes (**3.4**), (**4.2**) and (**4.6**).

Preliminary ethylene polymerisation studies on (**4.1**) and (**4.3**) with an excess of MAO showed them to act as moderate polymerisation catalysts.

4.7 Experimental

The following compounds were prepared following literature methods: $Zr(NEt_2)_2Cl_2(THF)_2$,[19] $Ti(NMe_2)_2Cl_2$.[20]

4.7.1 [2-(1-Cyclohexylimino-ethyl)-*N*-(2,4,6-trimethylphenyl)-anilide] zirconium chloride bis-diethylamide (4.1).

To a stirred and cooled (-78 °C) solution of $Zr(NEt_2)_2Cl_2(THF)_2$ (1.35 g, 3.0 mmol) in THF (50 cm^3) was added slowly *via* cannula a cooled (-78 °C) solution of (**2.9**) (1.02 g, 3.0 mmol) in THF (50 cm^3). The reaction was stirred at –78 °C for 1 h, allowed to reach room temperature and then stirred for 18 h. From the bright orange solution the volatiles were removed *in vacuo* and the residue extracted into petroleum (*ca.* 100 cm^3) and filtered through Celite. The bright orange filtrate was concentrated to *ca.* 15 cm^3 and cooled to –30 °C overnight to produce yellow, X-ray diffraction quality crystals.

Yield: 0.900 g, 50%.

$\delta_H(C_6D_6)$ 0.84 (12H, t, $N(CH_2CH_3)_2$), 1.10-2.80 (10H, m, cyclohexyl CH_2s), 2.02 (3H, s, imine CH_3), 2.15 (6H, s, mesityl CH_3s), 2.24 (3H, s, mesityl CH_3), 3.16-3.38 (8H, m, $N(CH_2CH_3)_2$), 3.74 (1H, br t, cyclohexyl CH α to imine N), 6.53 (1H, dt, aromatic), 6.62 (1H, d, aromatic), 6.86-6.95 (3H, m, mesityl aromatics and one aromatic), 7.24 (1H, dd, aromatic).

$^{13}C\{^1H\}$ $\delta_C(C_6D_6)$ 13.25 ($N(CH_2CH_3)_2$), 20.25 (mesityl CH_3s), 21.62 (mesityl CH_3), 23.75 (imine CH_3), 26.24, 27.02, 32.35 (cyclohexyl CH_2s), 41.48 ($N(CH_2CH_3)_2$), 65.85 (cyclohexyl CH α to imine N), 117.42, 120.50 (aromatic CHs), 122.86, 129.07 (quaternary aromatics), 130.32, 131.77, 133.25 (aromatic CHs), 134.19, 135.61, 150.71 (quaternary aromatics), 169.75 (ArC(Me)=N(Cy)).

(Found: C, 61.3; H, 8.3; N, 9.3. $C_{31}H_{49}ClN_4Zr$ requires C, 61.6; H, 8.2; N, 9.3%).

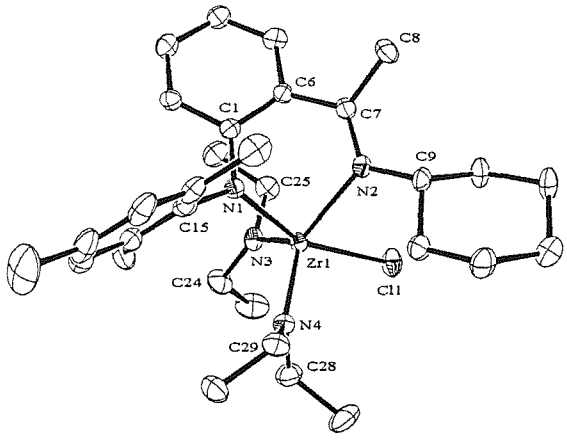

Figure 4.9: ORTEP representation of the crystal structure of [2-(1-cyclohexylimino-ethyl)-*N*-(2,4,6-trimethylphenyl)-anilide] zirconium chloride bis-diethylamide **(4.1)** (50% probability thermal ellipsoids). Hydrogens are omitted for clarity.

Table 4.1: Selected bond lengths (Å) and angles (°) for **(4.1)**.

N(1)-Zr(1)	2.180(2)	N(2)-Zr(1)	2.315(2)
N(3)-Zr(1)	2.027(2)	N(4)-Zr(1)	1.999(2)
Cl(1)-Zr(1)	2.5228(9)	N(1)-C(15)	1.443(3)
N(1)-C(1)	1.377(3)	C(1)-C(6)	1.424(4)
C(6)-C(7)	1.474(4)	C(7)-C(8)	1.500(4)
N(2)-C(7)	1.300(3)	N(2)-C(9)	1.503(3)
N(3)-C(25)	1.452(4)	N(3)-C(24)	1.459(4)
N(4)-C(29)	1.467(3)	N(4)-C(28)	1.468(4)
N(1)-Zr(1)-Cl(1)	156.71(6)	N(1)-Zr(1)-N(2)	75.51(8)
N(2)-Zr(1)-N(3)	129.04(9)	N(3)-Zr(1)-N(4)	110.35(10)
N(4)-Zr(1)-N(2)	120.58(9)	C(1)-N(1)-Zr(1)	112.18(16)
C(1)-N(1)-C(15)	115.2(2)	C(15)-N(1)-Zr(1)	131.22(17)
C(7)-N(2)-C(9)	117.9(2)	C(9)-N(2)-Zr(1)	123.39(17)
C(7)-N(2)-Zr(1)	118.69(17)	N(1)-C(1)-C(6)	122.1(2)
C(1)-C(6)-C(7)	120.3(2)	C(6)-C(7)-N(2)	120.7(2)
C(6)-C(7)-C(8)	114.3(2)	C(8)-C(7)-N(2)	124.7(2)
C(24)-N(3)-Zr(1)	131.42(19)	C(25)-N(3)-Zr(1)	113.03(18)
C(24)-N(3)-C(25)	114.3(2)	C(29)-N(4)-Zr(1)	131.60(19)
C(28)-N(4)-Zr(1)	113.35(17)	C(28)-N(4)-C(29)	114.6(2)

4.7.2 [2-(1-Cyclohexylamido-vinyl)-*N*-(2,4,6-trimethylphenyl)-anilide] zirconium chloride diethylamide tetrahydrofuran (4.2).

Crystallising two crops of crystalline (**4.1**) from the mother liquor of the above reaction gave samples that were predominantly (**4.2**).

$\delta_H(C_6D_6)$ 0.75-1.80 (10H, cyclohexyl C*H*$_2$s), 0.90 (6H, t, N(CH$_2$C*H*$_3$)$_2$), 1.26 (4H, br t, THF), 2.19 (3H, s, mesityl C*H*$_3$), 2.27 (3H, s, mesityl C*H*$_3$), 2.56 (3H, s, mesityl C*H*$_3$), 2.85-3.0 (2H, m, N(C*H*$_2$CH$_3$)$_2$), 3.10-3.25 (1H, m, cyclohexyl C*H* α to cyclohexylamide N), 3.35-3.55 (2H, m, N(C*H*$_2$CH$_3$)$_2$), 3.78 (4H, br t, THF), 4.52 (1H, s, C=C*H*$_2$), 4.96 (1H, s, C=C*H*$_2$), 6.11 (1H, d, aromatic), 6.76 (1H, t, aromatic), 6.90-7.05 (3H, m, aromatics), 7.41 (1H, d, aromatic).

$^{13}C\{^1H\}$ $\delta_C(C_6D_6)$ 13.14 (N(CH$_2$*C*H$_3$)$_2$), 19.37, 19.74, 21.80 (mesityl *C*H$_3$s), 25.98 (THF), 26.24, 26.97, 35.18, 36.91, 37.12 (cyclohexyl *C*H$_2$s), 41.26 (N(*C*H$_2$CH$_3$)$_2$), 61.06 (cyclohexyl *C*H α to cyclohexylamide N), 71.75 (THF), 102.77 (ArC(NCy)=*C*H$_2$), 112.87 (aromatic *C*H), 113.48 (quaternary aromatic), 117.51, 128.08 (aromatic *C*Hs), 129.80 (quaternary aromatic), 130.25, 131.12, 131.25 (aromatic *C*Hs), 135.14, 142.61, 152.84, 155.92 (quaternary aromatics), 171.71 (Ar*C*(NCy)=CH$_2$).

4.7.3 [2-(1-Cyclohexylimino-ethyl)-*N*-(2,4,6-trimethylphenyl)-anilide] zirconium trichloride (4.3).

To a stirred solution of (**4.1**) (0.80 g, 1.33 mmol) in benzene (20 cm^3) was added trimethylchlorosilane (0.7 cm^3, 5.5 mmol). Upon addition of the trimethylchlorosilane the benzene solution remained a bright orange colour, but after stirring for 30 minutes a bright yellow precipitate was produced. The reaction was stirred for a total of 3 h before the product was collected by filtration and washed with petrol (*ca.* 50 cm^3) before drying *in vacuo* to yield a yellow solid.

Yield: 0.590 g, 84%.

$\delta_H(d^8$-THF) 1.30-2.20 (10H, m, cyclohexyl C*H*$_2$s), 2.26 (6H, s, mesityl C*H*$_3$s), 2.39 (3H, s, C*H*$_3$), 2.97 (3H, s, C*H*$_3$), 5.08 (1H, br t, cyclohexyl C*H* α to imine N), 6.41 (1H, d, aromatic), 6.97-7.05 (3H, m, aromatic), 8.03 (1H, d, aromatic).

$^{13}C\{^1H\}$ $\delta_C(d^8$-THF) 21.24 (mesityl *C*H$_3$s), 22.26, 26.56 (*C*H$_3$s), 27.79, 28.70, 28.89, 32.18, 36.40 (cyclohexyl *C*H$_2$s) 66.17 (cyclohexyl *C*H α to imine N),

119.90, 121.35(aromatic *C*Hs), 130.50 (quaternary aromatic), 131.53, 132.85, 134.39 (aromatic *C*Hs), 137.70, 137.86, 139.00, 151.54 (quaternary aromatics), 177.48 (Ar*C*(Me)=N(Cy)).

4.7.4 [2-(1-cyclohexylimino-ethyl)-*N*-(2,4,6-trimethylphenyl)-anilide] zirconium tetrachloride diethylammonium salt (4.4).

Complex (**4.3**) (*ca.* 0.10 g) was dissolved in THF (*ca.* 10 cm^3) and layered with petroleum (*ca.* 10 cm^3) in a Schlenk tube. The tube was left to stand for *ca.* one week and afforded a small crop of yellow crystals of (**4.4**) as well as non-crystalline yellow solid.

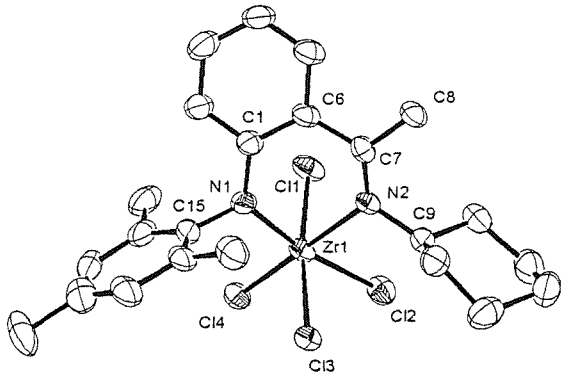

Figure 4.10: ORTEP representation of the crystal structure of the anion from the [2-(1-cyclohexylimino-ethyl)-*N*-(2,4,6-trimethylphenyl)-anilide] zirconium tetrachloride diethylammonium salt (**4.4**) (50% probability thermal ellipsoids). Hydrogens are removed for clarity.

Table 4.2: Selected bond lengths (Å) and angles (°) for (**4.4**).

N(1)-Zr(1)	2.118(4)	N(2)-Zr(1)	2.289(3)
Cl(1)-Zr(1)	2.4779(13)	Cl(2)-Zr(1)	2.5716(13)
Cl(3)-Zr(1)	2.4611(13)	Cl(4)-Zr(1)	2.4577(12)
N(1)-C(15)	1.447(6)	N(1)-C(1)	1.389(5)
C(1)-C(6)	1.419(6)	C(6)-C(7)	1.495(6)
C(7)-C(8)	1.521(6)	C(7)-N(2)	1.293(5)
C(9)-N(2)	1.514(5)		

N(1)-Zr(1)-Cl(2)	169.51(10)	N(2)-Zr(1)-Cl(4)	178.27(9)
Cl(1)-Zr(1)-Cl(3)	173.20(5)	N(1)-Zr(1)-N(2)	79.85(13)
C(15)-N(1)-Zr(1)	117.7(3)	C(15)-N(1)-C(1)	116.6(4)
Zr(1)-N(1)-C(1)	125.3(3)	N(1)-C(1)-C(6)	121.5(4)
C(1)-C(6)-C(7)	123.9(4)	C(6)-C(7)-C(8)	114.1(4)
C(8)-C(7)-N(2)	123.6(4)	C(6)-C(7)-N(2)	122.3(4)
C(7)-N(2)-Zr(1)	125.7(3)	C(7)-N(2)-C(9)	122.2(4)
Zr(1)-N(2)-C(9)	112.1(3)		

4.7.5 bis-[2-(1-Cyclohexylimino-ethyl)-*N*-(3,5-dimethylphenyl)-anilide] zirconium dichloride (4.5).

To a cooled (-78 °C), stirred solution of $CpZrCl_3$ (0.131 g, 0.50 mmol) in toluene (15 cm^3) was added *via* cannula a cooled (-78 °C) solution of (**2.7**) (0.163 g, 0.50 mmol) in toluene (10 cm^3). The reaction was stirred at –78 °C for 1 h before being allowed to reach RT and stirring for 15 h. This gave a yellow solution with a colourless precipitate that was removed by filtration through Celite. The volatiles were removed *in vacuo* and the residue dissolved in petrol (20 cm^3), which was concentrated to *ca.* 10 cm^3 and cooled to –30 °C to yield (**4.5**) as a small crop of X-ray diffraction quality, orange crystals.

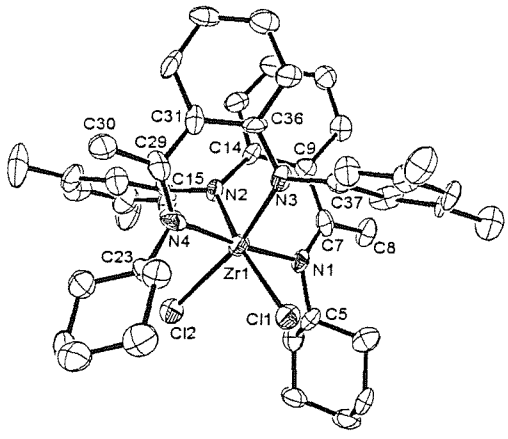

Figure 4.11: ORTEP representation of the crystal structure of isomer A of bis-[2-(1-cyclohexylimino-ethyl)-*N*-(2,4,6-trimethylphenyl)-anilide] zirconium dichloride (**4.5A**) (50% probability thermal ellipsoids). Hydrogens are omitted for clarity.

Table 4.3: Selected bond lengths (Å) and angles (°) for **(4.5A)**.

Zr(1)-N(1)	2.260(10)	Zr(1)-N(2)	2.108(10)
Zr(1)-N(3)	2.126(10)	Zr(1)-N(4)	2.246(11)
Zr(1)-Cl(1)	2.476(4)	Zr(1)-Cl(2)	2.447(4)
N(1)-C(5)	1.493(16)	N(1)-C(7)	1.307(16)
N(2)-C(14)	1.390(15)	N(2)-C(15)	1.435(15)
N(4)-C(23)	1.478(17)	N(4)-C(29)	1.300(16)
N(3)-C(36)	1.392(15)	N(3)-C(37)	1.436(15)
C(7)-C(8)	1.484(17)	C(7)-C(9)	1.474(18)
C(9)-C(14)	1.421(16)	C(29)-C(30)	1.545(17)
C(29)-C(31)	1.429(18)	C(31)-C(36)	1.403(17)
N(1)-Zr(1)-N(2)	78.5(4)	N(3)-Zr(1)-N(4)	76.8(4)
Cl(1)-Zr(1)-Cl(2)	94.91(12)	N(2)-Zr(1)-N(3)	90.9(4)
N(1)-Zr(1)-N(4)	174.5(4)	N(2)-Zr(1)-Cl(1)	168.8(3)
N(3)-Zr(1)-Cl(2)	164.5(3)	Zr(1)-N(1)-C(5)	112.4(8)
C(5)-N(1)-C(7)	123.5(11)	C(7)-N(1)-Zr(1)	124.0(8)
Zr(1)-N(2)-C(14)	119.0(7)	C(14)-N(2)-C(15)	112.7(10)
C(15)-N(2)-Zr(1)	128.0(8)	C(23)-N(4)-C(29)	123.1(12)
C(29)-N(4)-Zr(1)	123.4(9)	Zr(1)-N(4)-C(23)	113.6(8)
C(36)-N(3)-C(37)	117.0(10)	C(37)-N(3)-Zr(1)	123.7(8)
Zr(1)-N(3)-C(36)	119.3(8)	N(2)-C(14)-C(9)	121.0(11)
C(14)-C(9)-C(7)	123.9(12)	C(9)-C(7)-C(8)	116.5(13)
C(8)-C(7)-N(1)	124.9(13)	C(9)-C(7)-N(1)	118.5(12)
N(3)-C(36)-C(31)	121.0(12)	C(36)-C(31)-C(29)	123.0(13)
C(31)-C(29)-N(4)	120.8(12)	C(31)-C(29)-C(30)	116.0(12)
C(30)-C(29)-N(4)	123.1(13)		

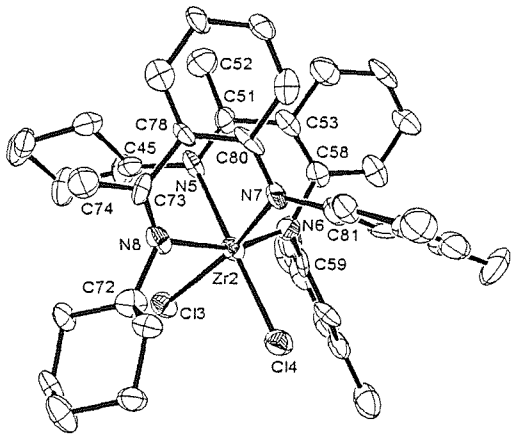

Figure 4.12: ORTEP representation of the crystal structure of isomer B of bis-[2-(1-cyclohexylimino-ethyl)-*N*-(2,4,6-trimethylphenyl)-anilide] zirconium dichloride (**4.5B**) (50% probability thermal ellipsoids). Hydrogens are omitted for clarity.

Table 4.4: Selected bond lengths (Å) and angles (°) for (**4.5B**).

Zr(2)-N(5)	2.320(10)	Zr(2)-N(6)	2.075(12)
Zr(2)-N(7)	2.124(10)	Zr(2)-N(8)	2.296(11)
Zr(2)-Cl(3)	2.456(3)	Zr(2)-Cl(4)	2.434(4)
N(5)-C(45)	1.490(15)	N(5)-C(51)	1.292(15)
N(6)-C(58)	1.423(16)	N(6)-C(59)	1.437(17)
N(8)-C(72)	1.503(16)	N(8)-C(73)	1.317(16)
N(7)-C(80)	1.393(17)	N(7)-C(81)	1.441(16)
C(58)-C(53)	1.441(18)	C(53)-C(51)	1.453(18)
C(51)-C(52)	1.513(18)	C(80)-C(78)	1.407(18)
C(78)-C(73)	1.475(18)	C(73)-C(74)	1.489(18)
N(5)-Zr(2)-N(6)	77.7(4)	N(7)-Zr(2)-N(8)	75.6(4)
Cl(3)-Zr(2)-Cl(4)	91.65(12)	N(6)-Zr(2)-N(8)	160.4(4)
N(5)-Zr(2)-Cl(4)	178.7(3)	N(7)-Zr(2)-Cl(3)	165.2(3)
Zr(2)-N(5)-C(45)	116.1(7)	Zr(2)-N(5)-C(51)	120.9(8)
C(45)-N(5)-C(51)	122.9(10)	Zr(2)-N(6)-C(59)	127.3(8)
Zr(2)-N(6)-C(58)	119.4(9)	C(58)-N(6)-C(59)	113.2(11)
Zr(2)-N(8)-C(72)	109.4(9)	Zr(2)-N(8)-C(73)	128.8(9)
C(72)-N(8)-C(73)	121.3(11)	Zr(2)-N(7)-C(80)	119.6(8)
Zr(2)-N(7)-C(81)	125.0(9)	C(80)-N(7)-C(81)	115.3(11)
N(6)-C(58)-C(53)	119.6(12)	C(58)-C(53)-C(51)	122.4(12)
C(53)-C(51)-N(5)	122.3(12)	C(53)-C(51)-C(52)	114.5(12)
C(52)-C(51)-N(5)	123.2(12)	N(7)-C(80)-C(78)	124.7(11)
C(80)-C(78)-C(73)	121.5(12)	C(78)-C(73)-N(8)	117.1(12)
C(78)-C(73)-C(74)	116.8(13)	C(74)-C(73)-N(8)	126.0(13)

Table 4.5: Crystallographic parameters for **(4.1)**, **(4.4)** and **(4.5)**.

Compound	**(4.1)**	**(4.4)**	**(4.5)**
Chemical Formula	$C_{31}H_{49}Cl_1N_4Zr_1$	$C_{27}H_{41}Cl_4N_3Zr_1$	$C_{92}H_{118}Cl_4N_8O_1Zr_2$
Formula Weight	604.41	640.65	1676.18
Crystal System	Monoclinic	Monoclinic	Triclinic
Space Group	$P2_1/c$	$P2_1/c$	P-1
a/Å	17.199(7)	19.245(3)	14.1489(10)
b/Å	12.774(5)	11.4615(19)	18.9314(16)
c/Å	14.655(4)	17.391(3)	19.1389(18)
α/°	90	90	104.905(5)
β/°	98.410(10)	112.964(4)	98.766(6)
γ/°	90	90	111.332(3)
V/Å^3	3185(2)	3532.0(10)	4439.0(6)
Z	4	4	2
T/K	120	120	120
μ/mm^{-1}	0.454	0.632	0.404
F(000)	1280	1328	1764
No. Data collected	13616	31784	14178
No. Unique data	7191	5670	8244
R_{int}	0.0479	0.0853	0.1230
Final $R(\|F\|)$ for $I>2\sigma(I)$	0.0456	0.0528	0.0844
Final $R(F^2)$ for all data	0.0952	0.1360	0.2084

4.7.6 [2-(1-Cyclohexylimino-ethyl)-*N*-(3,5-dimethylphenyl)-anilide] [2-(1-cyclohexylamido-vinyl)-*N*-(3,5-dimethylphenyl)-anilide] zirconium chloride (4.6).

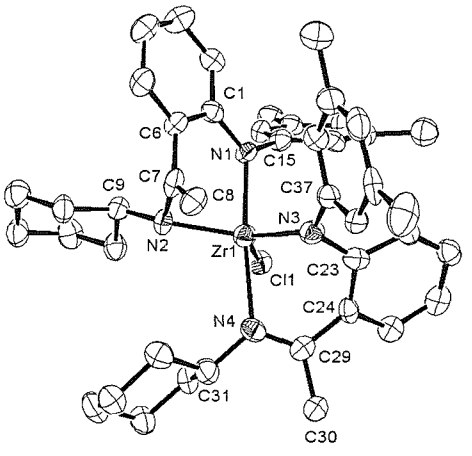

Figure 4.13: ORTEP representation of the crystal structure of [2-(1-cyclohexylimino-ethyl)-*N*-(3,5-dimethylphenyl)-anilide] [2-(1-cyclohexylamido-vinyl)-*N*-(3,5-dimethylphenyl)-anilide] zirconium chloride **(4.6)** (50% probability thermal ellipsoids). Hydrogens are omitted for clarity.

Table 4.6: Selected bond lengths (Å) and angles (°) for **(4.6)**.

Zr(1)-N(1)	2.172(4)	Zr(1)-N(2)	2.054(5)
Zr(1)-N(3)	2.122(5)	Zr(1)-N(4)	2.356(5)
Zr(1)-C(7)	2.506(6)	Zr(1)-C(8)	2.856(6)
Zr(1)-Cl(1)	2.3947(17)	N(1)-C(15)	1.431(7)
N(1)-C(1)	1.390(7)	C(1)-C(6)	1.417(8)
C(6)-C(7)	1.492(8)	C(7)-N(2)	1.416(8)
N(2)-C(9)	1.479(7)	C(7)-C(8)	1.329(8)
N(3)-C(37)	1.440(8)	N(3)-C(23)	1.403(8)
C(23)-C(24)	1.409(8)	C(24)-C(29)	1.484(8)
C(29)-N(4)	1.296(7)	N(4)-C(31)	1.502(7)
C(29)-C(30)	1.510(7)		

N(2)-Zr(1)-N(3)	129.9(2)	N(3)-Zr(1)-Cl(1)	119.94(15)
Cl(1)-Zr(1)-N(2)	110.03(14)	N(1)-Zr(1)-N(4)	172.69(19)
Cl(1)-Zr(1)-C(8)	164.53(13)	Cl(1)-Zr(1)-C(7)	139.20(15)
N(2)-Zr(1)-C(8)	54.54(18)	N(2)-Zr(1)-C(7)	34.41(19)
N(1)-Zr(1)-N(2)	84.01(18)	Zr(1)-N(1)-C(15)	117.4(4)
Zr(1)-N(1)-C(1)	124.9(4)	C(15)-N(1)-C(1)	117.4(5)
N(1)-C(1)-C(6)	116.9(5)	C(1)-C(6)-C(7)	117.2(5)
C(6)-C(7)-N(2)	116.7(5)	C(7)-N(2)-Zr(1)	90.5(3)
C(6)-C(7)-C(8)	123.0(6)	C(8)-C(7)-N(2)	118.5(6)
C(7)-N(2)-C(9)	115.3(5)	C(9)-N(2)-Zr(1)	136.8(4)
N(3)-Zr(1)-N(4)	80.04(18)	Zr(1)-N(3)-C(37)	134.7(4)
Zr(1)-N(3)-C(23)	107.5(4)	C(23)-N(3)-C(37)	114.9(5)
N(3)-C(23)-C(24)	121.2(6)	C(23)-C(24)-C(29)	125.1(6)
C(24)-C(29)-N(4)	120.7(5)	C(29)-N(4)-Zr(1)	114.7(4)
C(24)-C(29)-C(30)	115.9(5)	C(30)-C(29)-N(4)	123.4(6)
C(29)-N(4)-C(31)	117.7(5)	C(31)-N(4)-Zr(1)	126.4(4)

4.7.7 [2-(1-Cyclohexylamido-1-dimethylamino-ethyl)-*N*-(3,5-dimethylphenyl)-anilide] titanium chloride dimethylamide (4.7) and [2-(1-cyclohexylamido-1-dimethylamino-ethyl)-*N*-(3,5-dimethylphenyl)-anilide] titanium dichloride (4.8).

To a stirred, cooled (-78 °C) solution of $Ti(NMe_2)_2Cl_2$ (0.104 g, 0.5 mmol) in THF (15 cm^3) was added slowly a solution of **(2.7)** (0.163 g, 0.5 mmol) in THF (15 cm^3). The dark red solution was allowed to reach room temperature over *ca.* 15 h before stirring for a further 2 h. Volatiles were removed *in vacuo* and the residue extracted into petroleum (2 x 30 cm^3) and filtered through Celite. The bright red solution was concentrated to *ca.* 20 cm^3 and cooled at –30 °C for 48 h to give an orange/red solid. A saturated petroleum solution was cooled to –30 °C to give X-ray diffraction quality crystals of **(4.8)**.

Major product (**4.7**):

$\delta_H(C_6D_6)$ 0.80-1.80 (10H, m, cyclohexyl C*H*$_2$s), 1.40 (3H, s, ArC(NMe$_2$)(NCy)C*H*$_3$), 1.94 (3H, s, amine C*H*$_3$), 2.18 (6H, s, xylyl C*H*$_3$s), 2.51 (3H, s, amine C*H*$_3$), 3.17 (6H, s, dimethylamide C*H*$_3$s), 3.30-3.50 (1H, m, cyclohexyl C*H* α to cyclohexylamide N), 6.73 (1H, s, xylyl aromatic), 6.77-6.86 (2H, m, aromatics), 7.01 (1H, dt, aromatic), 7.13 (1H, dd, aromatic), 7.24 (2H, xylyl aromatics).

Minor product (**4.8**):

$\delta_H(C_6D_6)$ 0.70-2.70 (10H, m, cyclohexyl C*H*$_2$s), 1.26 (3H, s, ArC(NMe$_2$)(NCy)C*H*$_3$), 1.92 (3H, amine C*H*$_3$), 2.13 (6H, s, xylyl C*H*$_3$s), 2.25 (3H, s, amine C*H*$_3$), 2.40-2.60 (1H, m, cyclohexyl C*H* α to cyclohexylamide N), 6.35 (1H, dd, aromatic), 6.70 (2H, s, xylyl aromatics), 6.79 (1H, dt, aromatic), 6.87 (1H, dt, aromatic), 6.99 (1H, dd, aromatic), 7.15 (1H, s, xylyl aromatic).

$^{13}C\{^1H\}$ $\delta_C(C_6D_6)$ 16.26 (ArC(NMe$_2$)(NCy)*C*H$_3$), 21.90 (xylyl *C*H$_3$s), 26.30, 27.05, 27.30, 35.07, 37.19 (cyclohexyl *C*H$_2$s), 40.52, 43.24 (amine *C*H$_3$s), 67.30 (cyclohexyl *C*H α to cyclohexylamide N), 86.12 (Ar*C*(NMe$_2$)(NCy)CH$_3$), 112.47, 123.64, 128.03, 129.00 (aromatic *C*Hs), 129.68 (quaternary aromatic), 129.84, 130.46 (aromatic *C*Hs), 140.75, 144.90, 151.56 (quaternary aromatics).

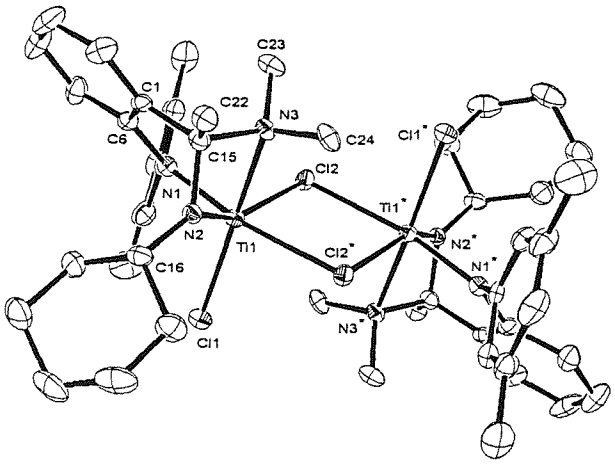

Figure 4.14: ORTEP representation of the crystal structure of [2-(1-cyclohexylamido-1-dimethylamino-ethyl)-*N*-(3,5-dimethylphenyl)-anilide] titanium dichloride (**4.8**) (50% probability thermal ellipsoids). Hydrogens are omitted for clarity.

Table 4.7: Selected bond lengths (Å) and angles (°) for **(4.8)**.

Ti(1)-N(1)	1.954(3)	Ti(1)-N(2)	1.890(3)
Ti(1)-N(3)	2.224(3)	Ti(1)-Cl(1)	2.3185(11)
Ti(1)-Cl(2)	2.4968(11)	Ti(1)-Cl(2*)	2.5349(11)
N(1)-C(7)	1.440(5)	N(1)-C(6)	1.415(5)
C(6)-C(1)	1.417(5)	C(1)-C(15)	1.514(5)
C(15)-N(2)	1.470(4)	N(2)-C(16)	1.476(4)
C(15)-C(22)	1.526(5)	C(15)-N(3)	1.535(4)
N(3)-C(23)	1.470(4)	N(3)-C(24)	1.479(4)
N(1)-Ti(1)-N(2)	90.11(12)	N(2)-Ti(1)-N(3)	65.64(11)
N(1)-Ti(1)-N(3)	87.35(11)	Cl(2)-Ti(1)-Cl(2*)	77.47(3)
Cl(1)-Ti(1)-Cl(2)	105.93(4)	Cl(1)-Ti(1)-Cl(2*)	84.69(3)
N(1)-Ti(1)-Cl(2*)	165.27(9)	N(2)-Ti(1)-Cl(2)	153.93(9)
N(3)-Ti(1)-Cl(1)	163.93(8)	Ti(1)-N(1)-C(6)	123.0(2)
N(1)-C(6)-C(1)	120.3(3)	C(6)-C(1)-C(15)	119.8(3)
C(1)-C(15)-N(2)	109.2(3)	C(15)-N(2)-Ti(1)	101.54(19)
N(2)-C(15)-N(3)	96.8(2)	C(15)-N(3)-Ti(1)	86.17(18)
Ti(1)-N(1)-C(7)	120.5(2)	C(7)-N(1)-C(6)	115.8(3)
C(16)-N(2)-C(15)	118.7(3)	C(16)-N(2)-Ti(1)	136.7(2)
C(23)-N(3)-C(24)	107.6(3)		

4.7.8 [2-(1-Cyclohexylamido-1-dimethylamino-ethyl)-*N*-(2,4,6-trimethylphenyl)-anilide] titanium chloride dimethylamide (4.9) and [2-(1-cyclohexylamido-1-dimethylamino-ethyl)-*N*-(2,4,6-trimethylphenyl)-anilide] titanium dichloride (4.10).

To a stirred, cooled (-78 °C) solution of $Ti(NMe_2)_2Cl_2$ (0.104 g, 0.5 mmol) in THF (15 cm^3) was added slowly a solution of **(2.9)** (0.170 g, 0.5 mmol) in THF (15 cm^3). The dark red solution was allowed to reach room temperature over *ca.* 15 h before stirring for a further 2 h. Volatiles were removed *in vacuo* and the residue extracted into petroleum (60 cm^3 then 2 x 30 cm^3) and filtered through Celite. The bright red solution was concentrated to *ca.* 20 cm^3 and cooled at –30 °C for 48 h to give an orange/red solid. A saturated petroleum solution was cooled to –30 °C to give X-ray diffraction quality crystals of **(4.9)**.

Major product **(4.9)**:

$\delta_H(C_6D_6)$ 0.80-1.65 (10H, m, cyclohexyl CH_2s), 1.47 (3H, s, $ArC(NMe_2)(NCy)CH_3$), 1.96 (3H, s, amine CH_3), 2.12 (3H, s, mesityl CH_3), 2.22 (3H, s, mesityl CH_3), 2.46 (3H, s, mesityl CH_3), 2.49 (3H, s, amine CH_3), 3.13 (6H, s, dimethylamide CH_3s), 3.27 (1H, tt, cyclohexyl CH α to cyclohexylamide N),

6.08 (1H, dd, aromatic), 6.81 (1H, dt, aromatic), 6.87-6.98 (3H, m, mesityl aromatics and one aromatic), 7.13 (1h, dd, aromatic).

$^{13}C\{^{1}H\}$ $\delta_C(C_6D_6)$ 17.87 (ArC(NMe$_2$)(NCy)*C*H$_3$), 19.88, 20.34, 21.70 (mesityl *C*H$_3$s), 27.02, 27.33, 27.60, 36.34, 37.66 (cyclohexyl *C*H$_2$s), 39.58, 42.56 (amine *C*H$_3$s), 46.46 (dimethylamide *C*H$_3$s), 66.66 (cyclohexyl *C*H α to cyclohexylamide N), 86.59 (Ar*C*(NMe$_2$)(NCy)CH$_3$), 110.91, 121.34, 128.00, 129.53 (aromatic *C*Hs), 129.74 (quaternary aromatic), 130.50, 131.89 (aromatic *C*Hs), 135.69, 137.36, 138.17, 140.24, 148.71 (quaternary aromatics).

Minor product (**4.10**):

$\delta_H(C_6D_6)$ 0.80-2.00 (10H, m, cyclohexyl C*H*$_2$s), 1.29 (3H, s, ArC(NMe$_2$)(NCy)C*H*$_3$), 1.78 (3H, s, amine C*H*$_3$), 2.13 (3H, s, mesityl C*H*$_3$), 2.19 (3H, s, mesityl C*H*$_3$), 2.25 (3H, s, mesityl C*H*$_3$), 2.28 (3H, s, amine C*H*$_3$), 3.05 (1H, tt, cyclohexyl C*H* α to cyclohexylamide N), 6.00 (1H, dd, aromatic), 6.75-6.90 (4H, m, mesityl aromatics and two aromatics), 7.01 (1H, dd, aromatics).

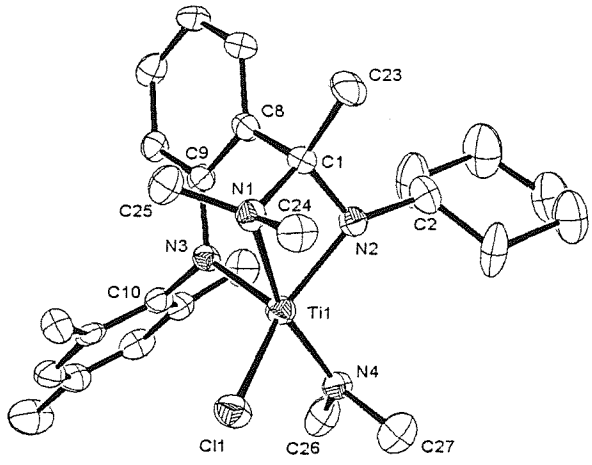

Figure 4.15: ORTEP representation of the crystal structure of [2-(1-cyclohexylamido-1-dimethylamino-ethyl)-*N*-(2,4,6-trimethylphenyl)-anilide] titanium chloride diethylamide (**4.9**) (50% probability thermal ellipsoids). Hydrogens are omitted for clarity.

Table 4.8: Selected bond lengths (Å) and angles (°) for **(4.9)**.

N(3)-Ti(1)	1.934(4)	N(2)-Ti(1)	1.914(4)
N(1)-Ti(1)	2.291(4)	N(4)-Ti(1)	1.918(4)
Cl(1)-Ti(1)	2.3757(15)	C(10)-N(3)	1.444(6)
C(9)-N(3)	1.414(5)	C(8)-C(9)	1.416(6)
C(1)-C(8)	1.544(7)	C(1)-N(2)	1.480(6)
C(1)-C(23)	1.534(6)	C(1)-N(1)	1.524(6)
N(2)-C(2)	1.462(6)	N(1)-C(24)	1.476(6)
N(1)-C(25)	1.469(6)	N(4)-C(26)	1.415(6)
N(4)-C(27)	1.462(6)		
N(2)-Ti(1)-N(3)	95.19(16)	N(1)-Ti(1)-N(3)	87.04(16)
N(1)-Ti(1)-N(2)	64.95(15)	N(3)-Ti(1)-Cl(1)	118.74(12)
N(2)-Ti(1)-Cl(1)	132.94(13)	N(1)-Ti(1)-N(4)	159.36(17)
Ti(1)-N(3)-C(10)	121.4(3)	C(9)-N(3)-C(10)	116.5(4)
C(9)-N(3)-Ti(1)	122.1(3)	N(3)-C(9)-C(8)	120.5(4)
C(9)-C(8)-C(1)	121.0(4)	C(8)-C(1)-N(2)	109.7(4)
N(1)-C(1)-N(2)	98.8(3)	C(1)-N(2)-Ti(1)	100.0(3)
C(1)-N(2)-C(2)	117.9(4)	Ti(1)-N(2)-C(2)	140.1(3)
C(1)-N(1)-Ti(1)	84.0(2)	Ti(1)-N(4)-C(26)	132.4(4)
Ti(1)-N(4)-C(27)	115.7(3)	C(26)-N(4)-C(27)	110.3(4)

Table 4.9: Crystallographic parameters for compounds **(4.6)**, **(4.8)** and **(4.9)**.

Compound	**(4.6)**	**(4.8)**	**(4.9)**
Chemical Formula	$C_{44}H_{53}Cl_1N_4Zr_1$	$C_{48}H_{66}Cl_4N_6Ti_2$	$C_{27}H_{41}Cl_1N_4Ti_1$
Formula Weight	764.57	964.67	504.99
Crystal System	Monoclinic	Triclinic	Monoclinic
Space Group	$P2_1/c$	P-1	$P2_1/c$
a/Å	15.8871(7)	8.6874(12)	14.891(2)
b/Å	14.0906(8)	11.0077(15)	19.812(3)
c/Å	18.9208(11)	15.197(2)	9.1479(7)
α/°	90	96.648(3)	90
β/°	114.233(3)	98.987(4)	100.210(8)
γ/°	90	108.334(4)	90
V/Å^3	3862.4(4)	1341.3(3)	2656.1(6)
Z	4	1	4
T/K	120	120	120
μ/mm^{-1}	0.390	0.533	0.445
F(000)	1608	508	1080
No. Data collected	26129	7610	13708
No. Unique data	8748	2271	4295
R_{int}	0.1939	0.0376	0.1296
Final $R(\|F\|)$ for $I>2\sigma(I)$	0.0861	0.0337	0.0728
Final $R(F^2)$ for all data	0.1611	0.0937	0.1496

4.7.9 Ethylene polymerisation catalysis.

Complex (**4.1**) (0.060 g, 0.10 mmol) was dissolved in toluene (100 cm^3) in a glass pressure bottle. MAO (10% weight in toluene) (66.3 ml, 100 mmol) was added to the solution of (**4.1**). This was stirred for 30 minutes at room temperature. The toluene solution was then saturated with ethylene at a pressure of 7 bar for 2 h. A white solid was formed in the toluene solution during the catalysis run. After 2 h the ethylene was blown off the system and the polymerization quenched by the addition of ethanol (5 ml). The polymeric solid that was produced was filtered away from the toluene solution and stirred overnight in a 20 vol% ethanolic hydrochloric acid solution, then washed with water and ethanol and dried *in vacuo*.

Average yield of polyethylene produced: 3.81 g. This corresponds to a catalyst activity of 2.7 g $mmol^{-1}$ bar^{-1} h^{-1}.

This procedure was followed for (**4.3**) and the yield of polyethylene was 5.70 g. This corresponds to a catalyst activity of 4.1 g $mmol^{-1}$ bar^{-1} h^{-1}.

4.8 References

1. L. Bourget-Merle, M. F. Lappert, J. R. Severn, *Chem. Rev.*, 2002, **102**, 3031.

2. W.-K. Kim, M. J. Fevola, L. M. Liable-Sands, A. L. Rheingold, K. H. Theopold, *Organometallics*, 1998, **17**, 4541.

3. P. H. M. Budzelaar, A. B. van Oort, A. G. Orpen, *Eur. J. Inorg. Chem.*, 1998, 1485.

4. L. Kakaliou, W. J. Scanlon, B. Qian, S. W. Beek, M. R. Smith, D. H. Motry, *Inorg. Chem.*, 1999, **38**, 5964.

5. B. Qian, W. J. Scanlon, S. W. Beek, M. R. Smith, D. H. Motry, *Organometallics*, 1999, **18**, 1693.

6. M. Rahim, N. J. Taylor, S. Xin, S. Collins, *Organometallics*, 1998, **17**, 1315.

7. P. G. Hayes, G. C. Welch, D. J. H. Emslie, C. L. Noack, W. E. Piers, M. Parvez, *Organometallics*, 2003, **22**, 1577.

8. R. M. Porter, S. Winston, A. A. Danopoulos, M. B. Hursthouse, *J. Chem. Soc., Dalton Trans.*, 2002, 3290.

9. P. R. Woodman, N. W. Alcock, I. J. Munslow, C. J. Sanders, P. Scott, *J. Chem. Soc., Dalton Trans.*, 2000, 3340.

10. P. D. Knight, A. J. Clarke, B. S. Kimberley, R. A. Jackson, P. Scott, *Chem. Commun.*, 2002, 352.

11. D. J. H. Emslie, W. E. Piers, M. Parvez, *J. Chem. Soc., Dalton Trans.*, 2003, 2615.

12. D. J. H. Emslie, W. E. Piers, M. Parvez, R. MacDonald, *Organometallics*, 2002, **21**, 4226.

13. D. J. H. Emslie, W. E. Piers, R. MacDonald, *J. Chem. Soc., Dalton Trans.*, 2002, 293.

14. P. Mehrkodavandi, P. J. Bonitatebus, R. R. Schrock, *J. Am. Chem. Soc.*, 2000, **122**, 7841.

15. M. Mitani, J. Mohri, Y. Yoshida, J. Saito, S. Ishii, K. Tsuru, S. Matsui, R. Furuyama, T. Nakano, H. Tanaka, S. Kojoh, T. Matsugi, N. Kashiwa, T. Fujita, *J. Am. Chem. Soc.*, 2002, **124**, 3327.

16. J. Saito, M. Mitani, J. Mohri, Y. Yoshida, S. Matsui, S. Ishii, S. Kojoh, N. Kashiwa, T. Fujita, *Angew. Chem. Int. Ed.*, 2001, **40**, 2918.

17. S. Matsui, M. Mitani, J. Saito,Y. Tohi, H. Makio, N. Matsukawa, Y. Takagi, K. Tsuru, M. Nitabaru, T. Nakano, H. Tanaka, N. Kashiwa, T. Fujita, *J. Am. Chem. Soc.*, 2001, **123**, 6847.

18. W. Kaminsky, R. Engehausen, K. Zoumis, *Makromol. Chem.*, 1992, **193**, 1643.

19. S. Brenner, R. Kempe, P. Arndt, *Z. Anorg. Allg. Chem.*, 1995, **621**, 2021.

20. E. Benzing, W. Kornicker, *Chem. Ber.*, 1961, **94**, 2263.

Chapter 5

Phenoxyimine and Related Complexes of Titanium(IV), Zirconium(IV) and Niobium(V)

5.1 Introduction

The salicylaldiminato or phenoxyimine class of ligands has been the subject of intense study in recent years. They are monoanionic ligands combining the hard phenoxide group with the neutral, softer imine moiety. The ligands offer ready accessibility and their steric and electronic properties are readily modified by altering the substituents R^1-R^4 (Figure 5.2). These factors have lead to a huge interest in the study of phenoxyimine complexes as olefin polymerisation catalysts.[1]

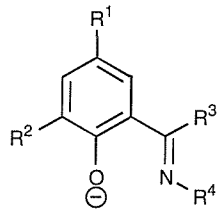

Figure 5.1: General structure of the phenoxyimine ligand.

The main area of study has focused on bis-phenoxyimine titanium and zirconium complexes (Figure 5.2). Fujita and co-workers at Mitsui Chemicals have reported a large volume of work concerned with the polymerisation behaviour of this class of complexes.[1-4, 16-18] This class of titanium complexes was found to be highly active catalysts for the polymerisation of ethylene. Fujita claimed that the electrophilicity of the titanium centre plays a dominant role in determining the catalytic activity for bis-phenoxyimine ligands. Complexes where the imine substituent is a fluorinated aryl group show very high ethylene polymerisation activities.[2,3] One bis-phenoxyimine titanium complex in which the imine bears a fluorinated aryl group displayed living polymerisation activity when activated with MAO even at high temperatures.[4] On the basis of DFT calculations it has been suggested that an *ortho* fluorine atom of the *N*-aryl group of the phenoxyimine

ligand interacts with the β-H of the growing polymer chain. This prevents β-H elimination by the titanium centre and results in living behaviour at high temperature.[2,4]

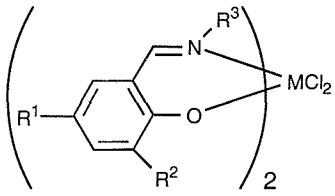

Figure 5.2: Bis-phenoxyimine titanium complexes studied by Fujita.

Coates reported a similar bis-phenoxyimine titanium complex that when activated with MAO displayed highly syndiospecific living olefin polymerisation.[5] The catalyst was used to produce syndiotactic polypropylene as well as block copolymers from ethylene and propylene.

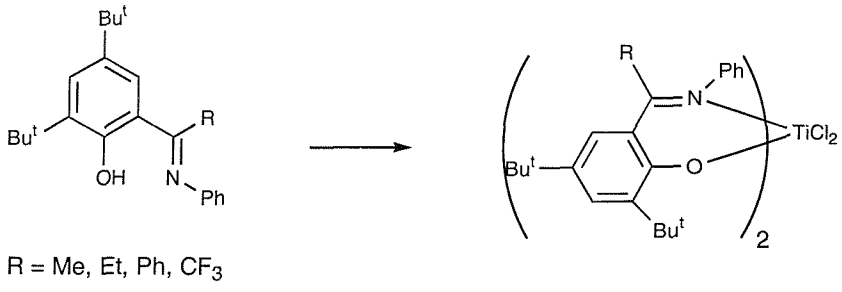

Scheme 5.1: A series of ketiminophenol ligands and bis-phenoxyketimine titanium complexes reported by Coates.

The phenoxyimine ligands that are usually studied contain an aldimine group. Coates has synthesised a range of phenoxyimine ligands that contain the ketimine moiety and used them to synthesis bis-phenoxyimine titanium complexes.[6] The rationale behind the choice of the ketimine group was that it might better resist insertion into a Ti-alkyl bond. The ligands were synthesised *via* Friedel-Crafts reactions from 2,4-di-tert-butylphenol with the corresponding imidoyl chlorides. The four bis-phenoxyketimine titanium complexes synthesised were all found to be active ethylene polymerisation catalysts when activated with MAO. A comparison

with the bis-phenoxyaldimine titanium complex showed the ketimine complexes to have inferior catalyst activities.

Although most of the complexes synthesised and studied contain two phenoxyimine ligands, a smaller number of reports have been concerned with mono-phenoxyimine complexes. Work reported by Ladipo included a mono-phenoxyimine titanium trichloride and a mono-phenoxyimine titanium tris-dimethylamide complex.[7] Both complexes were tested for ethylene polymerisation activity and were found to be about 30-60 times less active than Cp_2ZrCl_2.

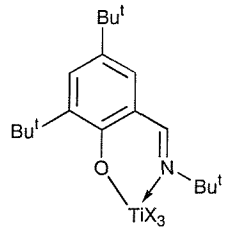

X = Cl, NMe_2

Figure 5.3: Mono-phenoxyimine titanium complexes reported by Ladipo.

Bochmann reported work focusing on titanium and zirconium complexes containing a phenoxyimine ligand as well as a cyclopentadienyl ligand.[8] The complexes were all found to be active for the polymerisation of ethylene but were between 10-1000 times less active than Cp_2TiCl_2 and Cp_2ZrCl_2.

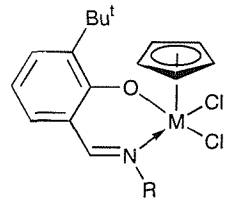

M = Ti, Zr; R = 2,4,6-trimethylphenyl, pentafluorophenyl, cyclohexyl

Figure 5.4: Monocyclopentadienyl phenoxyimine complexes reported by Bochmann.

The phenoxyimine ligand can be incorporated into larger ligand architectures through the imine substituent. One example of this is a diphenoxy-monoimine ligand reported by Ladipo in which the imine substituent is an *o*-phenol.[7] A more common example of the versatility of the phenoxyimine group is a di-phenoxyimine ligand generated by linking two phenoxyimine groups through the imine nitrogens. Examples of the different linking groups that have been utilised are: a cyclohexyl group,[9] ferrocene,[10] and a biaryl group.[11,12,13]

Results and Discussion

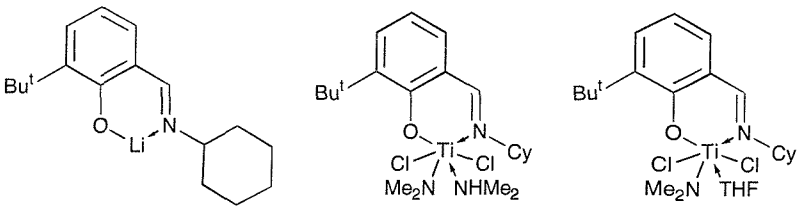

(5.1)

(5.2)

(5.3)

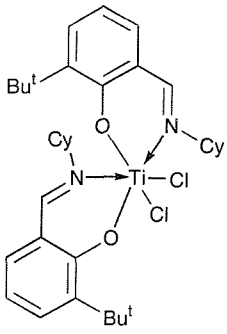

(5.4)

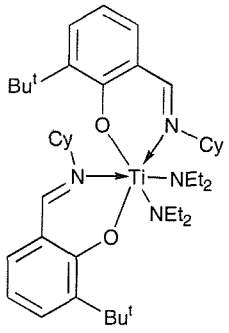

(5.5)

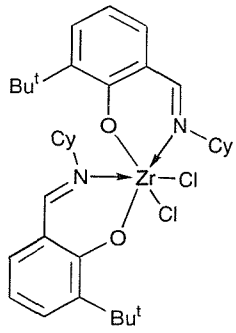

(5.6)

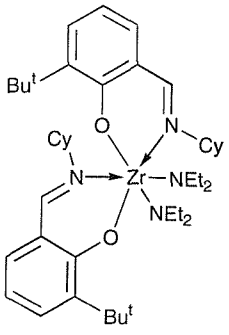

(5.7)

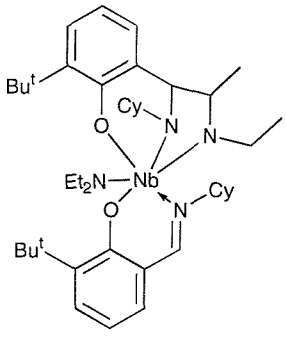

(5.8)

Figure 5.5: Lithium phenoxyimine **(5.1)**, titanium complexes **(5.2)**-**(5.5)**, zirconium complexes **(5.6)**-**(5.7)**, and niobium complex **(5.8)** synthesised.

5.2 Ligand Synthesis

The 2-*tert*-butyl-6-cyclohexyliminomethyl-phenol ligand was synthesised by reaction of 3-*tert*-butyl-2-hydroxybenzaldehyde with cyclohexylamine in toluene using *p*-toluenesulfonic acid monohydrate as a catalyst. The synthesis was essentially identical to that reported by Bochmann.[14]

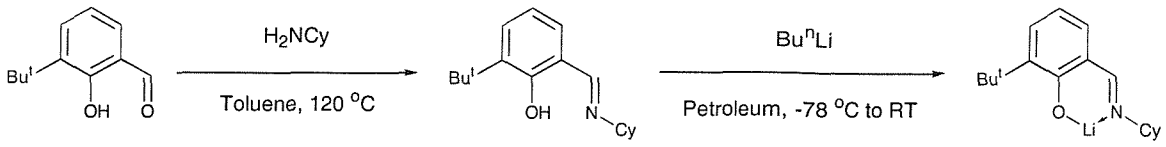

Scheme 5.2: Synthesis of 2-*tert*-butyl-6-cyclohexyliminomethyl-phenol and lithium 2-*tert*-butyl-6-cyclohexyliminomethyl-phenoxide (**5.1**).

The iminophenol ligand was deprotonated by reaction with Bu^{n}Li in petroleum to give the lithium phenoxyimine ligand (**5.1**). The extremely air and moisture sensitive white solid was isolated in good yield by filtration. Despite this the product has partial solubility in petroleum and a second crop of product was obtained by concentrating and cooling the supernatant solution to –30 °C. Despite the air and moisture sensitivity of the compound, as with the lithium amido/imino ligands (Chapter 2), it can be stored indefinitely under N_2 in a glovebox.

5.2.1 NMR spectroscopy for (5.1)

The absence of a peak in the ^{1}H NMR spectrum above 10 ppm demonstrates that the iminophenol ligand has been deprotonated by the Bu^{n}Li to give the lithium phenoxyimine species. The furthest downfield peak is due to the imine proton, which is further downfield than the aromatics and appears at 7.96 ppm. The phenoxy-bearing carbon is shifted to 169.05 ppm in the ^{13}C{H} NMR spectrum, making it further downfield than the imine carbon (166.55 ppm). The cyclohexyl group now appears as six signals in the ^{13}C{H} NMR spectrum, unlike in the starting material, where it appeared as four signals. The methine cyclohexyl CH is shifted downfield to 72.35 ppm in the ^{13}C{H} NMR spectrum and upfield to *ca.* 2.6 ppm in the ^{1}H NMR spectrum. The *tert*-butyl resonances appear at approximately the same positions as in the iminophenol ligand.

5.3 Titanium complexes bearing one phenoxyimine ligand

The first step in the study of reactions of the phenoxyimine ligand with titanium and zirconium complexes bearing dialkylamide ligands was to react one equivalent of the lithium phenoxyimine (**5.1**) with $Ti(NMe_2)_2Cl_2$. The result was complex (**5.2**). It is a titanium(IV) complex consisting of one phenoxyimine ligand, two chlorides, one dimethylamide ligand and a dimethlyamine. The complex was characterised by NMR spectroscopy and a single crystal X-ray diffraction study, but the mechanism of its formation is unclear. It appeared possible that the lithium phenoxyimine ligand had been reprotonated before reacting with the $Ti(NMe_2)_2Cl_2$ and eliminating a molecule of dimethylamine, which then coordinated to the titanium complex.

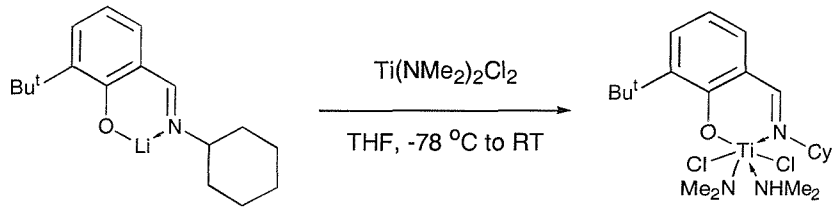

Scheme 5.3: Synthesis of (**5.2**).

To test this hypothesis the reaction between the neutral iminophenol ligand and one equivalent of $Ti(NMe_2)_2Cl_2$ was performed. The result of the reaction was complex (**5.3**), as identified by NMR spectroscopy. As with (**5.2**), the complex bears one phenoxyimine ligand, two chlorides and one dimethylamide ligand. But a molecule of THF completes the coordination sphere instead of a dimethylamine ligand.

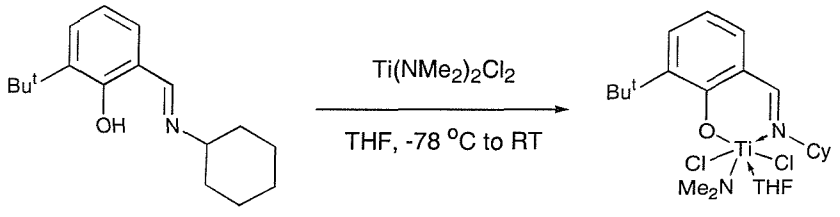

Scheme 5.4: Synthesis of (**5.3**).

Given that the protonolysis reaction of the iminophenol ligand with $Ti(NMe_2)_2Cl_2$ eliminates one equivalent of dimethylamine and the complex favours the coordination of a THF molecule, it is unlikely that the formation of **(5.2)** occurs by a simple reprotonation of the lithium phenoxyimine ligand followed by dimethylamine elimination. As such the mechanism of formation of **(5.2)** remains unclear and requires further study. Similar reactions could be carried out with other $Ti(NR_2)_2Cl_2$ complexes or analogous zirconium complexes, which might offer some insight into the formation of **(5.2)**.

The isolation of **(5.2)** and **(5.3)** shows that it is possible to synthesise mono-phenoxyimine $LTi(NMe_2)Cl_2L'$ type complexes (where L=phenoxyimine; L'=$NHMe_2$, THF). The phenoxyimine ligand does not undergo the rearrangement observed in the titanium complexes **(4.7)**, **(4.8)**, **(4.9)** and **(4.10)**. With the reduced steric demands of the phenoxyimine ligand compared to the arylamido/imino ligands, it is possible that a reduction of steric crowding about the titanium centre is the driving force for the rearrangement to a tripodal ligand in **(4.7)**, **(4.8)**, **(4.9)** and **(4.10)**. The evidence here suggests that a reduction of the steric crowding is not necessary for the less sterically demanding phenoxyimine ligand. It is also possible that better π-donation by the arylamido ligand may make a dialkylamide ligand more nucleophilic and therefore more prone to migration.

5.3.1 NMR spectroscopy for (5.2) and (5.3)

The resonances due to the phenoxyimine ligand in both **(5.2)** and **(5.3)** appear in very similar positions (see Table 5.1). The dimethylamide resonances appear in the same region in both complexes [**(5.2)** ^1H 3.56, $^{13}C\{^1H\}$ 54.06; **(5.3)** ^1H 3.54, $^{13}C\{^1H\}$ 53.48 ppm]. The peaks are located further downfield than those of the Ti-NMe_2 groups in complexes **(4.7)** and **(4.9)** which appear in the proton spectra at *ca.* 3.1 ppm and in the carbon NMR spectra at *ca.* 46 ppm. The methyls of the dimethylamine group in **(5.2)** resonate at 1.84 (^1H) and 40.35 ($^{13}C\{^1H\}$) ppm and the N*H* appears as a signal at 7.16 ppm. The imine group is identifiable by the downfield resonances at *ca.* 8.3 in the ^1H and 164.5 in the $^{13}C\{^1H\}$ NMR spectra. The NMR spectra of **(5.2)** and **(5.3)** are similar to the mono-phenoxyimine titanium tris-dimethylamide and mono-phenoxyimine titanium trichloride complexes reported by Ladipo.[7]

Table 5.1: A comparison of selected ^{1}H and $^{13}C\{^{1}H\}$ NMR data for **(5.2)** and **(5.3)**.[a]

Compound	(5.2)	(5.3)
Imine *H*	8.25	8.30
Cy *CH* α to N	4.55-4.70	4.40-4.60
$C(CH_3)_3$	1.55	1.57
Ti-N$(CH_3)_2$	3.56	3.54
Imine *C*	164.62	164.51
Cy *C*H α to N	67.61	67.24
$C(CH_3)_3$ [b]	30.63, 34.86	30.55, 35.92
Ti-N$(CH_3)_2$	54.06	53.48

[a] Spectral data expressed in ppm; solvent = C_6D_6.

[b] The first value given is that of the methyl carbons, followed by the tertiary carbon.

5.3.2 X-ray diffraction study on (5.2)

X-ray diffraction quality crystals of **(5.2)** were grown by cooling a saturated toluene solution to –30 °C to give the product as dark red blocks.

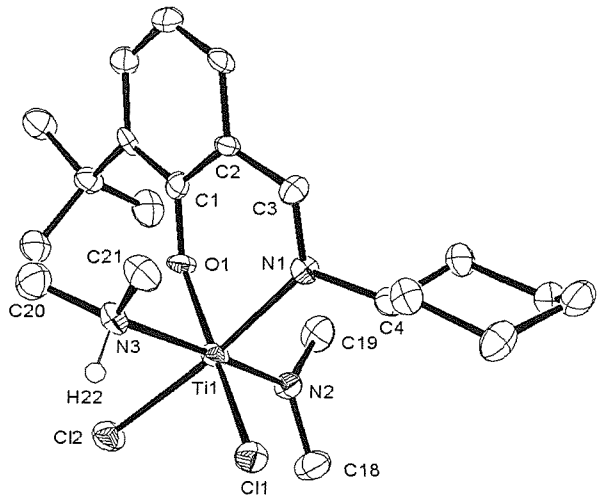

Figure 5.6: ORTEP representation of the crystal structure of (2-*tert*-butyl-6-cyclohexyliminomethyl-phenoxy) titanium dimethylamide dichloride dimethylamine **(5.2)** (50% probability thermal ellipsoids). Hydrogens are omitted for clarity.

The six-coordinate complex **(5.2)** adopts a distorted octahedral geometry. The phenoxyimine ligand occupies two *cis* sites with a bite angle of 82.6(2)°. The two chloride ligands occupy mutually *cis* sites and are separated by an angle of 91.74(8)°. The remaining dimethylamide and dimethylamine ligands are located *trans* to one another. The bonds between the metal centre and the phenoxyimine ligand [Ti(1)-O(1) 1.871(5); Ti(1)-N(1) 2.170(6)Å] are typical of the phenoxyimine complexes reported here and in the literature.[4,8,15] The titanium-imine bond length lies approximately half way between the Ti-dimethylamide [Ti(1)-N(2) 1.885(6)Å] and the Ti-dimethylamine bond lengths [Ti(1)-N(3) 2.404(6)Å]. The dimethylamine ligand is clearly identifiable due to the increased length of the Ti-N bond compared to the dimethylamide ligand, and the pyramidal geometry of the amine nitrogen. The two Ti-Cl bond lengths are equal [Ti(1)-Cl(1) 2.371(2); Ti(1)-Cl(2) 2.383(2)Å] despite one chloride being *trans* to the phenoxide and the other *trans* to the imine. The imine bond length of 1.292(8)Å is typical and comparable to that of the amido/imino ligands in the complexes reported in Chapters 3 and 4.

5.4 Titanium and zirconium complexes bearing two phenoxyimine ligands

Four bis-phenoxyimine complexes of titanium and zirconium were synthesised by reaction of two equivalents of the 2-*tert*-butyl-6-cyclohexyliminomethyl-phenol ligand with $Ti(NEt_2)_2Cl_2$, $Ti(NEt_2)_4$, $Zr(NEt_2)_2Cl_2(THF)_2$, and $Zr(NEt_2)_4$ to give compounds **(5.4)**, **(5.5)**, **(5.6)** and **(5.7)** respectively (Scheme 5.5). In each case, two equivalents of diethylamine were cleaved off the metal centre.

The additions were all carried out in THF at -78 °C before rising quickly to RT and stirring overnight. The resultant complexes were readily crystallised by cooling saturated toluene or petroleum solutions to –30 °C to give the compounds as crystalline solids in 39-60% yield. This is quite low given that the proton NMR spectra of aliquots from these reactions showed them to be essentially quantitative.

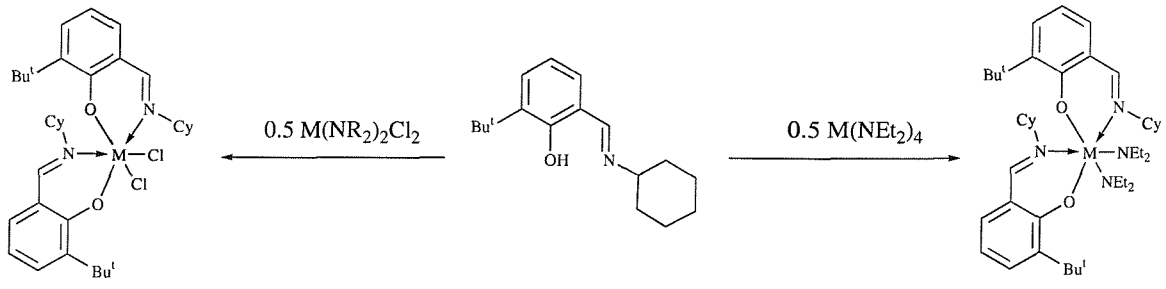

M = Ti, **(5.4)**
M = Zr, **(5.6)**

M = Ti, **(5.5)**
M = Zr, **(5.7)**

Scheme 5.5: Synthesis of **(5.4)**, **(5.5)**, **(5.6)** and **(5.7)**.

The formation of these four complexes showed that it was possible to have this phenoxyimine ligand bound to titanium and zirconium centres bearing the bulky diethylamide ligand without promoting the migration of the dimethylamide to the imine carbon to generate a new ligand architecture. This shows that the process is more common with the more sterically demanding amido/imino ligands and their complexes reported in Chapters 3 and 4.

Complexes **(5.4)** and **(5.6)** have previously been reported by Fujita and co-workers.[16,17] Both complexes were synthesised by a different method and only their ^{1}H NMR data were reported due to the focus of the report being their behaviour as polymerisation catalysts.

5.4.1 X-ray diffraction studies on (5.4), (5.5) and (5.7)

The three complexes all adopt the same distorted octahedral geometry with the two oxygen atoms mutually *trans* to one another and the imine nitrogens occupying mutually *cis* sites. The two remaining donor atoms (chlorides or amide nitrogens) are thus arranged *trans* to the imine nitrogens and *cis* to each other. This geometry makes the complexes C_2-symmetric.

Table 5.2: A comparison of selected structural data between **(5.4)**, **(5.5)** (M=Ti) and **(5.7)** (M=Zr).[a]

Compound	(5.4)	(5.5)	(5.7)
M-O	1.863(4)	1.963(4)	2.050(4)
M-N [b]	2.189(6)	2.286(4)	2.411(6)
M-X [c]	2.3091(20)	1.939(4)	2.072(5)
C=N	1.287(8)	1.290(7)	1.283(8)
O-M-O	172.06(14)	163.00(11)	157.22(12)
N-M-N [b]	80.19(13)	82.70(11)	81.17(13)
O-M-N [b]	81.90(19)	81.50(16)	77.06(18)
X-M-X [c]	100.09(6)	97.93(13)	99.41(15)
M-O-C	145.0(4)	141.9(3)	145.1(4)

[a] Mean bond lengths in Å, angles in °.

[b] Imine nitrogen.

[c] **(5.4)** (X=Cl);**(5.5)**, **(5.7)** (X=NEt_2).

A comparison of the bis-phenoxyimine titanium dichloride complex **(5.4)** and the bis-phenoxyimine titanium bis-diethylamide complex **(5.5)** shows that the bonds between the phenoxyimine ligand and the metal are *ca.* 0.1Å longer in **(5.5)**. Despite this the bite angle of the ligand is essentially the same in both complexes. The bonds are a further *ca.* 0.1Å longer to zirconium in **(5.7)** than they are in **(5.5)**. Complex **(5.4)** adopts the geometry that is closest to octahedral with a O-Ti-O angle of 172.06(14)°. When the ligands are changed from chlorides to bulkier diethylamides in **(5.5)**, the O-Ti-O angle is 163.00(11)° and the complex adopts a more distorted octahedral geometry. The combination of diethylamide ligands with a larger metal centre of zirconium in **(5.7)** results in a greater distortion of the

octahedral geometry, with a O-Zr-O angle of 157.22(12)°. The bite angle of the ligand in **(5.7)** is *ca.* 4-5° smaller than in the titanium complexes.

5.4.1.1 X-ray diffraction study on compound (5.4)

X-ray diffraction quality crystals of **(5.4)** were grown by cooling a saturated toluene solution to –30 °C to give the product as dark red blocks.

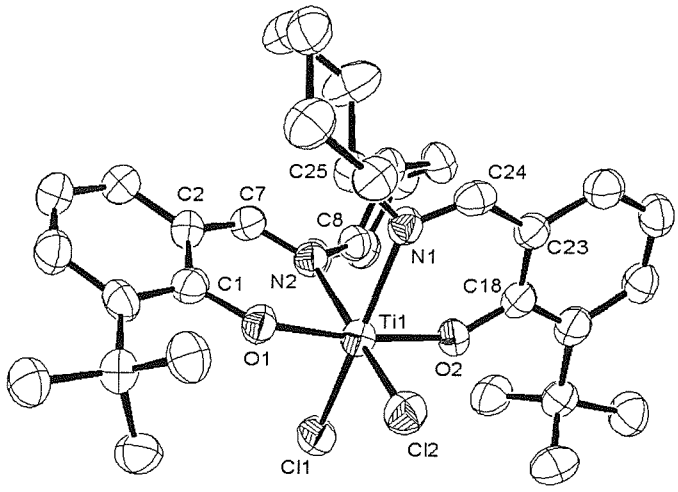

Figure 5.7: ORTEP representation of the crystal structure of bis-(2-*tert*-butyl-6-cyclohexyliminomethyl-phenoxy) titanium dichloride **(5.4)** (50% probability thermal ellipsoids). Hydrogens are omitted for clarity.

Compound **(5.4)** crystallizes as a monomer with two molecules in the asymmetric unit as well as four molecules of toluene. The complex possesses C_2-symmetry and the geometry about the titanium centre is distorted octahedral. As with the majority of bis-phenoxyimine L_2MCl_2 type complexes, the coordination geometry consists of *trans* oxygens, *cis* imine nitrogens and *cis* chlorides. The mean phenoxyimine bite angle is 81.90(19)° and the mean Ti-O bond length is 1.863(4)Å. The mean Ti-N(imine) bond length is 2.189(6)Å and the N-Ti-N angle is 80.19(13)°. The mean imine bond length is 1.287(8)Å and the geometry about the imine bond is planar. The Cl-Ti-Cl angle is 100.09(5)° with a mean Ti-Cl bond length of 2.3091(20)Å. The data is agreeable with bis-phenoxyimine L_2TiCl_2 type complexes reported in the literature.[4,8,15]

5.4.1.2 X-ray diffraction study on compound (5.5)

X-ray diffraction quality crystals of (**5.5**) were grown by cooling a saturated petroleum solution to –30 °C to give the product as orange plates.

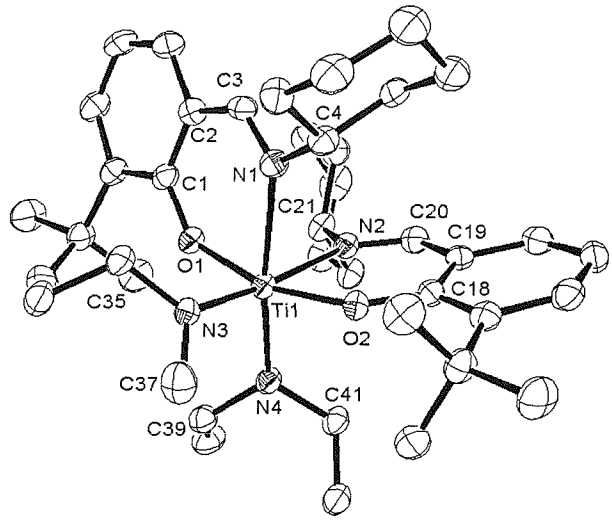

Figure 5.8: ORTEP representation of the crystal structure of bis-(2-*tert*-butyl-6-cyclohexyliminomethyl-phenoxy) titanium bis-diethylamide (**5.5**) (50% probability thermal ellipsoids). Hydrogens are omitted for clarity.

Compound (**5.5**) is distorted octahedral and adopts the same geometry about the titanium centre as (**5.4**) but with *cis* diethylamides instead of *cis* chlorides. The phenoxy-oxygens are again located *trans* to one another. The mean phenoxyimine bite angle is 81.50(16)° with a mean Ti-O bond length of 1.963(4)Å, whilst the mean titanium-nitrogen bond length to the imine is 2.286(4)Å. The mean imine bond length is 1.290(7)Å and the imine group possesses the same planar geometry as in (**5.4**). The mean titanium-diethylamide bond length is 1.939(4)Å and the N-Ti-N angle between the two diethylamide groups is 97.93(13)°.

5.4.1.3 X-ray diffraction study on compound (5.7)

X-ray diffraction quality crystals of **(5.7)** were grown by cooling a saturated toluene solution to –30 °C to give the product as bright yellow plates.

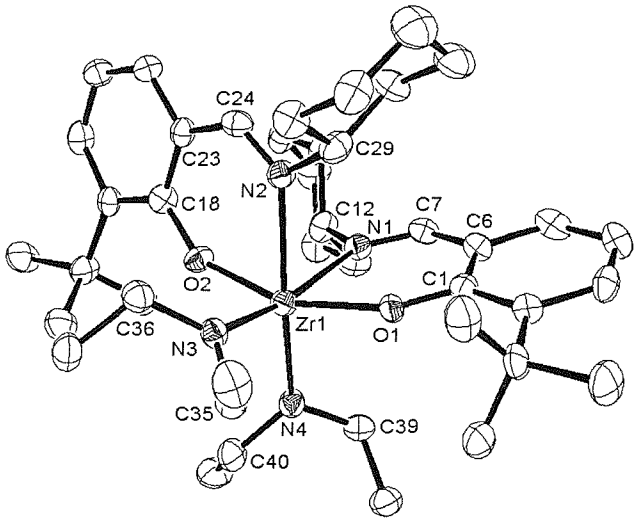

Figure 5.9: ORTEP representation of the crystal structure of bis-(2-*tert*-butyl-6-cyclohexyliminomethyl-phenoxy) zirconium bis-diethylamide **(5.7)** (50% probability thermal ellipsoids). Hydrogens are omitted for clarity.

The complex possesses a distorted octahedral geometry about the zirconium centre similar to that adopted by the two titanium complexes **(5.4)** and **(5.5)**. It also adopts the same coordination geometry of *trans* phenoxy groups, *cis* imine nitrogens, and *cis* diethylamide ligands. The mean Zr-O bond length of 2.050(4)Å is longer than the Ti-O distances observed in **(5.4)** and **(5.5)**. The O-Zr-O angle of 157.22(12)° shows greater distortion from the ideal octahedral geometry than is displayed in **(5.4)** and **(5.5)**. The mean zirconium-nitrogen bond length to the imine [2.411(6)Å] is also longer than in the titanium analogues. The mean bite angle of the phenoxyimine ligand is 77.06(18)° and the imine bond length remains the same as in the titanium examples [1.283(8)Å]. The mean zirconium-diethylamide distance is 2.072(5)Å and so is longer than the titanium-diethylamide distances of **(5.5)** [1.939(4)Å].

The structural data of **(5.7)** is very similar to that of two di-phenoxyimine zirconium bis-dimethylamide complexes reported by Erker.[15] The ligands

employed are 2-alkyliminomethyl-phenoxide groups and so there is no second substituent *ortho* to the phenoxy group. The lack of this substituent would make the ligands less sterically demanding than the *tert*-butyl substituted ligand studied here. However, all the major bond lengths and angles of these two complexes are comparable to those of **(5.7)** and the two phenoxyimine ligands adopt the same *trans*-phenoxides and *cis*-imines geometry as **(5.7)**.

The Zr-O bond lengths in **(5.7)** are *ca.* 0.1Å longer than those in two bis-phenoxyimine zirconium dichloride complexes reported in the literature.[8,18] This is most likely due to the stronger electron donating nature of the diethylamide ligands of **(5.7)** compared to the chlorides of the literature examples.

5.4.2 NMR spectroscopy for (5.4), (5.5), (5.6) and (5.7)

The most indicative aspect of the ^{1}H NMR spectra of the reaction aliquots that suggests that the reactions have occurred is the disappearance of the phenolic O*H* resonance. For complexes **(5.5)** and **(5.7)** the CH_2 resonance of the diethylamide groups changes from a simple quartet in the starting material to a more complex pattern in the product.

Table 5.3: A comparison of selected ^{1}H and $^{13}C\{^{1}H\}$ NMR data of **(5.4)**, **(5.5)** (M = Ti) and **(5.6)**, **(5.7)** (M = Zr).[a]

Compound	(5.4)	(5.5)	(5.6)	(5.7)
Imine *H*	7.82	8.01	7.89	8.02
Cy C*H* α to N	4.06	3.68	4.00	3.82
$C(CH_3)_3$	1.79	1.80	1.72	1.77
$M\text{-}N(CH_2CH_3)_2$	-	4.00, 4.20	-	3.65-3.85
$M\text{-}N(CH_2CH_3)_2$	-	1.07	-	1.17
Imine *C*	163.89	164.44	167.52	166.19
Cy *C*H α to N	67.24	61.89	63.68	62.26
$C(CH_3)_3$ [b]	30.86, 36.20	31.34, 36.26	30.72, 36.10	31.07, 36.21
$M\text{-}N(CH_2CH_3)_2$	-	48.43	-	43.74
$M\text{-}N(CH_2CH_3)_2$	-	15.19	-	15.66

[a] Spectral data expressed in ppm; solvent = C_6D_6.

[b] The first value given is that of the methyl carbons, followed by the tertiary carbon.

The position of the imine proton resonance does not vary significantly between the different complexes and is typical of phenoxyimine complexes of titanium and zirconium. It appears at a slightly higher frequency when the other ligands in the coordination sphere are diethylamides rather than chlorides. The diethylamide groups appear as two resonances in the $^{13}C\{^{1}H\}$ NMR spectra with the methyl groups appearing at *ca.* 15 ppm and the methylene groups at *ca.* 50 ppm. Whilst the methyl groups appear as a single triplet in the ^{1}H NMR spectra (*ca.* 1.1 ppm), the methylene groups are seen as two resonances. In the titanium complex **(5.5)** the four methylene groups appear as two sextets at 4.00 and 4.20 ppm and the zirconium complex **(5.7)** has two overlapping multiplets between 3.55 and 3.95 ppm also overlapping with the resonance of the methine cyclohexyl C*H*.

The NMR data suggests that the complexes all adopt the same C_2-symmetric distorted octahedral geometry that they possess in the solid state. There was no evidence of other isomers present in solution.

5.4.3 Decomposition studies of complexes (5.5) and (5.7)

Solutions of (**5.5**) and (**5.7**) in d^8-toluene were heated in Young's tap NMR tubes in order to see if the phenoxyimine ligand would undergo a migratory insertion of a diethylamide group under more forceful conditions. The samples were heated to 100 °C for 48 h with no changes in the ^{1}H NMR spectra.

5.5 Formation and characterisation of a niobium(V) complex of the type [Nb^{V}LL'(NEt$_2$)] from Nb(NEt$_2$)$_4$

An attempt was made to synthesise a $L_2Nb(NEt_2)_2$ type complex of the Group 5 metal niobium in its +4 oxidation state using the 2-*tert*-butyl-6-cyclohexyliminomethyl-phenol ligand. Using [Nb(NEt$_2$)$_4$] as the starting material it was anticipated that the reaction would proceed in the same way as that used to form the analogous zirconium complex (**5.7**). However, the product isolated from this reaction was a niobium(V) complex bearing one phenoxyimine ligand (**L**), one diethylamide and a novel tridentate phenoxy-diamide ligand (**L'**) (Scheme 5.6). The new ligand (**L'**) consists of the phenoxyimine ligand linked to a diethylamide group through a new carbon-carbon bond. The bond links the imine carbon to a methylene carbon of the diethylamide ligand. This has resulted in the conversion of the imine double bond into a single bond and the neutral imine nitrogen into an amide group.

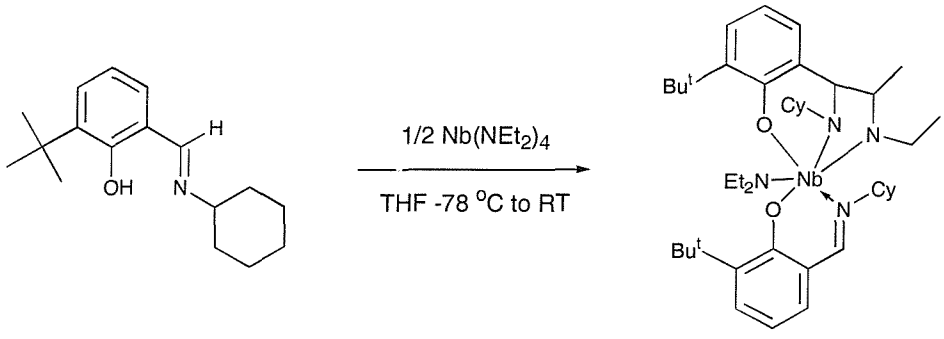

(5.8)

Scheme 5.6: Formation of (**5.8**)

5.5.1 X-ray diffraction study of compound (5.8)

X-ray diffraction quality crystals of **(5.8)** were grown by cooling a saturated petroleum solution to –30 °C to give the product as as orange blocks.

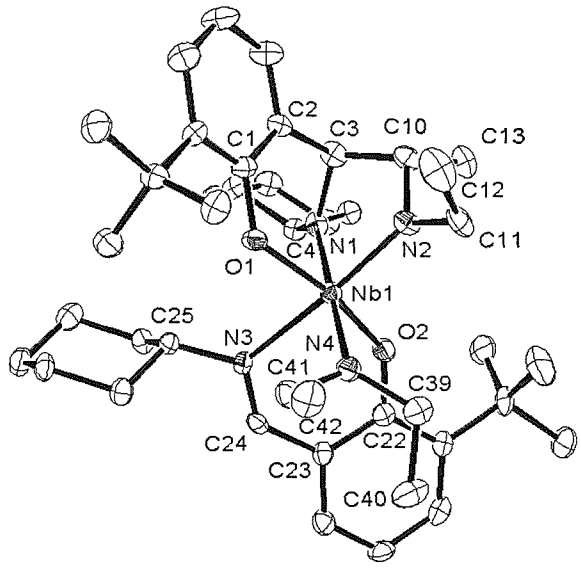

Figure 5.10: ORTEP representation of the crystal structure of (2-*tert*-butyl-6-cyclohexyliminomethyl-phenoxy) [2-*tert*-butyl-6-(1-cyclohexylamido-2-ethylamido-propyl)-phenoxy] niobium diethylamide **(5.8)** (50% probability thermal ellipsoids). Hydrogens are omitted for clarity.

The complex possesses a distorted octahedral geometry about the niobium(V) centre with the tridentate ligand adopting a *fac* conformation. The two phenoxy groups are *trans* to one another as in the complexes **(5.4)**, **(5.5)** and **(5.7)**. The O-Nb-O angle is 165.99° and the two Nb-O distances are very similar [**(L')**: O(1)-Nb(1) 2.019(3)Å; **(L)**: O(2)-Nb(1) 2.051(3)Å]. The cyclohexylamide nitrogen of **(L')** is *trans* to the remaining diethylamide [N(1)-Nb(1)-N(4) 177.58(13)°]. The ethylamide nitrogen of **(L')** is thus *trans* to the imine group of L [N(2)-Nb(1)-N(3) 172.15(12)°]. The three niobium-amide bond lengths [N(1)-Nb(1) 2.002(3)Å; N(2)-Nb(1) 1.986(3)Å; N(4)-Nb(1) 2.027(3)Å] are significantly shorter than the niobium-imine distance [N(3)-Nb(1) 2.336(3)Å]. The new carbon-carbon bond between C(7) and C(18) is a typical C-C single bond [C(7)-C(18) 1.529(6)Å]. The conversion in **(L')** of the imine to an amide has resulted in the C-N bond length increasing to 1.488(5)Å compared to the normal imine bond length [N(3)-C(28)

1.298(5)Å] observed for the intact imine moiety of **(L)**.

The tridentate ligand **(L')** binds to the niobium centre forming a six-membered chelate ring [through O(1) and N(1)] and a five-membered chelate ring [through N(1) and N(2)]. These two chelate rings are fused along the C(7)-N(1) bond. The three bite angles of **(L')** are: N(1)-Nb(1)-O(1) 87.80(11)°; N(2)-Nb(1)-O(1) 92.17(12)° and N(2)-Nb(1)-N(1) 81.65(13)°. The bite angle between the two amide nitrogens is the smallest of the three due to them being part of the five-membered chelate ring. Both of the amide groups are planar [sum of the angles about the nitrogen atom: N(1) 360°; N(2) 359.7°].

5.5.2 NMR spectroscopy for (5.8)

The ^{1}H and $^{13}C\{^{1}H\}$ NMR spectra of **(5.8)** were more complicated compared to those of the di-phenoxyimine L_2MX_2 type complexes due to **(5.8)** containing two different ligands based on the same framework. The aryl regions of both the ^{1}H and $^{13}C\{^{1}H\}$ NMR spectra are quite simple. There is only one resonance in both spectra for the imine group. This is because C(7) of L' is no longer sp^2 hybridised and so appears much further upfield. C(7) appears at 72.54 ppm in the $^{13}C\{^{1}H\}$ NMR spectrum (d^8-toluene) with C(18) at 74.86 ppm. The proton of C(7) appears as a singlet at 4.42 ppm in the ^{1}H NMR spectrum. It should be coupled to the proton of C(18) but with the geometry adopted by **(L')** the dihedral angle H-C(7)-C(18)-H is close to 90°. From the Karplus relationship this gives the minimum theoretical value of the coupling constant *J*. This could then make the resonance of C(7) appear as a broad singlet instead of a doublet. C(18) appears at *ca.* 4.2 ppm as multiplet.

The methine cyclohexyl carbon of **(L')** [C(12)] bonded to the amide nitrogen appears at 63.50 ppm. This is further downfield than the corresponding carbon in **(L)** (60.87 ppm), which is bonded to a neutral nitrogen atom. The remaining CH_2 [C(20)] group of the "diethylamide section" of **(L')** appears at 51.40 ppm, further downfield than the CH_2s of the diethylamide ligand (45.13). The two protons on C(20) are diastereotopic, appearing at 3.37 and 3.99 ppm. The CH_2s of the diethylamide are also diastereotopic, appearing at *ca.* 4.1 and 4.5 ppm. The resonances of the two methyl groups of **(L')**, C(19) and C(21), are quite separated in both the ^{1}H and $^{13}C\{^{1}H\}$ NMR spectra. C(19) appears as a doublet at 1.35 ppm in the ^{1}H NMR spectrum and a peak at 20.55 ppm in the $^{13}C\{^{1}H\}$ NMR spectrum.

C(21) appears as a triplet at 0.96 ppm in the proton NMR spectrum and a signal at 15.90 ppm in the $^{13}C\{^{1}H\}$ NMR spectrum. The methyl groups of the diethylamide ligand appear at *ca.* 0.80 ppm (^{1}H) and 14.10 ppm ($^{13}C\{^{1}H\}$).

5.5.3 Formation of (5.8)

The fact that the niobium atom in **(5.8)** has undergone a one electron oxidation from Nb(IV) to Nb(V) suggests that a radical mechanism is involved in the formation of the new ligand **(L')**. A very similar niobium(V) complex to **(5.8)**, arising from the reaction between a linked bis-phenoxyimine ligand with $Nb(NEt_2)_4$ has been reported by Scott.[11] The complex contains a tetradentate ligand in which one half is an intact phenoxyimine group and the other half is a phenoxyamide group. The coordination sphere is completed by two diethylamide ligands. The bis-phenoxyimine ligand has become fused with a diethylamine group through one of the imine carbons and a CH_2 of the diethylamine. This has resulted in the formation of a tetradentate trianionic ligand because the pendant "diethylamine" group is non-coordinating. This ligand is clearly analogous to the coupling of the phenoxyimine and the phenoxydiamide ligands in **(5.8)**.

Scott also reports the identification of a second niobium complex from the same reaction. This contains the intact bis-phenoxyimine ligand, one diethylamide ligand and an ethylimido ligand. He proposed that the ligand would initially react with $Nb(NEt_2)_4$ to form the $LNb(NEt_2)_2$ niobium(IV) complex and two equivalents of diethylamine. An ethyl radical is then lost from a diethylamide group to yield the imide and to oxidise the niobium centre. This ethyl radical is then quenched by a molecule of diethylamine to form the more stable 1-ethylaminoethyl radical. This radical then reacts with further $LNb(NEt_2)_2$ and adds to the imine group to give the niobium(V) species and the "diethylamine-part" of the new ligand.

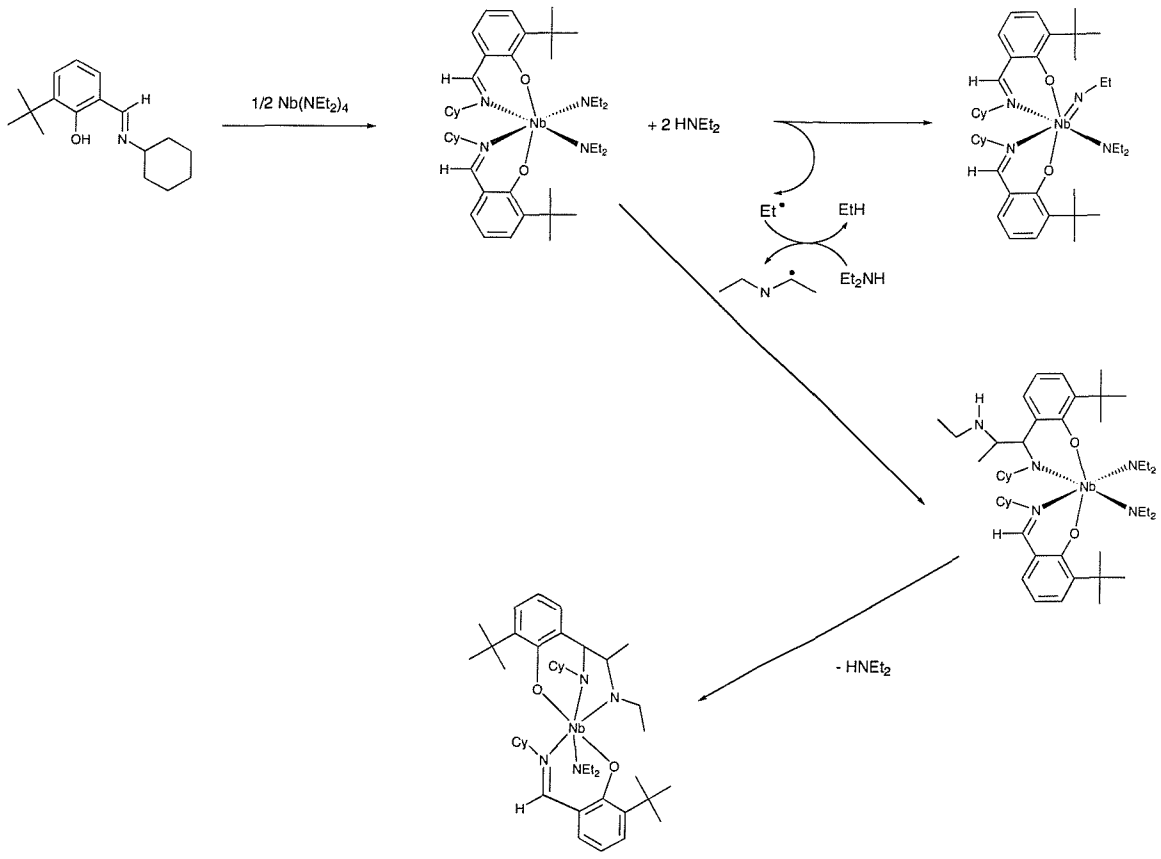

Scheme 5.7: Possible mechanism for the formation of **(5.8)**.

Based on this mechanism, it is possible that the formation of **(5.8)** follows the same mechanism but then contains an extra step. Because Scott's ligand has two linked phenoxyimine groups, the geometry of the donor atoms is more rigidly enforced than in the case of **(5.8)**, where there were probably two separate phenoxyimine ligands coordinating the niobium centre. With more flexibility it is plausible that the diethylamine group that is fused to the phenoxyamide ligand could perform an intramolecular diethylamine elimination of one of the two diethylamide ligands. This elimination would be driven by the chelate effect and result in the formation of complex **(5.8)**.

There was no evidence of the presence of the proposed imido complex in the material crystallised from petroleum that yielded the X-ray crystal structure and NMR spectra of **(5.8)**. The mother liquor that yielded the crystals of **(5.8)** was not subjected to NMR analysis so it is unknown whether or not the imido complex was produced by the reaction. In light of the proposed mechanism the reaction requires further study to try and detect the imido compound. If the complex was detected it

would provide strong evidence to support the proposed mechanism. Regardless of whether Scott's proposed mechanism is correct it is apparent that his complex and **(5.8)** were formed by a common mechanism and that **(5.8)** was possibly formed by a further elimination of diethylamine by the "dangling diethylamine" moiety to yield the trianionic ligand.

5.5.4 Formation of complex (5.8) by reaction of one equivalent of phenoxyimine ligand with $Nb(NEt_2)_4$

The reaction of one equivalent of 2-*tert*-butyl-6-cyclohexyliminomethyl-phenol with $Nb(NEt_2)_4$ was also attempted. It was anticipated that a (phenoxy-imine)$Nb(NEt_2)_3$ complex would be formed. Crystals suitable for X-ray diffraction were again grown from a petroleum solution of the reaction mixture, but proved to be complex **(5.8)** again. The fact that this complex was formed in preference to the anticipated 1:1 complex suggests that complex **(5.8)** is very thermodynamically stable.

5.6 Conclusions

The lithium salt of 2-*tert*-butyl-6-cyclohexyliminomethyl-phenol was synthesised by reaction of the iminophenol ligand with Bu^nLi to give **(5.1)** as a colourless solid. The lithium phenoxyimine was thermally stable and could be stored under N_2 indefinitely. The result of a salt metathesis reaction between **(5.1)** and $Ti(NMe_2)_2Cl_2$ was the mono-phenoxyimine titanium dimethylamide dichloride dimethylamine complex **(5.2)**. The similar mono-phenoxyimine titanium dimethylamide dichloride tetrahydrofuran complex **(5.3)** was prepared by a protonolysis reaction between 2-*tert*-butyl-6-cyclohexyliminomethyl-phenol and $Ti(NMe_2)_2Cl_2$. Neither complex displayed any evidence of an insertion of the imine double bond into a titanium-dimethylamide bond, as observed with the amido/imino ligands and $Ti(NMe_2)_2Cl_2$ [complexes **(4.7)**, **(4.8)**, **(4.9)** and **(4.10)**, Chapter 4]. This suggests that the increased steric bulk of the amido/imino ligand may be the reason for the rearrangements observed in **(4.7)**, **(4.8)**, **(4.9)** and **(4.10)**. The mechanism that lead to the formation of **(5.2)** is unclear, but the formation of **(5.3)** *via* the protonolysis reaction suggests that **(5.2)** is not the result of reprotonated iminophenol ligand performing a protonolysis reaction with $Ti(NMe_2)_2Cl_2$.

The formation of the bis-phenoxyimine titanium dichloride and bis-phenoxyimine zirconium dichloride complexes (**5.4**) and (**5.6**) demonstrate that the L_2MCl_2 type complexes are accessible by reaction of two equivalents of iminophenol ligand with $M(NR_2)_2Cl_2$ starting materials. This route to bis-phenoxyimine metal complexes is an alternative to the established salt metathesis methodology employing metal tetrachlorides as starting materials.

Two bis-phenoxyimine complexes of titanium (**5.5**) and zirconium (**5.7**) bearing two diethylamide ligands were synthesised by reacting two equivalents of the iminophenol ligand with $Ti(NEt_2)_4$ and $Zr(NEt_2)_4$ respectively. The isolation of these complexes demonstrated that the phenoxyimine ligands are stable to insertion of the imine double bond into the metal-diethylamide bond even when there are two phenoxyimine ligands on the metal centre.

When an attempt was made to synthesise an analogous bis-phenoxyimine niobium(IV) bis-diethylamide complex the unusual phenoxyimine phenoxydiamido niobium diethylamide complex (**5.8**) was isolated. The niobium centre had been oxidised to niobium(V) and one phenoxyimine ligand had been fused to a diethylamide ligand through the imine carbon and a methine carbon of the diethylamide. This resulted in the conversion of the imine group to an amido group. The mechanism of the formation of (**5.8**) is currently unclear, but the single electron oxidation is suggestive of a radical process.

5.7 Experimental

The following compounds were prepared following literature methods: 2-*tert*-butyl-6-cyclohexyliminomethyl-phenol,[14] $Ti(NMe_2)_2Cl_2$,[19] $Zr(NEt_2)_2Cl_2(THF)_2$,[20] $Ti(NEt_2)_4$,[21] $Ti(NEt_2)_2Cl_2$,[22] $Nb(NEt_2)_4$.[23]

5.7.1 Lithium 2-*tert*-butyl-6-cyclohexyliminomethyl-phenoxide (5.1).

A 2-neck 100 ml RB flask was charged with 2-*tert*-butyl-6-cyclohexyliminomethyl-phenol (2.57 g, 9.91 mmol) and petroleum (30 cm^3). The bright yellow solution was cooled to –78 °C and Bu^nLi (4.5 cm^3 of 2.45 M solution in hexanes, 10.90 mmol) was added slowly *via* cannula to the stirred solution. Immediately upon complete addition of the Bu^nLi solution, the bright yellow reaction became colourless. The reaction was stirred at -78 °C for 1 h before being allowed to reach room temperature and then stirred for a further 16 h. This afforded the crude product as a white suspension. The supernatant was removed by filtration and the resultant solid washed with petroleum (10 cm^3), to yield the product as a white, extremely air and moisture sensitive solid (1.90 g). The mother liquor was cooled to –30 °C to yield a second crop of **(5.1)** (0.30 g).

Yield: 2.20 g, 84%.

Mp: 145 °C (dec).

$\delta_H(C_6D_6)$ 0.60-1.80 (10H, m, cyclohexyl CH_2s), 1.58 (9H, s, $ArC(CH_3)_3$), 2.55-2.70 (1H, m, cyclohexyl C*H* α to imine N), 6.67 (1H, t, aromatic), 7.08 (1H, dd, aromatic), 7.41 (1H, dd, aromatic), 7.96 (1H, s, ArC(*H*)=NCy).

$^{13}C\{^1H\}$ $\delta_C(C_6D_6)$ 25.76, 25.89, 25.94 (cyclohexyl CH_2s), 31.76 ($ArC(CH_3)_3$), 34.67 (cyclohexyl CH_2), 35.41 ($ArC(CH_3)_3$), 35.70 (cyclohexyl CH_2), 72.35 (cyclohexyl *C*H α to imine N), 114.60 (aromatic *C*H), 125.05 (quaternary aromatic), 131.11, 134.49 (aromatic *C*Hs), 141.89 (quaternary aromatic), 166.55 (Ar*C*(H)=NCy), 169.05 (quaternary aromatic).

5.7.2 (2-*tert*-Butyl-6-cyclohexyliminomethyl-phenoxy) titanium dimethylamide dichloride dimethylamine (5.2).

An ampoule was charged with $Ti(NMe_2)_2Cl_2$ (0.104 g, 0.5 mmol) and THF (15 cm^3) and cooled to –78 °C. To this was added slowly *via* cannula a cooled (-78 °C) solution of lithium **(5.1)** (0.133 g, 0.5 mmol) in THF (15 cm^3). The

resultant dark red solution was allowed to reach room temperature over *ca.* 15 h before stirring for a further 2 h. This produced a yellow/orange solution with a fine precipitate. Volatiles were removed *in vacuo* and the residue extracted into toluene (40 cm^3) and filtered through Celite. The solution was concentrated to *ca.* 10 cm^3 and cooled at -30 °C for 48 h to give the product as dark red, X-ray diffraction quality crystals.

Yield: 0.050 g, 21%.

$\delta_H(C_6D_6)$ 0.80-1.80 (10H, m, cyclohexyl C*H*$_2$s), 1.55 (9H, s, ArC(C*H*$_3$)$_3$), 1.84 (6H, br. s, HN(C*H*$_3$)$_2$), 3.56 (6H, s, N(C*H*$_3$)$_2$), 4.55-4.70 (1H, m, cyclohexyl C*H* α to imine N), 6.79 (1H, t, aromatic), 7.04 (1H, dd, aromatic), 7.16 (1H, s, *H*N(CH$_3$)$_2$), 7.41 (1H, dd, aromatic), 8.25 (1H, s, ArC(*H*)=NCy).

$^{13}C\{^1H\}$ $\delta_C(C_6D_6)$ 26.63, 26.83 (cyclohexyl *C*H$_2$s), 30.63 (ArC(*C*H$_3$)$_3$), 31.01 (cyclohexyl *C*H$_2$), 34.86 (Ar*C*(CH$_3$)$_3$), 35.90, 36.05 (cyclohexyl *C*H$_2$s), 40.35 (HN(*C*H$_3$)$_2$), 54.06 (N(*C*H$_3$)$_2$), 67.61(cyclohexyl *C*H α to imine N), 121.01, 126.34, 129.98, 132.95, 133.39, 160.51 (aromatics), 164.62 (Ar*C*(H)=NCy).

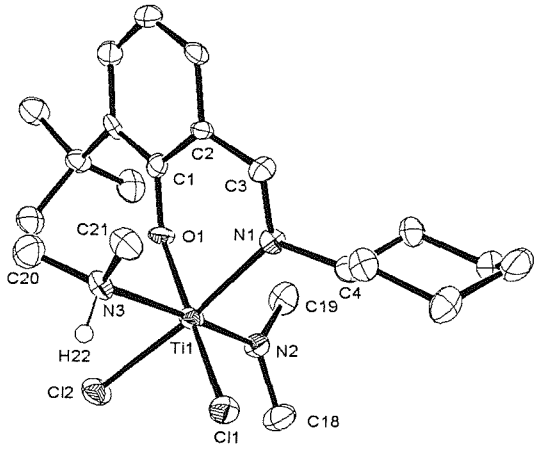

Figure 5.11: ORTEP representation of the crystal structure of (2-*tert*-butyl-6-cyclohexyliminomethyl-phenoxy) titanium dimethylamide dichloride dimethylamine **(5.2)** (50% probability thermal ellipsoids). Hydrogens are omitted for clarity.

Table 5.4: Selected bond lengths (Å) and angles (°) for **(5.2)**.

Ti(1)-O(1)	1.871(5)	Ti(1)-N(1)	2.170(6)
Ti(1)-N(2)	1.885(6)	Ti(1)-N(3)	2.404(6)
Ti(1)-Cl(1)	2.371(2)	Ti(1)-Cl(2)	2.383(2)
O(1)-C(1)	1.332(7)	C(1)-C(2)	1.426(9)
C(2)-C(3)	1.442(9)	N(1)-C(3)	1.292(8)
N(1)-C(4)	1.498(8)		
O(1)-Ti(1)-N(1)	82.6(2)	Cl(1)-Ti(1)-Cl(2)	91.74(8)
O(1)-Ti(1)-Cl(1)	163.34(16)	N(1)-Ti(1)-Cl(2)	172.68(17)
N(2)-Ti(1)-N(3)	177.3(2)	C(1)-O(1)-Ti(1)	138.9(4)
O(1)-C(1)-C(2)	117.6(6)	C(1)-C(2)-C(3)	121.8(6)
C(3)-N(1)-Ti(1)	123.5(5)	C(3)-N(1)-C(4)	116.8(6)
C(4)-N(1)-Ti(1)	119.7(4)	C(18)-N(2)-C(19)	111.1(6)
C(18)-N(2)-Ti(1)	124.1(5)	C(19)-N(2)-Ti(1)	124.6(5)
C(20)-N(3)-C(21)	110.2(6)	C(20)-N(3)-Ti(1)	117.2(4)
C(21)-N(3)-Ti(1)	119.7(4)		

5.7.3 (2-*tert*-Butyl-6-cyclohexyliminomethyl-phenoxy) titanium dimethylamide dichloride tetrahydrofuran (5.3).

An ampoule was charged with $Ti(NMe_2)_2Cl_2$ (0.060 g, 0.28 mmol) and THF (5 cm^3) and cooled to –78 °C. To this was added slowly *via* cannula a cooled (-78 °C) solution of 2-*tert*-butyl-6-cyclohexyliminomethyl-phenol (0.072 g, 0.28 mmol) in THF (5 cm^3). The ampoule was closed under reduced pressure and the reaction was allowed to quickly reach room temperature and stirred for 16 h to give a dark red solution. The volatiles were removed *in vacuo* and the residue extracted into petroleum (40 cm^3). The solution was concentrated to *ca.* 10 cm^3 before cooling to -30 °C for 24 h to yield the product as an orange powder (0.063 g) which was isolated by filtration and dried *in vacuo*.

Yield: 0.063 g, 46%.

$\delta_H(C_6D_6)$ 0.80-1.90 (10H, m, cyclohexyl CH_2s), 1.28 (4H, t, THF), 1.57 (9H, s, $ArC(CH_3)_3$), 3.54 (6H, s, $N(CH_3)_2$), 3.61 (4H, t, THF), 4.40-4.60 (1H, m, cyclohexyl CH α to imine N), 6.83 (1H, t, aromatic), 7.11 (1H, dd, aromatic), 7.42 (1H, dd, aromatic) 8.30 (1H, s, ArC(*H*)=NCy).

$^{13}C\{^1H\}$ $\delta_C(C_6D_6)$ 26.31, 26.58, 26.85 (cyclohexyl CH_2s), 30.55 ($ArC(CH_3)_3$), 34.82 (THF), 35.92 ($ArC(CH_3)_3$), 53.48 ($N(CH_3)_2$), 67.24 (cyclohexyl CH α to imine N), 69.35 (THF), 121.22 (aromatic CH), 125.65 (quaternary aromatic), 132.78, 133.22 (aromatic CHs), 139.13, 161.08 (quaternary

aromatics), 164.51 (Ar*C*(H)=NCy).

5.7.4 Bis-(2-*tert*-butyl-6-cyclohexyliminomethyl-phenoxy) titanium dichloride (5.4).

An ampoule was charged with $Ti(NMe_2)_2Cl_2$ (0.071 g, 0.35 mmol) and THF (5 cm^3) and cooled to –78 °C. To this was added slowly *via* cannula a cooled (-78 °C) solution of 2-*tert*-butyl-6-cyclohexyliminomethyl-phenol (0.179 g, 0.70 mmol) in THF (10 cm^3). The ampoule was closed under reduced pressure and the reaction was allowed to quickly reach room temperature and stirred for 16 h to give a dark red solution. The volatiles were removed *in vacuo* and the residue extracted into hot toluene (20 cm^3) which was allowed to cool to room temperature before cooling to -30 °C for 24 h. This yielded the product as a dark orange powder (0.080 g) that was isolated by filtration. The mother liquor was again cooled to –30 °C for 48 h to yield a second crop of **(5.4)** as dark red, X-ray diffraction quality crystals (0.030 g).

Yield: 0.110 g, 49%.

$\delta_H(C_6D_6)$ 0.50-2.35 (20H, m, cyclohexyl C*H*$_2$s), 1.79 (18H, s, ArC(C*H*$_3$)$_3$), 4.00-4.12 (2H, m, cyclohexyl C*H* α to imine N), 6.72 (2H, t, aromatic), 6.84 (2H, dd, aromatic), 7.43 (2H, dd, aromatic) 7.82 (2H, s, ArC(*H*)=NCy).

$^{13}C\{^1H\}$ $\delta_C(C_6D_6)$ 26.32, 26.66, 26.72 (cyclohexyl *C*H$_2$s), 30.86 (ArC(*C*H$_3$)$_3$), 34.82, 35.15 (cyclohexyl *C*H$_2$s), 36.20 (Ar*C*(CH$_3$)$_3$), 67.24 (cyclohexyl *C*H α to imine N), 121.66, 126.43, 132.92, 134.04, 140.37, 161.40 (aromatics), 163.89 (Ar*C*(H)=NCy).

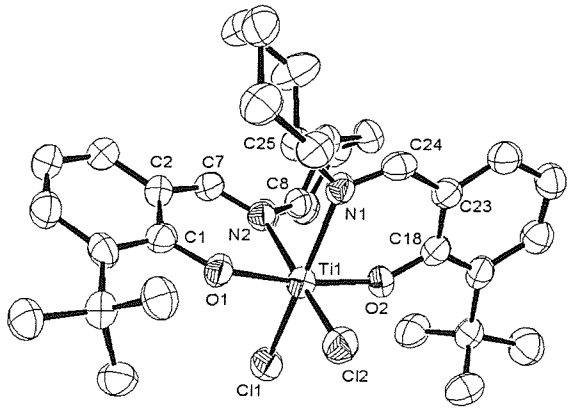

Figure 5.12: ORTEP representation of the crystal structure of bis-(2-*tert*-butyl-6-cyclohexyliminomethyl-phenoxy) titanium dichloride **(5.4)** (50% probability thermal ellipsoids). Hydrogens are omitted for clarity.

Table 5.5: Selected bond lengths (Å) and angles (°) for **(5.4)**.

O(1)-Ti(1)	1.858(3)	O(2)-Ti(1)	1.867(3)
N(1)-Ti(1)	2.186(4)	N(2)-Ti(1)	2.191(4)
Cl(1)-Ti(1)	2.3211(14)	Cl(2)-Ti(1)	2.2971(14)
C(1)-O(1)	1.327(5)	C(1)-C(2)	1.407(6)
C(7)-N(2)	1.296(6)	C(2)-C(7)	1.453(6)
C(8)-N(2)	1.495(5)		
O(1)-Ti(1)-N(2)	81.78(13)	O(2)-Ti(1)-N(1)	82.01(14)
O(1)-Ti(1)-O(2)	172.06(14)	N(1)-Ti(1)-N(2)	80.19(13)
Cl(1)-Ti(1)-Cl(2)	100.09(5)	N(1)-Ti(1)-Cl(1)	165.87(11)
N(2)-Ti(1)-Cl(2)	169.68(11)	C(1)-O(1)-Ti(1)	145.0(3)
O(1)-C(1)-C(2)	117.6(4)	C(1)-C(2)-C(7)	121.8(4)
C(2)-C(7)-N(2)	127.4(5)	C(7)-N(2)-Ti(1)	125.4(3)
C(8)-N(2)-Ti(1)	119.7(3)	C(7)-N(2)-C(8)	115.0(4)

5.7.5 Bis-(2-*tert*-butyl-6-cyclohexyliminomethyl-phenoxy) titanium bis-diethylamide (5.5).

An ampoule was charged with $Ti(NEt_2)_4$ (0.113 g, 0.334 mmol) and THF (5 cm^3) and cooled to –78 °C. To this was added slowly *via* cannula a cooled (-78 °C) solution of 2-*tert*-butyl-6-cyclohexyliminomethyl-phenol (0.174 g, 0.67 mmol) in THF (10 cm^3). The ampoule was closed under reduced pressure and the reaction was allowed to quickly reach room temperature and stirred for 16 h to

give a red solution. The volatiles were removed *in vacuo* and the residue extracted into toluene (20 cm^3), filtered and concentrated to *ca.* 5 cm^3. The solution was cooled to -30 °C for 24 h to yield the product as orange, X-ray diffraction quality crystals (0.093 g)

Yield: 0.093 g, 39%.

$\delta_H(C_6D_6)$ 0.45-1.78 (20H, m, cyclohexyl C*H*$_2$s), 1.07 (12H, t, N(CH_2CH_3)$_2$), 1.80 (18H, s, ArC(CH_3)$_3$), 3.68 (2H, tt, cyclohexyl C*H* α to imine N), 4.00 (4H, sextet, N(CH_2CH_3)$_2$), 4.20 (4H, sextet, N(CH_2CH_3)$_2$), 6.80 (2H, t, aromatic), 7.07 (2H, dd, aromatic), 7.55 (2H, dd, aromatic), 8.01 (2H, s, ArC(*H*)=NCy).

$^{13}C\{^1H\}$ $\delta_C(C_6D_6)$ 15.19 (N(CH_2CH_3)$_2$), 26.53, 26.67, 26.73 (cyclohexyl CH_2s), 31.34 (ArC(CH_3)$_3$), 34.28, 35.56 (cyclohexyl CH_2s), 36.26 ((ArC(CH_3)$_3$), 48.43 (N(CH_2CH_3)$_2$), 61.89 (cyclohexyl *C*H α to imino N), 117.63, (aromatic *C*H), 125.13 (quaternary aromatic), 131.97, 133.98 (aromatic *C*Hs), 139.79, 163.47 (quaternary aromatics), 164.44 (Ar*C*(H)=NCy).

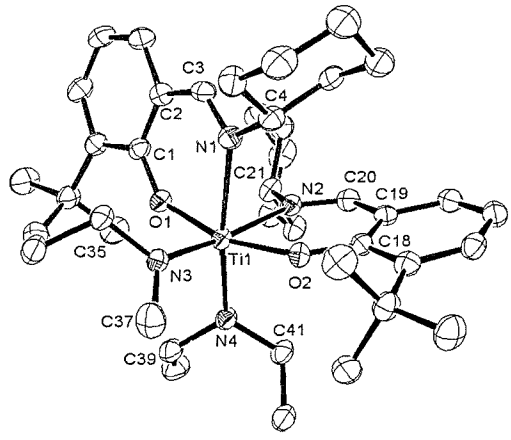

Figure5.13: ORTEP representation of the crystal structure of bis-(2-*tert*-butyl-6-cyclohexyliminomethyl-phenoxy) titanium bis-diethylamide **(5.5)** (50% probability thermal ellipsoids). Hydrogens are omitted for clarity.

Table 5.6: Selected bond lengths (Å) and angles (°) for **(5.5)**.

Ti(1)-O(1)	1.961(3)	Ti(1)-O(2)	1.964(3)
Ti(1)-N(1)	2.300(3)	Ti(1)-N(2)	2.272(3)
Ti(1)-N(3)	1.936(3)	Ti(1)-N(4)	1.941(3)
O(1)-C(1)	1.329(4)	C(1)-C(2)	1.426(5)
C(2)-C(3)	1.444(6)	N(1)-C(3)	1.290(5)
N(1)-C(4)	1.488(5)		
O(1)-Ti(1)-N(1)	81.30(11)	O(2)-Ti(1)-N(2)	81.70(11)
O(1)-Ti(1)-O(2)	163.00(11)	N(3)-Ti(1)-N(2)	173.78(12)
N(4)-Ti(1)-N(1)	170.76(12)	N(2)-Ti(1)-N(1)	82.70(11)
N(3)-Ti(1)-N(4)	97.93(13)	C(1)-O(1)-Ti(1)	142.2(2)
O(1)-C(1)-C(2)	119.1(3)	C(1)-C(2)-C(3)	123.4(3)
C(2)-C(3)-N(1)	128.8(3)	C(3)-N(1)-Ti(1)	124.1(3)
C(3)-N(1)-C(4)	114.2(3)	C(4)-N(1)-Ti(1)	121.7(2)
C(35)-N(3)-Ti(1)	123.5(2)	C(37)-N(3)-Ti(1)	123.9(2)
C(35)-N(3)-C(37)	112.5(3)	C(39)-N(4)-Ti(1)	121.5(2)
C(41)-N(4)-Ti(1)	124.7(2)	C(39)-N(4)-C(41)	113.8(3)

Table 5.7: Crystallographic parameters for **(5.2)**, **(5.4)** and **(5.5)**.

Compound	**(5.2)**	**(5.4)**	**(5.5)**
Chemical Formula	$C_{21}H_{37}Cl_2N_3O_1Ti_1$	$C_{48}H_{64}Cl_2N_2O_2Ti_1$	$C_{42}H_{68}N_4O_2Ti_1$
Formula Weight	466.34	819.81	708.90
Crystal System	Monoclinic	Tetragonal	Monoclinic
Space Group	$P2_1/c$	$P\text{-}4$	$P2_1/n$
a/Å	7.4024(3)	25.2383(6)	10.8799(3)
b/Å	41.996(2)	25.2383(6)	24.4770(8)
c/Å	8.8849(4)	14.3015(5)	15.2713(4)
α/°	90	90	90
β/°	118.350(3)	90	92.0460(10)
γ/°	90	90	90
V/Å^3	2430.79(19)	9109.7(4)	4064.3(2)
Z	4	8	4
T/K	120	120	120
μ/mm^{-1}	0.588	0.344	0.249
F(000)	992	3504	1544
No. Data collected	8820	40737	58361
No. Unique data	3773	18675	7146
R_{int}	0.1103	0.0626	0.2782
Final $R(\|F\|)$ for $I>2\sigma(I)$	0.0869	0.0580	0.0801
Final $R(F^2)$ for all data	0.1716	0.1435	0.1793

5.7.6 Bis-(2-*tert*-butyl-6-cyclohexyliminomethyl-phenoxy) zirconium dichloride (5.6).

An ampoule was charged with $Zr(NEt_2)_2Cl_2(THF)_2$ (0.123 g, 0.27 mmol) and THF (5 cm^3) and cooled to –78 °C. To this was added slowly *via* cannula a cooled (-78 °C) solution of 2-*tert*-butyl-6-cyclohexyliminomethyl-phenol (0.142 g, 0.55 mmol) in THF (10 cm^3). The ampoule was closed under reduced pressure and the reaction was allowed to quickly reach room temperature and stirred for 16 h to give a yellow solution. The volatiles were removed *in vacuo* and the residue extracted into toluene (3 x 10 cm^3) and filtered. The solution was concentrated to 10 cm^3 before cooling to -30 °C for 24 h. This yielded the product as a bright yellow solid (0.080 g) that was isolated by filtration.

Yield: 0.080 g, 43%.

$\delta_H(C_6D_6)$ 0.40-2.30 (20H, m, cyclohexyl CH_2s), 1.72 (18H, s, ArC(CH_3)$_3$), 4.00 (2H, br t, cyclohexyl C*H* α to imine N), 6.71 (2H, t, aromatic), 6.81 (2H, dd, aromatic), 7.43 (2H, dd, aromatic), 7.89 (2H, s, ArC(*H*)=NCy).

$^{13}C\{^1H\}$ $\delta_C(C_6D_6)$ 26.20, 26.40, 26.55 (cyclohexyl *C*H_2s), 30.72 (ArC(*C*H_3)$_3$), 34.41, 34.59 (cyclohexyl *C*H_2s), 36.10 (Ar*C*(CH$_3$)$_3$), 63.68 (cyclohexyl *C*H α to imine N), 120.61 (aromatic *C*H), 124.99 (quaternary aromatic), 133.52, 134.29 (aromatic *C*Hs), 141.28, 160.07 (quaternary aromatics), 167.52 (Ar*C*(H)=NCy).

5.7.7 Bis-(2-*tert*-butyl-6-cyclohexyliminomethyl-phenoxy) zirconium bis-diethylamide (5.7).

An ampoule was charged with $Zr(NEt_2)_4$ (0.098 g, 0.26 mmol) and THF (5 cm^3) and cooled to –78 °C. To this was added slowly *via* cannula a cooled (-78 °C) solution of 2-*tert*-butyl-6-cyclohexyliminomethyl-phenol (0.134 g, 0.52 mmol) in THF (10 cm^3). The ampoule was closed under reduced pressure and the reaction was allowed to quickly reach room temperature and stirred for 16 h to give a yellow solution. The volatiles were removed *in vacuo* and the residue extracted into toluene (20 cm^3), filtered and concentrated to *ca.* 5 cm^3. The solution was cooled to -30 °C for 24 h to yield the product as yellow, X-ray diffraction quality crystals (0.113 g)

Yield: 0.113 g, 58%.

$\delta_H(C_6D_6)$ 0.35-1.95 (20H, m, cyclohexyl CH_2s), 1.17 (12H, t, $N(CH_2CH_3)_2$), 1.77 (18H, s, $ArC(CH_3)_3$), 3.55-3.95 (10H, m, NEt_2 and cyclohexyl CH α to imine N), 6.77 (2H, t, aromatic), 7.02 (2H, dd, aromatic), 7.51 (2H, dd, aromatic), 8.02 (2H, s, ArC(*H*)=NCy).

$^{13}C\{^1H\}$ $\delta_C(C_6D_6)$ 15.66 ($N(CH_2CH_3)_2$), 26.46, 26.54, 26.70 (cyclohexyl CH_2s), 31.07 ($ArC(CH_3)_3$), 34.04, 35.03 (cyclohexyl CH_2s), 36.21 ($ArC(CH_3)_3$), 43.74 ($N(CH_2CH_3)_2$), 62.26 (cyclohexyl CH α to imino N), 118.07 (aromatic CH), 125.17 (quaternary aromatic), 132.44, 134.23 (aromatic CHs), 140.68, 162.15 (quaternary aromatics), 166.19 (ArC(H)=NCy).

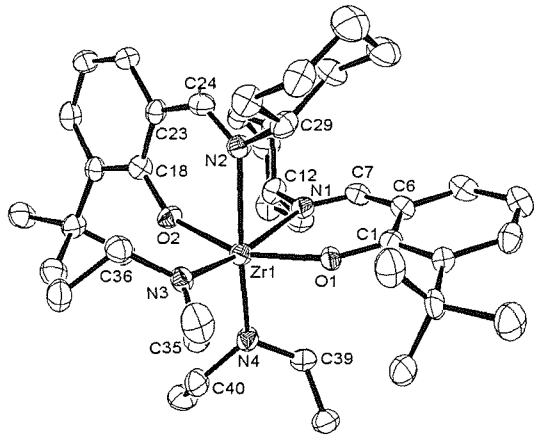

Figure 5.14: ORTEP representation of the crystal structure of bis-(2-*tert*-butyl-6-cyclohexyliminomethyl-phenoxy) zirconium bis-diethylamide **(5.7)** (50% probability thermal ellipsoids). Hydrogens are omitted for clarity.

Table 5.8: Selected bond lengths (Å) and angles (°) for **(5.7)**.

O(1)-Zr(1)	2.046(3)	O(2)-Zr(1)	2.053(3)
N(1)-Zr(1)	2.429(4)	N(2)-Zr(1)	2.392(4)
N(3)-Zr(1)	2.066(4)	N(4)-Zr(1)	2.078(3)
C(1)-O(1)	1.336(5)	C(1)-C(6)	1.423(7)
C(6)-C(7)	1.436(7)	C(7)-N(1)	1.274(6)
C(12)-N(1)	1.497(6)		
O(1)-Zr(1)-N(1)	76.87(13)	O(2)-Zr(1)-N(2)	77.25(12)
O(1)-Zr(1)-O(2)	157.22(12)	N(2)-Zr(1)-N(4)	172.49(15)
N(1)-Zr(1)-N(3)	169.08(14)	N(1)-Zr(1)-N(2)	81.17(13)
N(3)-Zr(1)-N(4)	99.41(15)	C(1)-O(1)-Zr(1)	145.3(3)

O(1)-C(1)-C(6)	118.2(4)	C(1)-C(6)-C(7)	124.5(5)
C(6)-C(7)-N(1)	129.3(5)	C(7)-N(1)-Zr(1)	125.2(3)
C(7)-N(1)-C(12)	115.2(4)	C(12)-N(1)-Zr(1)	119.5(3)
C(35)-N(3)-Zr(1)	121.8(3)	C(36)-N(3)-Zr(1)	125.2(3)
C(35)-N(3)-C(36)	112.9(4)	C(39)-N(4)-Zr(1)	122.7(3)
C(40)-N(4)-Zr(1)	124.1(3)	C(39)-N(3)-C(40)	113.1(4)

5.7.8 (2-*tert*-Butyl-6-cyclohexyliminomethyl-phenoxy) [2-*tert*-butyl-6-(1-cyclohexylamido-2-ethylamido-propyl)-phenoxy] niobium diethylamide (5.8).

5.7.8.1 1:1 Reaction.

An ampoule was charged with $Nb(NEt_2)_4$ (0.296 g, 0.78 mmol) and THF (8 cm^3) and cooled to –78 °C. To this was added slowly *via* cannula a cooled (-78 °C) solution of 2-*tert*-butyl-6-cyclohexyliminomethyl-phenol (0.201 g, 0.78 mmol) in THF (8 cm^3). The ampoule was closed under reduced pressure and the reaction was allowed to quickly reach room temperature and stirred for 16 h to give a dark orange/brown solution. The volatiles were removed *in vacuo* and the residue extracted into petroleum (10 cm^3). The solution was concentrated to *ca.* 5 cm^3 and cooled to -30 °C to yield **(5.8)** as orange, X-ray diffraction quality crystals (0.052 g).

Yield (0.052 g, 9%).

5.7.8.2 2:1 Reaction.

An ampoule was charged with $Nb(NEt_2)_4$ (0.199 g, 0.52 mmol) and THF (10 cm^3) and cooled to –78 °C. To this was added slowly *via* cannula a cooled (-78 °C) solution of 2-*tert*-butyl-6-cyclohexyliminomethyl-phenol (0.270 g, 1.04 mmol) in THF (10 cm^3). The ampoule was closed under reduced pressure and the reaction was allowed to quickly reach room temperature and stirred for 16 h to give a dark orange/brown solution. The volatiles were removed *in vacuo* and the residue extracted into petroleum (10 cm^3). The solution was left to stand at RT to yield **(5.8)** as orange, X-ray diffraction quality crystals (0.085 g).

Yield: (0.085 g, 22%).

$\delta_H(C_6D_6)$ 0.72-2.15 (20H, m, cyclohexyl CH_2s), 0.82 (6H, t, $N(CH_2CH_3)_2$), 0.98 (3H, t, $ArCH(NCy)CH(CH_3)NCH_2CH_3$), 1.34 (3H, d, $ArCH(NCy)CH(CH_3)NCH_2CH_3$), 1.62 (9H, s, $ArC(CH_3)_3$), 1.76 (9H, s, $ArC(CH_3)_3$), 3.41 (1H, m, $ArCH(NCy)CH(CH_3)NCH_2CH_3$), 3.55-3.78 (3H, m,

cyclohexyl C*H* α to amide N and N($C\mathit{H}_2CH_3)_2$), 4.01 (1H, sextet, ArCH(NCy)CH(CH_3)N$C\mathit{H}_2CH_3$), 4.10-4.24 (2H, m, cyclohexyl C*H* α to imine N and ArCH(NCy)C*H*(CH_3)NCH_2CH_3), 4.38-4.60 (2H, br s, N($C\mathit{H}_2CH_3)_2$), 4.45 (1H, s, ArC*H*(NCy)CH(CH_3)NCH_2CH_3),6.72 (1H, t, aromatic), 6.89 (1H, t, aromatic), 6.98-7.05 (2H, m, aromatics), 7.40-7.52, (2H, m, aromatics), 8.20 (1H, s, ArC(*H*)=NCy).

$^{13}C\{^1H\}$ $\delta_C(C_6D_6)$ 14.81 (N($CH_2\mathit{C}H_3)_2$), 16.60 (ArCH(NCy)CH(CH_3)N$CH_2\mathit{C}H_3$), 21.25 (ArCH(NCy)CH($\mathit{C}H_3$)NCH_2CH_3), 26.27, 26.55, 26.88, 27.15, 27.37 (cyclohexyl $\mathit{C}H_2$s), 31.52, 32.19 (ArC($\mathit{C}H_3)_3$s), 34.33, 34.42, 35.22, 35.84 (cyclohexyl $\mathit{C}H_2$s), 36.06, 36.12, (Ar$\mathit{C}(CH_3)_3$s), 45.84 (N($\mathit{C}H_2CH_3)_2$), 52.17 (ArCH(NCy)CH(CH_3)N$\mathit{C}H_2CH_3$), 61.55 (cyclohexyl *C*H α to imine N), 64.17 (cyclohexyl *C*H α to amide N), 73.21 (Ar*C*H(NCy)CH(CH_3)NCH_2CH_3), 75.43 (ArCH(NCy)*C*H(CH_3)NCH_2CH_3), 117.68, 119.27 (aromatic *C*Hs), 124.24 (quaternary aromatic), 126,57, 128.21, 132.89, 133.74 (aromatic *C*Hs), 138.16, 140.20, 162.64, 164.09 (quaternary aromatics), 166.78 (Ar*C*(H)=NCy).

$\delta_H(C_6D_5CD_3)$ 0.75-2.15 (20H, m, cyclohexyl $C\mathit{H}_2$s), 0.82 (6H, t, N($CH_2\mathit{C}H_3)_2$), 0.96 (3H, t, ArCH(NCy)CH(CH_3)N$CH_2\mathit{C}H_3$), 1.35 (3H, d, ArCH(NCy)CH($\mathit{C}H_3$)NCH_2CH_3), 1.60 (9H, s, ^{t}Bu RC($\mathit{C}H_3)_3$s), 1.74 (9H, s, ^{t}Bu RC($\mathit{C}H_3$)s), 3.37 (1H, sextet, ArCH(NCy)CH(CH_3)N$\mathit{C}H_2CH_3$), 3.55-3.70 (3H, m, cyclohexyl C*H* α to amide N and N($C\mathit{H}_2CH_3)_2$), 3.99 (1H, sextet, ArCH(NCy)CH(CH_3)N$\mathit{C}H_2CH_3$), 4.07-4.20 (2H, m, cyclohexyl C*H* α to imine N and ArCH(NCy)C*H*(CH_3)NCH_2CH_3), 4.37-4.55 (2H, br s, N($C\mathit{H}_2CH_3)_2$), 4.42 (1H, s, ArC*H*(NCy)CH(CH_3)NCH_2CH_3), 6.70 (1H, t, aromatic), 6.83 (aromatic), 6.96 (1H, dd, aromatic), 6.99 (1H, dd, aromatic), 7.37 (1H, dd, aromatic), 7.44 (1H, dd, aromatic), 8.20 (1H, s, ArC(*H*)=NCy).

$^{13}C\{^1H\}$ $\delta_C(C_6D_5CD_3)$ 14.10 (N($CH_2\mathit{C}H_3)_2$), 15.90 (ArCH(NCy)CH(CH_3)N$CH_2\mathit{C}H_3$), 20.55 (ArCH(NCy)CH($\mathit{C}H_3$)NCH_2CH_3), 25.69, 25.98, 26.24, 26.51, 26.68 (cyclohexyl $\mathit{C}H_2$s), 30.82, 31.50 (ArC($\mathit{C}H_3)_3$s), 33.68, 33.89, 34.56, 35.15 (cyclohexyl $\mathit{C}H_2$s), 35.39, 35.43 (Ar$\mathit{C}(CH_3)_3$s), 45.13 (N($\mathit{C}H_2CH_3)_2$), 51.40 (ArCH(NCy)CH(CH_3)N$\mathit{C}H_2CH_3$), 60.87 (cyclohexyl *C*H α to imine N), 63.50 (cyclohexyl *C*H α to amide N), 72.54 (Ar*C*H(NCy)CH(CH_3)NCH_2CH_3), 74.86 (ArCH(NCy)*C*H(CH_3)NCH_2CH_3),

117.01, 118.64 (aromatic *C*Hs), 123.58 (quaternary aromatic), 125.83, 127.50 (aromatic *C*Hs), 132.02 (quaternary aromatic), 132.14, 133.07 (aromatic *C*Hs), 139.51, 161.92, 163.46 (quaternary aromatics), 166.14 (Ar*C*(H)=NCy).

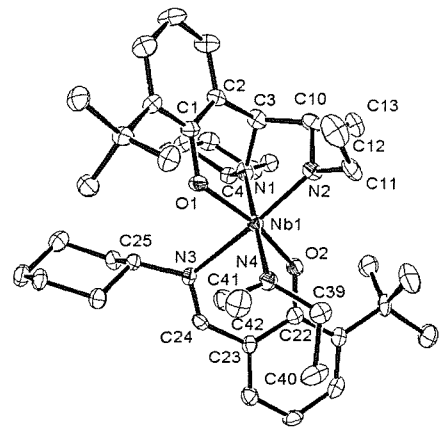

Figure 5.15: ORTEP representation of the crystal structure of (2-*tert*-butyl-6-cyclohexyliminomethyl-phenoxy) [2-*tert*-butyl-6-(1-cyclohexylamido-2-ethylamido-propyl)-phenoxy] niobium diethylamide **(5.8)** (50% probability thermal ellipsoids). Hydrogens are omitted for clarity.

Table 5.9: Selected bond lengths (Å) and angles (°) for **(5.8)**.

O(1)-Nb(1)	2.019(3)	O(2)-Nb(1)	2.051(3)
N(1)-Nb(1)	2.002(3)	N(2)-Nb(1)	1.987(3)
N(3)-Nb(1)	2.336(3)	N(4)-Nb(1)	2.027(3)
C(1)-O(1)	1.359(4)	C(1)-C(2)	1.413(5)
C(2)-C(3)	1.519(5)	C(3)-N(1)	1.488(5)
C(4)-N(1)	1.460(5)	C(3)-C(10)	1.530(6)
C(10)-N(2)	1.484(5)	C(10)-C(13)	1.520(5)
C(11)-N(2)	1.453(5)	C(11)-C(12)	1.525(6)
C(22)-O(2)	1.320(5)	C(22)-C(23)	1.412(5)
C(23)-C(24)	1.440(5)	C(24)-N(3)	1.298(5)
C(25)-N(3)	1.486(5)	C(39)-N(4)	1.480(5)
C(41)-N(4)	1.469(5)	C(39)-C(40)	1.520(6)
C(41)-C(42)	1.529(6)		
N(2)-Nb(1)-N(1)	81.65(13)	N(2)-Nb(1)-O(1)	92.18(12)
N(1)-Nb(1)-O(1)	87.79(11)	C(1)-O(1)-Nb(1)	125.7(2)
C(3)-N(1)-C(4)	117.3(3)	C(4)-N(1)-Nb(1)	135.6(2)
C(3)-N(1)-Nb(1)	107.2(2)	C(10)-N(2)-C(11)	114.2(3)
C(11)-N(2)-Nb(1)	130.6(3)	C(10)-N(2)-Nb(1)	114.9(2)

N(1)-C(3)-C(2)	113.0(3)	N(1)-C(3)-C(10)	106.1(3)
C(2)-C(3)-C(10)	111.7(3)	N(2)-C(10)-C(13)	111.2(3)
N(2)-C(10)-C(3)	106.0(3)	C(13)-C(10)-C(3)	114.2(3)
O(1)-C(1)-C(2)	121.5(3)	C(1)-C(2)-C(3)	123.8(4)
C(22)-O(2)-Nb(1)	134.0(2)	C(24)-N(3)-Nb(1)	120.6(2)
C(24)-N(3)-C(25)	116.2(3)	C(25)-N(3)-Nb(1)	122.8(2)
O(2)-C(22)-C(23)	119.5(4)	C(22)-C(23)-C(24)	122.6(4)
N(3)-C(24)-C(23)	128.9(4)	C(39)-N(4)-C(41)	112.5(3)
C(39)-N(4)-Nb(1)	126.2(3)	C(41)-N(4)-Nb(1)	121.2(3)
N(1)-Nb(1)-N(4)	177.59(13)	O(1)-Nb(1)-O(2)	165.97(10)
N(2)-Nb(1)-N(3)	172.15(12)		

Table 5.10: Crystallographic parameters for **(5.7)** and **(5.8)**.

Compound	**(5.7)**	**(5.8)**
Chemical Formula	$C_{42}H_{68}N_4O_2Zr_1$	$C_{42}H_{67}N_4Nb_1O_2$
Formula Weight	752.22	752.91
Crystal System	Monoclinic	Monoclinic
Space Group	$P2_1/n$	$P2_1/n$
a/Å	11.0808(9)	13.0405(6)
b/Å	24.488(2)	14.3836(5)
c/Å	15.3939(12)	21.5695(11)
α/°	90	90
β/°	92.399	100.335(2)
γ/°	90	90
V/Å^3	4173.5(6)	3980.1(3)
Z	4	4
T/K	120	120
μ/mm^{-1}	0.301	0.342
F(000)	1616	1616
No. Data collected	44564	24410
No. Unique data	8885	8968
R_{int}	0.2474	0.1175
Final $R(\|F\|)$ for $I>2\sigma(I)$	0.0663	0.0587
Final $R(F^2)$ for all data	0.1356	0.1157

5.8 References

1. Y. Suzuki, H. Terao, T. Fujita, *Bull. Chem. Soc. Jpn.*, 2003, **76**, 1493.

2. M. Mitani, J. Mohri, Y. Yoshida, J. Saito, S. Ishii, K. Tsuru, S. Matsui, R. Furuyama, T. Nakano, H. Tanaka, S. Kojoh, T. Matsugi, N. Kashiwa, T. Fujita, *J. Am. Chem. Soc.*, 2002, **124**, 3327.

3. M. Mitani, R. Furuyama, J. Mohri, J. Saito, S. Ishii, H. Terao, T. Nakano, H. Tanaka, T. Fujita, *J. Am. Chem. Soc.*, 2003, **125**, 4293.

4. J. Saito, M. Mitani, J. Mohri, Y. Yoshida, S. Matsui, S. Ishii, S. Kojoh, N. Kashiwa, T. Fujita, *Angew. Chem. Int. Ed.*, 2001, **40**, 2918.

5. J. Tian, P. D. Hustad, G. W. Coates, *J. Am. Chem. Soc.*, 2001, **123**, 5134.

6. S. Reinartz, A. F. Mason, E. B. Lobkovsky, G. W. Coates, *Organometallics*, 2003, **22**, 2542.

7. D. Owiny, S. Parkin, F. T. Ladipo, *J. Organomet. Chem.*, 2003, **678**, 134.

8. R. K. J. Bott, D. L. Hughes, M. Schormann, M. Bochmann, S. J. Lancaster, *J. Organomet. Chem.*, 2003, **665**, 135.

9. G. M. Sammis, E. N. Jacobsen, *J. Am. Chem. Soc.*, 2003, **125**, 4442.

10. A. Shafir, D. Fiedler, J. Arnold, *J. Chem. Soc., Dalton Trans.*, 2002, 555.

11. P. R. Woodman, C. J. Sanders, N. W. Alcock, P. B. Hitchcock, P. Scott, *New. J. Chem.*, 1999, **23**, 815.

12. P. R. Woodman, N. W. Alcock, I. J. Munslow, C. J. Sanders, P. Scott, *J. Chem. Soc., Dalton Trans.*, 2000, 3340.

13. P. D. Knight, A. J. Clarke, B. S. Kimberley, R. A. Jackson, P. Scott, *Chem. Commun.*, 2002, 352.

14. A. Lara-Sanchez, A. Rodriguez, D. L. Hughes, M. Schormann, M. Bochmann, *J. Organomet. Chem.*, 2002, **663**, 63.

15. J. Strauch, T. H. Warren, G. Erker, R. Fröhlich, P. Saarenketo, *Inorg. Chim. Acta*, 2000, **300**, 810.

16. Y. Nakayama, H. Bando, Y. Sonobe, H. Kaneko, N. Kashiwa, T. Fujita, *J. Catal.*, 2003, **215**, 171.

17. S. Ishii, M. Mitani, J. Saito, S. Matsuura, S. Kojoh, N. Kashiwa, T. Fujita, *Chem. Lett.*, 2002, 741.

18. S. Matsui, T. Fujita, *Catal. Today*, 2001, **66**, 63.

19. E. Benzing, W. Kornicker, *Chem. Ber.*, 1961, **94**, 2263.

20. S. Brenner, R. Kempe, P. Arndt, *Z. Anorg. Allg. Chem.*, 1995, **621**, 2021.

21. D. C. Bradley, I. M. Thomas, *J. Chem. Soc.*, 1960, 3857.

22. H. Bürger, H. J. Neese, *Z. Anorg. Allg. Chem.*, 1969, **365**, 243.

23. D. C. Bradley, I. M. Thomas, *Can. J. Chem.*, 1962, **40**, 449.

Chapter 6

Synthesis of Dianionic Tridentate Diamidoxanthene and Diamidodibenzofuran "NON-Ligands" and Their Titanium Complexes

6.1 Introduction

The work reported here represents the beginning of a program to investigate the use of rigid, tridentate diamide ligands in early transition metal chemistry. The ligands studied thus far are based on 4,5-diamidoxanthene (**A**) and 4,5-diamidodibenzofuran (**B**) architectures (Scheme 6.1) which were anticipated to bind to the metal through the two amide nitrogens and the neutral oxygen atom. The fact that the ligand backbones are two phenyl rings linked in two places will ensure their rigidity and ensure that the ligand should bind metal centres in a *mer* fashion. In analogous ligands that feature three donor atoms but with a more flexible backbone the ligand can bind either in a *mer* or a *fac* fashion.

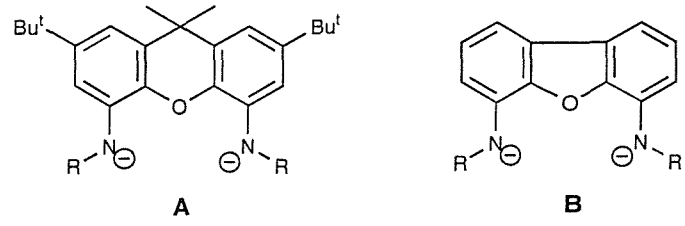

Scheme 6.1: 4,5-diamidoxanthene (**A**) and 4,5-diamidodibenzofuran (**B**) based ligands studied.

These ligand designs were chosen because they offer the opportunity to study the effect of the bite angle of the different ligands on metal centres and catalytic reactions. The dibenzofuran-based ligands should locate the amide groups further apart from each other than in the xanthene-based ligands. This is due to the constrained nature of the central furan. This difference in the distance between the two donor-nitrogens should result in differences in the properties of metal complexes upon coordination. As well as a difference in the N-M-N angle and the

M-O distance there might be increased strain in complexes of the dibenzofuran-based ligands. Suitable complexes of each ligand type could be tested for polymerisation catalytic activity to test if there are significant differences due to the bite angle of the ligand.

The 4,5-diamidoxanthene and 4,5-diamidodibenzofuran ligands are similar to a class of tridentate diamido ligands studied by Schrock.[1-8] These ligands feature two anilide donors linked by an *ortho*-aryl ether moiety (Scheme 6.2).

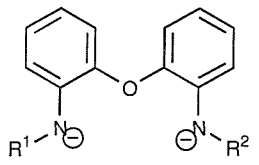

$R^1 = R^2 = C(CD_3)_2CH_3$
$R^1 = R^2 = i\text{-Pr}$
$R^1 = R^2 = Cy$
$R^1 = R^2 = SiMe_3$
$R^1 = R^2 = 0.5\ Me_2SiCH_2CH_2SiMe_2$
$R^1 = R^2 = 2,4,6\text{-}Me_3C_6H_2$

Scheme 6.2: Series of tridentate diamido ligands of the type $[(RN\text{-}o\text{-}C_6H_4)_2O]^{2-}$ prepared by Schrock.

The ligands of Scheme 6.2 were used to form complexes of Ti, Zr and Hf that were studied for α-olefin polymerisation activity. The typical method of preparation of the metal complexes involves reaction of the diamine ligand with a $M(NMe_2)_4$ complex to give the $(NON)M(NMe_2)_2$ species. The dimethylamide ligands remaining on the metal centre are then substituted for halides (by reaction with trimethylchlorosilane) before reaction with methyl-Grignard to give the dimethyl complexes. Schrock reports that whether the tridentate ligands adopt a *mer* or *fac* geometry depends on the steric interaction between the amide substituent and other co-ligands. It is thought that the *mer* structure is preferred for steric reasons up to the point where steric clash between the amide substituents and the R' ligands becomes significant. Crystallographic data suggests that these complexes prefer to adopt the *fac* structure but the NMR data suggests that the two inequivalent R' ligands rapidly exchange on the NMR time scale in solution *via* a *mer* structure. Cationic species are then formed from $(NON)MR'_2$ by alkyl abstraction with $B(C_6F_5)_3$, $[Ph_3C][B(C_6F_5)_4]$ or $[PhNMe_2H][B(C_6F_5)_4]$. These cationic species are generally unstable in solution and decompose in hours at room temperature but are stable at –30 °C.

Schrock and co-workers have also reported similar tridentate dianionic "NON-ligands" with an aliphatic backbone. One type is the $[(ArylNCH_2CH_2)_2O]^{2-}$ ligand [(**A**), Scheme 6.3],[9] which was used to synthesise zirconium complexes of the same type as discussed above. Crystallographic data showed this class of $(NON)MR_2$ complexes adopt a *mer* structure, most probably due to the planar nature of the aryl amide substituents resulting in lower steric clash than with the tetrahedral alkyl and silyl groups.

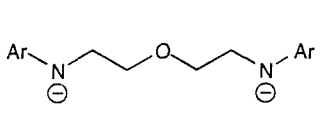

(A)

Ar = 2,6-$Me_2C_6H_3$
Ar = 2,6-$Et_2C_6H_3$
Ar = 2,6-*i*-$Pr_2C_6H_3$

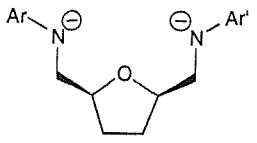

(B)

Ar = Ar' = 2,6-$Me_2C_6H_3$
Ar = 2,6-$Me_2C_6H_3$, Ar' =2,6-*i*-$Pr_2C_6H_3$

Scheme 6.3: Two types of tridentate dianionic "NON-ligands" reported by Schrock.

The second type of ligand was a tridentate diamido "NON-ligand" with restricted geometry [(**B**), Scheme 6.3].[10] This *cis*-2,5-bis-((arylamido)methyl)-tetrahydrofuran ligand could be prepared either with symmetrical (R = R' = 2,6-$Me_2C_6H_3$) or unsymmetrical (R = 2,6-$Me_2C_6H_3$, R' = 2,6-*i*-PrC_6H_3) *N*-substitution. This ligand was used to prepare a zirconium complex of the type $(NON)ZrMe_2$ in which the "NON-ligand" was shown to occupy the *mer* sites. Cationic species derived from $(NON)ZrMe_2$ were shown to be active for the polymerisation of propylene and 1-hexene.

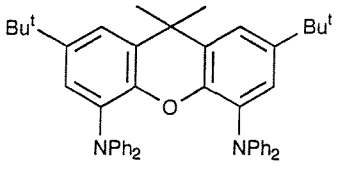

Figure 6.1: Diaminoxanthene-based ligand reported by van Leeuwen.

A similar ligand (Figure 6.1) to the diamidoxanthene-based ligand reported here has been employed by van Leeuwen and co-workers in the study of palladium catalysed allylic alkylation[11] and rhodium catalysed hydroformylation.[12] The nitrogen atoms each bear two phenyl groups and the ligand is thus used as a neutral diamine ligand.

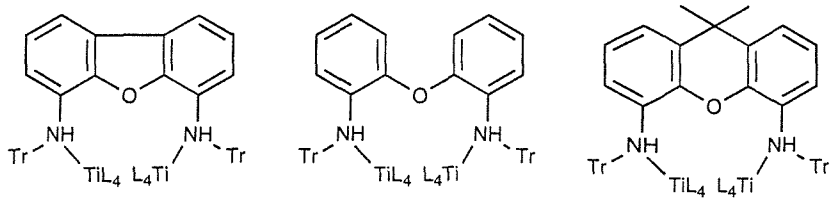

Scheme 6.4: Series of titanium complexes utilising NON-ligands reported by Maruoka and co-workers (Tr = trityl).

A series of NON-ligands (Scheme 6.4) including diaminodibenzofuran and diaminoxanthene have been employed by Maruoka and co-workers to support titanium(IV) oxide complexes.[13] The trityl-substituted secondary amino moieties bridge between two titanium centres. These complexes are used as catalysts for the asymmetric allylation of aldehydes and aryl ketones.

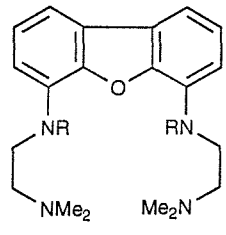

R = H, Me

Figure 6.2: Dibenzofuran-bridged bis-diamine ligands studied by Hagadorn.

A pair of ligands featuring two diamine groups located on a dibenzofuran backbone have been synthesised by Hagadorn and co-workers (Figure 6.2).[14] The ligand containing the secondary amine groups (R = H) was deprotonated to yield a dianionic bis-amidoamine coordinating to two lithium atoms. It was also coordinated to Zn and Al centres, bridging between two metal centres in each case.

Results and Discussion

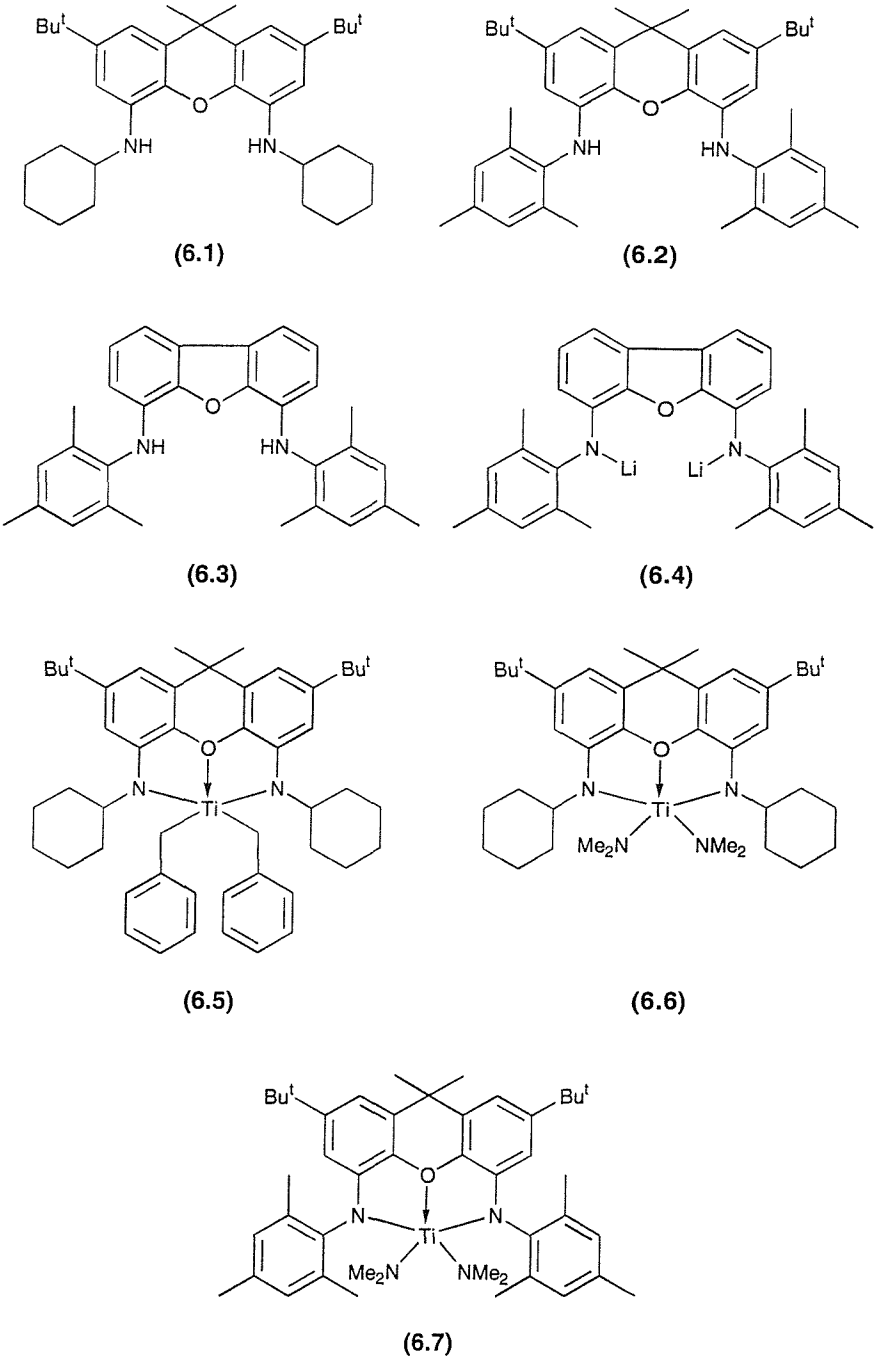

Figure 6.3: Diaminoxanthene ligands (**6.1**) and (**6.2**), diaminodibenzofuran ligand (**6.3**), dilithium diamidodibenzofuran complex (**6.4**), and diamidoxanthene titanium complexes (**6.5**)-(**6.7**) synthesised.

6.2 Synthesis of diaminoxanthene and diaminodibenzofuran ligands

The two diaminoxanthene compounds **(6.1)** and **(6.2)** were synthesised *via* a palladium catalysed coupling reaction between 4,5-dibromo-2,7-di-*tert*-butyl-9,9-dimethyl-xanthene and a primary amine. The catalytic procedure followed was that used to couple *o*-(1-cyclohexylimino-ethyl)-aniline with bromomesitylene (see Chapter 2) and so employed a palladium(0) carbene complex as catalyst. The reaction was performed in 1,4-dioxane and the palladium(0) carbene complex was generated from $Pd(dba)_2$, 1,3-bis-(2,6-diisopropylphenyl)imidazolinium chloride and base ($NaOBu^t$). The catalytic loading was 3% Pd (based on 4,5-dibromo-2,7-di-*tert*-butyl-9,9-dimethyl-xanthene) for **(6.1)** and 5% Pd for **(6.2)**. The reactions were followed by ^1H NMR spectroscopy and appeared to show quantitative conversion after *ca.* 3 days at 100 °C.

The amine used to synthesise compound **(6.1)** was cyclohexylamine. This gave the 4,5-dicyclohexylamino-2,7-di-*tert*-butyl-9,9-dimethyl-xanthene product in 76% yield as a pale yellow solid following recrystallisation from petroleum.

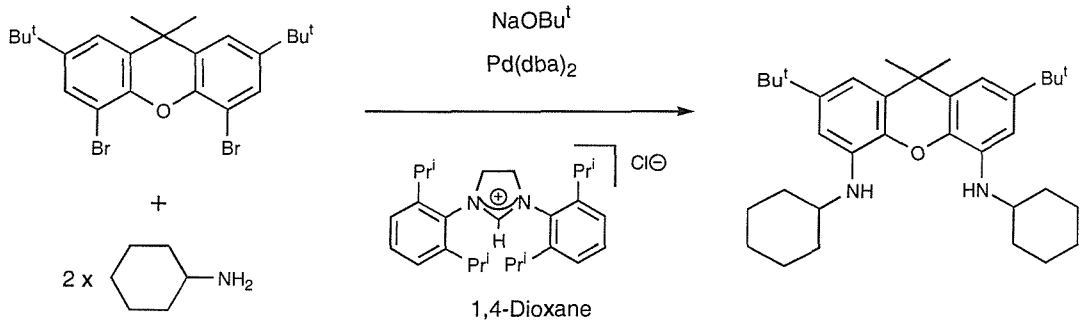

Scheme 6.5: Synthesis of **(6.1)**.

The analogous reaction between 4,5-dibromo-2,7-di-*tert*-butyl-9,9-dimethyl-xanthene and mesitylaniline gave 4,5-di-(2,4,6-trimethylanilino)-2,7-di-*tert*-butyl-9,9-dimethyl-xanthene **(6.2)** in 69% yield as a white solid following recrystallisation from ethanol.

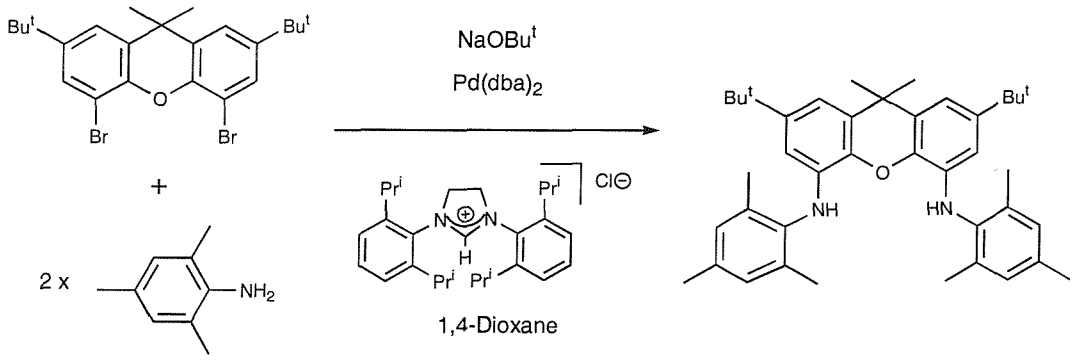

Scheme 6.6: Synthesis of **(6.2)**.

The 4,5-di-(2,4,6-trimethylanilino)-dibenzofuran **(6.3)** ligand was synthesised using the same catalytic system as **(6.1)** and **(6.2)** employing 5% Pd. The ligand was prepared as a white solid from 4,5-dibromo-dibenzofuran and mesitylaniline. The yield was 61% following recrystallisation from ethanol.

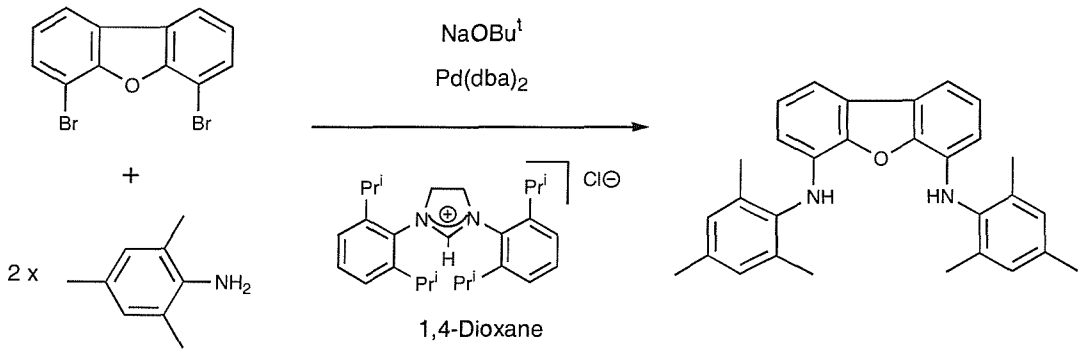

Scheme 6.7: Synthesis of **(6.3)**.

6.2.1 NMR spectroscopy for (6.1), (6.2) and (6.3)

The NMR data of the two diaminoxanthene ligands **(6.1)** and **(6.2)** are very similar. The ^{1}H NMR spectra of both compounds contains two aromatic signals as singlets between *ca.* 6-7 ppm due to the xanthene backbone. The *tert*-butyl methyl groups appear at *ca.* 1.3-1.4 ppm in the proton spectra and at *ca.* 32 ppm in the carbon NMR spectra. The methyls of the xanthene backbone resonate at 1.62 ppm in the ^{1}H NMR spectrum of **(6.1)** and at 1.89 ppm for **(6.2)** whilst appearing in a similar position to the *tert*-butyl methyls in the ^{13}C{^{1}H} NMR spectra of both compounds (*ca.* 32 ppm). The position of the resonance of the amine proton is

sensitive to the nature of the amino substituent. The resonance of the alkyl-substituted amine proton of **(6.1)** appears at 4.03 ppm in the proton NMR spectrum whilst that of the aryl-substituted amine of **(6.2)** appears at 5.73 ppm. The N*H* resonance of **(6.1)** appears as a doublet due to coupling to the methine CH of the cyclohexyl group. The cyclohexyl groups of **(6.1)** appear as several multiplets in the proton NMR spectrum but the fact that they appear as only four signals in the $^{13}C\{^{1}H\}$ NMR spectrum shows that they are flipping fast in than the NMR timescale. Similarly, the NMR data for **(6.2)** of only one signal for the mesityl aromatic CHs and two signals in a 2:1 ratio for the mesityl methyl groups shows that the mesityl rings are freely rotating about the C-N bond.

Table 6.1: A comparison of selected ^{1}H and $^{13}C\{^{1}H\}$ NMR data for **(6.1)** and **(6.2)**.[a]

Compound	(6.1)	(6.2)
Xanthene C*H*$_3$S	1.62	1.89
Xanthene C(C*H*$_3$)$_3$S	1.35	1.39
N*H*	4.03	5.73
Xanthene *C*H$_3$S	32.25	32.15
Xanthene *C*(CH$_3$)$_3$S	32.32	32.20

[a] Spectral data expressed in ppm; solvent = $CDCl_3$.

The aromatic protons of the dibenzofuran backbone of **(6.3)** appear in the ^{1}H NMR spectrum as two doublets at 6.28 and 7.33 ppm and a triplet at 7.09 ppm whilst the amine N*H* resonance appears at 5.69 ppm. This position of the N*H* is almost identical to that for **(6.2)**, which essentially features the same substitution of the amine moiety. The resonances due to the mesityl groups of **(6.3)** are located in practically identical positions to those of **(6.2)** in both the proton and carbon NMR spectra (see Table 6.2).

Table 6.2: A comparison of selected ^{1}H and $^{13}C\{^{1}H\}$ NMR data for (**6.2**) and (**6.3**).[a]

Compound	(6.2)	(6.3)
Mesityl C*H*$_3$s	2.38, 2.44	2.28, 2.36
Mesityl aromatic C*H*s	7.09	7.01
N*H*	5.73	5.69
Mesityl *C*H$_3$s	18.98, 21.55	18.94, 21.64
Mesityl aromatic *C*Hs	129.86	129.98

[a] Spectral data expressed in ppm; solvent = $CDCl_3$.

6.3 Synthesis of dilithium 4,5-di-(2,4,6-trimethylanilido)-dibenzofuran (6.4)

It was possible to deprotonate (**6.3**) with *n*-butyllithium to give the dilithium 4,5-di-(2,4,6-trimethylanilido)-dibenzofuran (**6.4**) species. The reaction was performed in petroleum (40/60) with the addition of *n*-butyllithium to (**6.3**) at -78 °C. After allowing to reach RT and stirring for 15 h the product was formed as a white solid that was isolated by filtration in 85% yield. The compound was extremely air and moisture sensitive but could be stored indefinitely under N_2 in a glovebox.

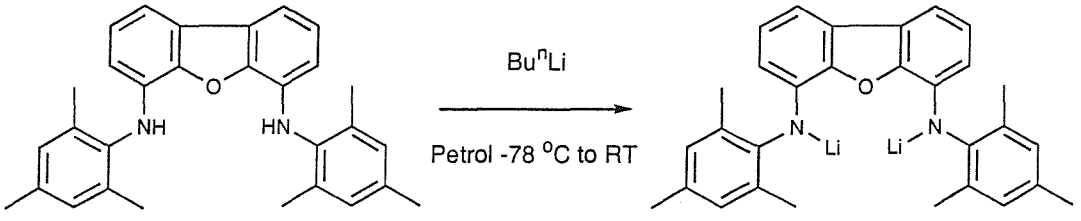

Scheme 6.8: Synthesis of (**6.4**).

6.3.1 NMR spectroscopy for (6.4)

The absence of a peak assignable to the amine N*H* in the ^{1}H NMR spectrum of (**6.4**) was strong evidence that deprotonation of both amine groups of (**6.3**) had occurred. The aromatic protons of the dibenzofuran backbone appear as a doublet at 6.32 ppm and two overlapping signals centred at *ca.* 7 ppm integrating as four protons. The mesityl aromatic CHs appear as a singlet at 6.63 ppm in the ^{1}H NMR spectrum and one signal at 131.27 ppm in the $^{13}C\{^{1}H\}$ NMR spectrum. The

mesityl methyls appear as two signals in a 2:1 ratio in the ^{1}H NMR spectrum and as two signals in the $^{13}C\{^{1}H\}$ NMR spectrum which indicates that the mesityl rings are freely rotating about the C-N bonds in (**6.4**) as they were in the neutral diamine precursor (**6.3**).

6.4 Synthesis of 4,5-dicyclohexylamido-2,7-di-*tert*-butyl-9,9-dimethyl-xanthene titanium dibenzyl (6.5)

A small scale reaction was conducted between 4,5-dicyclohexylamino-2,7-di-*tert*-butyl-9,9-dimethyl-xanthene (**6.1**) and titanium tetrabenzyl. The reaction was performed in the absence of light in a Young's tap NMR tube in d^8-PhMe. After leaving the NMR tube at RT overnight the proton NMR spectrum showed evidence of reaction based on the appearance of peaks not assignable to starting materials. Heating the NMR tube at 80 °C for three hours resulted in the disappearance of the peaks due to the starting materials in the proton NMR spectrum. The spectrum now contained peaks assignable to 4,5-dicyclohexylamido-2,7-di-*tert*-butyl-9,9-dimethyl-xanthene titanium dibenzyl (**6.5**) as well as free toluene as a result of protonolysis of two of the benzyl groups on each titanium centre. Removal of the volatiles from this sample *in vacuo* and redissolving the residue in d^8-PhMe gave a dark red solution. Proton and carbon NMR supported the identification of the species as 4,5-dicyclohexylamido-2,7-di-*tert*-butyl-9,9-dimethyl-xanthene titanium dibenzyl. Attempts to scale up this reaction and isolate the product were unfortunately unsuccessful. Proton NMR analysis of the reactions revealed that a mixture of unidentified species and (**6.5**) was obtained.

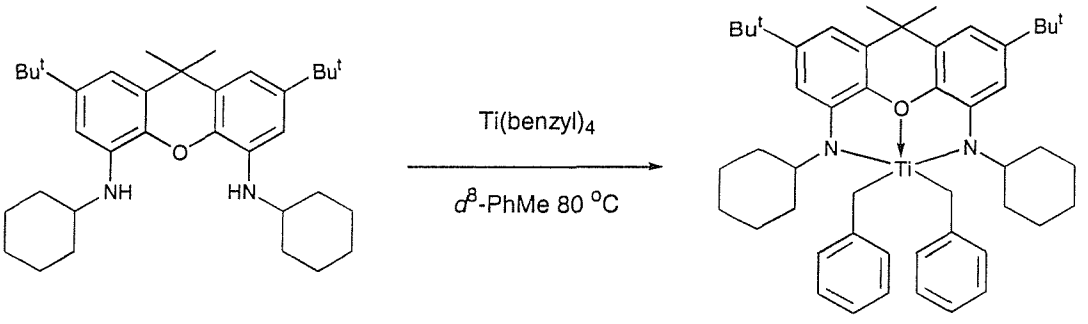

Scheme 6.9: Synthesis of (**6.5**).

6.4.1 NMR spectroscopy for (6.5)

The proton NMR spectrum of **(6.5)** does not contain a resonance assignable to the amino protons of the ligand. The CH_2s of the two benzyl groups appear as a singlet at 2.92 ppm in the ^1H NMR spectrum and one peak at 84.53 ppm in the $^{13}C\{^1H\}$ NMR spectrum. The *tert*-butyl and methyl groups of the xanthene backbone each give rise to one set of peaks in the NMR spectra. The two cyclohexyl groups appear as six peaks in the $^{13}C\{^1H\}$ NMR spectrum. These observations suggest that the complex possesses C_2 symmetry. The aromatic protons of the complex give rise to three multiplets due to overlapping signals with a total integral of fourteen. The $^{13}C\{^1H\}$ NMR spectrum allows for more detailed assignment of the aromatics as it shows signals due to five aromatic CHs and five quaternary carbons. The symmetric diamidoxanthene ligand gives rise to two aromatic CHs and four quaternary aromatics and the benzyl ligands are observed as three aromatic CHs and one quaternary aromatic.

6.5 Synthesis of 4,5-diamidoxanthene titanium bis-dimethylamide complexes

Attempts to synthesise titanium complexes of the 4,5-diamidoxanthene ligands followed the strategy shown below (Scheme 6.10). It involved *in situ* double deprotonation of the 4,5-diaminoxanthene precursor followed by reaction of the resultant dilithium-diamide species with $Ti(NMe_2)_2Cl_2$. This would then give the 4,5-diamidoxanthene titanium bis-dimethylamide species as well as LiCl.

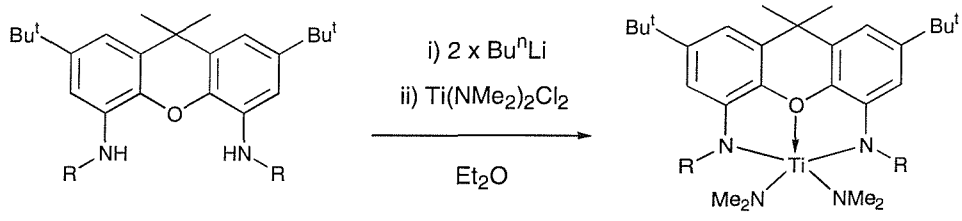

Scheme 6.10: Synthesis of **(6.6)** (R=cyclohexyl) and **(6.7)** (R=mesityl).

There were great problems involved in the isolation of **(6.6)** which contained the cyclohexylamide groups. NMR analysis of the reaction mixture showed it to be a mixture of the free ligand **(6.1)** and other species containing dimethylamide groups. It did not prove possible to isolate the desired product in large amounts due

to the extremely high solubility of both **(6.1)** and **(6.6)** in petroleum, diethyl ether and toluene. Solutions of *ca.* 1 cm^3 precipitated no solid when cooled to –30 °C. A very small crop of crystals suitable for X-ray diffraction studies was obtained from a very small amount of diethyl ether, however it was such a small amount that all were taken out of the Schlenk tube to obtain the crystal structure. As a result of this failure to isolate the pure product, satisfactory NMR spectra were not recorded for complex **(6.6)**. The small crop of crystals obtained from diethyl ether did yield the crystal structure of **(6.6)**.

The mesitylamide containing complex **(6.7)** was obtained pure in good yield by crystallisation from petroleum to give the product as an orange solid.

6.5.1 NMR spectroscopy for (6.7)

The proton NMR spectrum does not contain a peak assignable to an amino proton. The complex appears to have C_2-symmetry similar to **(6.5)** with the two *tert*-butyl and two methyl groups of the xanthene backbone each giving rise to one set of peaks in the ^1H and $^{13}C\{^1H\}$ NMR spectra. The mesityl methyl groups appear as two signals in both of the ^1H and $^{13}C\{^1H\}$ NMR spectra with the integrals of the two peaks in the proton spectrum having the ratio of 2:1. The two dimethylamide groups appear as one signal in each of the ^1H and $^{13}C\{^1H\}$ NMR spectra.

6.5.2 X-ray diffraction study on compound (6.6)

X-ray diffraction quality crystals of **(6.6)** were grown by cooling a saturated diethyl ether solution to –30 °C to give the product as red blocks. One of the *tert*-butyl groups of the xanthene backbone was disordered and was modelled as two staggered *tert*-butyl groups sharing one tertiary carbon. The structure also features a highly disordered molecule of diethyl ether in the unit cell.

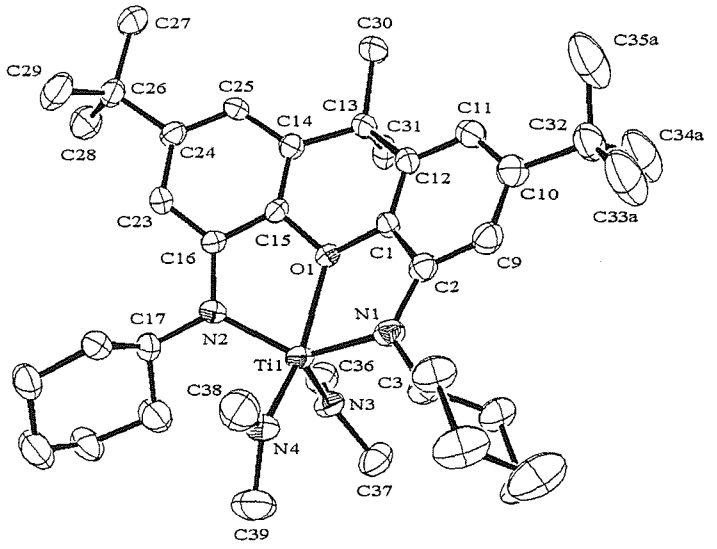

Figure 6.4: ORTEP representation of the crystal structure of 4,5-di-cyclohexylamido-2,7-di-*tert*-butyl-9,9-dimethyl-xanthene titanium bis-dimethylamide (**6.6**) (50% probability thermal ellipsoids). A disordered molecule of diethyl ether is removed for clarity. Hydrogens are omitted for clarity.

The geometry of the complex is best described as distorted trigonal bipyramidal with the dimethylamide nitrogens and the xanthene oxygen occupying the equatorial positions with the nitrogens of the diamidoxanthene ligand in the apical sites. The angles between the equatorial atoms [N(3)-Ti(1)-O(1) 99.88°; N(4)-Ti(1)-O(1) 154.75(16)°; N(3)-Ti(1)-N(4) 105.30(19)°] and the angle between the apical nitrogens [N(1)-Ti(1)-N(2) 139.01(16)°] show how distorted from the ideal trigonal bipyramidal geometry the complex is. The diamidoxanthene ligand coordinates in a *mer* fashion as anticipated. The nitrogen-titanium bond lengths of the ligand [Ti(1)-N(1) 2.056(4)Å; Ti(1)-N(2) 2.039(4)Å] are significantly longer than those to the dimethylamide groups [Ti(1)-N(3) 1.888(4)Å; Ti(1)-N(2) 1.892(4)Å]. The bond between the metal and the xanthene oxygen [Ti(1)-O(1) 2.131(3)Å] is longer than the titanium-xantheneamide bonds. The two bite angles of the bidentate ligand are the same [N(1)-Ti(1)-O(1) 73.66(13)°; N(2)-Ti(1)-O(1) 73.73(13)°]. The planar geometry about the nitrogens of the diamidoxanthene ligands indicates a high degree of π-donation to the metal.

The Ti-N bond lengths of the diamidoxanthene ligand here are shown to be long when compared to analogous titanium alkyl complexes reported by Schrock.

In the [t-BuNON]$TiMe_2$ complex[5] [t-BuNON = $((t\text{-}BuN\text{-}o\text{-}C_6H_4)_2O)^{2-}$] the NON-ligand adopts a *fac* geometry and the Ti-N bonds [Ti-N(1) 1.944(4)Å; Ti-N(2) 1.936(4)Å] are shorter than in **(6.6).** The bond between the metal and the ether oxygen is much longer in Schrock's complex [Ti-O 2.402(4)Å] than in **(6.6)**. Schrock reports a structure for a titanium alkyl complex of a similar ligand.[4] In the [*i*-PrNON]$Ti(CH_2CHMe_2)_2$ [*i*-PrNON = $((i\text{-}PrN\text{-}o\text{-}C_6H_4)_2O)^{2-}$] complex the NON ligand adopts a *mer* geometry and the Ti-O distance is 2.149(3)Å, very similar to that of **(6.6)**. The Ti-N bond lengths to the NON ligand [Ti-N(1) 1.993(3)Å; Ti-N(2) 1.993(3)Å] are very similar to those of the previous complex reported by Schrock in which the ligand adopted the *fac* conformation.

6.6 Conclusions

The work reported in this chapter represents the beginning of a study of the conformationally restricted 4,5-diamidoxanthene and 4,5-diamidodibenzofuran ligands. The 4,5-dicyclohexylamino-2,7-di-*tert*-butyl-9,9-dimethyl-xanthene **(6.1)**, 4,5-di-(2,4,6-trimethylanilino)-2,7-di-*tert*-butyl-9,9-dimethyl-xanthene **(6.2)** and 4,5-di-(2,4,6-trimethylanilino)-dibenzofuran **(6.3)** compounds have been prepared in high yields by palladium catalysed amination of the appropriate dibromoxanthene or dibromodibenzofuran starting materials.

4,5-Di-(2,4,6-trimethylanilino)-dibenzofuran **(6.3)** was doubly deprotonated with Bu^nLi to give dilithium 4,5-di-(2,4,6-trimethylanilido)-dibenzofuran **(6.4)** as an extremely air and moisture sensitive white solid. A NMR reaction between 4,5-dicyclohexylamino-2,7-di-*tert*-butyl-9,9-dimethyl-xanthene **(6.1)** and titanium tetrabenzyl gave the titanium alkyl complex 4,5-dicyclohexylamido-2,7-di-*tert*-butyl-9,9-dimethyl-xanthene titanium dibenzyl **(6.5)**.

In situ deprotonation of both **(6.1)** and **(6.2)** followed by reaction with $Ti(NMe_2)_2Cl_2$ gave 4,5-di-cyclohexylamido-2,7-di-*tert*-butyl-9,9-dimethyl-xanthene titanium bis-dimethylamide **(6.6)** and 4,5-di-(2,4,6-trimethylanilido)-2,7-di-*tert*-butyl-9,9-dimethyl-xanthene titanium bis-dimethylamide **(6.7)** respectively. There were difficulties in isolating pure **(6.6)** in reasonable quantities, so it was only analysed by single crystal X-ray diffraction. Complex **(6.7)** was isolated in good yield as an orange solid.

6.7 Experimental

The following compounds were prepared following literature methods: 4,5-dibromo-2,7-di-*tert*-butyl-9,9-dimethyl-xanthene,[15] 4,5-dibromo-dibenzofuran,[16] $Ti(benzyl)_4$,[17] $Ti(NMe_2)_2Cl_2$.[18]

6.7.1 4,5-Dicyclohexylamino-2,7-di-*tert*-butyl-9,9-dimethyl-xanthene (6.1).

An ampoule was charged with 4,5-dibromo-2,7-di-*tert*-butyl-9,9-dimethyl-xanthene (2.80 g, 5.83 mmol), sodium *tert*-butoxide (1.70 g, 17.5 mmol), $Pd(dba)_2$ (0.10 g, 0.175 mmol), 1,3-bis-(2,6-diisopropylphenyl)imidazolinium chloride (0.15 g, 0.35 mmol) and 1,4-dioxane (40 cm^3). To this was added cyclohexylamine (1.27 g, 12.83 mmol) and the ampoule was closed under reduced pressure and heated at 100 °C for 60 h. The reaction was allowed to cool and water (40 cm^3) was added before extracting the reaction into diethyl ether (2 x 100 cm^3 then 50 cm^3). The organic extracts were combined, filtered through Celite and dried with $MgSO_4$. Volatiles were removed *in vacuo* to yield a pale yellow solid that was recrystallised from boiling petroleum (60/80) to give **(6.1)** as a pale yellow solid.

Yield: 2.29 g, 76%.

Mp: 190-195 °C.

$\delta_H(CDCl_3)$ 1.20-2.15 (20H, m, cyclohexyl C*H*$_2$s), 1.35 (18H, s, C(C*H*$_3$)$_3$s), 1.62 (6H, s, xanthene C*H*$_3$s), 3.40-3.50 (2H, m, cyclohexyl C*H* α to amine N), 4.03 (2H, d, N*H*), 6.62 (2H, s, aromatics), 6.77 (2H, s, aromatics).

$^{13}C\{^1H\}$ $\delta_C(CDCl_3)$ 25.30, 26.75 (cyclohexyl *C*H$_2$s), 32.25 (xanthene *C*H$_3$s), 32.32 (C(*C*H$_3$)$_3$s), 34.07 (cyclohexyl *C*H$_2$s), 35.30, 35.58 (tertiary carbons), 52.04 (cyclohexyl *C*H α to amine N), 107.61, 110.58 (aromatic *C*Hs), 130.12, 135.59, 137.36, 146.13 (quaternary aromatics).

6.7.2 4,5-Di-(2,4,6-trimethylanilino)-2,7-di-*tert*-butyl-9,9-dimethyl-xanthene (6.2).

An ampoule was charged with 4,5-dibromo-2,7-di-*tert*-butyl-9,9-dimethyl-xanthene (3.00 g, 6.25 mmol), sodium *tert*-butoxide (1.80 g, 18.75 mmol), $Pd(dba)_2$ (0.18 g, 0.3 mmol), 1,3-bis-(2,6-diisopropylphenyl)imidazolinium chloride (0.26 g, 0.6 mmol) and 1,4-dioxane (60 cm^3). To this was added 2,4,6-trimethylaniline (1.86 g, 13.74 mmol) and the ampoule was closed under reduced

pressure and heated at 105 °C for 4 days. The reaction was allowed to cool and water (40 cm^3) was added before extracting the reaction into diethyl ether (3 x 100 cm^3). The organic extracts were combined, filtered through Celite and dried with $MgSO_4$. Volatiles were removed *in vacuo* and the residue recrystallised from boiling ethanol to yield the product as a cream coloured solid.

Yield: 2.53 g, 69%.

Mp: 193-196 °C.

$\delta_H(CDCl_3)$ 1.39 (18H, s, $C(CH_3)_3s$), 1.89 (6H, s, xanthene CH_3s), 2.38 (12H, s, mesityl CH_3s), 2.44 (6H, s, mesityl CH_3s), 5.73 (2H, s, N*H*), 6.37 (2H, s, xanthene aromatics), 7.03 (2H, s, xanthene aromatics), 7.09 (4H, s, mesityl aromatics).

$^{13}C\{^1H\}$ $\delta_C(CDCl_3)$ 18.98, 21.55 (mesityl CH_3s), 32.15 (xanthene CH_3s), 32.20 ($C(CH_3)_3s$), 35.18, 35.67 (tertiary carbons), 108.34, 111.49 (xanthene aromatic *C*Hs), 129.86 (mesityl aromatic *C*Hs), 130.35, 134.60, 135.43, 135.77, 136.45, 137.55, 146.11 (quaternary aromatics).

6.7.3 4,5-Di-(2,4,6-trimethylanilino)-dibenzofuran (6.3).

An ampoule was charged with 4,5-dibromo-dibenzofuran (1.00 g, 3.1 mmol), sodium *tert*-butoxide (0.88 g, 9.2 mmol), $Pd(dba)_2$ (0.18 g, 0.3 mmol), 1,3-bis-(2,6-diisopropylphenyl)imidazolinium chloride (0.26 g, 0.6 mmol) and 1,4-dioxane (20 cm^3). To this was added 2,4,6-trimethylaniline (0.99 g, 7.3 mmol) and the ampoule was closed under reduced pressure and heated at 105 °C for 18 h. The reaction was allowed to cool and water (100 cm^3) was added before extracting the reaction into diethyl ether (3 x 100 cm^3). The organic extracts were combined, filtered through Celite and dried with $MgSO_4$. Volatiles were removed *in vacuo* and the residue recrystallised from boiling ethanol to yield the product as a colourless solid.

Yield: 0.82 g, 61%.

Mp: 162-165 °C.

$\delta_H(CDCl_3)$ 2.28 (12H, s, mesityl CH_3s), 2.36 (6H, s, mesityl CH_3s), 5.69 (2H, s, N*H*), 6.28 (2H, d, dibenzofuran aromatics), 7.01 (4H, s, mesityl aromatics), 7.09 (2H, t, dibenzofuran aromatics), 7.33 (2H, d, dibenzofuran aromatics).

$^{13}C\{^1H\}$ $\delta_C(CDCl_3)$ 18.94, 21.64 (mesityl *C*H$_3$s), 109.86, 110.46, 124.27 (dibenzofuran aromatic *C*Hs), 125.85 (quaternary aromatic), 129.98 (mesityl aromatic *C*Hs), 133.23, 135.55, 136.43, 136.79, 145.01 (quaternary aromatics).

6.7.4 Dilithium 4,5-di-(2,4,6-trimethylanilido)-dibenzofuran (6.4).

To a stirred, cooled (-78 °C) solution of **(6.3)** (0.22 g, 0.5 mmol) in petroleum (20 cm^3), was added slowly *via* cannula Bu^{n}Li (0.4 cm^3 of 2.45 M solution in hexanes, 1.0 mmol). The mixture was stirred at –78 °C for 1 h, allowed to reach room temperature and stirred for 15 h. This gave a colourless precipitate that was isolated by filtration and dried *in vacuo* to yield **(6.4)** as a white solid.

Yield: 0.190 g, 85%.

$\delta_H(C_6D_6)$ 1.65 (12H, s, mesityl C*H*$_3$s), 2.09 (6H, s, mesityl C*H*$_3$s), 6.32 (2H, d, dibenzofuran aromatics), 6.63 (4H, s, mesityl aromatics), 6.90-7.05 (4H, m, dibenzofuran aromatics).

$^{13}C\{^1H\}$ $\delta_C(C_6D_6)$ 19.70, 21.33 (mesityl *C*H$_3$s), 107.27, 112.15 (dibenzofuran aromatic *C*Hs), 126.94 (quaternary aromatics), 127.84 (dibenzofuran aromatic *C*Hs), 131.27 (mesityl aromatic *C*Hs), 131.94, 132.12, 142.25, 145.49, 146.40 (quaternary aromatics).

6.7.5 4,5-Di-cyclohexylamido-2,7-di-*tert*-butyl-9,9-dimethyl-xanthene titanium dibenzyl (6.5).

In reduced light, a Young's tap NMR tube wrapped in foil was charged with a C_6D_6 solution of **(6.1)** (0.020 g, 0.039 mmol) and Ti(Bz)$_4$ (0.016 g, 0.039 mmol). The sample was left at RT for *ca.* 15 h before the before being heated at 80 °C for 3 h. The volatiles were removed *in vacuo* and the dark red residue redissolved in C_6D_6 to obtain the spectra of **(6.5)**.

$\delta_H(C_6D_6)$ 1.10-2.65 (20H, m, cyclohexyl C*H*$_2$s), 1.35 (18H, s, C(C*H*$_3$)$_3$s), 1.57 (6H, s, xanthene C*H*$_3$s), 2.92 (4H, s, benzyl C*H*$_2$s), 5.78 (2H, br m, cyclohexyl C*H* α to amide N), 6.70-6.85 (4H, m, aromatics), 6.95-7.05 (6H, m, aromatics), 7.10-7.20 (4H, m, aromatics).

$^{13}C\{^1H\}$ $\delta_C(C_6D_6)$ 27.57, 28.24, 29.86 (cyclohexyl *C*H$_2$s), 32.57 (C(*C*H$_3$)$_3$s), 33.05 (xanthene *C*H$_3$s), 35.02, 35.74 (cyclohexyl *C*H$_2$s), 38.56, 38.86 (tertiary carbons), 60.57 (cyclohexyl *C*H α to amide N), 84.53 (benzyl *C*H$_2$s), 107.85,

111.75, 123.50 (aromatic *C*Hs), 127.94 (quaternary aromatic), 128.02, 129.16 (aromatic *C*Hs), 142.32, 143.74, 148.52, 149.01 (quaternary aromatics).

6.7.6 4,5-Di-cyclohexylamido-2,7-di-*tert*-butyl-9,9-dimethyl-xanthene titanium bis-dimethylamide (6.6).

To a stirred, cooled (-78 °C) solution of (**6.1**) (0.180 g, 0.35 mmol) in diethyl ether (40 cm^3), was added slowly *via* cannula Bu^nLi (0.29 cm^3 of 2.45 M solution in hexanes, 0.70 mmol). The mixture was stirred at –78 °C for 1 h, allowed to reach room temperature and stirred for a further hour to give an orange solution with a colourless precipitate. The mixture was cooled to –25 °C and a cooled (-25 °C) solution of $Ti(NMe_2)_2Cl_2$ (0.072 g, 0.35 mmol) in diethyl ether (10 cm^3) was added slowly *via* cannula. The reaction was slowly allowed to reach RT and stirred for *ca.* 15 h to give a dark red solution and grey precipitate. The volatiles were removed *in vacuo* and the residue extracted into petroleum (20 cm^3) and filtered through Celite. The petroleum was removed *in vacuo*, the residue dissolved in diethyl ether (5 cm^3) and cooled to –30 °C to give (**6.6**) as a small crop of red X-ray diffraction quality crystals.

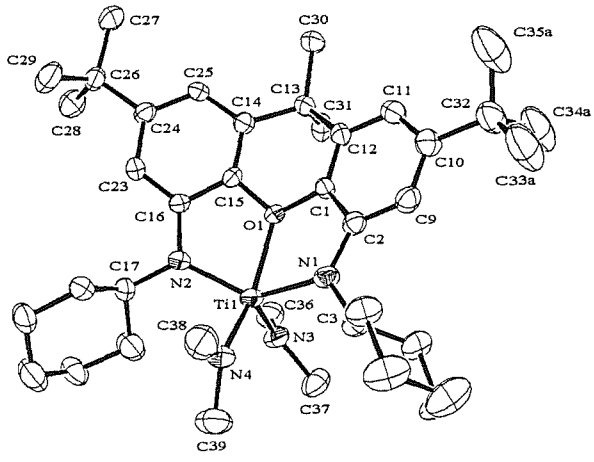

Figure 6.5: ORTEP representation of the crystal structure of 4,5-di-cyclohexylamido-2,7-di-*tert*-butyl-9,9-dimethyl-xanthene titanium bis-dimethylamide (**6.6**) (50% probability thermal ellipsoids). Hydrogens are omitted for clarity.

Table 6.3: Selected bond lengths (Å) and angles (°) for **(6.6)**.

Ti(1)-N(1)	2.056(4)	Ti(1)-N(2)	2.039(4)
Ti(1)-O(1)	2.131(3)	Ti(1)-N(3)	1.888(4)
Ti(1)-N(4)	1.892(4)	N(1)-C(3)	1.477(6)
N(1)-C(2)	1.399(6)	C(2)-C(1)	1.390(6)
C(1)-O(1)	1.406(5)	O(1)-C(15)	1.403(5)
C(15)-C(16)	1.383(6)	C(16)-N(2)	1.403(6)
N(2)-C(17)	1.475(6)	N(3)-C(36)	1.473(7)
N(3)-C(37)	1.454(6)	N(4)-C(38)	1.447(7)
N(4)-C(39)	1.465(7)		

N(1)-Ti(1)-N(2)	139.01(16)	N(1)-Ti(1)-O(1)	73.66(13)
N(2)-Ti(1)-O(1)	73.73(13)	N(3)-Ti(1)-O(1)	99.88(16)
N(4)-Ti(1)-O(1)	154.75(16)	N(3)-Ti(1)-N(4)	105.30(19)
N(3)-Ti(1)-N(2)	103.91(17)	N(4)-Ti(1)-N(2)	101.57(17)
N(3)-Ti(1)-N(1)	105.55(17)	N(4)-Ti(1)-N(1)	97.44(17)
C(3)-N(1)-Ti(1)	119.2(3)	C(3)-N(1)-C(2)	119.8(4)
C(2)-N(1)-Ti(1)	120.5(3)	N(1)-C(2)-C(1)	114.7(4)
C(2)-C(1)-O(1)	112.4(4)	C(1)-O(1)-C(15)	116.3(3)
O(1)-C(15)-C(16)	112.6(4)	C(15)-C(16)-N(2)	114.4(4)
C(16)-N(2)-Ti(1)	120.3(3)	C(16)-N(2)-C(17)	114.7(4)
C(17)-N(2)-Ti(1)	125.0(3)	Ti(1)-N(3)-C(36)	123.2(3)
Ti(1)-N(3)-C(37)	123.8(3)	C(36)-N(3)-C(37)	111.2(4)
Ti(1)-N(4)-C(38)	119.4(4)	Ti(1)-N(4)-C(39)	130.4(4)
C(38)-N(4)-C(39)	110.1(5)		

Table 6.4: Crystallographic parameters for **(6.6)**.

Compound	**(6.6)**
Chemical Formula	$C_{43}H_{72}N_4O_2Ti_1$
Formula Weight	724.95
Crystal System	Triclinic
Space Group	P -1
a/Å	10.2581(4)
b/Å	12.2629(6)
c/Å	18.6460(11)
α/°	94.693(2)
β/°	95.234(3)
γ/°	107.671(2)
V/Å^3	2210.69(19)
Z	2
T/K	150(2)
μ/mm^{-1}	0.230
F(000)	792
No. Data collected	23300

No. Unique data	7739
R_{int}	0.0981
Final $R(\|F\|)$ for $I>2\sigma(I)$	0.0955
Final $R(F^2)$ for all data	0.1547

6.7.7 4,5-Di-(2,4,6-trimethylanilido)-2,7-di-*tert*-butyl-9,9-dimethyl-xanthene titanium bis-dimethylamide (6.7).

To a stirred, cooled (-78 °C) solution of **(6.2)** (0.24 g, 0.41 mmol) in diethyl ether (10 cm^3), was added slowly *via* cannula Bu^nLi (0.34 cm^3 of 2.45 M solution in hexanes, 0.81 mmol). The mixture was stirred at –78 °C for 1 h, allowed to reach room temperature and stirred for a further hour to give an orange solution with a colourless precipitate. The mixture was cooled to –25 °C and a cooled (-25 °C) solution of $Ti(NMe_2)_2Cl_2$ (0.085 g, 0.41 mmol) in diethyl ether (7 cm^3) was added slowly *via* cannula. The reaction was slowly allowed to reach RT and stirred for *ca.* 15 h to give a red solution and grey precipitate. The volatiles were removed *in vacuo* and the residue extracted into petroleum (20 cm^3) and filtered through Celite. The petroleum solution was concentrated and cooled to –30 °C to give **(6.7)** as an orange solid.

Yield: 0.157 g, 53%.

$\delta_H(C_6D_6)$ 1.23 (18H, s, $C(CH_3)_3$s), 1.74 (6H, s, xanthene CH_3s), 2.17 (6H, s, mesityl CH_3s), 2.22 (12H, s, mesityl CH_3s), 2.83 (12H, s, $N(CH_3)_2$s), 6.26 (2H, s, xanthene aromatics), 6.80-7.00 (6H, m, aromatics).

$^{13}C\{^1H\}$ $\delta_C(C_6D_6)$ 19.92, 21.64 (mesityl CH_3s), 29.20 (xanthene CH_3s), 32.64 ($C(CH_3)_3$s), 35.76, 37.38 (tertiary carbons), 45.99 ($N(CH_3)_2$s), 108.18, 109.01 (xanthene aromatic CHs), 129.79 (mesityl aromatic CHs), 132.04, 133.66, 134.23, 142.57, 147.73, 148.01, 149.39 (quaternary aromatics).

6.8 References

1. R. Baumann, W. M. Davis, R. R. Schrock, *J. Am. Chem. Soc.*, 1997, **119**, 3830.
2. D. D. Graf, W. M. Davis, R. R. Schrock, *Organometallics*, 1998, **17**, 5820.
3. R. Baumann, R. R. Schrock, *J. Organomet. Chem.*, 1998, **557**, 69.
4. R. Baumann, R. Stumpf, W. M. Davis, L. C. Liang, R. R. Schrock, *J. Am. Chem. Soc.*, 1999, **121**, 7822.
5. R. R. Schrock, R. Baumann, S. M. Reid, J. T. Goodman, R. Stumpf, W. M. Davis, *Organometallics*, 1999, **18**, 3649.

6. L. C. Liang, R. R. Schrock, W. M. Davis, *Organometallics*, 2000, **19**, 2526.

7. J. T. Goodman, R. R. Schrock, *Organometallics*, 2001, **20**, 5205.

8. R. R. Schrock, L. C. Liang, R. Baumann, W. M. Davis, *J. Organomet. Chem.*, 1999, **591**, 163.

9. M. Aizenberg, L. Turculet, W. M. Davis, F. Schattenmann, R. R. Schrock, *Organometallics*, 1998, **17**, 4795.

10. M. A. Flores, M. R. Manzoni, R. Baumann, W. M. Davis, R. R. Schrock, *Organometallics*, 1999, **18**, 3220.

11. R. J. van Haaren, P. K. Keeven, L. A. van der Veen, K. Goubitz, G. P. F. van Strijdonck, H. Oevering, J. N. H. Reek, P. C. J. Kamer, P. W. N. M. van Leeuwen, *Inorg. Chim. Acta*, 2002, **327**, 108.

12. L. A. van der Veen, P. K. Keeven, P. C. J. Kamer, P. W. N. M. van Leeuwen, *J. Chem. Soc., Dalton Trans.*, 2000, 2105.

13. H. Hanawa, S. Kii, K. Maruoka, *Adv. Synth. Catal.*, 2001, **343**, 57.

14. M. L. Hlavinka, J. R. Hagadorn, *Chem. Commun.*, 2003, 2686.

15. J. S. Nowick, P. Ballester, F. Ebmeyer, J. Rebek, *J. Am. Chem. Soc.*, 1990, **112**, 8902.

16. E. B. Schwartz, C. B. Knobler, D. J. Cram, *J. Am. Chem. Soc.*, 1992, **114**, 10775.

17. A. van der Linden, C. J. Schaverien, N. Meijboom, C. Ganter, A. G. Orpen, *J. Am. Chem. Soc.*, 1995, **117**, 3008.

18. E. Benzing, W. Kornicker, *Chem. Ber.*, 1961, **94**, 2263.

Chapter 7
Conclusions

7.1 Amido/imino complexes of zirconium and titanium

This work demonstrates the practical and high yielding syntheses of four different anilino/ketimino ligands based on a 2-(1-cyclohexylimino-ethyl)-aniline framework as well as their respective lithium amido/imino derivatives. Two of these ligands, 2-(1-cyclohexylimino-ethyl)-*N*-(trimethylsilyl)-aniline (**2.2**) and 2-(1-cyclohexylimino-ethyl)-*N*-(*tert*-butyldimethylsilyl)-aniline (**2.4**), feature a trialkylsilyl group as the second substituent of the secondary anilino nitrogen and demonstrate how the steric properties of the ligand can readily be varied. It was possible to deprotonate the secondary silyl-amino nitrogen of these two compounds to give the respective lithium-[2-(1-cyclohexylimino-ethyl)-*N*-(trimethylsilyl)-anilide] (**2.3**) and lithium-[2-(1-cyclohexylimino-ethyl)-*N*-(*tert*-butyldimethylsilyl)-anilide] (**2.5**), as isolable extremely air and moisture sensitive white solids.

The second two anilino/ketimino ligands featured the same 2-(1-cyclohexylimino-ethyl)-aniline framework but possessed an aryl group as the second substituent on the anilino nitrogen. This aryl ring was introduced onto the nitrogen *via* a palladium catalysed arylation of the aniline with an arylbromide. Employing 3,5-dimethylbromobenzene and 2,4,6-trimethylbromobenzene as the arylbromides, 2-(1-cyclohexylimino-ethyl)-*N*-(3,5-dimethylphenyl)-aniline (**2.6**) and 2-(1-cyclohexylimino-ethyl)-*N*-(2,4,6-trimethylphenyl)-aniline (**2.8**) were obtained as products, respectively. Both (**2.6**) and (**2.8**) were deprotonated to give lithium-[2-(1-cyclohexylimino-ethyl)-*N*-(3,5-dimethylphenyl)-anilide] (**2.7**) and lithium-[2-(1-cyclohexylimino-ethyl)-*N*-(2,4,6-trimethylphenyl)-anilide] (**2.9**) as bright yellow and bright orange solids, respectively. The structural data obtained for the lithium amides show that the adopted structures are dependant on the steric characteristics of the ligand. Bulkier *N*-groups give rise to structures of lower aggregation.

An attempt to synthesise an analogous anilino/aldimino ligand based on a 2-cyclohexyliminomethyl-aniline framework, bearing an aryl group on the anilino nitrogen, by the palladium catalysed arylation of the 2-cyclohexyliminomethyl-

aniline with 2,4,6-trimethylbromobenzene however, did not work. Slow coupling to form 2-(cyclohexyliminomethyl)-*N*-(2,4,6-trimethylphenyl)-aniline was realised by performing a palladium catalysed amination of 2-cyclohexyliminomethyl-bromobenzene with 2,4,6-trimethylaniline. The reaction proceeded very slowly to give the desired product (**2.10**) in moderate yield on a small scale. These findings demonstrate the subtle electronic and steric factors that are involved in palladium-catalysed aminations.

The lithium amido/imino complexes (**2.3**), (**2.5**) and (**2.9**) were used to synthesise zirconium complexes of the type $LZr(NR_2)_2Cl$ in which L = amido/imino ligand and NR_2 = dimethylamide or diethylamide. These complexes were [2-(1-cyclohexylimino-ethyl)-*N*-(trimethylsilyl)-anilide] zirconium chloride bis-dimethylamide (**3.1**); [2-(1-cyclohexylimino-ethyl)-*N*-(*tert*-butyldimethylsilyl)-anilide] zirconium chloride bis-dimethylamide (**3.2**); [2-(1-cyclohexylimino-ethyl)-*N*-(trimethylsilyl)-anilide] zirconium chloride bis-diethylamide (**3.3**); and [2-(1-cyclohexylimino-ethyl)-*N*-(2,4,6-trimethylphenyl)-anilide] zirconium chloride bis-diethylamide (**4.1**). They were obtained in moderate to good yield as yellow or orange crystalline solids and identified by a combination of NMR spectroscopy, single crystal X-ray diffraction and analytical methods. The amido/imino ligand seemed to place large steric demands on the metal centre and it was not possible to introduce a second amido/imino ligand *via* a salt metathesis reaction to give the $L_2Zr(NR_2)_2$ type complexes.

It was possible to convert several of these $LZr(NR_2)_2Cl$ type complexes to the corresponding amido/imino zirconium trichloride complexes of the type $LZrCl_3$ by reaction with chlorotrimethylsilane. Repeated attempts to react these $LZrCl_3$ complexes with alkylating agents gave only intractable mixtures.

It appears that the steric bulk of the ligand is the driving force behind the rearrangement observed in two complexes giving rise to [2-(1-cyclohexylamido-vinyl)-*N*-(*tert*-butyldimethylsilyl)-anilide] zirconium chloride diethylamide tetrahydrofuran (**3.4**) and [2-(1-cyclohexylamido-vinyl)-*N*-(2,4,6-trimethylphenyl)-anilide] zirconium chloride diethylamide tetrahydrofuran (**4.2**). The amido/imino ligand has been converted into a dianionic arylamido/vinylamido ligand. We propose that this occurs *via* the insertion of the cyclohexylimino group into a zirconium-diethylamide bond to convert the imine nitrogen into an amide,

followed by elimination of diethylamine to give the vinyl group *via* an E1 type mechanism.

A similar argument can be invoked to explain the results of salt metathesis reactions of the lithium arylamido/imino complexes with $Ti(NMe_2)_2Cl_2$. In this case, the resultant complexes that were isolated featured a dianionic arylamido/ cyclohexylamido/dimethylamino pseudo tripodal tridentate ligand of the type 2-(1-cyclohexylamido-1-dimethylamino-ethyl)-*N*-(aryl)-anilide (aryl = 3,5-dimethylphenyl and 2,4,6-trimethylphenyl). The ligand formally originates by insertion of the imine group into a titanium-dimethylamide bond. Two examples of this type of species were characterised crystallographically. When attempts were made to react the free amino/imino ligands **(2.6)** and **(2.8)** with $Ti(NMe_2)_2Cl_2$, no reactions were observed. Despite this the ligand may have interesting properties and warrants further study. It would be interesting to investigate whether a rational synthesis for the free ligand could be found or whether it is only obtainable *via* a titanium based rearrangement.

Although no transamination reactions were achieved with the free arylamino/imino ligands **(2.6)** and **(2.8)**, one example in which the trimethylsilyl-substituted ligand **(2.2)** was introduced onto zirconium *via* a transamination reaction with $Zr(NMe_2)_4$ was studied by NMR spectroscopy to give [2-(1-cyclohexylimino-ethyl)-*N*-(trimethylsilyl)-anilide] zirconium tris-dimethylamide **(3.7)**. When the reaction was attempted with two equivalents of **(2.2)** under more forcing conditions an imido/imino zirconium bis-dimethylamide complex **(3.8)** was isolated and characterised crystallographically. The trimethylsilyl-substituent had been eliminated from the ligand and demonstrates a potential decomposition route of the trialkylsilyl-substituted amido/imino ligands.

Despite the large steric bulk of the ligands, a bis-amido/imino zirconium complex was isolated in low yield as bis-[2-(1-cyclohexylamido-vinyl)-*N*-(*tert*-butyldimethylsilyl)-anilide] zirconium dichloride **(3.6)** following reaction of two equivalents of **(2.4)** with $ZrCl_4(THT)_2$.

Several of the amido/imino zirconium complexes were tested for their activity as catalysts for the polymerisation of ethylene when activated with an excess of MAO. The complexes **(3.1)**, **(3.6)**, **(4.1)** and **(4.3)** all had low to moderate activity under the polymerisation conditions employed.

Given the wide variety of ligand rearrangements observed for these amido/imino ligands their coordination chemistry is worthy of further study. As they stand the ligands are probably too reactive and prone to rearrangements to act as effective supporting ligands for single-site polymerisation of olefins. If the imine group can be stabilised towards the insertion reaction they may prove more viable supporting ligands. Given that these rearrangement reactions are occurring under relatively mild conditions it is highly likely that similar reactions are occurring under the harsher conditions of polymerisation catalysis. It is also possible that the vinyl-containing diamido ligands and the tripodal diamido/monoamino ligands may prove suitable supporting ligands and they too warrant further study.

7.2 Salicylaldiminato complexes of zirconium and titanium and a related complex of niobium

Following the instances in which the imine group of the amido/imino ligand inserted into a metal-dialkylamide bond an effort was undertaken to investigate whether the analogous salicylaldiminato ligand would undergo similar rearrangements when bound to titanium and zirconium centres bearing dialkylamide ligands. Initial efforts focused on mono-salicylaldiminato complexes of titanium(IV). The reaction of lithium 2-*tert*-butyl-6-cyclohexyliminomethyl-phenoxide (**5.1**) with $Ti(NMe_2)_2Cl_2$ gave (2-*tert*-butyl-6-cyclohexyliminomethyl-phenoxy) titanium dimethylamide dichloride dimethylamine (**5.2**) as the product. Whilst it is unclear how (**5.2**) was formed, given that it is not the anticipated $LTi(NMe_2)_2Cl$ type complex, the product contained the intact salicylaldiminato ligand with no evidence of any insertion of the imine group into a titanium-dimethylamide bond. When a reaction between the neutral salicylaldimine and $Ti(NMe_2)_2Cl_2$ was performed in THF the product was (2-*tert*-butyl-6-cyclohexyliminomethyl-phenoxy) titanium dimethylamide dichloride tetrahydrofuran (**5.3**) following a protonolysis reaction to eliminate one equivalent of dimethylamine.

To investigate whether increasing the steric crowding around the metal centre could induce the insertion of the imine group into the metal-amide bond, reactions were attempted between two equivalents of the neutral salicylaldimine with zirconium and titanium complexes bearing bulkier diethylamide ligands. The

reactions with $Ti(NEt_2)_2Cl_2$ and $Zr(NEt_2)_2Cl_2(THF)_2$ gave the bis-salicylaldiminato metal dichloride complexes bis-(2-*tert*-butyl-6-cyclohexyliminomethyl-phenoxy) titanium dichloride (**5.4**) and bis-(2-*tert*-butyl-6-cyclohexyliminomethyl-phenoxy) zirconium dichloride (**5.6**) with no evidence of the insertion reaction. Reaction of two equivalents of the neutral salicylaldimine with $Ti(NEt_2)_4$ and $Zr(NEt_2)_4$ gave bis-(2-*tert*-butyl-6-cyclohexyliminomethyl-phenoxy) titanium bis-diethylamide (**5.5**) and bis-(2-*tert*-butyl-6-cyclohexyliminomethyl-phenoxy) zirconium bis-diethylamide (**5.7**). Again there was no evidence of the insertion reaction, even when these two complexes were heated to 100 °C in d^8-PhMe.

These results show that salicylaldiminato ligand is not prone to the insertion of the imine group into a Group(IV) metal-dialkylamide bond whilst the amido/imino ligands studied here, are. It seems possible that this is due to the increased steric demands of the amido/imino ligand due to the presence of a second substituent on the amide nitrogen, which is not present on the phenoxide oxygen of the salicylaldiminato ligand.

A rearrangement involving the imine group of the salicylaldiminato ligand was observed following the reaction of two equivalents of the neutral salicylaldimine with the niobium(IV) complex $Nb(NEt_2)_4$. The niobium(V) complex (2-*tert*-butyl-6-cyclohexyliminomethyl-phenoxy) [2-*tert*-butyl-6-(1-cyclohexylamido-2-ethylamido-propyl)-phenoxy] niobium diethylamide (**5.8**) was isolated from the reaction in good yield and identified by both single crystal X-ray crystallography and NMR spectroscopy. The complex contains one intact salicylaldiminato ligand and one that has been fused with a diethylamide ligand through the imine carbon of the salicylaldiminato and one of the methylene carbons of the diethylamide group. This has resulted in the conversion of the imine group to an amide giving a trianionic phenoxide/diamide ligand. Given the single electron oxidation of Nb(IV) to Nb(V) it is most likely that the mechanism of formation of the new ligand is radical based.

7.3 Diamidoxanthene and diamidodibenzofuran ligands and their titanium complexes

The synthesis of two 4,5-diaminoxanthene molecules was achieved using palladium-catalysed amination reactions of 4,5-dibromo-2,7-di-*tert*-butyl-9,9-dimethyl-xanthene. The two compounds were 4,5-dicyclohexylamino-2,7-di-*tert*-

butyl-9,9-dimethyl-xanthene (**6.1**) and 4,5-di-(2,4,6-trimethylanilino)-2,7-di-*tert*-butyl-9,9-dimethyl-xanthene (**6.2**). An analogous dibenzofuran-based ligand was synthesised using the same palladium catalysis method but with 4,5-dibromo-dibenzofuran to give 4,5-di-(2,4,6-trimethylanilino)-dibenzofuran (**6.3**). These three complexes were synthesised in good yields. The rationale behind the synthesis of the xanthene and the dibenzofuran based ligands is that they will offer different bite angles when coordinated to metals and so have differing influences on the other ligands bound to the metal centre.

The dilithium 4,5-di-(2,4,6-trimethylanilido)-dibenzofuran (**6.4**) complex was synthesised by reaction of two equivalents of Bu^nLi with (**6.3**). An NMR scale reaction between (**6.1**) and titanium tetrabenzyl yielded the diamido titanium dibenzyl complex 4,5-dicyclohexylamido-2,7-di-*tert*-butyl-9,9-dimethyl-xanthene titanium dibenzyl (**6.5**). Another two titanium complexes were synthesised by *in situ* formation of dilithium diamide species from (**6.1**) and (**6.2**) and subsequent reaction with one equivalent of $Ti(NMe_2)_2Cl_2$. The two complexes 4,5-di-cyclohexylamido)-2,7-di-*tert*-butyl-9,9-dimethyl-xanthene titanium bis-dimethylamide (**6.6**) and 4,5-di-(2,4,6-trimethylanilido)-2,7-di-*tert*-butyl-9,9-dimethyl-xanthene titanium bis-dimethylamide (**6.7**) were identified through a combination of single crystal X-ray crystallography and NMR spectroscopy.

The work reported here on these diamidoxanthene and diamidodibenzofuran ligands represents the beginning of an investigation into their coordination behaviour and the ability of their metal complexes to act as single-site polymerisation catalysts. They require and warrant further study.

Appendix

Experimental Techniques and Instrumentation

Experimental Techniques

Unless otherwise stated, experiments were performed under dry dinitrogen using standard Schlenk line techniques or in an inert atmosphere dry box (Braun UNILAB) containing dry dinitrogen, constantly monitoring oxygen levels. Glassware was pre-dried before use. Solvents were dried and then distilled from sodium benzophenone ketyl [light petroleum ether (bp 40-60 °C), Et_2O and THF], from sodium (toluene, xylenes, 1,4-dioxane) or from calcium hydride (dichloromethane), under a slow continuous stream of dinitrogen. Solvents were thoroughly degassed by purging with dinitrogen prior to use. Deuterated solvents were dried (d^6-benzene and d^8-toluene over sodium/potassium alloy; d^8-THF over potassium; d^2-dichloromethane over calcium hydride; and d^1-chloroform over molecular sieves), distilled and degassed by freeze-pump-thaw cycles prior to use. Unless otherwise stated, commercial reagents and solvents were used as received from Acros, Aldrich, and Avocado.

Instrumentation

NMR experiments were performed on Bruker 300 and 400 MHz spectrometers. The spectra were referenced internally using the signal from the residual protio-solvent (^1H) or the signal from the solvent ($^{13}C\{^1H\}$), or externally relative to LiCl in D_2O (^7Li).

Gas chromatographic mass spectra were recorded on a Thermoquest TraceMS machine from dried dichloromethane solutions.

Elemental analyses were carried out by the University College London Microanalytical Laboratory.

Crystallography

All data sets were collected on a Enraf Nonius Kappa CCD area detector diffractometer with rotating anode FR591 and an Oxford Cryosystems low-temperature device, operating in omega scanning mode with phi scans to fill the Ewald sphere. The crystals were isolated under dinitrogen, covered with Fomblin

vacuum oil and mounted on a glass fibre with silicon grease. Structures were solved and refined using SHELX[1] and WinGX[2] software packages. Non-hydrogen atoms were refined with anisotropic thermal parameters. Compound (**4.4**) crystallises with one molecule of THF and compound (**4.8**) crystallises with one molecule of diethyl ether per dimer, in both cases, these were highly disordered and were handled using the PLATON SQUEEZE procedure.[3]

References

1. G. M. Sheldrick, SHELX97. Programs for Crystal Structure Analysis (Release 97-2). University of Göttingen, Germany.

2. L. J. Farrugia, *J. Appl. Cryst.*, 1999, **32**, 83.

3. P. van der Sluis and A. L. Spek, *Acta. Cryst. A*, 1990, **46**, 194.